

Documentation and Verification of VST2D:
A Model for Simulating Transient, **V**ariably
Saturated, Coupled Water-Heat-Solute
Transport in Heterogeneous, Anisotropic,
2-Dimensional, Ground-Water Systems with
Variable Fluid Density

Water-Resources Investigations Report 00–4105

Documentation and Verification of VST2D: A Model for Simulating Transient, **V**ariably **S**aturated, Coupled Water-Heat-Solute Transport in Heterogeneous, Anisotropic, **2-D**imensional, Ground-Water Systems with Variable Fluid Density

By Michael J. Friedel

Water-Resources Investigations Report 00-4105

U.S. DEPARTMENT OF THE INTERIOR
GALE A. NORTON, Secretary

U.S. GEOLOGICAL SURVEY
Charles G. Groat, Director

The use of firm, trade, and brand names in this report is for identification purposes only and does not constitute endorsement by the U.S. Geological Survey.

For additional information write to:

District Chief
U.S. Geological Survey
221 North Broadway Avenue
Urbana, Illinois 61801

Copies of this report can be purchased from:

U.S. Geological Survey
Branch of Information Services
Box 25286
Denver, CO 80225-0286

PREFACE

The computer model described in this report, called VST2D, was designed to simulate coupled water-heat-solute transport in heterogeneous, anisotropic, two-dimensional, ground-water systems with variable fluid density. The VST2D model was verified against analytic and numerical solutions for problems of water transport under isohaline and isothermal conditions, heat transport under isobaric and isohaline conditions, and solute transport under isobaric and isothermal conditions. The coupled water-heat-solute transport problem was compared to measured laboratory results for which no known analytic solutions or numerical models are available.

Whereas these test results indicate that VST2D is accurate and applicable for a wide range of conditions, including when water (liquid and vapor), heat (sensible and latent), and solute (single species) are coupled, future applications of this program could reveal errors not previously detected. Users are requested to notify the author if errors are found in either the VST2D report or the computer program. The user is further reminded that achieving a successful simulation is not dependent solely on applying a well-formulated numerical model. The user's knowledge and understanding of ground-water hydraulics, heat transfer, chemical processes, and model limitations are equally important in arriving at a well-posed simulation.

The code for this model is available for downloading over the Internet from a U.S. Geological Survey (USGS) software repository, accessible from the USGS Water Resources Information and Illinois District Web pages at URL <http://water.usgs.gov/software> and <http://il.water.usgs.gov/usgs/computers/vst2d/>, respectively.

CONTENTS

Abstract	1
Introduction	2
Theoretical Background	3
Governing Equations	3
Water Transport	3
Heat Transport	11
Solute Transport	13
Properties and Parametric Relations	15
Hydraulic	16
Thermal	23
Water	29
Chemical	29
Assumptions	30
Numerical Methods	31
Finite-Element Method	31
Residual Equations for Elements	35
Individual Element Matrices and Vectors	41
Derivative Boundary Conditions, Point Sources and Sinks	46
Solution Procedure	48
Time Discretization	49
Combined Element Matrices and Vectors	54
Dirichlet Conditions	56
Neumann Conditions	59
Initial Conditions	59
Picard Iteration	59
Peclet and Courant Numbers	60
Mass and Energy Balance	60
Assumptions	63
Model Documentation	63
General Program Structure	63
Main Program and Related Subroutines	65
Data Input Files	67
Data Output Files	70
Model Verification	71
Case 1: Water Transport Under Nonisobaric, Isothermal, Isohaline Conditions	71
Case 2: Heat Transport Under Isobaric, Nonisothermal, Isohaline Conditions	73
Case 3: Solute Transport Under Isobaric, Isothermal, Nonisohaline Conditions	73
Case 4: Coupled Water-Heat-Solute Transport Under Nonisobaric, Nonisothermal, Nonisohaline Conditions	77
Summary	78
References	87
Appendix 1. Elemental Matrix-Vector Representation for Water, Heat, and Solute Equations	91
Appendix 2. Input/Output for Finite-Element GRID Generator (GRID)	95
Appendix 3. Model Input Files in Case 1 Validation (Water Transport)	97
Appendix 4. Model Input File in Case 2 Validation (Heat Transport)	105
Appendix 5. Model Input File in Case 3 Validation (Solute Transport)	111
Appendix 6. Model Input File in Case 4 Validation (Coupled Water-Heat-Solute Transport)	119

Figures

1-2. Diagrams showing:	
1. Representative control volume	4
2. Relation of local and global coordinates	9
3-6. Graphs showing:	
3. Moisture retention function fitted to desorption measurements for Ida silt loam	17
4. Temperature dependent water properties: (A) liquid density, (B) saturated vapor density, (C) surface tension, and (D) viscosity.....	19
5. Relative conductivity and moisture capacity as a function of effective saturation for Ida silt loam	24
6. Effect of temperature on pressure head for Ida silt loam	28
7. Flowchart depicting (a) operational and (b) matrix sequencing for the VST2D model.....	64
8. Diagram showing finite-element mesh used in the verification of water transport under isothermal and isohaline conditions.....	74
9-10. Graphs showing:	
9. Comparison of transient pressure head profiles for vertical water transport simulated under isothermal and isohaline conditions using the VST2D and VARSAT2D models	75
10. Comparison of transient (A) moisture and (B) saturation profiles for vertical water transport simulated under isothermal and isohaline conditions using the VST2D model.....	76
11. Diagram showing finite-element mesh used in the verification of heat transport under isobaric and isohaline conditions.....	78
12-13. Graphs showing:	
12. Comparison of transient temperature profiles simulated under isobaric and isohaline conditions using VST2D and HEAT2	79
13. Comparison of transient solute profiles simulated under isobaric and isothermal conditions using VST2D and ALVE2.....	81
14. Diagram showing finite-element mesh used in the verification of solute transport simulated under isobaric and isothermal conditions.....	82
15. Diagram showing finite-element mesh used in the verification of steady-state water-heat-solute transport conditions	83
16. Graphs showing the comparison of measured and simulated steady-state profiles within a moist, salinized, horizontal column subject to differential heat: (A) temperature, (B) moisture content, (C) solute concentration	85
17. Concepts for finite-element mesh generation using GRID	86

Tables

1. Summary of empirical relations for selected water and thermal properties used in the VST2D model.....	26
2. Summary of properties used in the VST2D model validation process involving Ida silt loam	72
3. Summary of properties used in the VST2D model validation process involving crystalline rock	72
4. Summary of conditions used in the VST2D validation process for water transport.....	73
5. Summary of conditions used in the VST2D validation process for heat transport.....	77
6. Summary of conditions used in the VST2D model validation process for solute transport.....	80
7. Summary of conditions used in the VST2D validation process for coupled water-heat-solute transport	84

CONVERSION FACTORS

Multiply	By	To obtain
Length		
nanometer (nm)	0.00003937	inch
centimeter (cm)	0.3937	inch
centimeter (cm)	0.03281	foot
meter (m)	3.281	foot
Mass		
kilogram (kg)	2.205	pound (avoirdupois)
Density		
kilogram per cubic meter (kg m ⁻³)	0.06242	pound per cubic foot
Energy		
joule (J)	4.187	calorie
Force		
Newton (N)	1	joule per meter
Power		
Watt (W)	1	joule per second
Watt (W)	1	kilogram meter squared per cubic second
Pressure head		
Newton per meter squared (N m ⁻²)	10 ⁻⁵	bar
centimeter (cm)	10.2	centibar
Volumetric Heat capacity		
Joule per cubic meter degree Kelvin (J m ⁻³ K ⁻¹)	.000000239	calorie per cubic centimeter degree Celsius
Thermal Conductivity		
Watt per meter degree Kelvin (W m ⁻¹ K ⁻¹)	20460	calorie per meter day degree Celsius
Heat flux		
Watt per meter squared (W m ⁻²)	0.000048461	calorie per meter squared day
Liquid flux		
meter per day (m d ⁻¹)	3.281	feet per day

Temperature in degrees Celsius (°C) may be converted to degrees Fahrenheit (°F) as follows:

$$^{\circ}\text{F} = (1.8 \times ^{\circ}\text{C}) + 32.$$

To convert degree Celsius (°C) to degree Kelvin (K) use the following formula:

$$\text{K} = ^{\circ}\text{C} + 273.$$

To convert pressure head to potential multiply by the product of fluid density (ρ_L) and gravitational constant (g).

LIST OF SYMBOLS

a	mean ionic solution activity [dimensionless]
a_i, a_j, a_k	coefficients used in interpolation functions, where $a_i = x_i y_k - x_k y_j, a_j = x_k y_i - x_i y_k,$ $a_k = x_i y_j - x_j y_i$ [m^2]
A^e	element area [m^2]
A_s	surface area of clay particle [m^2]
$A_{\psi L}, A_{\psi V}, A_{\psi \psi}$	three-node element capacitance-type coefficients arising because of time dependence in the water equation [m^2], [m^2], [$kg\ m^{-2}$], [$cal\ kg\ mol^{-1}\ m^{-1}$]
$A_{TL}, A_{T\psi}, A_{TT}, A_{TC}$	three-node element capacitance-type coefficients arising because of time dependence in the heat equation [$cal\ m^{-1}$], [$cal\ m^{-2}$], [$cal\ m^{-1}\ ^\circ C^{-1}$], [$cal\ kg\ mol^{-1}\ m^{-1}$]
$A_{CL}, A_{C\psi}, A_{CC}$	three-node element capacitance-type coefficients arising because of time dependence in the solute equation [$mol\ kg^{-1}\ m^2$], [$mol\ kg^{-1}\ m$], [m^2]
b	one-half of the water film thickness [nm]
b_ψ, b_T, b_C	three-node forcing coefficients for water, heat and solute equations [m^2], [$cal\ m^{-1}$], [$m^2\ mol\ kg^{-1}$]
b_i, b_j, b_k	coefficients used in interpolation functions, where $b_i = y_j - y_k, b_j = y_k - y_i,$ and $b_k = y_i - y_j$, [m]
c_i, c_j, c_k	coefficients used in interpolation functions, where $c_i = x_k - x_j, c_j = x_i - x_k,$ and $c_k = x_j - x_i$ [m]
$B_{\psi\psi}, B_{\psi T}, B_{\psi C}$	three-node element conductance-type coefficient associated with the water equation [$kg\ m^{-2}\ d^{-1}$], [$kg\ m^{-1}\ d^{-1}\ ^\circ C^{-1}$], [$kg\ mol^{-1}\ m^{-1}\ d^{-1}$]
$B_{T\psi}, B_{TT}, B_{TC}$	three-node element conductance-type coefficient associated with the heat equation [$cal\ m^{-2}\ d^{-1}$], [$cal\ m^{-1}\ ^\circ C^{-1}\ d^{-1}$], [$cal\ kg\ m^{-1}\ mol^{-1}\ d^{-1}$]
$B_{C\psi}, B_{CT}, B_{CC}$	three-node element conductance-type coefficient associated with the solute equation [$m\ mol\ kg^{-1}\ d^{-1}$], [$m^2\ mol\ kg^{-1}\ ^\circ C^{-1}\ d^{-1}$], [$m^2\ d^{-1}$]
$C_{\psi\psi}$	three-node element capacitance-type coefficient because of time dependence [m],
C	solute concentration [$mol\ kg^{-1}$]
C_0, C_e	initial and boundary exit concentrations [$mol\ kg^{-1}$]
C_M, C_o, C_L and C_a	volumetric heat capacities of minerals, organic matter, liquid water, and air [$cal\ m^3\ ^\circ C^{-1}$]
C_d	volumetric heat capacity of dry soil or rock [$cal\ m^{-3}\ ^\circ C^{-1}$]
c_L	specific heat of liquid water [$cal\ gm^{-1}\ ^\circ C^{-1}$]
c_p	specific heat of water vapor at constant pressure [$cal\ gm^{-1}\ ^\circ C^{-1}$]
c_L	specific heat of liquid water [$cal\ gm^{-1}\ ^\circ C^{-1}$]
C_p	volumetric heat capacity of water vapor [$cal\ m^{-3}\ ^\circ C^{-1}$]
C_L	volumetric heat capacity of liquid water [$cal\ m^{-3}\ ^\circ C^{-1}$]
C_ψ^*	critical capacitance ψ^* [m^{-1}]
W^*	differential heat of wetting [$cal\ m^{-3}$].
C_v	volumetric heat capacity of bulk soil or rock [$cal\ m^{-3}\ ^\circ C^{-1}$]
C_ψ	moisture capacity [m^{-1}]
C^*	amount of chemical sorbed to the soil-rock mass [$mol\ kg^{-1}$],

dt	simulation time step [d]
D	molecular diffusivity of water vapor in air [$\text{m}^2 \text{d}^{-1}$]
D_C	solute moisture diffusivity [$\text{m}^2 \text{d}^{-1} \text{kg mol}^{-1}$]
D_{CC}	moisture diffusivity because of solute concentration [$\text{m}^2 \text{d}^{-1} \text{kg mol}^{-1}$]
D_{CL}	liquid water diffusivity because of solute concentration [$\text{m}^2 \text{d}^{-1} \text{kg mol}^{-1}$]
D_{CV}	vapor diffusivity in soil because of solute concentration [$\text{m}^2 \text{d}^{-1} \text{kg mol}^{-1}$]
$D_{C\theta}$	diffusion tensor because of salt sieving [$\text{m}^2 \text{mol kg}^{-1} \text{d}^{-1}$]
D_h	hydrodynamic dispersion tensor [$\text{m}^2 \text{d}^{-1}$]
D_x, D_y	physical property coefficients oriented along principal directions
D_0	solute diffusion coefficient because of concentration gradient [$\text{m}^2 \text{d}^{-1}$]
D_{siev}	diffusion coefficient because of salt sieving [$\text{m}^2 \text{d}^{-1} \text{mol kg}^{-1}$]
D_T	thermal moisture diffusivity [$\text{m}^2 \text{d}^{-1} \text{°C}^{-1}$]
D_{TS}	thermal solute diffusion coefficient because of a temperature gradient [$\text{m}^2 \text{d}^{-1} \text{mol kg}^{-1} \text{°C}^{-1}$]
D_{TL}	thermal liquid diffusivity [$\text{m}^2 \text{d}^{-1} \text{°C}^{-1}$]
D_{TV}	vapor thermal diffusivity [$\text{m}^2 \text{d}^{-1} \text{°C}^{-1}$]
D_{xx}	dispersion coefficient in principal direction xx [$\text{m}^2 \text{d}^{-1}$]
D_{yy}	dispersion coefficient in principal direction yy [$\text{m}^2 \text{d}^{-1}$]
D_{xy}	dispersion coefficient in the xy (and yx) direction [$\text{m}^2 \text{d}^{-1}$]
D_θ	isothermal moisture diffusivity [$\text{m}^2 \text{d}^{-1}$]
$D_{\theta L}$	isothermal liquid diffusivity [$\text{m}^2 \text{d}^{-1}$]
$D_{\theta V}$	isothermal vapor diffusivity [$\text{m}^2 \text{d}^{-1}$]
e	element
E	elevation head [m]
f_1	bulk heat capacitance type term [$\text{cal m}^{-3} \text{°C}^{-1}$]
f_2	bulk latent heat type term [cal m^{-3}]
f_3	bulk latent heat type term [$\text{cal m}^{-3} \text{kg mol}^{-1}$]
f_c	fractional clay content [dimensionless]
$f_{\psi L}, f_{\psi \psi}, f_{\psi V}, f_{\psi V \psi}$	three-node element forcing coefficients that arise because of Neumann conditions and time derivative associated with water equations [kg m^{-1}], [kg m^{-1}], [kg m^{-1}], [kg m^{-1}]
$f_{T \psi}, f_{TL}$	three-node element forcing coefficients that arise because of Neumann conditions and time derivative associated with water equations [cal m^{-1}], [cal m^{-1}]
f_{TH}, f_{TT}	three-node element forcing coefficients that arise because of applying a Taylor series expansion about the heat content with respect to temperature [cal m^{-1}], [cal m^{-1}]
f_{TC}, f_{TCH}	three-node element forcing coefficients that arise because of applying a Taylor series expansion about the heat content with respect to concentration [cal m^{-1}], [cal m^{-1}]
$f_{CL}, f_{C \psi}, f_{CC}$	three-node element forcing coefficients that arise because of Neumann conditions and time derivative associated with water equations [cal m^{-1}], [cal m^{-1}], [cal m^{-1}]
F	Faraday's constant [$96,485 \text{ col mol}^{-1}$]

F_{ψ}, F_T, F_C	total forcing coefficients that arise because of Neumann conditions and time derivatives associated with water, temperature, and solute equations [kg m^{-1}], [cal m^{-1}], [$\text{m}^2 \text{mol kg}^{-1}$]
g	gravitational acceleration [9.81 m s^{-2}]
$G_{\psi T}$	gain factor used to compensate for underestimation of temperature-induced changes when only surface tension is considered
H	total heat content [cal m^{-3}]
h_r	relative humidity [dimensionless]
h_m	relative humidity because of soil matric potential [dimensionless]
h_o	relative humidity because of an osmotic potential [dimensionless]
i, j, k	subscripts indicating element node
L, V	subscripts indicating water phases: liquid and vapor, respectively
k	intrinsic permeability [m^2]
k_x, k_y	intrinsic permeability along principal directions [m^2]
\bar{k}	unit vertical vector, $0i + 0j + 1k$ or $\{0,0,1\}$
K	degree Kelvin
K	hydraulic conductivity tensor [m d^{-1}]
K_r	relative hydraulic conductivity (a function of effective saturation or moisture content)
K_{xx}	principal component of hydraulic conductivity in xx direction [m d^{-1}]
K_{xy}	principal component of hydraulic conductivity in xy direction [m d^{-1}]
K_{yx}	principal component of hydraulic conductivity in yx direction [m d^{-1}]
K_{yy}	principal component of hydraulic conductivity in yy direction [m d^{-1}]
K_x, K_y	hydraulic conductivity values in principal directions of element [m d^{-1}]
K_{sx}, K_{sy}	saturated hydraulic conductivity values in the principal directions of element [m d^{-1}]
K_d	distribution coefficient [L kg^{-1}]
K_{OC}	partition coefficient with respect to the organic fraction [$\text{m}^3 \text{kg}^{-1}$]
K_{OW}	octanol-water partition coefficient [$\text{m}^3 \text{kg}^{-1}$]
K_s	saturated hydraulic conductivity [m d^{-1}]
L	latent heat of vaporization [cal gm^{-1}]
L_0	latent heat of vaporization at reference temperature (585 cal g^{-1} at $20 \text{ }^\circ\text{C}$)
L_{ψ}, L_T, L_C	differential operators for water, heat and solute equations [d^{-1}], [$\text{cal m}^{-3}\text{d}^{-1}$], [$\text{mol kg}^{-1}\text{d}^{-1}$]
m, n	empirically derived constants used in moisture retention function
M	molecular weight of liquid water [$4.615 \times 10^6 \text{ erg gm}^{-1} \text{ }^\circ\text{C}^{-1}$]
M_C	total solute mass [mol kg^{-1}],
$M_{\psi\psi}, M_{\psi T}, M_{\psi C}$	global three-node element conductance-type coefficients for water equation [kg m^{-2}], [$\text{kg m}^{-1} \text{ }^\circ\text{C}^{-1}$], [mol m^{-1}]
$M_{T\psi}, M_{TT}, M_{TC}$	global three-node element conductance-type coefficients for heat equation [cal m^{-2}], [$\text{cal m}^{-1} \text{ }^\circ\text{C}^{-1}$], [$\text{cal kg m}^{-1} \text{ mol}^{-1}$]
$M_{C\psi}, M_{CT}, M_{CC}$	global three-node element conductance-type coefficients for solute equation [m mol kg^{-1}], [$\text{m}^2 \text{mol kg}^{-1} \text{ }^\circ\text{C}^{-1}$], [m^2]
N	number of soil/rock constituents

N_i	element interpolation function at node i
N_j	element interpolation functions at node j
N_k	element interpolation functions at node k
p, d	subscripts indicating point and distributed sources in the water equation, respectively
p_w	water pressure [N m ⁻²]
P	is the number of discrete node points in the solution domain
q_C	noninteracting solute flux [mol m ⁻² d ⁻¹]
q'_C	total mass solute flux [mol m ⁻² d ⁻¹ kg m ⁻³]
q_H	total heat flux [cal d ⁻¹ m ⁻³]
q'_L	liquid water flux (specific discharge) [m d ⁻¹]
q'_{Ln}	liquid water flux along solution domain boundary [m d ⁻¹]
q'_w	water flux [m d ⁻¹]
q_w	total mass water flux [kg m ⁻² d ⁻¹]
q_V	water vapor mass flux [kg m ⁻² d ⁻¹]
q_L	liquid water mass flux [kg m ⁻² d ⁻¹]
q_{Lx}	specific discharge along the x-direction [m d ⁻¹]
q_{Ly}	specific discharge along the y-direction [m d ⁻¹].
q'_{Lb}	liquid water flux [kg m ⁻² d ⁻¹]
Q_{Lp}, Q_{Ld}	liquid water flux point and distributed source or sink [m d ⁻¹]
Q_{Hp}, Q_{Hd}	heat flux point and distributed source or sink [cal m ⁻³ d ⁻¹]
Q_{Cp}, Q_{Cd}	solute flux point and distributed source or sink [mol ⁻¹ kg d ⁻¹]
r_s	hydrated radius of the solute [nm]
r_w	radius of a water molecule [nm]
r_w, r_T, r_C	residual error that arises due discrete dependent variable approximations [m, °C, mol kg ⁻¹]
R	universal gas constant [4.615×10 ⁶ erg gm ⁻¹ °C ⁻¹]
R	retardation factor [dimensionless]
$R_\theta, R_C, \text{ and } R_H$	solution domain residual errors for water [m ³], solute [m ³ mol kg ⁻¹], and heat [cal]
S	coefficients that depends on the applied boundary condition
t	time [d]
T	temperature [°C]
T	absolute temperature [K]
T_0	reference temperature [°C]
S_e	effective saturation [dimensionless]
S_e^*	critical value of effective saturation (0.001) [dimensionless]
V	absolute magnitude of elemental pore velocity [m d ⁻¹]
V_z	velocity of solid particles in the vertical direction [m s ⁻¹]
V_{Lx}, V_{Ly}	average bulk velocities of solution in the x- and y- directions [m d ⁻¹],
x, y	Cartesian coordinates (horizontal or vertical)
X_M, X_L, X_o, X_a	volume fractions of minerals, organic matter, liquid water, water vapor
$X_{snd}, X_{slt}, X_{cly}$	volume fraction of minerals: sand, silt, and clay
α_L, α_T	longitudinal and transverse dispersivity [m]

α	empirically derived constant used in retention function [m^{-1}]
α_0	reference values for the van Genuchten parameter [m^{-1}]
β	derivative of saturated water vapor density with respect to temperature [$\text{kg m}^{-3} \text{ }^\circ\text{C}^{-1}$]
β'	salt sieving coefficient representing the relative restriction of solute to solvent (equal in magnitude to osmotic coefficient, ϕ) [dimensionless]
δ	angle between element and solution domain principal axes [degrees]
γ_1^0, γ_2^0	limiting ionic conductivity of ions in liquid water [dimensionless]
γ	surface tension of water over air [mN m^{-1}]
γ_0	reference value for surface tension [mN m^{-1}]
γ_T'	temperature coefficient [$^\circ\text{C}^{-1}$]
γ_C'	concentration coefficient [kg mol^{-1}]
ε	tortuosity factor [dimensionless]
ε_z	strain in vertical direction [$\text{m}^{-1}/\text{m}^{-1}$]
ζ	change in pressure head with temperature [$\text{m }^\circ\text{C}^{-1}$]
η	factor accounting for microscopic exceeding macroscopic thermal gradients [dimensionless]
λ	solute decay coefficient [d^{-1}]
λ^*	thermal conductivity of variably saturated soil or rock [$\text{mcal cm}^{-1} \text{ }^\circ\text{C}^{-1} \text{ s}^{-1}$]
$\lambda_{cl}, \lambda_{org}, \lambda_{slt}$	thermal conductivities of clay, organic matter, and silt [$\text{cal m}^{-1} \text{ }^\circ\text{C}^{-1} \text{ d}^{-1}$]
$\lambda_a, \lambda_q, \lambda_{NaCl}$	thermal conductivities of air, quartz, sodium chloride solution defined by empirical relations given in table 1. [$\text{cal m}^{-1} \text{ }^\circ\text{C}^{-1} \text{ d}^{-1}$],
Λ	dimensionless storativity-type term
Λ'	storativity-type term [m^{-1}]
μ	fluid kinematic viscosity [N s m^{-2}]
μ_0	fluid kinematic viscosity at a reference temperature and concentration [N s m^{-2}],
ν	number of ions per molecule for an ionizing solute [dimensionless]
ν_1, ν_2	number of cations and anions [dimensionless]
θ	total water content [dimensionless]
θ_A	air filled porosity [dimensionless]
θ_L	liquid water (moisture) content [$\text{cm}^3 \text{ cm}^{-3}$]
θ_r	residual liquid water content at field capacity [$\text{cm}^3 \text{ cm}^{-3}$]
θ_s	saturated moisture content (porosity) [$\text{cm}^3 \text{ cm}^{-3}$]
θ_V	water-vapor content [$\text{cm}^3 \text{ cm}^{-3}$]
Θ	the angle of the boundary flux to the outward normal
ρ_b	bulk density [kg m^{-3}]
ρ_L	density of liquid [kg m^{-3}]
ρ_0	saturated water vapor density [kg m^{-3}]
σ_0	osmotic efficiency coefficient
σ	effective thermal conductivity term associated with a temperature gradient [cal m^{-2}]
σ'	effective latent heat term associated with a pressure gradient [$\text{cal m}^{-3} \text{ }^\circ\text{C}^{-1}$]
σ''	effective latent heat term associated with a concentration gradient [$\text{cal m}^{-3} \text{ kg mol}^{-1}$]

σ_e	effective stress [N m^{-2}]
σ_T	total stress [N m^{-2}]
ϕ	osmotic coefficient [dimensionless]
ϕ_b	unknown value on boundary of the solution domain
ψ	pressure head [m]
ψ^*	critical value of pressure head [m]
Ω	porous medium coefficient of vertical compressibility [$\text{m}^2 \text{N}^{-1}$]
ω	fluid compressibility [$\text{m}^2 \text{N}^{-1}$]
Γ	integration boundary along element surface
Π_i	ratio of average temperature gradient in the i th constituent to the average temperature gradient of the bulk medium.
$\partial\gamma/\partial T$	change in surface tension with temperature [$\text{mN m}^{-1} \text{ }^\circ\text{C}^{-1}$]
$\partial\gamma/\partial C$	change in surface tension with concentration [$\text{mN m}^{-1} \text{ kg}^{-1} \text{ mol}^{-1}$]
$\partial O/\partial T$	change in osmotic head with temperature [$\text{m }^\circ\text{C}^{-1}$]
$\partial O/\partial C$	change in osmotic head with concentration [m kg mol^{-1}]
∂	partial differential operator
\int	integral operator
∇	gradient operator [m^{-1}]
ΔV	control volume [m^3]
$\Delta x, \Delta y, \Delta z$	length of control volume sides [m]
$\Delta S_\theta, \Delta S_C, \text{ and } \Delta S_H$	changes in solution domain storage for water [m^3], solute [$\text{m}^3 \text{ mol kg}^{-1}$], and heat [cal];
$\Delta Q_\theta, \Delta Q_C, \text{ and } \Delta Q_H$	solution domain net fluxes along the permeable boundaries and at internal source/sinks
!	factorial
[]	matrix
{ }	vector
$\{R_\psi\}$	vector of residual equations for water transport [$\text{m}^2 \text{ d}^{-1}$]
$\{R_T\}$	vector of residual equations for heat transport [$\text{cal m}^{-1} \text{ d}^{-1}$]
$\{R_C\}$	vector of residual equations for solute transport [$\text{m}^2 \text{ d}^{-1} \text{ mol kg}^{-1}$]
$\{I_{bc}\}, \{I_i\}$	vector boundary and interior contributions, respectively
$[N]$	row vector of interpolation functions $\{N_i, N_j, N_k\}$
$[N]^T$	transpose of row vector $[N]$
$[G]^e$ and $[G]^{eT}$	element gradient vector and its transpose, and
$[K]^e$	element conductivity matrix

Documentation and Verification of VST2D: A Model for Simulating Transient, Variably Saturated, Coupled Water-Heat-Solute Transport in Heterogeneous, Anisotropic, 2-Dimensional, Ground-Water Systems with Variable Fluid Density

By M.J. Friedel

Abstract

This report describes a model for simulating transient, Variably Saturated, coupled water-heat-solute Transport in heterogeneous, anisotropic, 2-Dimensional, ground-water systems with variable fluid density (VST2D). VST2D was developed to help understand the effects of natural and anthropogenic factors on quantity and quality of variably saturated ground-water systems. The model solves simultaneously for one or more dependent variables (pressure, temperature, and concentration) at nodes in a horizontal or vertical mesh using a quasi-linearized general minimum residual method. This approach enhances computational speed beyond the speed of a sequential approach. Heterogeneous and anisotropic conditions are implemented locally using individual element property descriptions. This implementation allows local principal directions to differ among elements and from the global solution domain coordinates. Boundary conditions can include time-varying pressure head (or moisture content), heat, and/or concentration; fluxes distributed along domain boundaries and/or at internal node points; and/or convective moisture, heat, and solute fluxes along the domain boundaries; and/or unit hydraulic gradient along domain boundaries. Other model features include temperature and concentration dependent density (liquid and vapor) and viscosity, sorption and/or decay of a solute, and capability to determine moisture content beyond residual to zero. These features are described in the documentation together with development of the governing equations, application of the finite-element formulation (using the Galerkin approach), solution procedure, mass and energy balance considerations, input requirements, and output options.

The VST2D model was verified, and results included solutions for problems of water transport under isohaline and isothermal conditions, heat transport under isobaric and isohaline conditions, solute transport under isobaric and isothermal conditions, and coupled water-heat-solute transport. The first three problems considered in model verification were compared to either analytical or numerical solutions, whereas the coupled problem was compared to measured laboratory results for which no known analytic solutions or numerical models are available. The test results indicate the model is accurate and applicable for a wide range of conditions, including when water (liquid and vapor), heat (sensible and latent), and solute are coupled in ground-water systems. The cumulative residual errors for the coupled problem tested was less than 10^{-8} cubic centimeter per cubic centimeter, 10^{-5} moles per kilogram, and 10^2 calories per cubic meter for liquid water content, solute concentration and heat content, respectively. This model should be useful to hydrologists, engineers, and researchers interested in studying coupled processes associated with variably saturated transport in ground-water systems.

INTRODUCTION

Understanding the effects that natural and anthropogenic factors have on the quantity and quality of ground-water recharge and/or discharge in the United States is of practical interest to hydrologists, engineers, and policy makers for accurate water-resource assessment and to minimize the potential for contamination of drinking-water supplies. In many regions, ground-water recharge and/or discharge occur through an unsaturated (or vadose) zone subject to complex time-space variations in natural and anthropogenic factors. Examples of natural factors affecting ground-water recharge and/or discharge include subsurface properties (physical, chemical, and biological), topography, ambient conditions (water content, temperature, and chemical concentration), and climatic conditions (evaporation, temperature, and precipitation). Some anthropogenic factors affecting the ground-water system include application of fertilizers and pesticides, pumping of irrigation and domestic supply wells, and use of agricultural drainage systems. In response to these factors, the quantity and quality of ground-water recharge and/or discharge is directly related to the simultaneous coupling of gravitational, pressure, temperature and osmotic potentials. The coupled effect of these potentials is poorly understood and a major deficiency in current ground-water models.

In recent years, researchers and engineers have developed relevant theories and related numerical models to study certain coupled problems in saturated, unsaturated, and variably saturated (saturated and/or unsaturated) ground-water systems. A coupled problem is governed by a set of linear (saturated ground water) or nonlinear (variably saturated ground water) partial differential equations derived from mass conservation laws that describe water-solute transport, water-heat transport, or water-heat-solute transport. The actual number of governing mathematical equations is equal to the number of State variables, for example, pressure, temperature, and/or solute concentration. Examples of saturated water-solute transport models are numerous, with reviews provided by the National Research Council (1990) and Segol (1994). Saturated water-solute transport models will not be discussed further because this report focuses on variably saturated transport. Examples of coupled unsaturated or variably saturated water-solute transport models include those developed by Voss, 1984; Healy, 1990; Yeh and others, 1993; and Simunke and others, 1994.

The first mathematical theory that explained coupled water-heat transport in unsaturated porous media was developed by Philip and de Vries (1957). In that theory, equations were developed that described movement of liquid and vapor as a consequence of gradients in temperature and water content. By introducing the pressure head as a dependent variable instead of water content, Milly (1982) generalized the Philip and de Vries' equations to heterogeneous soils. Several numerical models were developed on the basis of this theory and used to simulate unsaturated water-heat transport in the laboratory and field (Schieldge, 1982; Milly, 1984; Passerat de Silans and others, 1989; Scanlon and Milly, 1994; Braud and others, 1995; Friedel and Nieber, 1995; Healy and Ronan, 1996). Voss (1984) developed a numerical model to account for density-dependent water flow in variably saturated ground-water systems with either thermal energy or solute transport. Laboratory observations of solute redistribution subject to moisture, temperature, and osmotic gradients (Nassar and Horton, 1989a) motivated development of a generalized set of coupled governing equations for water-heat-solute transport in unsaturated porous media (Nassar and Horton, 1992). These equations were incorporated into a one-dimensional, steady-state, numerical model for verification of these laboratory observations (Nassar and Horton, 1992). Later, Scanlon and Milly (1994) used a transient one-dimensional unsaturated transport model to study the response of water (liquid and vapor) and heat flux to atmospheric forcing in the Chihuahuan Desert of Texas. Recently, Noborio and others (1996) developed a transient unsaturated water (liquid, no vapor)-heat-solute transport model to study the redistribution of mass and energy in a homogeneous and isotropic furrow-irrigated Midwest soil. Currently, the coupled subsurface transport of mass and energy under variably saturated, heterogeneous, and anisotropic conditions with variable fluid density is poorly understood and a major deficiency in existing numerical models.

The purpose of this report is to document, describe, and verify a numerical model for simulating transient, Variably Saturated, coupled water-heat-solute Transport in heterogeneous, anisotropic, 2-Dimensional (VST2D), ground-water systems with variable fluid density. To more effectively study natural and anthropogenic factors on coupled variably saturated subsurface transport phenomena, mathematical equations were developed to describe the simultaneous and coupled movement of mass (water and solute) and energy (heat). The ability to describe

coupled transport phenomena in variably saturated ground-water systems is achieved through spatial discretization of pressure head, temperature, and chemical concentration for each equation. Next, these equations are transformed into a set of nonlinear algebraic equations using the Galerkin finite-element formulation to transform space derivatives, and the finite-difference method to discretize time. Various model properties, boundary conditions, and a nonlinear solution method are implemented to arrive at a numerical solution for which various problems are evaluated. Finally, a section on verification of the VST2D model is included for problems of water transport under isohaline and isothermal conditions, heat transport under isobaric and isohaline conditions, solute transport under isobaric and isothermal conditions, and coupled water-heat-solute transport.

THEORETICAL BACKGROUND

Governing Equations

In the subsurface, temperature gradients affect the water potential and induce liquid and vapor movement in ground-water systems. Reciprocally, water potential gradients cause water movement that transports heat and solutes. The simultaneous occurrence of temperature, pressure head, and chemical concentration gradients in geologic materials cause the transport of heat, water, and solute. The development of equations for coupling of water, heat, and solute transport under field conditions is described in the following sections.

Water Transport

In deriving an equation for water transport, the law of mass conservation is applied. The law of mass conservation (or continuity principle) states that the difference between the mass flux in and out is equal to the rate change of mass stored in a control volume of the aquifer (fig. 1). Considering only the liquid mass flux, the total mass inflow rate perpendicular to the y-z plane is

$$\rho_L q'_{Lx} \Delta y \Delta z, \quad (1)$$

where

q'_{Lx} is the liquid water flux (specific discharge) in the x-direction [m d^{-1}];

ρ_L is the density of liquid water [kg m^{-3}];

Δx , Δy , and Δz are the respective control volume lengths in the x-, y- and z-directions;

$\Delta y \Delta z$ is the area of elemental face perpendicular to the flux direction; and

L is a subscript indicating the liquid water phase.

Using a Taylor series expansion, the first-order approximation for outflow rate of fluid mass through the right face perpendicular to the y-z plane is given by

$$\left[\rho_L q'_{Lx} + \frac{\partial}{\partial x} (\rho_L q'_{Lx}) \Delta x \right] \Delta y \Delta z. \quad (2)$$

The net mass liquid water flux in the x-direction is then the difference between equations 1 and 2, expressed as

$$-\frac{\partial}{\partial x} (\rho_L q'_{Lx}) \Delta x \Delta y \Delta z. \quad (3)$$

EXPLANATION

LIQUID WATER FLUX (SPECIFIC DISCHARGE)

CHANGE IN LIQUID WATER FLUX
ALONG CARTESIAN AXES

LENGTH OF CONTROL VOLUME SIDES
ALONG CARTESIAN AXES

CARTESIAN AXES

$$q_L, \frac{\partial q_{Lz}}{\partial z}, \frac{\partial q_{Lx}}{\partial x}$$

$$\Delta x, \Delta y, \Delta z$$

X, Y, Z

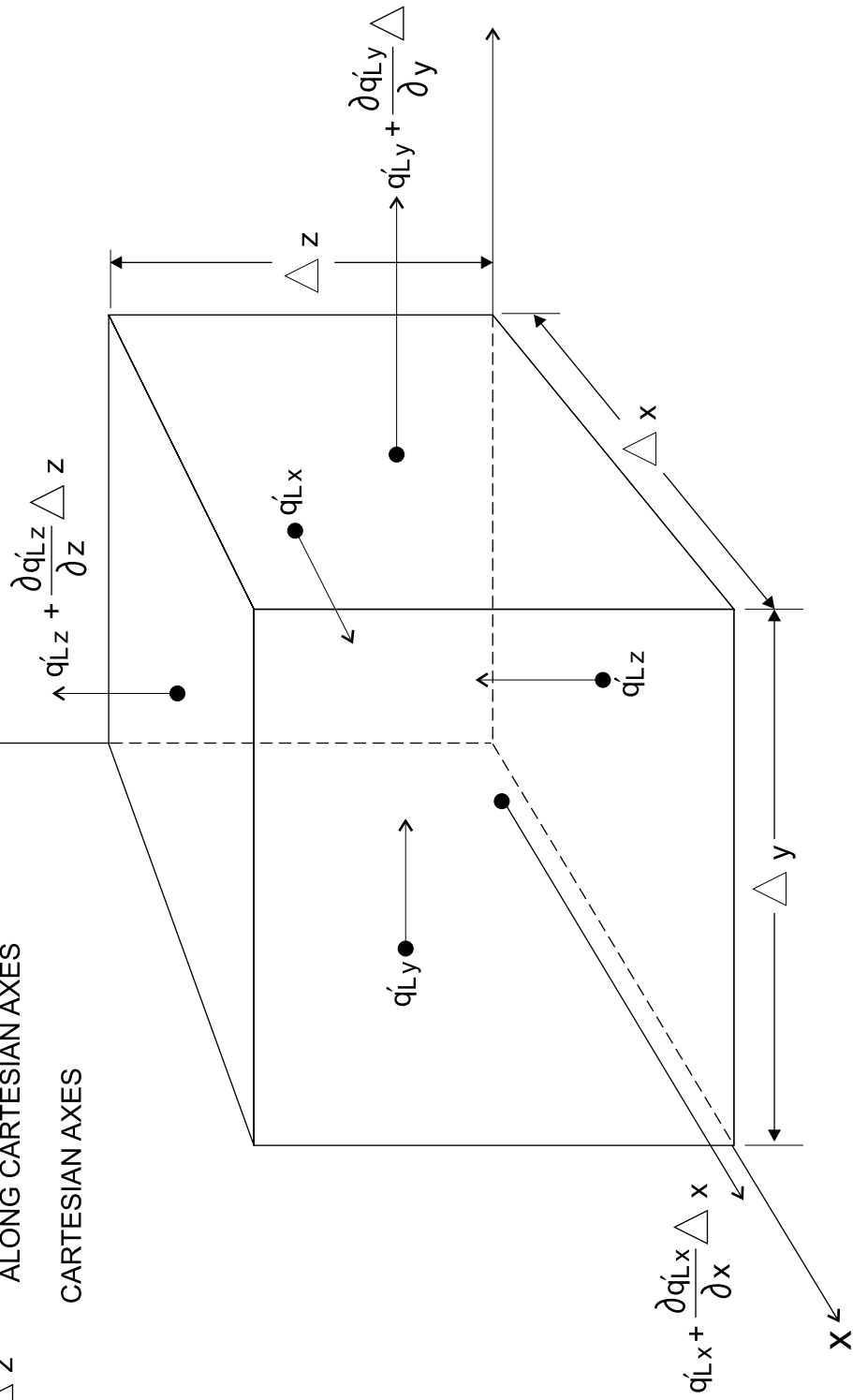


Figure 1. Representative control volume.

Similarly, the net fluxes along the y- and z-directions are calculated and combined to represent the net flux associated with the control volume. Summing these three net fluxes and allowing for a point and distributed source and/or sink in the control volume results in

$$-\nabla(\rho_L q'_L)\Delta V + Q_{Lp}\rho_L\Delta V + Q_{Ld}\rho_L\Delta V, \quad (4)$$

where

$\nabla = \{\partial/\partial x, \partial/\partial y, \partial/\partial z\}^T$ or $\partial/\partial x i + \partial/\partial y j + \partial/\partial z k$, is the gradient operator [m^{-1}],
 $\{ \}^T$ is the transpose of vector $\{ \}$,
 $\Delta V = \Delta x \Delta y \Delta z$ is the control volume,
 q'_L is a vector of discharge values, and
 Q_{Lp}, Q_{Ld} are the respective point and distributed source and/or sink for liquid water [m d^{-1}].

The rate change of liquid water mass, or storage, in the control volume can be described by

$$\frac{\partial}{\partial t}(\rho_L \theta_S S \Delta V). \quad (5)$$

where

θ_S is the saturated moisture content (or porosity) [$\text{cm}^3 \text{cm}^{-3}$],
 t is time [d], and
 S is the saturation $0 \leq S \leq 1$).

By equating the net liquid water flux in equation 4 and storage term in equation 5 and dividing through by the control volume, the mass balance expression becomes

$$\frac{\partial}{\partial t}(\rho_L \theta_S S) = -\nabla(\rho_L q'_L) + Q_{Lp}\rho_L + Q_{Ld}\rho_L. \quad (6)$$

Taking the ΔV out of the time derivative assumes the dimensions of the control volume do not change with time.

Using the chain rule, the storage term given on the left-hand-side of equation 6 can be expanded to

$$\frac{\partial}{\partial t}(\rho_L \theta_S S) = \theta_S S \frac{\partial \rho_L}{\partial t} + \rho_L S \frac{\partial \theta_S}{\partial t} + \theta_S \rho_L \frac{\partial S}{\partial t}. \quad (7)$$

The first term relates to the fluid compressibility, the second term relates to the compressibility of the porous matrix, and the third term relates to the change in fluid saturation. Because the fluid density is a function of pressure head, using the chain rule and accounting for fluid compressibility gives

$$\frac{\partial \rho_L}{\partial t} = \frac{\partial \rho_L}{\partial \psi} \frac{\partial \psi}{\partial t} = \varpi \rho_L g \rho_L \frac{\partial \psi}{\partial t}, \quad (8)$$

where

ψ is the water pressure head, [m],
 g is the gravitational acceleration [m s^{-2}],
 $\varpi = \rho_L^{-1} d\rho_L/dP$ is the fluid compressibility [$4.40 \times 10^{-10} \text{m}^2 \text{N}^{-1}$],
 $P = P_0 + \rho_L g \psi$ is pressure at a point in the aquifer [N m^{-2}],
 P_0 is the atmospheric pressure [N m^{-2}], and
 $dP = \rho_L g d\psi$.

By convention, water pressure head is positive in the saturated zone and negative in the unsaturated zone. Writing the saturation as a function of pressure head and using the chain rule, the fluid saturation term in equation 8 results in

$$\theta_s \frac{\partial S}{\partial t} = \theta_s \frac{\partial S}{\partial \psi} \frac{\partial \psi}{\partial t} = \frac{\partial \theta}{\partial \psi} \frac{\partial \psi}{\partial t} = C_\psi \frac{\partial \psi}{\partial t}, \quad (9)$$

where

$C_\psi = \partial \theta_L / \partial \psi$ is the moisture capacity [m^{-1}].

At saturation ($S = 1$ and $\theta_L = \theta_s$), the moisture capacity and this term becomes equal to zero. Therefore, this term is effective only under unsaturated conditions ($S < 1$). The porous medium compressibility (inverse of modulus of elasticity) can be described, assuming vertical strain is much greater than the horizontal strain, by

$$\frac{\partial \theta_s}{\partial t} = \frac{\partial V_z}{\partial z} = \frac{\partial \epsilon_z}{\partial t} = -\Omega \frac{\partial \sigma_e}{\partial t} = \Omega \frac{\partial p_L}{\partial t} = \Omega \rho_L g \frac{\partial \psi}{\partial t}, \quad (10)$$

where

V_z is the velocity of solid particles in the vertical direction [m s^{-1}],
 ϵ_z is the strain in vertical direction [$\text{m}^{-1}/\text{m}^{-1}$],
 $\sigma_e = \sigma_T - p_w$ is the effective stress [N m^{-2}],
 σ_T is the total stress [N m^{-2}],
 $p_w = \psi \rho_L g$ is the water pressure [N m^{-2}],
 Ω is the porous medium coefficient of vertical compressibility [$\text{m}^2 \text{N}^{-1}$],
 g is the gravitational acceleration [m s^{-2}], and
 $\rho_L g$ is the specific unit weight of water [N m^{-3}].

Substituting the results for fluid compressibility (equation 8), fluid saturation (equation 9), and porous medium compressibility (equation 10) into the equation of mass conservation (equation 6), and dividing through by the liquid density gives

$$\rho_L \Lambda' \frac{\partial \psi}{\partial t} + \rho_L C_\psi \frac{\partial \psi}{\partial t} = -\nabla(\rho_L q'_L) + \rho_L Q_{Lp} + \rho_L Q_{Lpd}, \quad (11)$$

where

$\Lambda' = \theta_s S \omega \rho_L g + S \Omega \rho_L g$, is a storativity-type term [m^{-1}]. This term is important only where changes in porous media and fluid compressibility exceed changes in saturation, for example, in the pumping of confined saturated ground-water systems.

Using variable substitution for the capacitance term and generalizing mass conservation for water to include liquid and vapor, this expression becomes

$$\rho_L \Lambda \frac{\partial \theta_L}{\partial t} + \rho_L \frac{\partial \theta_V}{\partial t} = -\nabla(\rho_L q'_L) + \rho_L Q_{Lp} + Q_{Ld} + \rho_L Q_{Vp} + \rho_L Q_{Vd} \quad (12)$$

where

$\Lambda = \Lambda' C_\psi^{-1} + 1$ is a dimensionless storativity-type term,
 $\theta_w = \theta_L + \theta_V$ is the total water content,
 $\theta_L = \theta_s - \theta_A$ is the liquid water content,
 $\theta_V = \theta_A \rho_V \rho_L^{-1}$ is the water vapor content,
 $\rho_V = \rho_o h_r$ is the water vapor density [kg m^{-3}],

ρ_o is the saturated water vapor density [kg m^{-3}],
 h_r is the relative humidity,
 $\theta_A = \theta_S - \theta_w$ is the volumetric air content,
 $\dot{q}_w = \dot{q}_V + q_L$ is the total water flux [m d^{-1}],
 q_V is the water vapor flux [m d^{-1}], and

L, V are subscripts indicating water phases: liquid and vapor, respectively.

Using water content time derivative terms is advantageous because this form is mass conservative.

An equation for total water flux (vapor and liquid) that takes into account the coupling of matric, temperature, osmotic, and gravitational potentials can be written (Philip and DeVries, 1957; Nassar and Horton, 1989, Naborio and others, 1996) as

$$\dot{q}'_w = \frac{q_w}{\rho_L} = -D_\theta \nabla \theta_L - D_T \nabla T + D_C \nabla C - K \nabla E, \quad (13)$$

where

$q_w = q_V + q_L$ is the total mass water flux [$\text{kg m}^{-2} \text{d}^{-1}$];

q_V is the mass water vapor flux [$\text{kg m}^{-2} \text{d}^{-1}$];

q_L is the mass liquid water flux [$\text{kg m}^{-2} \text{d}^{-1}$];

$\theta, C,$ and T are subscripts indicating dependent variables:
 water content, solute concentration, and
 temperature, respectively;

$D_T = D_{TV} + D_{TL}$ is the thermal moisture diffusivity [$\text{m}^2 \text{d}^{-1} \text{ } ^\circ\text{C}^{-1}$];

$D_\theta = D_{\theta V} + D_{\theta L}$ is the isothermal moisture diffusivity [$\text{m}^2 \text{d}^{-1}$];

$D_C = D_{CV} + D_{CL}$ is the solute moisture diffusivity [$\text{m}^2 \text{d}^{-1} \text{ kg mol}^{-1}$];

$D_{TV} = DLa\beta\eta h_r \rho_L^{-1}$ is the thermal vapor diffusivity [$\text{m}^2 \text{d}^{-1} \text{ } ^\circ\text{C}^{-1}$];

$D_{TL} = K(\psi G_{\psi T} \gamma_T - \sigma_0 \partial O / \partial T)$ is the thermal liquid diffusivity [$\text{m}^2 \text{d}^{-1} \text{ } ^\circ\text{C}^{-1}$];

$D_{\theta V} = C_\psi^{-1} MD\varepsilon\theta_V \rho_o h_r g / \rho_L RT$ is the isothermal vapor diffusivity [$\text{m}^2 \text{d}^{-1}$];

$D_{\theta L} = K C_\psi^{-1}$ is the isothermal liquid diffusivity [$\text{m}^2 \text{d}^{-1}$];

$D_{CV} = D\varepsilon\theta_V \rho_o h_r g \rho_L^{-1} M\phi_V$ is the solute vapor diffusivity [$\text{m}^2 \text{d}^{-1} \text{ kg mol}^{-1}$];

$D_{CL} = K(\psi \gamma_C - \sigma_0 \partial O / \partial C)$ is the solute liquid water diffusivity
 [$\text{m}^2 \text{d}^{-1} \text{ kg mol}^{-1}$];

D is the molecular diffusivity of water vapor in air
 [$\text{m}^2 \text{d}^{-1}$];

$\theta_V = \theta_S - \theta_L$ is the air-filled porosity;

a is the mean ionic solution activity;

$b = \theta_L A_s^{-1} \rho_b^{-1} (\theta_L < \theta_r)$ or $b = \theta_r A_s^{-1} \rho_b^{-1} (\theta_L \geq \theta_r)$ is the one-half of the water film thickness [nm];

C is the solute concentration [mol kg^{-1}];

E is the elevation head [m];

f_c is the fractional clay content;

g is the gravitational acceleration constant
 [9.81 m s^{-2}];

$G_{\psi T}$ is a gain factor used to compensate for
 underestimation of temperature-induced
 changes when only surface tension is
 considered (Nimmo and Miller, 1986);

$h_r = h_m h_o$ is the relative humidity;

$h_m = \exp(g M \psi / RT)$ is the relative humidity because of a soil matric

potential;

$h_o = \exp(Mv\phi C)$ is the relative humidity because of an osmotic potential;

$K = \begin{bmatrix} K_{xx} & K_{xy} \\ K_{yx} & K_{yy} \end{bmatrix}$ is the hydraulic conductivity tensor (individual values are a function of moisture or pressure head, viscosity, temperature, and orientation) [m d⁻¹];

$K_{xx} = K_{x'}$
 $\cos^2 \delta + K_{y'} \sin^2 \delta,$
 $K_{xy} = K_{yx} = (K_{x'} - K_{y'}) \sin \delta \cos \delta,$
 $K_{yy} = K_{x'} \sin^2 \delta + K_{y'} \cos^2 \delta$ are the tensoral components of hydraulic conductivity that arise when principal directions of hydraulic conductivity in one or more elements do not coincide with the global domain coordinate axes (Strack, 1989);

$K_{x'}$ and $K_{y'}$ are values of hydraulic conductivity along principal directions in an element;

δ is the angle between local and global principal coordinate directions (see figure 2);

K is degrees Kelvin;

M is the molecular weight of liquid water [0.018015 kg mol⁻¹];

r_s is the hydrated radius of the solute [m];

r_w is the radius of a water molecule [nm];

R is the universal gas constant [8.3143 J mol⁻¹ K⁻¹];

t is the time [d];

T is the temperature [°C];

T is the temperature [K];

x and y are Cartesian coordinates (horizontal or vertical);

$\beta = \partial \rho_0 / \partial T$ [kg m⁻³ °C⁻¹];

γ is the surface tension of water over air [mN m⁻¹];

$\gamma_C' = \gamma^{-1} \partial \gamma / \partial C$ is a concentration coefficient [kg mol⁻¹];

$\gamma_T' = \gamma^{-1} \partial \gamma / \partial T$ is a temperature coefficient [°C⁻¹];

$\varepsilon = (\theta_S - \theta_L)^{2/3}$ is a factor accounting for tortuosity;

η is a factor used to adjust the underestimation of microscopic temperature gradients (greater than 1);

θ_L is the liquid water (moisture) content;

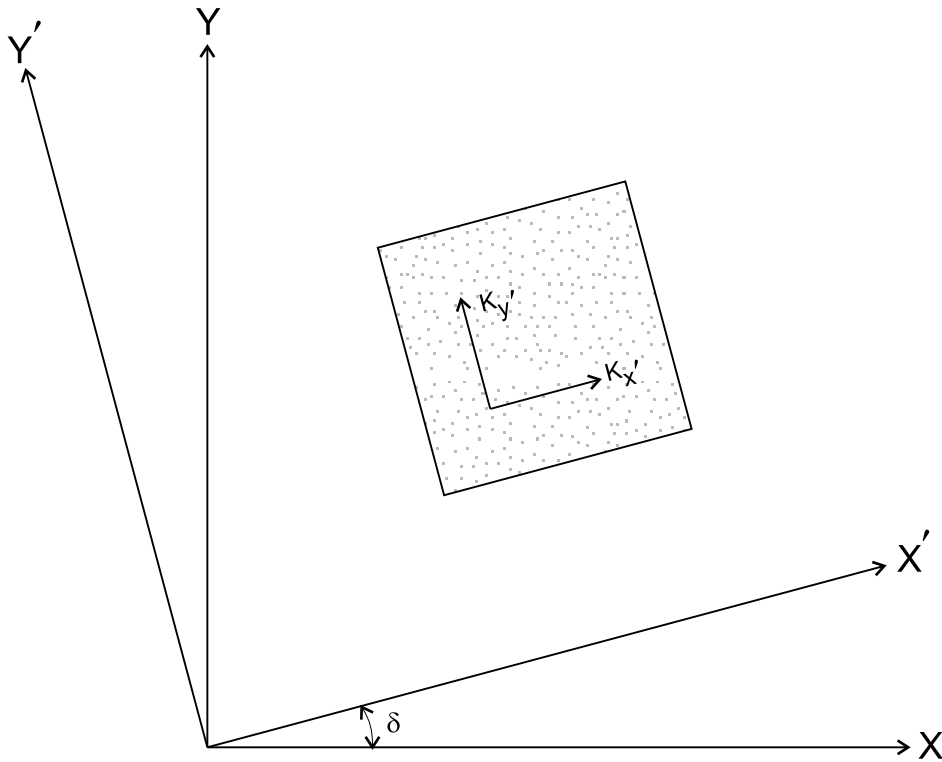
v is the number of ions per molecule for an ionizing solute;

ρ_b is the bulk density [kg m⁻³];

$\sigma_0 = (r_s - r_w) / (b - r_w)$ is the osmotic efficiency coefficient;

ϕ is an osmotic coefficient (Robinson and Stokes, 1965);

$\partial \gamma / \partial C$ is the change in surface tension with concentration [0.001634 mN kg mol⁻¹];



EXPLANATION

X, Y PRINCIPAL AXES ASSOCIATED WITH SOLUTION DOMAIN

X', Y' PRINCIPAL AXES ASSOCIATED WITH ELEMENT

δ ANGLE BETWEEN PRINCIPAL ELEMENT AND SOLUTION DOMAIN AXES

K'_y, K'_x PRINCIPAL ELEMENT ORIENTATION OF HYDRAULIC CONDUCTIVITY AXES

 ELEMENT WITH ARBITRARY MATERIAL

Figure 2. Relation of local and global coordinates.

$\partial\gamma/\partial T$ is the change in surface tension with temperature
[$\text{mNm}^{-1}\text{C}^{-1}$];

$\partial O/\partial T = RM^{-1}g^{-1}\ln(a) = R\phi v C g^{-1}$ is the change in osmotic head with temperature
[$\text{m } ^\circ\text{C}^{-1}$];

$\partial O/\partial C = TC^{-1} \partial O/\partial T$ ($C > 0.001 \text{ mol kg}^{-1}$) and

$\partial O/\partial C = -4091$ ($C \leq 0.001 \text{ mol kg}^{-1}$) are the change in osmotic head with concentration
[m kg mol^{-1}]; and

a is the mean ionic solution activity [dimensionless].

After variable substitution ($\partial\theta_L=C_\psi \partial\psi$), the equation for water flux becomes

$$q'_w = \frac{q_w}{\rho_L} = -D_{\theta_V}C_\psi \nabla\psi - D_{\theta_L}C_\psi \nabla\psi - D_{TV} \nabla T - D_{TL} \nabla T + D_{CV} \nabla C + D_{CL} \nabla C - K \nabla E. \quad (14)$$

Following insertion of the water flux into the continuity equation, the governing equation for water transport can be written (neglecting vapor sources/sinks) as

$$\begin{aligned} \rho_L \Lambda \frac{\partial\theta_L}{\partial t} + \rho_L \frac{\partial\theta_V}{\partial t} = & \nabla(D_{\theta_V}\rho_L C_\psi \nabla\psi) + \nabla(D_{\theta_L}\rho_L C_\psi \nabla\psi) + \nabla(D_{TV}\rho_L \nabla T) \\ & + \nabla(D_{TL}\rho_L \nabla T) - \nabla(D_{CV}\rho_L \nabla C) - \nabla(D_{CL}\rho_L \nabla C) + \nabla(\rho_L K \nabla E) + \rho_L Q_{Lp} + \rho_L Q_{Ld}. \end{aligned} \quad (15)$$

Considering expansion in two-dimensions, recognizing that D_{θ_L} , D_{TL} , and D_{CL} are functions of hydraulic conductivity (a tensor), and applying the gradient in the continuity equation gives

$$\begin{aligned} \rho_L \Lambda \frac{\partial\theta_L}{\partial t} + \rho_L \frac{\partial\theta_V}{\partial t} = & \frac{\partial}{\partial x} \left[D_{\theta_V} \rho_L C_\psi \frac{\partial\psi}{\partial x} + \rho_L K_{xx} \frac{\partial\psi}{\partial x} + \rho_L K_{xy} \frac{\partial\psi}{\partial y} + \rho_L K_{xx} \frac{\partial E}{\partial x} + \rho_L K_{xy} \frac{\partial E}{\partial y} \right. \\ & + D_{TV} \rho_L \frac{\partial T}{\partial x} + D_{TLxx} \rho_L \frac{\partial T}{\partial x} + D_{TLxy} \rho_L \frac{\partial T}{\partial y} - D_{CV} \rho_L \frac{\partial C}{\partial x} - D_{CLxx} \rho_L \frac{\partial C}{\partial x} - D_{CLxy} \rho_L \frac{\partial C}{\partial y} \left. \right] + \frac{\partial}{\partial y} \left[D_{\theta_V} \rho_L C_\psi \frac{\partial\psi}{\partial y} \right. \\ & + \rho_L K_{yx} \frac{\partial\psi}{\partial x} + \rho_L K_{yy} \frac{\partial\psi}{\partial y} + \rho_L K_{yy} \frac{\partial E}{\partial y} + \rho_L K_{yx} \frac{\partial E}{\partial x} + D_{TV} \rho_L \frac{\partial T}{\partial y} + D_{TLyx} \rho_L \frac{\partial T}{\partial x} \\ & \left. + D_{TLyy} \rho_L \frac{\partial T}{\partial y} - D_{CV} \rho_L \frac{\partial C}{\partial y} - D_{CLyx} \rho_L \frac{\partial C}{\partial x} - D_{CLyy} \rho_L \frac{\partial C}{\partial y} \right] + \rho_L Q_{Lp} + \rho_L Q_{Ld}. \end{aligned} \quad (16)$$

In this model, the global x, y coordinates are aligned along the horizontal and vertical axes with y pointing upward. In this case, the change in elevation head along x and y directions becomes 0 and 1, respectively, $\frac{\partial E}{\partial x} = 0$, $\frac{\partial E}{\partial y} = 1$, and the governing equation for water flow simplifies to

$$\begin{aligned} \rho_L \Lambda \frac{\partial\theta_L}{\partial t} + \rho_L \frac{\partial\theta_V}{\partial t} = & \frac{\partial}{\partial x} \left(D_{\theta_V} \rho_L C_\psi \frac{\partial\psi}{\partial x} \right) + \frac{\partial}{\partial x} \left(\rho_L K_{xx} \frac{\partial\psi}{\partial x} \right) + \frac{\partial}{\partial x} \left(\rho_L K_{xy} \frac{\partial\psi}{\partial y} \right) + \frac{\partial(\rho_L K_{xy})}{\partial x} + \frac{\partial}{\partial x} \left(D_{TV} \rho_L \frac{\partial T}{\partial x} \right) \\ & + \frac{\partial}{\partial x} \left(D_{TLxx} \rho_L \frac{\partial T}{\partial x} \right) + \frac{\partial}{\partial x} \left(D_{TLxy} \rho_L \frac{\partial T}{\partial y} \right) - \frac{\partial}{\partial x} \left(D_{CV} \rho_L \frac{\partial C}{\partial x} \right) - \frac{\partial}{\partial x} \left(D_{CLxx} \rho_L \frac{\partial C}{\partial x} \right) \\ & - \frac{\partial}{\partial x} \left(D_{CLxy} \rho_L \frac{\partial C}{\partial y} \right) + \frac{\partial}{\partial y} \left(D_{\theta_V} \rho_L C_\psi \frac{\partial\psi}{\partial y} \right) + \frac{\partial}{\partial y} \left(\rho_L K_{yx} \frac{\partial\psi}{\partial x} \right) + \frac{\partial}{\partial y} \left(\rho_L K_{yy} \frac{\partial\psi}{\partial y} \right) + \frac{\partial(\rho_L K_{yy})}{\partial y} + \frac{\partial}{\partial y} \left(\rho_L D_{TV} \frac{\partial T}{\partial y} \right) \\ & + \frac{\partial}{\partial y} \left(\rho_L D_{TLyx} \frac{\partial T}{\partial x} \right) + \frac{\partial}{\partial y} \left(\rho_L D_{TLyy} \frac{\partial T}{\partial y} \right) - \frac{\partial}{\partial y} \left(\rho_L D_{CV} \frac{\partial C}{\partial y} \right) - \frac{\partial}{\partial y} \left(\rho_L D_{CLyx} \frac{\partial C}{\partial x} \right) - \frac{\partial}{\partial y} \left(\rho_L D_{CLyy} \frac{\partial C}{\partial y} \right) + \rho_L Q_{Lp} \\ & + \rho_L Q_{Ld} \end{aligned} \quad (17)$$

In deriving the general equation for water transport, diffusion is assumed to be characterized as an isotropic process. In some cases, however, small-scale layering may give rise to directional dependence much like a hydraulic conductivity field. In addition to the subsurface transport of water, changing external and/or subsurface

conditions through natural (atmospheric, biologic, or chemical) and/or man-induced (subsurface injection and/or storage of hazardous or radioactive waste, or thermal energy) activities may give rise to heat and solute transport.

Heat Transport

To arrive at a suitable expression for heat transport, the law of conservation of energy (first law of thermodynamics) is applied. The continuity expression for conservation of energy in a control volume follows the derivation presented for water with the general form given by

$$\frac{\partial H}{\partial t} = -\nabla q_H + Q_{Hp} + Q_{Hd}, \quad (18)$$

where

H is the total heat content per unit volume of soil or rock [cal m^{-3}],

q_H is the total heat flux density [$\text{cal d}^{-1} \text{m}^{-2}$], and

Q_{Hp} , Q_{Hd} , are the respective point and distributed source and/or sink for heat [$\text{cal m}^{-3} \text{d}^{-1}$].

From this expression, a constant amount of energy exists within the control volume that can be neither lost nor increased; energy can, however, change form.

An equation used to describe the heat content (de Vries, 1958) is given by

$$H = C_d(T - T_0) + L_0\rho_L\theta_V + c_p\rho_L\theta_V(T - T_0) + c_L\rho_L\theta_L(T - T_0) - \rho_L \int_0^{\theta_L} W' d\theta_L, \quad (19)$$

where

C_d is the volumetric heat capacity of dry soil or rock [$\text{cal m}^{-3} \text{°C}^{-1}$],

T_0 is a reference temperature [°C],

L_0 is the latent heat of vaporization at the reference temperature [$585 \times 10^3 \text{cal kg}^{-1}$ at 20°C],

$c_p = C_P \rho_L^{-1}$ is the specific heat of water vapor at constant pressure [$\text{cal kg}^{-1} \text{°C}^{-1}$],

$c_L = C_L \rho_L^{-1}$ is the specific heat of liquid water [$\text{cal kg}^{-1} \text{°C}^{-1}$],

C_P is the volumetric heat capacity of water vapor [$\text{cal m}^{-3} \text{°C}^{-1}$],

C_L is the volumetric heat capacity of liquid water [$\text{cal m}^{-3} \text{°C}^{-1}$], and

W' is the differential heat of wetting [cal m^{-3}].

A general expression for heat flux (de Vries, 1958) is given by

$$q_H = -\lambda^* \nabla T + L_0 q_V + [c_p(T - T_0)q_V + c_L(T - T_0)q_L], \quad (20)$$

where

λ^* is the thermal conductivity of variably saturated soil or rock [$\text{cal m}^{-1} \text{°C}^{-1} \text{d}^{-1}$].

The three terms on the right-hand-side of this equation represent transfer by heat conduction, latent heat (associated with water vapor movement), and sensible heat (associated with vapor and liquid movement), respectively.

Following insertion of heat flux into the continuity equation and allowing for various substitutions, sources/sinks, rearrangement, and collecting coefficients, the governing equation for heat transport (modified after Nassar and Horton, 1992) can be written as

$$\begin{aligned}
f_1 \frac{\partial T}{\partial t} + f_2 \frac{\partial \theta_L}{\partial t} + f_3 \frac{\partial C}{\partial t} &= \nabla[(\lambda^* + L\rho_L D_{TV})\nabla T] + L\rho_L \nabla(D_{\theta_V} \nabla \theta_L) - L\rho_L \nabla(D_{CV} \nabla C) \\
&+ c_p \rho_L (D_{\theta_V} \nabla \theta_L + D_{TV} \nabla T - D_{CV} \nabla C) \nabla T + c_L \rho_L (D_{\theta_L} \nabla \theta_L + D_{TL} \nabla T - D_{CL} \nabla C + K \nabla E) \nabla T \\
&+ Q_{Hp} + Q_{Hd},
\end{aligned} \tag{21}$$

where

$$\begin{aligned}
f_1 &= (C_V + L(\theta_S - \theta_L) h_r \beta) \text{ is a global heat capacitance type term} \\
&\quad [\text{cal m}^{-3} \text{ }^\circ\text{C}^{-1}], \\
f_2 &= L(\theta_S - \theta) \rho_0 h_r (Mg/RT) C_\psi - L \rho_0 h_r + \rho_L g (\psi - T \zeta) \text{ is a global latent heat type term} [\text{cal m}^{-3}], \\
f_3 &= [L(S - \theta_L) \rho_0 h_r Mv\phi] \text{ is a global latent heat type term} \\
&\quad [\text{cal m}^{-3} \text{ kg mol}^{-1}], \\
C_V &\text{ is the global heat capacity of the porous} \\
&\quad \text{media} [\text{cal m}^{-3} \text{ }^\circ\text{C}^{-1}], \\
\zeta &= \partial\psi/\partial T [\text{m }^\circ\text{C}^{-1}], \text{ and} \\
L &= L_0 - (c_L - c_p)(T - T_0) \text{ is the latent heat of vaporization} [\text{cal kg}^{-1}].
\end{aligned}$$

The right-hand-side of equation 21 requires further expansion so that it can be evaluated using the finite-element method. In doing so, the liquid and vapor temperatures are assumed to be in local equilibrium; that is, $T_L = T_V$. Following these modifications and allowing for variable substitution ($\partial\theta_L = C_\psi \partial\psi$), the equation becomes

$$\begin{aligned}
f_1 \frac{\partial T}{\partial t} + f_2 \frac{\partial \theta_L}{\partial t} + f_3 \frac{\partial C}{\partial t} \\
&= \nabla[(\sigma' + C_L T D_{\theta_L} C_\psi) \nabla \psi] + \nabla[(\sigma + C_L T D_{TL}) \nabla T] \\
&- \nabla[\sigma'' + C_L T D_{CL}] \nabla C + \nabla[C_L T K \nabla E] + Q_{Hp} + Q_{Hd},
\end{aligned} \tag{22}$$

where

$$\begin{aligned}
\sigma &= \lambda^* + L\rho_L D_{TV} + C_p T D_{TV} \text{ is an effective thermal conductivity term} [\text{cal m}^{-1} \text{ }^\circ\text{C}^{-1} \text{ d}^{-1}], \\
\sigma' &= L\rho_L D_{\theta_V} C_\psi + C_p T D_{\theta_V} C_\psi \text{ is an effective latent heat term associated with a pressure gradient} \\
&\quad [\text{cal m}^{-2} \text{ d}^{-1}], \\
\sigma'' &= L\rho_L D_{CV} + C_p T D_{CV} \text{ is an effective latent heat term associated with a concentration gradient} \\
&\quad [\text{cal m}^{-1} \text{ d}^{-1} \text{ kg mol}^{-1}].
\end{aligned}$$

Considering a two-dimensional ground-water system and recognizing that D_{TL} , $D_{\theta L}$, D_{CL} are functions of K (tensor), the conservation of energy equation is expanded and terms collected resulting in

$$\begin{aligned}
& f_1 \frac{\partial T}{\partial t} + f_2 \frac{\partial \theta_L}{\partial t} + f_3 \frac{\partial C}{\partial t} \\
&= \frac{\partial}{\partial x} \left[\sigma' \frac{\partial \Psi}{\partial x} + C_L T K_{xx} \frac{\partial \Psi}{\partial x} + C_L T K_{xy} \frac{\partial \Psi}{\partial y} + \sigma \frac{\partial T}{\partial x} + C_L T D_{TLxx} \frac{\partial T}{\partial x} + C_L T D_{TLxy} \frac{\partial T}{\partial y} - \sigma'' \frac{\partial C}{\partial x} \right. \\
&\quad \left. - C_L T D_{CLxx} \frac{\partial C}{\partial x} - C_L T D_{CLxy} \frac{\partial C}{\partial y} \right] \\
&+ \frac{\partial}{\partial y} \left[\sigma' \frac{\partial \Psi}{\partial y} + C_L T K_{yx} \frac{\partial \Psi}{\partial x} + C_L T K_{yy} \frac{\partial \Psi}{\partial y} + \sigma \frac{\partial T}{\partial y} + C_L T D_{TLyy} \frac{\partial T}{\partial y} + C_L T D_{TLyx} \frac{\partial T}{\partial x} - \sigma'' \frac{\partial C}{\partial y} \right. \\
&\quad \left. - C_L T D_{CLyx} \frac{\partial C}{\partial x} - C_L T D_{CLyy} \frac{\partial C}{\partial y} \right] \\
&+ C_L T \frac{\partial E}{\partial x} \frac{\partial K_{xx}}{\partial x} + C_L K_{xx} \frac{\partial E}{\partial x} \frac{\partial T}{\partial x} + C_L T \frac{\partial E}{\partial y} \frac{\partial K_{xy}}{\partial x} + C_L K_{xy} \frac{\partial E}{\partial y} \frac{\partial T}{\partial y} \\
&+ C_L T \frac{\partial E}{\partial x} \frac{\partial K_{yx}}{\partial x} + C_L K_{yx} \frac{\partial E}{\partial x} \frac{\partial T}{\partial x} + C_L T \frac{\partial E}{\partial y} \frac{\partial K_{yy}}{\partial y} + C_L K_{yy} \frac{\partial E}{\partial y} \frac{\partial T}{\partial y} + Q_{Lp} + Q_{Ld}.
\end{aligned} \tag{23}$$

Recalling that the global x,y coordinates are aligned along the x (horizontal) and y (vertical) axes, the governing equation for heat transport then becomes

$$\begin{aligned}
& f_1 \frac{\partial T}{\partial t} + f_2 \frac{\partial \theta_L}{\partial t} + f_3 \frac{\partial C}{\partial t} \\
&= \frac{\partial}{\partial x} \left(\sigma' \frac{\partial \Psi}{\partial x} \right) + \frac{\partial}{\partial x} \left(C_L T K_{xx} \frac{\partial \Psi}{\partial x} \right) + \frac{\partial}{\partial x} \left(C_L T K_{xy} \frac{\partial \Psi}{\partial y} \right) + \frac{\partial}{\partial x} \left(\sigma \frac{\partial T}{\partial x} \right) + \frac{\partial}{\partial x} \left(C_L T D_{TLxx} \frac{\partial T}{\partial x} \right) \\
&\quad + \frac{\partial}{\partial x} \left(C_L T D_{TLxy} \frac{\partial T}{\partial y} \right) - \frac{\partial}{\partial x} \left(\sigma'' \frac{\partial C}{\partial x} \right) - \frac{\partial}{\partial x} \left(C_L T D_{CLxx} \frac{\partial C}{\partial x} \right) - \frac{\partial}{\partial x} \left(C_L T D_{CLxy} \frac{\partial C}{\partial y} \right) \\
&\quad + \frac{\partial}{\partial y} \left(\sigma' \frac{\partial \Psi}{\partial y} \right) + \frac{\partial}{\partial y} \left(C_L T K_{yx} \frac{\partial \Psi}{\partial x} \right) + \frac{\partial}{\partial y} \left(C_L T K_{yy} \frac{\partial \Psi}{\partial y} \right) + \frac{\partial}{\partial y} \left(\sigma \frac{\partial T}{\partial y} \right) + \frac{\partial}{\partial y} \left(C_L T D_{TLyy} \frac{\partial T}{\partial y} \right) \\
&\quad + \frac{\partial}{\partial y} \left(C_L T D_{TLyx} \frac{\partial T}{\partial x} \right) - \frac{\partial}{\partial y} \left(\sigma'' \frac{\partial C}{\partial y} \right) - \frac{\partial}{\partial y} \left(C_L T D_{CLyx} \frac{\partial C}{\partial x} \right) - \frac{\partial}{\partial y} \left(C_L T D_{CLyy} \frac{\partial C}{\partial y} \right) \\
&\quad + C_L T \frac{\partial K_{xy}}{\partial x} + C_L K_{xy} \frac{\partial T}{\partial x} + C_L T \frac{\partial K_{yx}}{\partial y} + C_L K_{yx} \frac{\partial T}{\partial y} + Q_{Lp} + Q_{Ld}.
\end{aligned} \tag{24}$$

Whereas a chemical gradient is incorporated in the water (17) and heat transport (24) equations, the transport of a dissolved chemical compound cannot be described using only these equations. Therefore, to account for the simultaneous field migration of water, heat, and chemicals, a third equation governing solute transport is incorporated into the model.

Solute Transport

A general partial-differential equation that accounts for time and space dependent chemical concentrations with additional source/sink terms for sorption and solute decay is obtained by considering the principles of mass conservation (see ‘‘Water Transport’’). The resulting equation is given by

$$\frac{\partial(\rho_b C^*)}{\partial t} + \frac{\partial(C\theta_L)}{\partial t} = -\nabla \cdot \left(\frac{q_c}{\rho_L} \right) + \lambda(\theta_L C + \rho_b K_d C) + Q_{Cp} + Q_{Cd}, \tag{25}$$

where

ρ_b is the bulk density of the porous material [kg m^{-3}],
 $C^* = K_d C$ [mol kg^{-1}] is the amount of chemical sorbed to the soil-rock mass,
 K_d is the distribution coefficient (slope of C^* and C) [L kg^{-1}],
 C is the solute described as mass concentration [mol L^{-1}],
 q_c is the solute mass flux [$\text{mol m}^{-2} \text{d}^{-1} \text{kg m}^{-3}$],
 λ is the solute decay coefficient [d^{-1}],

Q_{Cp} and Q_{Cd} are the point and distributed source/sink solute flux [$\text{mol kg}^{-1} \text{m d}^{-1}$].

The transport of solute in a variably saturated ground-water system is governed by various mechanisms. The predominant mechanisms affecting chemical movement include molecular diffusion, advection, hydrodynamic dispersion, and salt sieving (Nassar and Horton, 1992). Salt sieving is the relative restriction of solute to solvent (numerically equivalent to the dimensionless osmotic efficiency coefficient (ϕ), according to Letey and Kemper, 1969). This coefficient is purported to be important when the water content drops below field capacity and/or if the matrix clay content is relatively high.

In contrast to water and heat transport, no latent heat contribution is associated with solute transport. In addition to the traditional spatial discretization of solute concentration, application of the gradient operator to liquid-water content and temperature also is considered and written (Nassar and Horton, 1992) as

$$q_C' = \frac{q_C}{\rho_L} = D_{C\theta} \nabla \theta_L - D_{TS} \varepsilon \theta_L \nabla T - (D_0 \varepsilon \theta_L + D_h) \nabla C + v \theta_L C, \quad (26)$$

where

q_C' is the total solute flux [$\text{mol m}^{-2} \text{d}^{-1}$],

$D_{C\theta} = \begin{bmatrix} D_{C\theta_{xx}} & D_{C\theta_{xy}} \\ D_{C\theta_{yx}} & D_{C\theta_{yy}} \end{bmatrix}$ is the diffusion tensor associated with salt sieving [$\text{m}^2 \text{mol kg}^{-1} \text{d}^{-1}$] with
 $D_{C\theta_{xx}} = K_{xx} \beta' C C_\psi^{-1}$, $D_{C\theta_{xy}} = K_{xy} \beta' C C_\psi^{-1}$, $D_{C\theta_{yx}} = K_{yx} \beta' C C_\psi^{-1}$,
 $D_{C\theta_{yy}} = K_{yy} \beta' C C_\psi^{-1}$, $D_{TS} = (v_1 + v_2) \gamma_1^0 \gamma_2^0 R C \ln(\mathbf{a}) [v_1 Z_1 (\gamma_1^0 + \gamma_2^0) F^2]^{-1}$
is the thermal solute diffusion coefficient associated with a temperature
gradient [$\text{m}^2 \text{mol}^{-1} \text{kg}^{-1} \text{ }^\circ\text{C}^{-1} \text{d}^{-1}$];

\mathbf{a} is the mean ionic solution activity [dimensionless],

$D_O = \begin{bmatrix} D_{O_{xx}} & D_{O_{xy}} \\ D_{O_{yx}} & D_{O_{yy}} \end{bmatrix}$ is the isothermal/isobaric solute diffusion tensor [$\text{m}^2 \text{d}^{-1}$],

$D_{O_{xx}} = D_{O_{xy}} = D_{O_{yx}} = D_{O_{yy}}$ are the isotropic diffusion coefficients associated with a concentration gradient [$\text{m}^2 \text{d}^{-1}$];

$D_h = \begin{bmatrix} D_{h_{xx}} & D_{h_{xy}} \\ D_{h_{yx}} & D_{h_{yy}} \end{bmatrix}$ is the hydrodynamic dispersion tensor [$\text{m}^2 \text{d}^{-1}$] with
 $D_{h_{xx}} = (\alpha_T V_y^2 + \alpha_L V_x^2) V_L^{-1}$ [$\text{m}^2 \text{d}^{-1}$],
 $D_{h_{yy}} = (\alpha_T V_x^2 + \alpha_L V_y^2) V_L^{-1}$ [$\text{m}^2 \text{d}^{-1}$], and
 $D_{h_{xy}} = (\alpha_L - \alpha_T) V_{Lx} V_{Ly} V_L^{-1}$ [$\text{m}^2 \text{d}^{-1}$];

F is Faraday's constant [$96,485 \text{ col mol}^{-1}$],

V is the average bulk velocity of solution [m d^{-1}],

$V_L = (V_{Lx}^2 + V_{Ly}^2)^{1/2}$ is the resultant velocity [m d^{-1}],

V_{Lx} , V_{Ly} are the average bulk velocities of solution in the x- and y- directions [m d^{-1}],

β' is the salt-sieving coefficient [dimensionless],

ε is the tortuosity,

v_1 , v_2 are the number of cations and anions associated with the solute, and

γ_1^0 , γ_2^0 are the limiting ionic conductivity of water.

Applying the gradient operator to the right-hand-side results in

$$\begin{aligned} & \frac{\partial(K_d \rho_b C)}{\partial t} + \frac{\partial(C \theta_L)}{\partial t} = \\ & \frac{\partial}{\partial x} \left[D_{CCxx} \frac{\partial C}{\partial x} + D_{CCxy} \frac{\partial C}{\partial y} - D_{C\psi xx} \frac{\partial \psi}{\partial x} - D_{C\psi xy} \frac{\partial \psi}{\partial y} + D_{CT} \frac{\partial T}{\partial x} - V_{Lx} \theta_L C \right] + \\ & \frac{\partial}{\partial y} \left[D_{CCyy} \frac{\partial C}{\partial y} + D_{CCyx} \frac{\partial C}{\partial x} - D_{C\psi yy} \frac{\partial \psi}{\partial y} - D_{C\psi yx} \frac{\partial \psi}{\partial x} + D_{CT} \frac{\partial T}{\partial y} - V_{Ly} \theta_L C \right] \\ & - \lambda(\theta_L C + \rho_b K_d C) + Q_{Cp} + Q_{Cd}, \end{aligned} \quad (27)$$

where

$$\begin{aligned} D_{C\psi} &= D_{C\theta} C_{\psi} \text{ is the diffusivity because of a pressure gradient [m d}^{-1}\text{mol kg}^{-1}\text{]}, \\ D_{CT} &= D_{TS} \varepsilon \theta_L \text{ is the diffusivity because of a temperature gradient} \\ & \text{[m}^2\text{ d}^{-1}\text{mol kg}^{-1} \text{ }^\circ\text{C}^{-1}\text{]}, \text{ and} \end{aligned}$$

$$D_{CCxx} = D_{0xx} \varepsilon \theta_L + D_{hxx},$$

$$D_{CCxy} = D_{0xy} \varepsilon \theta_L + D_{hxy} = D_{CCyx},$$

$$D_{CCyy} = D_{0yy} \varepsilon \theta_L + D_{hyy} \text{ are components of the hydrodynamic dispersion tensor [m}^2\text{ d}^{-1}\text{].}$$

After applying the chain rule to the time derivative and velocity terms, applying the gradient operator, and combining like terms, the governing two-dimensional equation for conservation of chemical mass becomes

$$\begin{aligned} C \frac{\partial \theta_L}{\partial t} + \mathbf{R} \frac{\partial C}{\partial t} &= \frac{\partial}{\partial x} \left(D_{CCxx} \frac{\partial C}{\partial x} \right) + \frac{\partial}{\partial y} \left(D_{CCyy} \frac{\partial C}{\partial y} \right) + \frac{\partial}{\partial x} \left(D_{CCxy} \frac{\partial C}{\partial y} \right) + \frac{\partial}{\partial y} \left(D_{CCyx} \frac{\partial C}{\partial x} \right) - \frac{\partial}{\partial x} \left(D_{C\psi xx} \frac{\partial \psi}{\partial x} \right) \\ & - \frac{\partial}{\partial y} \left(D_{C\psi yy} \frac{\partial \psi}{\partial y} \right) - \frac{\partial}{\partial x} \left(D_{C\psi xy} \frac{\partial \psi}{\partial y} \right) - \frac{\partial}{\partial y} \left(D_{C\psi yx} \frac{\partial \psi}{\partial x} \right) + \frac{\partial}{\partial x} \left(D_{CT} \frac{\partial T}{\partial x} \right) + \frac{\partial}{\partial y} \left(D_{CT} \frac{\partial T}{\partial y} \right) \\ & - q_{Lx} \frac{\partial C}{\partial x} - q_{Ly} \frac{\partial C}{\partial y} - V_{Lx} C C_{\psi} \frac{\partial \psi}{\partial x} - V_{Ly} C C_{\psi} \frac{\partial \psi}{\partial y} - \theta_L C \frac{\partial V_{Lx}}{\partial x} - \theta_L C \frac{\partial V_{Ly}}{\partial y} - \lambda C \mathbf{R} + Q_{Cp} + Q_{Cd}, \end{aligned} \quad (28)$$

where

$$\mathbf{R} = \theta_L + K_d \rho_b \text{ is a dimensionless retardation factor,}$$

$$q_{Lx} = V_{Lx} \theta_L \text{ is the specific discharge along the x-direction [m d}^{-1}\text{], and}$$

$$q_{Ly} = V_{Ly} \theta_L \text{ is the specific discharge along the y-direction [m d}^{-1}\text{].}$$

This formulation assumes no time-dependent changes are associated with the distribution coefficient and bulk density. Also, the use of a lumped retardation factor (\mathbf{R}), herein, differs from the more conventional expression given by

$$R = \left(1 + \frac{K_d \rho_b}{\theta_L} \right). \quad (29)$$

In this model, the explicit coupling of governing equations through pressure head precludes simplification resulting from division through with the liquid water content.

Properties and Parametric Relations

The three previously derived governing partial differential equations (equations 17, 24, and 28) provide a mathematical means for describing the simultaneous interaction of pressure head, temperature and solute concentration. Because each equation involves pressure head, temperature, and solute concentration dependent diffusivities, describing their functional relation to field properties and related parameters is important. In the

following sections, the various parametric relations used to describe the hydraulic, thermal, water, and solute properties associated with soil and/or rock are presented.

Hydraulic

The pressure head and effective saturation relation, known as moisture retention, can be described using various analytic expressions. Using an analytic expression is advantageous because the expression completely describes a functional relation between two or more hydraulic properties. In the present model, the continuity of effective saturation and pressure head is modeled using a three-parameter power relation (van Genuchten, 1980) given by

$$S_e = \left(\frac{1}{1 + \alpha |\psi|^n} \right)^m, \quad \psi < 0, \quad (30)$$

where

α [m^{-1}], m , and n are empirically derived constants, and $S_e = (\theta_L - \theta_r) (\theta_s - \theta_r)^{-1}$ is the effective saturation.

The inverse of α is the effective pressure head required to overcome the air entry requirement for draining soil or rock.

On the basis of equation 30, retention parameters typically are determined by fitting this equation to either laboratory wetting or drainage measurements. One example of a soil moisture retention function fitted to drainage is for Ida silt loam ($\alpha = 0.5857 \text{ m}^{-1}$, $m = 0.3532$, $n=1.546$) shown in figure 3. Other important hydraulic properties are the relative conductivity (K_r) and moisture capacity, C_ψ (slope of the retention curve). Both parameters are functions of saturation (or equivalent pressure head) and, therefore, can be written in closed-form using the empirical moisture retention parameters (van Genuchten, 1980) as

$$K_r = S_e^{0.5} \left(1 - \left(1 - S_e^{1/m} \right)^m \right)^2, \quad m = 1 - \frac{1}{n}, \quad (31)$$

$$C_\psi = \alpha \theta_s (n-1) \left(1 - \frac{\theta_r}{\theta_s} \right) S_e^{1/m} \left(1 - S_e^{1/m} \right)^m. \quad (32)$$

In addition to the relative hydraulic conductivity dependence on saturation (or pressure head), the dependence on temperature and solute concentration are considered through changes in density and kinematic viscosity in the relation for saturated hydraulic conductivity given by

$$K_{sx'} = \frac{k_x' \rho_L g}{\mu}, \quad (33)$$

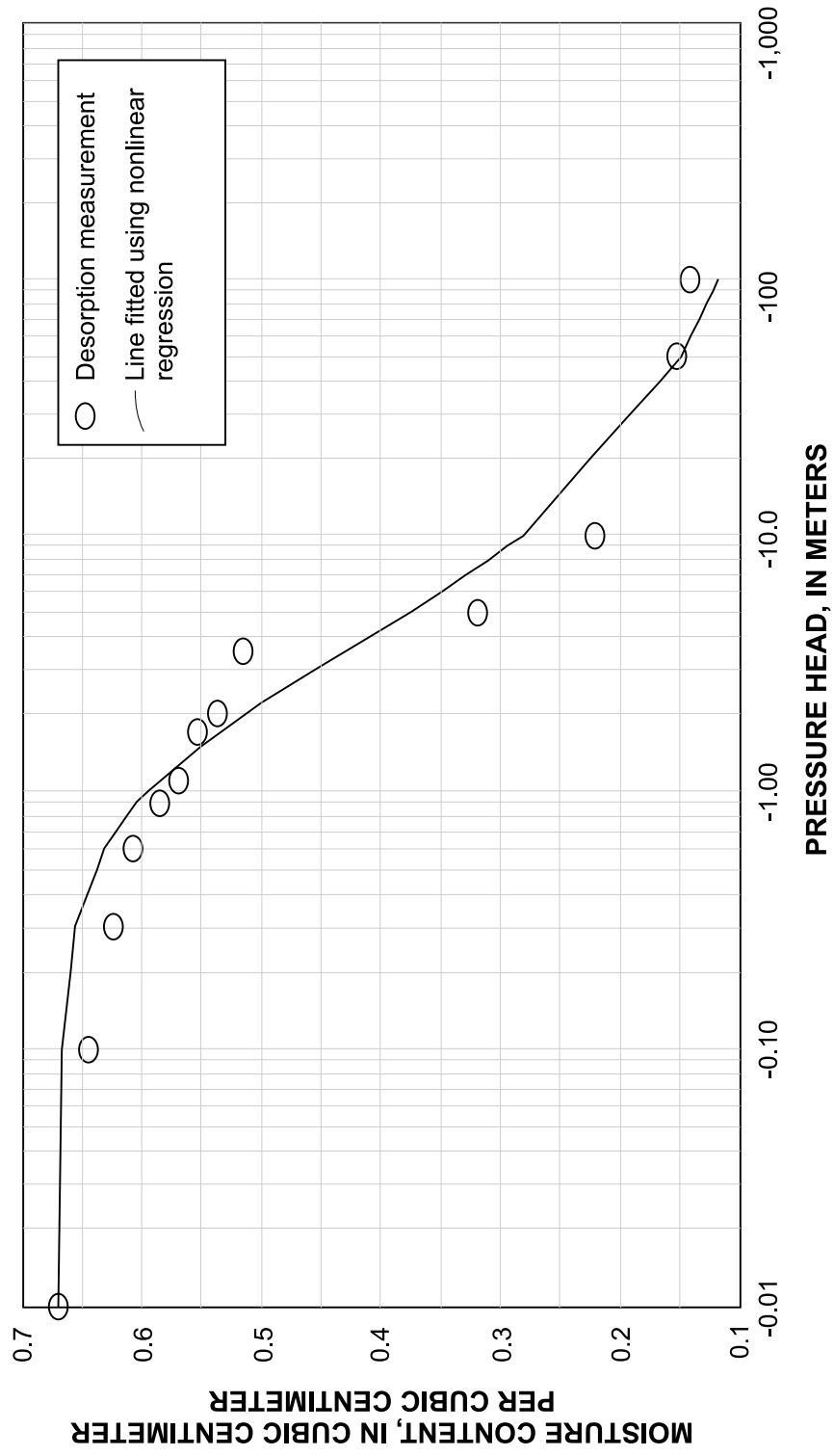


Figure 3. Moisture retention function fitted to desorption measurements for Ida silt loam.

$$K_{sy'} = \frac{k_{y'} \rho_L g}{\mu}, \quad (34)$$

where

$K_{sx'}$, $K_{sy'}$, $k_{x'}$, $k_{y'}$ are the respective value pairs of saturated hydraulic conductivity [m d^{-1}] and intrinsic permeability [m^2] along principal directions, and μ is the fluid kinematic viscosity [N s m^{-2}].

This formulation recognizes the strong dependence on density and viscosity on temperature and weak dependence of density and viscosity on solute concentration (fig. 4). By contrast, the permeability is an intrinsic function of the porous medium and not the fluid. Because the permeability is usually unknown, its magnitude is calculated after rearranging equations 33 and 34 to

$$k_{x'} = \frac{\mu_0 K_{s0x'}}{\rho_{L0} g}, \quad (35)$$

$$k_{y'} = \frac{\mu_0 K_{s0y'}}{\rho_{L0} g}, \quad (36)$$

where

$K_{s0x'}$ and $K_{s0y'}$ are saturated hydraulic conductivity along principal directions at a reference temperature and concentration,

μ_0 is the fluid kinematic viscosity [N s m^{-2}] at a reference temperature and concentration, and ρ_0 is fluid density at a reference temperature and concentration.

The local principal values of hydraulic conductivity then are calculated using

$$K_{x'} = K_{sx'} K_r, \quad (37)$$

$$K_{y'} = K_{sy'} K_r, \quad (38)$$

Using these values, the tensoral components of hydraulic conductivity with respect to the global coordinates then are calculated on the basis of

$$K_{xx} = K_{x'} \cos^2 \delta + K_{y'} \sin^2 \delta \quad (39)$$

$$K_{yy} = K_{x'} \sin^2 \delta + K_{y'} \cos^2 \delta \quad (40)$$

$$K_{xy} = (K_{x'} - K_{y'}) \sin \delta \cos \delta = K_{yx} \quad (41)$$

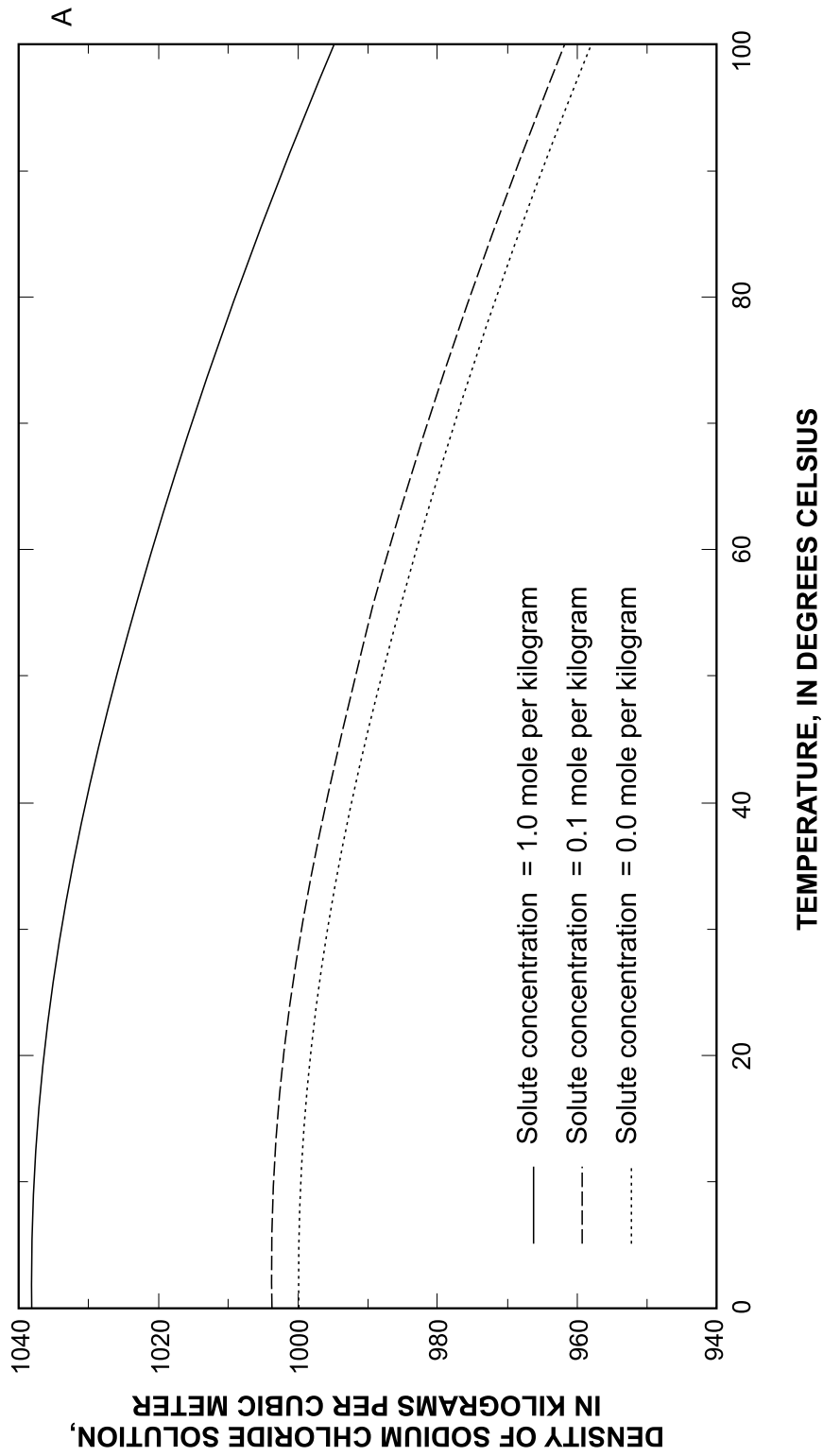


Figure 4. Temperature dependent water properties: (A) liquid density, (B) saturated vapor density, (C) surface tension, and (D) viscosity.

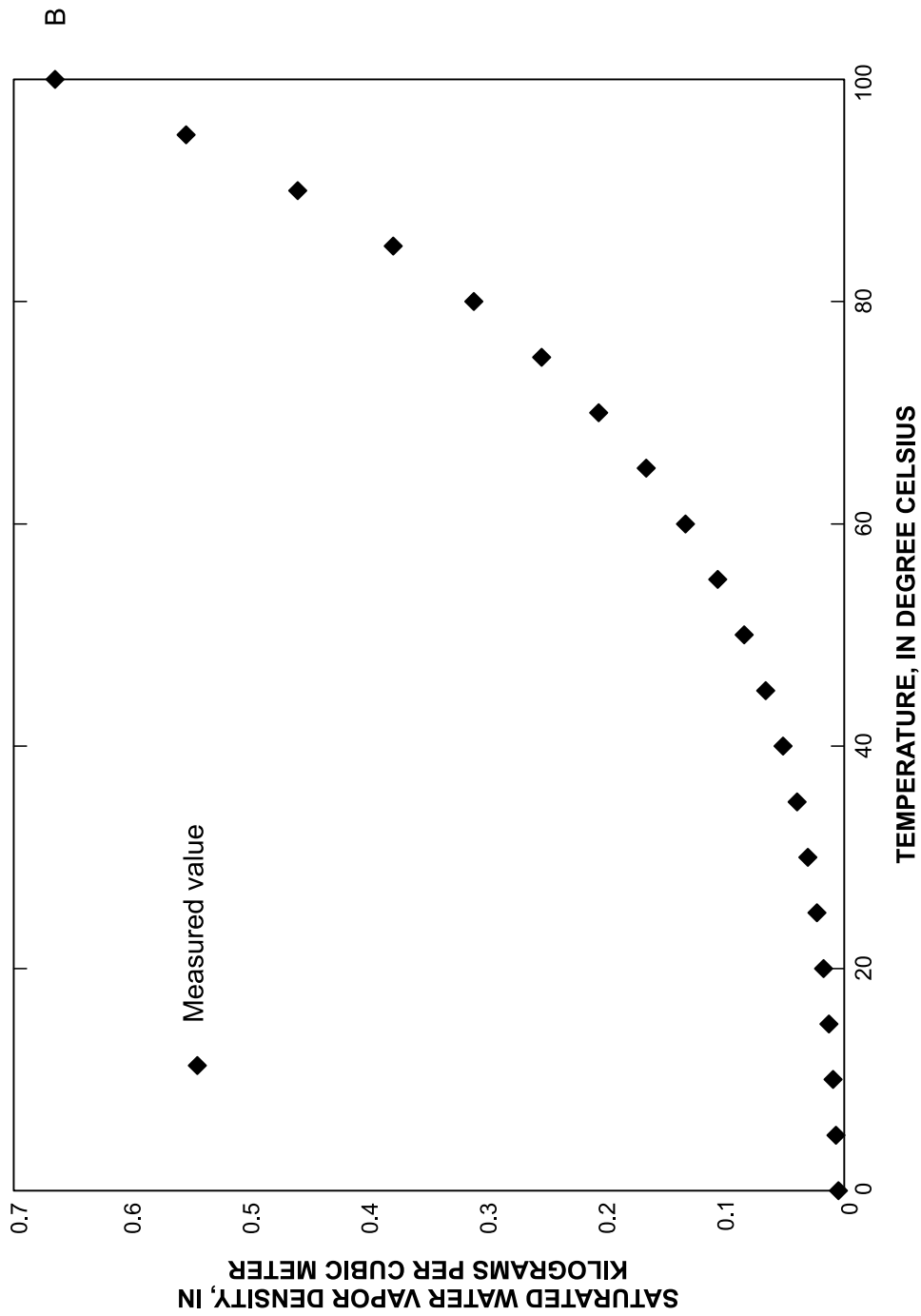


Figure 4. Temperature dependent water properties: (A) liquid density, (B) saturated vapor density, (C) surface tension, (D) viscosity—Continued.

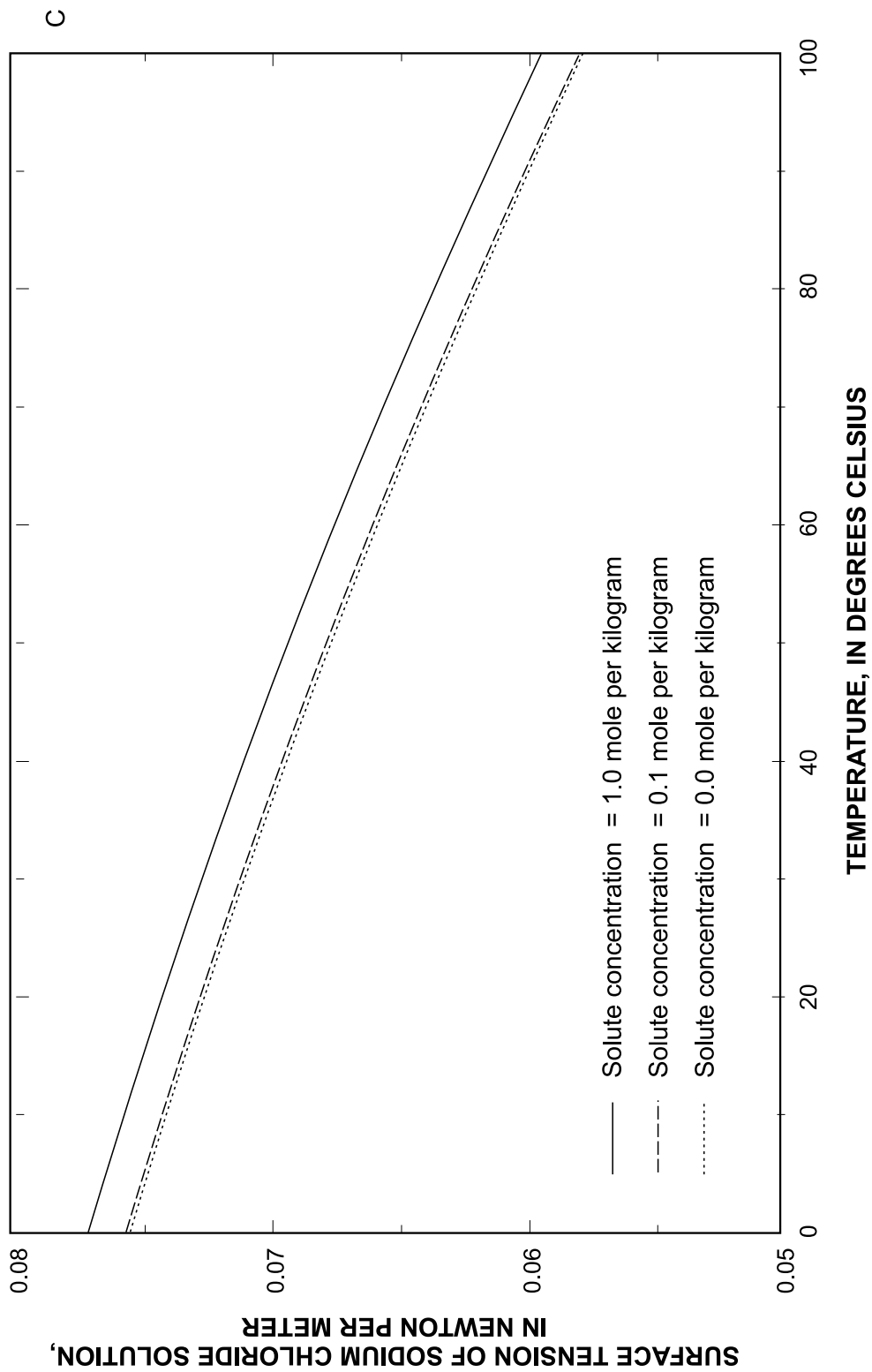


Figure 4. Temperature dependent water properties: (A) liquid density, (B) saturated vapor density, (C) surface tension, (D) viscosity—Continued.

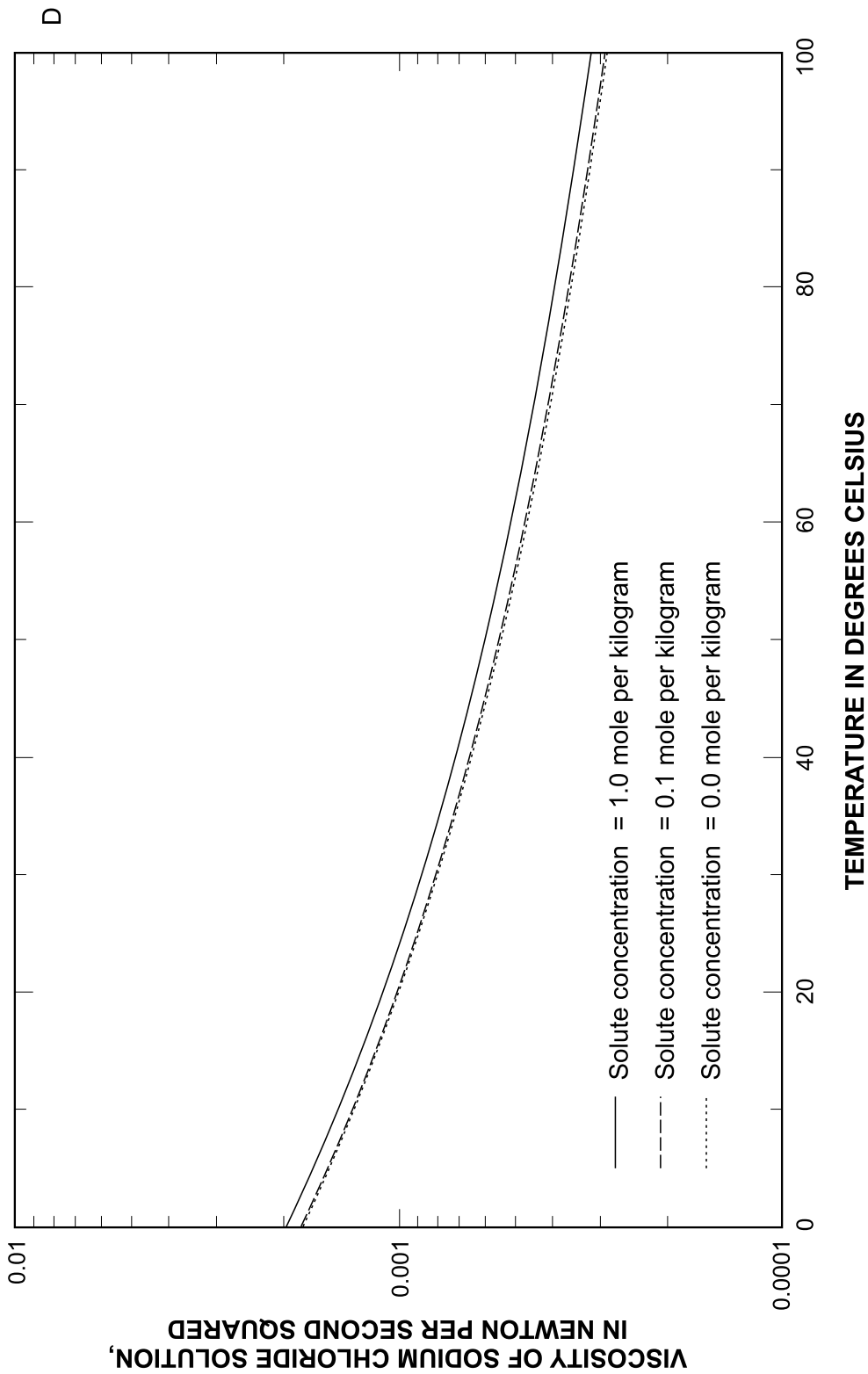


Figure 4. Temperature dependent water properties: (A) liquid density, (B) saturated vapor density, (C) surface tension, (D) viscosity—Continued.

where

δ is the angle between principal direction of hydraulic conductivity and global coordinate direction [degrees].

Using these equations 39-41, assuming homogeneous and isotropic (oriented along global coordinate axes, $\delta = 0$, and $K_{xx} = K_x$, $K_{yy} = K_y$, $K_{xy} = K_{yx} = 0$) properties, a uniform reference temperature (isothermal) of 20 °C and solute concentration (isohaline) of 0.0001 mol/kg, the Ida silt loam relative liquid conductivity and moisture capacity were computed and are shown in figure 5. Both functions are highly nonlinear with the moisture capacity and relative conductivity spanning 6 and 14 orders-of-magnitude, respectively.

One shortcoming in the previously described retention function (30) is that moisture content cannot be determined below the residual moisture content ($\theta(\psi) < \theta_r$). To overcome this limitation, the corresponding critical pressure head (ψ^*) is computed assuming an effective saturation (S_e^*) value of 0.001. When the pressure head drops below this critical value, the following linear expression is then used for calculating moisture content as

$$\theta_L = \theta_r - C_{\psi}^* \psi, \quad (42)$$

where the critical pressure ψ^* and critical moisture capacitance C_{ψ}^* are computed by

$$|\psi^*| = \alpha^{-1} \left(S_e^{*-1/m} \right)^{1/m}, \quad (43)$$

$$C_{\psi}^* = \alpha \theta_s (n-1) \left(1 - \frac{\theta_r}{\theta_s} \right) S_e^{*} e^{1/m} \left(1 - S_e^{*1/m} \right)^m. \quad (44)$$

Equation 42 describes the relation of moisture content between residual and zero ($\theta_L > 0$ when $\psi = -\frac{\theta_r}{C_{\psi}^*}$). Similar to hydraulic properties, thermal properties also are represented by various parametric forms. These thermal properties and parametric forms are discussed in the following section.

Thermal

The heat capacity (C_V) per unit volume of soil or rock is written as a linear combination of individual component capacities and volume fractions (DeVries, 1963) by

$$C_V = C_M X_M + C_o X_o + C_L X_L + C_a X_a, \quad (45)$$

where

C_M , C_o , C_L and C_a are the respective volumetric heat capacities of minerals, organic matter, liquid water, and air (known to be variable), 0.6, 1.0, 0.0003 cal m³ °C⁻¹;
 X_M , X_o , X_L and X_a are the respective dimensionless volume fractions of minerals, organic matter, liquid, and vapor.

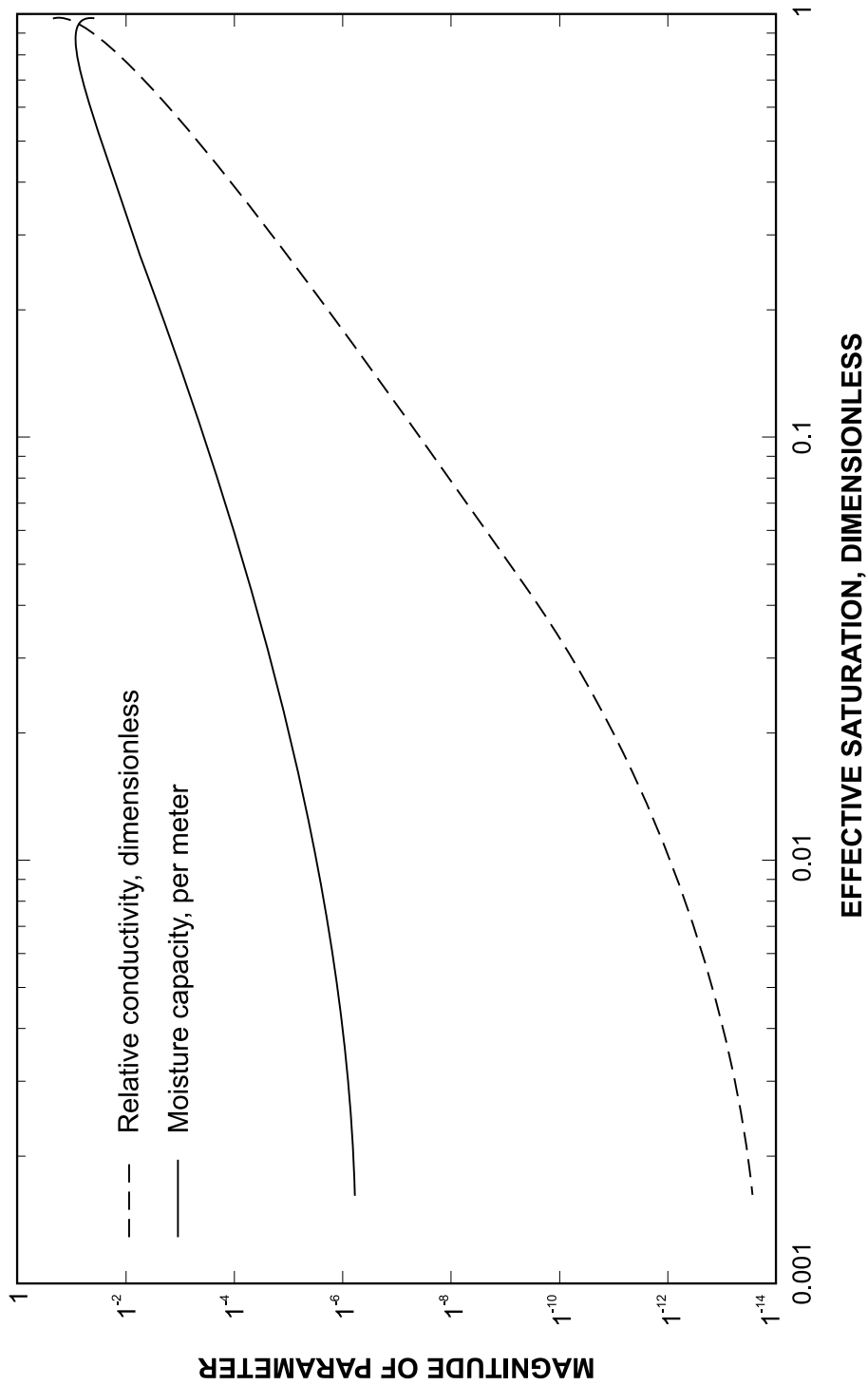


Figure 5. Relative conductivity and moisture capacity as a function of effective saturation for Ida silt loam.

The calculation of bulk thermal conductivity is performed using a weighted average of the thermal conductivities and associated volume fractions of soil or rock constituents in the subsurface. The method described by DeVries (1963) is used here and given by

$$\lambda = \frac{\sum_{i=1}^N \Pi_i X_i \lambda_i}{\sum_{i=1}^N \Pi_i X_i}, \quad (46)$$

where

- X_i is the dimensionless volume fraction of parameter i ;
- λ_i is the thermal conductivity of constituent i [$\text{cal m}^{-1} \text{ }^\circ\text{C}^{-1} \text{ d}^{-1}$],
- λ_{cly} , λ_{org} , and λ_{slt} are the thermal conductivities of clay, organic matter, and silt known to be 7, 0.6, and 10 [$\text{cal m}^{-1} \text{ }^\circ\text{C}^{-1} \text{ d}^{-1}$],
- λ_a , λ_q , and λ_{NaCl} are the thermal conductivities of air, quartz, sodium chloride solution defined by empirical relations given in table 1 [$\text{cal m}^{-1} \text{ }^\circ\text{C}^{-1} \text{ d}^{-1}$],
- N is the number of soil/rock constituents, and
- Π_i is the ratio of average temperature gradient in the i th constituent to the average temperature gradient of the bulk medium.

The values of Π_i are calculated using

$$\Pi_i = \frac{1}{3} \sum_{j=1}^3 \left(1 + \left[\frac{\lambda_j}{\lambda_0} - 1 \right] g_j \right)^{-1}, \quad (47)$$

where

- g_j is the j th particle shape factor with $g_1 + g_2 + g_3 = 1$ [dimensionless], and
 - λ_0 is the thermal conductivity of a continuous medium; for example, air, water or sand [$\text{cal m}^{-1} \text{ }^\circ\text{C}^{-1} \text{ d}^{-1}$].
- The thermal conductivities for air, water and sand are temperature dependent. The corresponding relations used to describe these thermal conductivities are included in table 1.

The air-shape factor, as given by Kimball and others (1976), is

$$g_{air} = 0.013 + \left[\frac{0.022}{\theta_L(\psi = -162m)} + \frac{0.298}{\theta_S} \right] \theta_L \quad \psi \leq -162 \text{ m}, \quad (48)$$

$$g_{air} = 0.035 + \left(\frac{0.298}{\theta_S} \right) \theta_L \quad \psi > -162 \text{ m}. \quad (49)$$

On the basis of these equations, the shape factor is assumed valid only to the approximate wilting point ($\psi = -162 \text{ m}$). The wilting point is that point at which plants cannot exert enough energy to remove water. At moisture contents below the wilting point, a liquid-phase discontinuity develops and linear interpolation is used to extend the calculation of shape factors to the hygroscopic point ($\psi = -316 \text{ m}$). Below the hygroscopic point, water is virtually bound and immobile.

Table 1. Summary of empirical relations for selected water and thermal properties used in the VST2D model

[kg m⁻³, kilogram per cubic meter; NaCl, sodium chloride; m² d⁻¹, meter squared per day; mol kg⁻¹, mole per kilogram; *T* is temperature in degree Celsius; and *T* are the absolute temperature in Kelvins]

Property	Parametric Equations	Reference
Activity of NaCl, a , [mol kg ⁻¹]	1. $C < 0.001$ mol kg ⁻¹ 1-3.1327×10 ⁻² C - 1.4553×10 ⁻³ C^2 $0.001 < C < 15$ mol kg ⁻¹ 0.202653 $C > 15$ mol kg ⁻¹	Robinson and Stokes, 1965
Density of pure water, ρ_w , [kg m ⁻³]	{1 - (T - 3.9863) ² (T + 288.9414) / [508929.2(T + 68.12963)]} × 10 ³	Harned and Owen, 1958
Density of NaCl solution, ρ_{NaCl} , [kg m ⁻³]	ρ_w (1 + 3.956×10 ⁻² C - 1.154×10 ⁻³ C^2) × 10 ³ [exp (31.3716 - 6014.79 T ⁻¹ - 7.92495×10 ⁻³ T)] T ⁻¹	Jessup, 1927
Density of saturated vapor, ρ_0 , [kg m ⁻³]	10 ⁻³ exp(19.84 - 4975.9 T ⁻¹)	Kimball and others, 1976
Diffusion coefficient of NaCl in water, D_0 , [m ² s ⁻¹]	7.26×10 ⁻⁶ + 2.63×10 ⁻¹¹ T + 2.18×10 ⁻¹² T^2	Lobo and Quaresma, 1989
Diffusion coefficient of water vapor in air D , [m ² d ⁻¹]	229 × 10 ⁻⁷ (T / 273.5) ^{1.75}	Kimball and others, 1976
Factor accounting for change in saturated vapor density with respect to temperature, $\beta = d\rho_0/dT$	4975.9 $\rho_0 T$ ⁻²	Derived by author
Factor accounting for micro-macro temperature gradients, η	9.5 + 6 θ_L - 8.5 exp{-(1 + 2.6 X_{cly} ^{-1/2}) θ_L } ⁴	Cass and others, 1984
Factor multiplying global latent heat term, ξ	$\psi(0)$ 0.003394×10 ^{0.001477 T}	Derived by author
Factor accounting for change in surface tention with temperature, dy/dC	-1.3595e-4 - 8.16e7 T	Derived by author
Osmotic coefficient, ϕ	0.9265 < or = 1 mol kg ⁻¹ 0.06455 C + 0.08648 > 1 mol kg ⁻¹	Derived by author
Surface tension of NaCl solution, γ_{NaCl} [N m ⁻¹]	7.5617×10 ⁻² - 1.3595×10 ⁻⁴ T - 4.0815×10 ⁻⁷ T^2 + 1.6342×10 ⁻³ C	Young and Harkins, 1928
Temperature coefficient, γ'_{NaCl} , [°C ⁻¹]	γ'_{NaCl} (-1.3595×10 ⁻⁴ - 8.164×10 ⁻⁷ T)	Derived by author
Thermal conductivity λ_a of air, [cal m ⁻¹ °C ⁻¹ d ⁻¹]	0.0237 + 6.41×10 ⁻⁵ T	Kimball and others, 1976
Thermal conductivity of quartz, λ_q , [cal m ⁻¹ °C ⁻¹ d ⁻¹]	-0.06621 T + 21.7804	de Vries, 1958
Thermal conductivity of NaCl solution, λ_{NaCl} , [cal m ⁻¹ °C ⁻¹ d ⁻¹]	0.599 (1-7.694×10 ⁻³ C) (0.94185 + 3.227×10 ⁻³ T - 1.533×10 ⁻⁵ T^2)	Jamieson and others, 1975
Viscosity of NaCl, μ , [N s m ⁻¹]	10 ^[-1.469+200.93/(T+116.71)] ×10 ⁻³ (1.0+9.359×10 ⁻²)	Chemical Society of Japan, 1975

To compute the global latent heat term f_2 (appearing in governing heat equation 24) requires functional knowledge of pressure head derivative with respect to temperature; that is, $\zeta = \partial\psi/\partial T$ [$\text{m } ^\circ\text{C}^{-1}$]. To arrive at a suitable means for computing ζ , first the pressure head is computed using

$$\psi = \alpha^{-1} \left(\frac{1}{S_e^{1/m}} - 1 \right). \quad (50)$$

Next, the temperature dependence is introduced using a temperature coefficient $\gamma' = [^\circ\text{C}^{-1}]$ given by

$$\gamma' = \gamma^{-1} \frac{\partial\gamma}{\partial T}. \quad (51)$$

Applying separation of variables the equation becomes

$$\int_{\gamma_0}^{\gamma} \gamma^{-1} d\gamma = \int_{T_0}^T \gamma' dT, \quad (52)$$

with the integration resulting in

$$\ln\gamma - \ln\gamma_0 = \gamma' \Delta T. \quad (53)$$

Assuming that the α parameter is proportional to surface tension, the equation can be written as

$$\frac{\alpha}{\alpha_0} = \frac{\gamma}{\gamma_0} = \exp(\gamma' \Delta T), \quad (54)$$

where

α_0 , and γ_0 represent reference values for the van Genuchten (1980) parameter and surface tension at reference temperature (T_0) and $\Delta T = T - T_0$.

Rearranging this equation provides a temperature dependent α parameter given by

$$\alpha(T) = \alpha_0 \exp(\gamma' \Delta T). \quad (55)$$

Applying equation 55 together with laboratory derived parameters for Ida loam soil (Nassar and Horton, 1989) and assuming effective saturation values of $S_e = 0.01$ ($\theta_L=0.056$), 0.1 ($\theta_L=0.112$), and 0.5 ($\theta_L=0.50$), the effect of temperature on pressure head is shown in figure 6. Taking the logarithm of the absolute value of pressure head, linear regression yields

$$\text{Log}(\psi) = m'T + \text{Log}[\psi(0)], \quad (56)$$

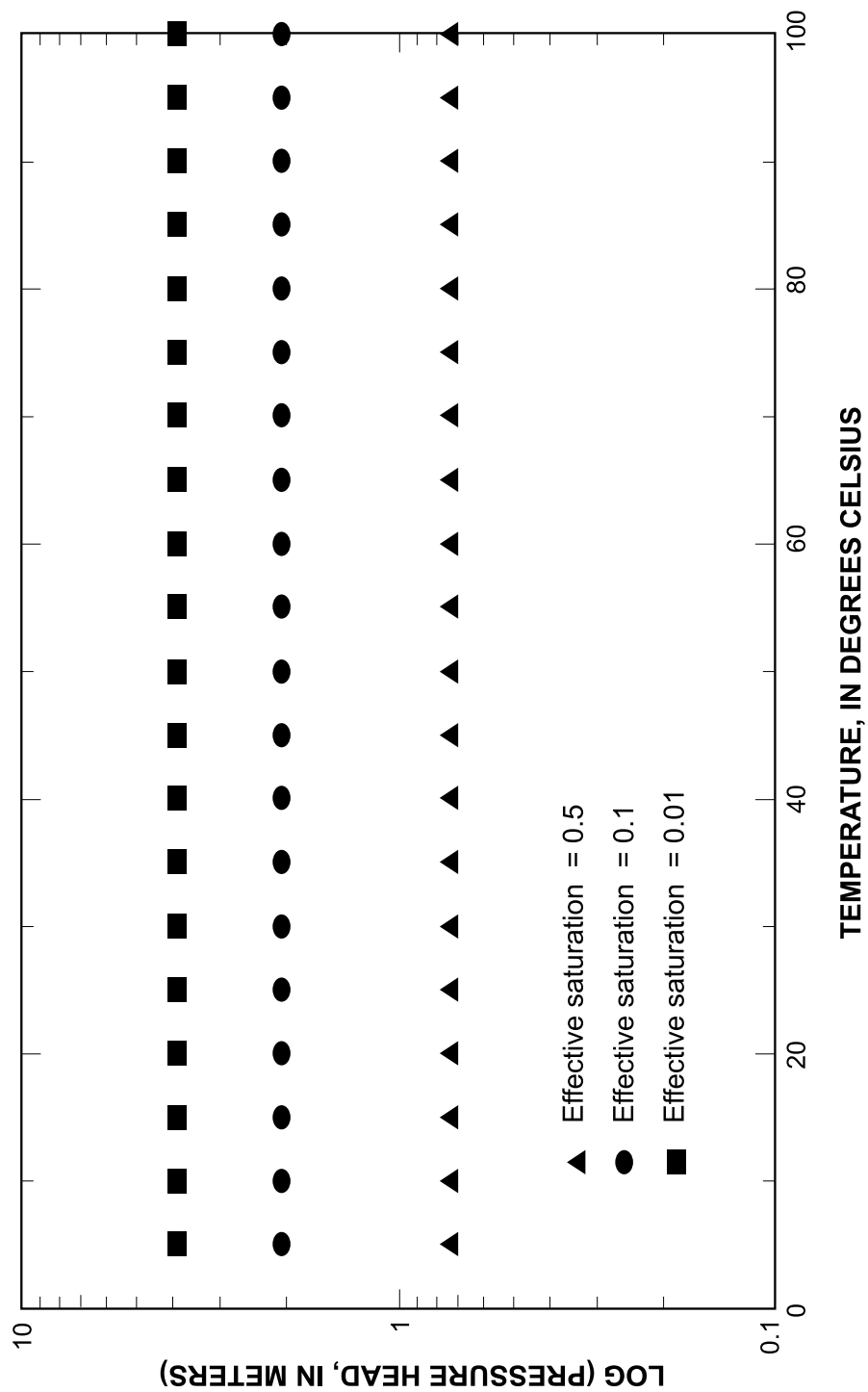


Figure 6. Effect of temperature on pressure head for Ida silt loam.

where $m' = 0.000147$ and $\text{Log}[\psi(0)]$ are the slope and intercept, respectively. Taking the inverse logarithm of equation 56 gives

$$\psi = \psi(0)10^{m'T}. \quad (57)$$

The change in pressure head with respect to temperature then is determined using the differentiation formula:

$$\frac{da^u}{dT} = a^u \frac{du}{dT} \ln a. \quad (58)$$

Letting $a= 10$, $u= m'T$, and applying to equation (57) results in

$$\zeta = \frac{d\psi}{dT} = \ln(10)m\psi(0)10^{m'T}. \quad (59)$$

Substitution of m' and converting the natural logarithm results in

$$\zeta = 2.3m'\psi(0)10^{m'T}. \quad (60)$$

Because dependent variables change during the Picard procedure (see “Picard Iteration”), this relation is used to compute ζ on a node-by-node basis for each iteration. Whereas m' is user defined (could assume that m' is similar to Ida silt loam, but this similarity has not been verified), $\psi(0)$ must be calculated using the current nodal value of S_e , setting $T = 0$, and equations 50 and 55.

Water

Certain properties of pore water also are temperature dependent. Examples of such temperature dependent model parameters include liquid and saturated water vapor densities (needed to compute the thermal vapor diffusivity, D_{TV} , and the global capacitance type term, f_1 , appearing in the governing heat equation), diffusion coefficients (water vapor in air and sodium chloride in water), surface tension, and viscosity. In some cases, certain properties of water also are dependent on the solute concentration. For example, the temperature-concentration dependent density, surface tension, and viscosity of a sodium chloride solution are shown in figure 4. A first-order nonlinear dependence on temperature is indicated but only a second-order dependence on concentration. In the present model, a flag in the input file allows the user to select either a temperature or temperature-concentration dependence in these parameters. A summary of all temperature and temperature-concentration dependent properties (liquid, vapor and solid) used in this model is provided in table 1.

Chemical

A chemical may be naturally and/or artificially removed from ground water through processes of sorption and/or decay. Sorption processes include adsorption, chemisorption, absorption, and ion exchange. In the VST2D model, no attempt is made to separate these processes, rather the sorption parameter is used to indicate the net result of these processes. From a practical view point, the important aspect is to quantify the removal of a chemical from the solution, irrespective of the process. In VST2D, a linear relation is assumed between the amount of a solute sorbed to a solid C^* and concentration of the solute C described by $C^* = K_d C$ [mol kg⁻¹].

If an aquifer constitutes at least 1 percent organic carbon (on a weight basis), partitioning of a solute will occur almost exclusively onto this fraction (Karickhoff and others, 1979). Under these circumstances, a partition coefficient with respect to the organic fraction, K_{OC} , can be defined as

$$K_{OC} = \frac{K_d}{X_O}. \quad (61)$$

In simulating the transport of an organic compound, it is important to note that the K_{OC} parameter may be estimated using an empirical relation to the octanol-water partition coefficient K_{OW} (Karickhoff, 1984). The use of this relation assumes that (1) sorption is primarily on the organic carbon, (2) sorption is hydrophobic (as compared with polar interactions, ionic bonding, or chemisorption), and (3) a linear relation exists between sorbed concentration and concentration of solute. Other processes that may remove chemicals from solution include radioactive and/or biological decay. In VST2D, either process is simulated by incorporating

$$\lambda(\theta_L C + \rho_b K_d C) \quad (62)$$

into the governing equation for solute transport.

Assumptions

The following list gives a summary of key assumptions invoked during the development of this theoretical mathematical model. The order does not indicate relative importance in model development and/or application. GENERAL for all

- Equations for water, heat, and solute are coupled in time and space.
- Anisotropy and heterogeneity are permitted throughout the solution domain.

WATER

- Critical value of effective saturation is 0.001.
- Drainage and wetting follow the same path (no hysteresis).
- Flow field is laminar (Darcy's Law is valid).
- Fluid density and viscosity can be described as temperature dependent using regression equations.
- Hydraulic conductivity varies with moisture content, density, and viscosity.
- Liquid water content is a linear function of pressure head between wilting and hygroscopic points.
- Mass conservation is maintained using a Taylor series expansion of the liquid water derivative.
- Moisture capacity is adequately described using a closed-form analytic expression.
- Moisture retention properties are adequately described using a three-parameter analytical function.
- Relative hydraulic conductivity is adequately described using a closed-form analytic expression.
- Soil matrix and water are assumed to be slightly compressible (no pressure dependent deformation).
- Taylor series expansion of change in vapor content with pressure head is approximately the conjugate of liquid water.
- Water transport is adequately characterized as a two-phase water system: liquid and vapor.
- Vapor transport is an isotropic and diffusive process.

HEAT:

- Density, surface tension, and viscosity can be described as temperature and concentration dependent using regression equations.
- Energy formulation is used assuming temperatures at or below 100 °C.
- Heat capacity is a linear combination of individual matrix and pore constituents.
- Particle shape factor is linear at moisture contents below the wilting point.

- Taylor series expansion of change in heat content with temperature is approximately linear.
- Temperature of each water phase is in local equilibrium ($T_L = T_V = T$).
- Thermal conductivities of clay, organic carbon, and silt are 7, 0.6, and 10.0 [mcal cm⁻¹ °C⁻¹ s⁻¹], respectively.
- Thermal conductivity of water is temperature and concentration dependent.
- Thermal conductivity of sand is adequately described as quartz.
- Thermal conductivity of the air and sand fraction is temperature dependent.
- Volumetric heat capacities of air and organic carbon are 0.0003, 0.6 [cal cm⁻³ °C⁻¹], respectively.
- Volumetric heat capacity of liquid water is temperature dependent.

SOLUTE

- Decay of chemicals is a first order process.
- Density, surface tension, and viscosity can be described as concentration and temperature dependent using regression equations.
- Formulation assumes that solute concentrations are at or below 15 mol kg⁻¹.
- Osmotic coefficient is constant at a concentration less than 1 mol kg⁻¹.
- Solute can be conservative or nonconservative (if decay is allowed).
- Sorption of a compound (organic or inorganic) is linear and reversible.
- Taylor series expansion of change in mass with concentration is approximately linear.

NUMERICAL METHODS

The principle limitation of analytical solutions is that they can be obtained only by imposing restrictive assumptions about aquifer properties, boundary conditions, and/or initial conditions. By contrast, numerical methods do not require such restrictive assumptions. Some examples of numerical methods include the finite-difference, variational and weighted residual approaches. Several variations of the weighted residual method differ only in the application of weighting functions. Examples of the weighted residual method include the collocation, subdomain, and Galerkin approaches. The Galerkin approach is the basis of the finite-element formulation described in the following section.

Finite-Element Method

This section describes application of the Galerkin finite-element method to obtain a discrete approximation for the governing mass and energy transport equations. The principal advantages of the finite-element method are the capability to (1) incorporate irregular aquifer boundaries, (2) incorporate heterogeneous and anisotropic aquifer properties (with arbitrary local principal directions that differ from global Cartesian coordinates), (3) incorporate nonlinear parameters, (4) incorporate complex time-dependent boundary conditions, and (6) modularize the program code.

In general, the finite-element method is a numerical procedure for solving physical problems governed by one or more governing partial differential equations. The two characteristics that distinguish the finite-element method from other numerical procedures are the use of an integral formulation to generate a system of algebraic equations and continuous piecewise smooth functions for approximating the unknown quantities (dependent variables). The finite-element method can be subdivided into five basic steps. First, the region is discretized into elements (in this case linear triangles). This discretization includes locating and numbering the node points and coordinate values. Second, an approximation is specified and equations are written in terms of unknown nodal values. Third, a system of nonlinear algebraic equations is developed. In using Galerkin's method, the weighting function for each unknown nodal value is defined and weighted residual integral evaluated. Application of this method generates one equation for each nodal value. In VST2D, three unknown dependent values result and, therefore, three equations are written for each node. Fourth, the system of equations is solved. These equations are intrinsically nonlinear because many parameters actually are unknown quantities that depend on the magnitude

of one or more dependent variables. For this reason, the equations are quasi-linearized using a Picard approach prior to solution. Fifth, the quantities of interest are calculated.

In the Galerkin method (and other weighted residual methods), the mathematically continuous dependent variables are replaced using a finite series (discrete approximations). In VST2D, the approximations used are given by

$$\Psi(x, y, t) \cong \sum_{p=1}^P N_p \psi_p(t) = [N]\{\psi\} \quad (63)$$

$$T(x, y, t) \cong \sum_{p=1}^P N_p T_p(t) = [N]\{T\} \quad (64)$$

$$C(x, y, t) \cong \sum_{p=1}^P N_p C_p(t) = [N]\{C\} , \quad (65)$$

where

$\tilde{\Psi}$, \tilde{T} , and \tilde{C} are continuous space and time dependent variables $\psi(x,y,t)$, $T(x,y,t)$, $C(x,y,t)$,

N is an interpolation function;

$[N]$ is a set of linearly independent interpolation (also called shape or basis) functions,

$\{\psi\}$, $\{T\}$, and $\{C\}$ are a set of dependent variable values at discrete points in the solution domain, and;

P is the number of discrete node points in the solution domain.

Even when the interpolation functions are chosen to satisfy all boundary conditions imposed on a problem, normally the interpolation functions will not satisfy the governing partial differential equation. For this reason, the governing differential equations are first rewritten in an equivalent form given as

Water:

$$\begin{aligned} L_{\psi}(x, y, \psi, T, C, t) = & \frac{\partial}{\partial x} \left(D_{\theta v} \rho_L C_{\psi} \frac{\partial \psi}{\partial x} \right) + \frac{\partial}{\partial x} \left(\rho_L K_{xx} \frac{\partial \psi}{\partial x} \right) + \frac{\partial}{\partial x} \left(\rho_L K_{xy} \frac{\partial \psi}{\partial y} \right) + \frac{\partial (\rho_L K_{xy})}{\partial x} \\ & + \frac{\partial}{\partial x} \left(\rho_L D_{TV} \frac{\partial T}{\partial x} \right) + \frac{\partial}{\partial x} \left(\rho_L D_{TLxx} \frac{\partial T}{\partial x} \right) + \frac{\partial}{\partial x} \left(\rho_L D_{TLxy} \frac{\partial T}{\partial y} \right) - \frac{\partial}{\partial x} \left(\rho_L D_{CV} \frac{\partial C}{\partial x} \right) - \frac{\partial}{\partial x} \left(\rho_L D_{CLxx} \frac{\partial C}{\partial x} \right) \\ & - \frac{\partial}{\partial x} \left(\rho_L D_{CLxy} \frac{\partial C}{\partial y} \right) + \frac{\partial}{\partial y} \left(D_{\theta v} \rho_L C_{\psi} \frac{\partial \psi}{\partial y} \right) + \frac{\partial}{\partial y} \left(\rho_L K_{yx} \frac{\partial \psi}{\partial x} \right) + \frac{\partial}{\partial y} \left(\rho_L K_{yy} \frac{\partial \psi}{\partial y} \right) + \frac{\partial (\rho_L K_{yy})}{\partial y} \\ & + \frac{\partial}{\partial y} \left(\rho_L D_{TV} \frac{\partial T}{\partial y} \right) + \frac{\partial}{\partial y} \left(\rho_L D_{TLyx} \frac{\partial T}{\partial x} \right) \\ & + \frac{\partial}{\partial y} \left(\rho_L D_{TLyy} \frac{\partial T}{\partial y} \right) - \frac{\partial}{\partial y} \left(\rho_L D_{CV} \frac{\partial C}{\partial y} \right) - \frac{\partial}{\partial y} \left(\rho_L D_{CLyx} \frac{\partial C}{\partial x} \right) - \frac{\partial}{\partial y} \left(\rho_L D_{CLyy} \frac{\partial C}{\partial y} \right) + \rho_L Q_{Lp} + \rho_L Q_{Ld} \\ & - \rho_L \Lambda \frac{\partial \theta_L}{\partial t} - \rho_L \frac{\partial \theta_v}{\partial t} \end{aligned} \quad (66)$$

Heat:

$$\begin{aligned}
L_T(x, y, T, \Psi, C, t) &= \frac{\partial}{\partial x} \left(\sigma' \frac{\partial \Psi}{\partial x} \right) + \frac{\partial}{\partial x} \left(C_L T K_{xx} \frac{\partial \Psi}{\partial x} \right) + \frac{\partial}{\partial x} \left(C_{Lp} T K_{xy} \frac{\partial \Psi}{\partial y} \right) + \frac{\partial}{\partial x} \left(\sigma \frac{\partial T}{\partial x} \right) + \frac{\partial}{\partial x} \left(C_L T D_{TLxx} \frac{\partial T}{\partial x} \right) \\
&+ \frac{\partial}{\partial x} \left(C_L T D_{TLxy} \frac{\partial T}{\partial y} \right) - \frac{\partial}{\partial x} \left(\sigma'' \frac{\partial C}{\partial x} \right) - \frac{\partial}{\partial x} \left(C_L T D_{CLxx} \frac{\partial C}{\partial x} \right) - \frac{\partial}{\partial x} \left(C_L T D_{CLxy} \frac{\partial C}{\partial y} \right) \\
&+ \frac{\partial}{\partial y} \left(\sigma' \frac{\partial \Psi}{\partial y} \right) + \frac{\partial}{\partial y} \left(C_L T K_{yx} \frac{\partial \Psi}{\partial x} \right) + \frac{\partial}{\partial y} \left(C_L T K_{yy} \frac{\partial \Psi}{\partial y} \right) + \frac{\partial}{\partial y} \left(\sigma \frac{\partial T}{\partial y} \right) + \frac{\partial}{\partial y} \left(C_L T D_{TLyx} \frac{\partial T}{\partial x} \right) \\
&+ \frac{\partial}{\partial y} \left(C_L T D_{TLyy} \frac{\partial T}{\partial y} \right) - \frac{\partial}{\partial y} \left(\sigma'' \frac{\partial C}{\partial y} \right) - \frac{\partial}{\partial y} \left(C_L T D_{CLyx} \frac{\partial C}{\partial x} \right) - \frac{\partial}{\partial y} \left(C_L T D_{CLyy} \frac{\partial C}{\partial y} \right) \\
&+ C_L T \frac{\partial K_{xy}}{\partial x} + C_L T \frac{\partial K_{yy}}{\partial y} + C_L K_{xy} \frac{\partial T}{\partial x} + C_L K_{yy} \frac{\partial T}{\partial y} + Q_{Lp} + Q_{Ld} - f_1 \frac{\partial T}{\partial t} - f_2 \frac{\partial \theta_L}{\partial t} - f_3 \frac{\partial C}{\partial t}, \tag{67}
\end{aligned}$$

Solute:

$$\begin{aligned}
L_C(x, y, \Psi, T, C, t) &= \frac{\partial}{\partial x} \left(D_{CCxx} \frac{\partial C}{\partial x} \right) + \frac{\partial}{\partial y} \left(D_{CCyy} \frac{\partial C}{\partial y} \right) + \frac{\partial}{\partial x} \left(D_{CCxy} \frac{\partial C}{\partial y} \right) + \frac{\partial}{\partial y} \left(D_{CCyx} \frac{\partial C}{\partial x} \right) \\
&- \frac{\partial}{\partial x} \left(D_{C\Psi xx} \frac{\partial \Psi}{\partial x} \right) - \frac{\partial}{\partial y} \left(D_{C\Psi yy} \frac{\partial \Psi}{\partial y} \right) - \frac{\partial}{\partial x} \left(D_{C\Psi xy} \frac{\partial \Psi}{\partial y} \right) - \frac{\partial}{\partial y} \left(D_{C\Psi yx} \frac{\partial \Psi}{\partial x} \right) + \frac{\partial}{\partial x} \left(D_{CT} \frac{\partial T}{\partial x} \right) + \frac{\partial}{\partial y} \left(D_{CT} \frac{\partial T}{\partial y} \right) - q_{Lx} \frac{\partial C}{\partial x} - q_{Ly} \frac{\partial C}{\partial y} \\
&- V_{Lx} C C_\Psi \frac{\partial \Psi}{\partial x} - V_{Ly} C C_\Psi \frac{\partial \Psi}{\partial y} - \theta_L C \frac{\partial V_{Lx}}{\partial x} - \theta_L C \frac{\partial V_{Ly}}{\partial y} - \lambda C R + Q_{Cp} + Q_{Cd} - C \frac{\partial \theta_L}{\partial t} - R \frac{\partial C}{\partial t}, \tag{68}
\end{aligned}$$

where

L_Ψ , L_T , and L_C are differential operators.

Substitution of the approximations (Ψ , T , and C) into equations 66-68 for ψ , T , C will result in some residual amount expressed as

$$L_\Psi(x, y, \Psi, T, C, t) = r_\Psi, \tag{69}$$

$$L_T(x, y, \Psi, T, C, t) = r_T, \text{ and} \tag{70}$$

$$L_C(x, y, \Psi, T, C, t) = r_C. \tag{71}$$

For this reason, selecting weighting coefficients such that they minimize these residuals is important. In the Galerkin approach, the weighting functions are chosen to be interpolation functions (one-per-node) in an integral formulation that forces the average domain residuals to be zero. The residuals can be expressed as

$$\{R_\Psi\} = \int_A [N]^T L_\Psi(x, y, \Psi, T, C, t) dA = 0, \tag{72}$$

$$\{R_T\} = \int_A [N]^T L_T(x, y, \Psi, T, C, t) dA = 0, \text{ and} \tag{73}$$

$$\{R_C\} = \int_A [N]^T L_C(x, y, \Psi, C, T, t) dA = 0, \quad (74)$$

where

$\{R_\Psi\}$, $\{R_T\}$, and $\{R_C\}$ are weighted residual vectors for water, heat and solute equations
 $[m^2 d^{-1}]$, $[cal m^{-1} d^{-1}]$, $[m^2 d^{-1} mol kg^{-1}]$,
 $[N]^T$ is the transpose of row vector of interpolation functions used to weight the
residual equations, and
 A is the solution domain area.

Because each interpolation function is defined over individual elements, first the integration is performed element-by-element. The corresponding set of element contributions to the set of residual equations then is

$$\{R_\Psi\}^e = \int_{A^e} [N]^e L_\Psi(x, y, \Psi, T, C, t)^e dA^e \neq 0, \quad (75)$$

$$\{R_T\}^e = \int_{A^e} [N]^e L_T(x, y, \Psi, T, C, t)^e dA^e \neq 0, \text{ and} \quad (76)$$

$$\{R_C\}^e = \int_{A^e} [N]^e L_C(x, y, \Psi, T, C, t)^e dA^e \neq 0, \quad (77)$$

where

$$\{R_\Psi\}^e = \begin{bmatrix} R_{\Psi i} \\ R_{\Psi j} \\ R_{\Psi k} \end{bmatrix}^e,$$

$$\{R_T\}^e = \begin{bmatrix} R_{T i} \\ R_{T j} \\ R_{T k} \end{bmatrix}^e, \text{ and}$$

$$\{R_C\}^e = \begin{bmatrix} R_{C i} \\ R_{C j} \\ R_{C k} \end{bmatrix}^e \text{ are column vectors of residual equations for element } e \text{ [m}^2 \text{ d}^{-1}\text{], [cal m}^{-1} \text{ d}^{-1}\text{], [m}^2 \text{ d}^{-1} \text{ mol kg}^{-1}\text{]};$$

$[N]^e = \{N_i, N_j, N_k\}$, and
 $N_i = 2A^{-1}(a_i + b_i x + c_i y)$,
 $N_j = 2A^{-1}(a_j + b_j x + c_j y)$,
 $N_k = 2A^{-1}(a_k + b_k x + c_k y)$ are the dimensionless element interpolation functions (equal to one at their respective node and zero at the other nodes);
 A^e is the element area $[m^2]$;
 e is the element;

$$\begin{aligned}
a_i &= x_i y_k - x_k y_j, \\
a_j &= x_k y_i - x_i y_k, \\
a_k &= x_i y_j - x_j y_i, \\
b_i &= y_j - y_k, \\
b_j &= y_k - y_i, \\
b_k &= y_i - y_j, \\
c_i &= x_k - x_j, \\
c_j &= x_i - x_k, \text{ and} \\
c_k &= x_j - x_i
\end{aligned}$$

a_i, b_i, c_i are variables associated with Cartesian coordinates for an element that are used in the interpolation functions [m] (Segerlind, 1984); and

i, j, k are local element nodes. The residuals on an element basis are not equal to zero.

These residual elemental contributions then are integrated over the solution domain to form a global set as

$$\{R_\Psi\} = \sum_e \int_{A^e} [N]^e L_\Psi(x, y, \Psi, T, C, t)^e dA^e = 0, \quad (78)$$

$$\{R_T\} = \sum_e \int_{A^e} [N]^e L_T(x, y, \Psi, T, C, t)^e dA^e = 0, \text{ and} \quad (79)$$

$$\{R_C\} = \sum_e \int_{A^e} [N]^e L_C(x, y, \Psi, T, C, t)^e dA^e = 0. \quad (80)$$

The remaining sections focus on the development of these residual element equations and their equivalent matrix-vector representation for a two-dimensional interactive water-heat-solute transport problem.

Residual Equations for Elements

Residual equations are derived using the Galerkin weighted integral formulation. For these equations, the element contributions to the global system can be written as

Water

$$\begin{aligned}
\{R_\Psi\}^e &= - \int_A [N]^e T \left[\frac{\partial}{\partial x} (D_{\theta V} \rho_L C_\Psi \frac{\partial \Psi}{\partial x}) + \frac{\partial}{\partial x} (\rho_L K_{xx} \frac{\partial \Psi}{\partial x}) + \frac{\partial}{\partial x} (\rho_L K_{xy} \frac{\partial \Psi}{\partial y}) + \frac{\partial (\rho_L K_{xy})}{\partial x} + \frac{\partial (\rho_L D_{TV} \frac{\partial T}{\partial x})}{\partial x} + \frac{\partial (\rho_L D_{TLxx} \frac{\partial T}{\partial x})}{\partial x} \right. \\
&+ \frac{\partial}{\partial x} (\rho_L D_{TLxy} \frac{\partial T}{\partial y}) - \frac{\partial}{\partial x} (\rho_L D_{CV} \frac{\partial C}{\partial x}) - \frac{\partial}{\partial x} (\rho_L D_{CLxx} \frac{\partial C}{\partial x}) - \frac{\partial}{\partial x} (\rho_L D_{CLxy} \frac{\partial C}{\partial y}) + \frac{\partial}{\partial y} (D_{\theta V} \rho_L C_\Psi \frac{\partial \Psi}{\partial y}) + \frac{\partial}{\partial y} (\rho_L K_{yx} \frac{\partial \Psi}{\partial x}) \\
&+ \frac{\partial}{\partial y} (\rho_L K_{yy} \frac{\partial \Psi}{\partial y}) + \frac{\partial (\rho_L K_{yy})}{\partial y} + \frac{\partial}{\partial y} (\rho_L D_{TV} \frac{\partial T}{\partial y}) + \frac{\partial}{\partial y} (\rho_L D_{TLyx} \frac{\partial T}{\partial x}) \\
&\left. + \frac{\partial}{\partial y} (\rho_L D_{TLyy} \frac{\partial T}{\partial y}) - \frac{\partial}{\partial y} (\rho_L D_{CV} \frac{\partial C}{\partial y}) - \frac{\partial}{\partial y} (\rho_L D_{CLyx} \frac{\partial C}{\partial x}) - \frac{\partial}{\partial y} (\rho_L D_{CLyy} \frac{\partial C}{\partial y}) + \rho_L Q_{Lp} + \rho_L Q_{Ld} - \rho_L \Lambda \frac{\partial \theta_L}{\partial t} - \rho_L \frac{\partial \theta_V}{\partial t} \right] dA^e \neq 0, \quad (81)
\end{aligned}$$

Heat

$$\begin{aligned}
\{R_T\}^e = & - \int_{A^e} [N]^{eT} \left[\frac{\partial}{\partial x} \left(\sigma' \frac{\partial \Psi}{\partial x} \right) + \frac{\partial}{\partial x} \left(C_L T K_{xx} \frac{\partial \Psi}{\partial x} \right) + \frac{\partial}{\partial x} \left(C_L T K_{xy} \frac{\partial \Psi}{\partial y} \right) + \frac{\partial}{\partial x} \left(\sigma \frac{\partial T}{\partial x} \right) \right. \\
& + \frac{\partial}{\partial x} \left(C_L T D_{TLxx} \frac{\partial T}{\partial x} \right) + \frac{\partial}{\partial x} \left(C_L T D_{TLxy} \frac{\partial T}{\partial y} \right) - \frac{\partial}{\partial x} \left(\sigma'' \frac{\partial C}{\partial x} \right) - \frac{\partial}{\partial x} \left(C_L T D_{CLxx} \frac{\partial C}{\partial x} \right) \\
& - \frac{\partial}{\partial x} \left(C_L T D_{CLxy} \frac{\partial C}{\partial y} \right) + \frac{\partial}{\partial y} \left(\sigma' \frac{\partial \Psi}{\partial y} \right) + \frac{\partial}{\partial y} \left(C_L T K_{yx} \frac{\partial \Psi}{\partial x} \right) + \frac{\partial}{\partial y} \left(C_L T K_{yy} \frac{\partial \Psi}{\partial y} \right) + \frac{\partial}{\partial y} \left(\sigma \frac{\partial T}{\partial y} \right) \\
& + \frac{\partial}{\partial y} \left(C_L T D_{TLyx} \frac{\partial T}{\partial x} \right) + \frac{\partial}{\partial y} \left(C_L T D_{TLyy} \frac{\partial T}{\partial y} \right) - \frac{\partial}{\partial y} \left(\sigma'' \frac{\partial C}{\partial y} \right) - \frac{\partial}{\partial y} \left(C_L T D_{CLyx} \frac{\partial C}{\partial x} \right) \\
& - \frac{\partial}{\partial y} \left(C_L T D_{CLyy} \frac{\partial C}{\partial y} \right) + C_L T \frac{\partial K_{xy}}{\partial x} + C_L T \frac{\partial K_{yy}}{\partial y} + C_L K_{xy} \frac{\partial T}{\partial x} + C_L K_{yy} \frac{\partial T}{\partial y} + Q_{Lp} + Q_{Ld} - f_1 \frac{\partial T}{\partial t} \\
& \left. - f_2 \frac{\partial \theta_L}{\partial t} - f_3 \frac{\partial C}{\partial t} \right] dA^e \neq 0, \text{ and}
\end{aligned} \tag{82}$$

Solute

$$\begin{aligned}
\{R_C\}^e = & - \int_{A^e} [N]^{eT} \left[\frac{\partial}{\partial x} \left(D_{CCxx} \frac{\partial C}{\partial x} \right) + \frac{\partial}{\partial y} \left(D_{CCyy} \frac{\partial C}{\partial y} \right) + \frac{\partial}{\partial x} \left(D_{CCxy} \frac{\partial C}{\partial y} \right) + \frac{\partial}{\partial y} \left(D_{CCyx} \frac{\partial C}{\partial x} \right) \right. \\
& - \frac{\partial}{\partial x} \left(D_{C\psi_{xx}} \frac{\partial \Psi}{\partial x} \right) - \frac{\partial}{\partial y} \left(D_{C\psi_{yy}} \frac{\partial \Psi}{\partial y} \right) - \frac{\partial}{\partial x} \left(D_{C\psi_{xy}} \frac{\partial \Psi}{\partial y} \right) - \frac{\partial}{\partial y} \left(D_{C\psi_{yx}} \frac{\partial \Psi}{\partial x} \right) + \frac{\partial}{\partial x} \left(D_{CT} \frac{\partial T}{\partial x} \right) + \frac{\partial}{\partial y} \left(D_{CT} \frac{\partial T}{\partial y} \right) \\
& - q_{Lx} \frac{\partial C}{\partial x} - q_{Ly} \frac{\partial C}{\partial y} - V_{Lx} C C \frac{\partial \Psi}{\partial x} - V_{Ly} C C \frac{\partial \Psi}{\partial y} - \theta_L C \frac{\partial V_{Lx}}{\partial x} - \theta_L C \frac{\partial V_{Ly}}{\partial y} - \lambda C R + Q_{Cp} + Q_{Cd} \\
& \left. - C \frac{\partial \theta_L}{\partial t} - R \frac{\partial C}{\partial t} \right] dA^e \neq 0,
\end{aligned} \tag{83}$$

In the finite-element approach, the hydraulic conductivity and diffusivity functions are assumed constant within each element (but they can vary from one element to another). In this case, the equations can be written as

Water

$$\begin{aligned}
\{R_\psi\}^e = & - \int_{A^e} [N]^{eT} \left[D_{\theta v} \rho_L C_\psi \frac{\partial^2 \Psi}{\partial x^2} + \rho_L K_{xx} \frac{\partial^2 \Psi}{\partial x^2} + \frac{\partial \rho_L K_{xx}}{\partial x} \frac{\partial \Psi}{\partial x} + \rho_L K_{xy} \frac{\partial^2 \Psi}{\partial x \partial y} + \frac{\partial \rho_L K_{xy}}{\partial x} \frac{\partial \Psi}{\partial y} + \frac{\partial \rho_L K_{xy}}{\partial x} \right. \\
& + \rho_L D_{TV} \frac{\partial^2 T}{\partial x^2} + \rho_L D_{TLxx} \frac{\partial^2 T}{\partial x^2} + \rho_L D_{TLxy} \frac{\partial^2 T}{\partial x \partial y} - \rho_L D_{CV} \frac{\partial^2 C}{\partial x^2} - \rho_L D_{CLxx} \frac{\partial^2 C}{\partial x^2} - \rho_L D_{CLxy} \frac{\partial^2 C}{\partial x \partial y} + D_{\theta v} \rho_L C_\psi \frac{\partial^2 \Psi}{\partial y^2} \\
& + \rho_L K_{yx} \frac{\partial^2 \Psi}{\partial y \partial x} + \frac{\partial \rho_L K_{yx}}{\partial y} \frac{\partial \Psi}{\partial x} + \rho_L K_{yy} \frac{\partial^2 \Psi}{\partial y^2} + \frac{\partial \rho_L K_{yy}}{\partial x} \frac{\partial \Psi}{\partial y} + \frac{\partial \rho_L K_{yy}}{\partial y} + \rho_L D_{TV} \frac{\partial^2 T}{\partial y^2} + \rho_L D_{TLyx} \frac{\partial^2 T}{\partial y \partial x} \\
& \left. + \rho_L D_{TLyy} \frac{\partial^2 T}{\partial y^2} - \rho_L D_{CV} \frac{\partial^2 C}{\partial y^2} - \rho_L D_{CLyx} \frac{\partial^2 C}{\partial y \partial x} - \rho_L D_{CLyy} \frac{\partial^2 C}{\partial y^2} + \rho_L Q_{Lp} + \rho_L Q_{Ld} - \rho_L \Lambda \frac{\partial \theta_L}{\partial t} - \rho_L \frac{\partial \theta_v}{\partial t} \right] dA^e \neq 0,
\end{aligned} \tag{84}$$

Heat

$$\begin{aligned}
\{R_T\}^e = & - \int_{A^e} [N]^e T \left[\sigma' \frac{\partial^2 \Psi}{\partial x^2} + C_L T K_{xx} \frac{\partial^2 \Psi}{\partial x^2} + C_L T \frac{\partial K_{xx}}{\partial x} \frac{\partial \Psi}{\partial x} + C_L T K_{xy} \frac{\partial^2 \Psi}{\partial x \partial y} + C_L T \frac{\partial K_{xy}}{\partial x} \frac{\partial \Psi}{\partial y} + \sigma \frac{\partial^2 T}{\partial x^2} \right. \\
& + C_L T D_{TLxx} \frac{\partial^2 T}{\partial x^2} + C_L T D_{TLxy} \frac{\partial^2 T}{\partial x \partial y} - \sigma'' \frac{\partial^2 C}{\partial x^2} - C_L T D_{CLxx} \frac{\partial^2 C}{\partial x^2} - C_L T D_{CLxy} \frac{\partial^2 C}{\partial x \partial y} + \sigma' \frac{\partial^2 \Psi}{\partial y^2} + C_L T K_{yx} \frac{\partial^2 \Psi}{\partial y \partial x} \\
& + C_L T \frac{\partial K_{yx}}{\partial y} \frac{\partial \Psi}{\partial x} + C_L T K_{yy} \frac{\partial^2 \Psi}{\partial y^2} + C_L T \frac{\partial K_{yy}}{\partial x} \frac{\partial \Psi}{\partial y} + \sigma \frac{\partial^2 T}{\partial y^2} + C_L T D_{TLyx} \frac{\partial^2 T}{\partial y \partial x} + C_L T D_{TLyy} \frac{\partial^2 T}{\partial y^2} - \sigma'' \frac{\partial^2 C}{\partial y^2} \\
& - C_L T D_{CLyx} \frac{\partial^2 C}{\partial y \partial x} - C_L T D_{CLyy} \frac{\partial^2 C}{\partial y^2} + C_L T \frac{\partial K_{xy}}{\partial x} + C_L T \frac{\partial K_{yy}}{\partial y} + C_L K_{xy} \frac{\partial T}{\partial x} + C_L K_{yy} \frac{\partial T}{\partial y} + Q_{Lp} + Q_{Ld} - f_1 \frac{\partial T}{\partial t} \\
& \left. - f_2 \frac{\partial \theta_L}{\partial t} - f_3 \frac{\partial C}{\partial t} \right] dA^e \neq 0, \text{ and}
\end{aligned} \tag{85}$$

Solute

$$\begin{aligned}
\{R_C\}^e = & - \int_{A^e} [N]^e T \left[D_{CCxx} \frac{\partial^2 C}{\partial x^2} + D_{CCyy} \frac{\partial^2 C}{\partial y^2} + D_{CCxy} \frac{\partial^2 C}{\partial x \partial y} + D_{CCyx} \frac{\partial^2 C}{\partial y \partial x} \right. \\
& + -D_{C\psi xx} \frac{\partial^2 \Psi}{\partial x^2} - D_{C\psi yy} \frac{\partial^2 \Psi}{\partial y^2} - D_{C\psi xy} \frac{\partial^2 \Psi}{\partial x \partial y} - D_{C\psi yx} \frac{\partial^2 \Psi}{\partial y \partial x} + D_{CT} \frac{\partial^2 T}{\partial x^2} + D_{CT} \frac{\partial^2 T}{\partial y^2} - q_{Lx} \frac{\partial C}{\partial x} - q_{Ly} \frac{\partial C}{\partial y} - V_{Lx} C C_\psi \frac{\partial \Psi}{\partial x} \\
& \left. - V_{Ly} C C_\psi \frac{\partial \Psi}{\partial y} - \theta_L C \frac{\partial V_{Lx}}{\partial x} - \theta_L C \frac{\partial V_{Ly}}{\partial y} - \lambda C R + Q_{Cp} + Q_{Cd} - C \frac{\partial \theta_L}{\partial t} - R \frac{\partial C}{\partial t} \right] dA^e \neq 0.
\end{aligned} \tag{86}$$

The second-order derivative terms appearing in these residual equations must be replaced by first-order derivative terms because interpolation functions do not have continuous derivatives across element boundaries.

The second-order derivative terms are replaced by applying the product rule for differentiation. For example, consider differentiation of the following quantities from the water equation (81):

$$\frac{\partial}{\partial x} \left([N]^T \frac{d\Psi}{dx} \right) = [N]^T \frac{\partial^2 \Psi}{\partial x^2} + \frac{\partial [N]^T}{\partial x} \frac{\partial \Psi}{\partial x} \text{ and} \tag{87}$$

$$\frac{\partial}{\partial x} \left([N]^T \frac{d\Psi}{dy} \right) = [N]^T \frac{\partial^2 \Psi}{\partial x \partial y} + \frac{\partial [N]^T}{\partial x} \frac{\partial \Psi}{\partial y}, \tag{88}$$

where

$\partial[N]^T/\partial x$ is a derivative of the interpolation function with respect to the x-direction:

$$\partial N_i/\partial x = b_i/2A, \quad \partial N_j/\partial x = b_j/2A, \quad \partial N_k/\partial x = b_k/2A \text{ and}$$

$\partial[N]^T/\partial y$ is a derivative of the interpolation function in the y-direction: $\partial N_i/\partial y = c_i/2A$, $\partial N_j/\partial y = c_j/2A$,

$$\partial N_k/\partial y = c_k/2A.$$

For example, applying these expressions to selected second order derivative terms in the water transport equation (84) results in

$$-\int_{A^e} [N]^{eT} \frac{\partial}{\partial x} \left(\rho_L K_{xx} \frac{\partial \Psi}{\partial x} \right) dA^e = -\int_{A^e} \rho_L K_{xx} \frac{\partial}{\partial x} \left([N]^{eT} \frac{\partial \Psi}{\partial x} \right) dA^e + \int_{A^e} \rho_L K_{xx} \frac{\partial [N]^{eT}}{\partial x} \frac{\partial \Psi}{\partial x} dA^e \quad \text{and} \quad (89)$$

$$-\int_{A^e} [N]^{eT} \frac{\partial}{\partial x} \left(\rho_L K_{xy} \frac{\partial \Psi}{\partial y} \right) dA^e = -\int_{A^e} \rho_L K_{xy} \frac{\partial}{\partial x} \left([N]^{eT} \frac{\partial \Psi}{\partial y} \right) dA^e + \int_{A^e} \rho_L K_{xy} \frac{\partial [N]^{eT}}{\partial x} \frac{\partial \Psi}{\partial y} dA^e. \quad (90)$$

The first integral on the right-hand-side of equations 89 and 90 can be replaced by an integral around the boundary on the basis of Green's Theorem (Olmstead, 1961). Application of this theorem results in

$$\int_{A^e} \frac{\rho_L K_{xx}}{\partial x} \frac{\partial}{\partial x} \left([N]^{eT} \frac{\partial \Psi}{\partial x} \right) dA^e = \int_{\Gamma^e} [N]^{eT} \frac{\rho_L K_{xx}}{\partial x} \frac{\partial \Psi}{\partial x} \cos \Theta_x d\Gamma^e \quad \text{and} \quad (91)$$

$$\int_{A^e} \frac{\rho_L K_{xy}}{\partial x} \frac{\partial}{\partial x} \left([N]^{eT} \frac{\partial \Psi}{\partial y} \right) dA^e = \int_{\Gamma^e} [N]^{eT} \frac{\rho_L K_{xy}}{\partial x} \frac{\partial \Psi}{\partial x} \cos \Theta_x d\Gamma^e, \quad (92)$$

where

$\{\Psi\}^e = \{\Psi_i, \Psi_j, \Psi_k\}$ is a vector,

Θ_x, Θ_y are the angles that the flux normal to the element boundary makes with the global (solution domain) Cartesian axes (x and y), and

Γ is the integration surface along an element boundary.

Substituting this result back into the residual water transport equation (84) gives

$$-\int_{A^e} [N]^{eT} \frac{\partial}{\partial x} \left(\rho_L K_{xx} \frac{\partial \Psi}{\partial x} \right) dA^e = -\int_{\Gamma^e} [N]^{eT} \rho_L K_{xx} \frac{\partial \Psi}{\partial x} \cos \Theta_x d\Gamma^e + \int_{A^e} \rho_L K_{xx} \frac{\partial [N]^{eT}}{\partial x} \frac{\partial \Psi}{\partial x} dA^e \quad \text{and} \quad (93)$$

$$-\int_{A^e} [N]^{eT} \frac{\partial}{\partial x} \left(\rho_L K_{xy} \frac{\partial \Psi}{\partial y} \right) dA^e = -\int_{\Gamma^e} [N]^{eT} \rho_L K_{xy} \frac{\partial \Psi}{\partial x} \cos \Theta_x d\Gamma^e + \int_{A^e} \rho_L K_{xy} \frac{\partial [N]^{eT}}{\partial x} \frac{\partial \Psi}{\partial y} dA^e. \quad (94)$$

A similar set of operations results in the yy- and yx- components resulting in

$$-\int_{A^e} [N]^{eT} \frac{\partial}{\partial y} \left(\rho_L K_{yy} \frac{\partial \Psi}{\partial y} \right) dA^e = -\int_{\Gamma^e} [N]^{eT} \rho_L K_{yy} \frac{\partial \Psi}{\partial y} \cos \Theta_y d\Gamma^e + \int_{A^e} \rho_L K_{yy} \frac{\partial [N]^{eT}}{\partial y} \frac{\partial \Psi}{\partial y} dA^e, \quad (95)$$

$$-\int_{A^e} [N]^{eT} \frac{\partial}{\partial y} \left(\rho_L K_{yx} \frac{\partial \Psi}{\partial x} \right) dA^e = -\int_{\Gamma^e} [N]^{eT} \rho_L K_{yx} \frac{\partial \Psi}{\partial x} \cos \Theta_y d\Gamma^e + \int_{A^e} \rho_L K_{yx} \frac{\partial [N]^{eT}}{\partial y} \frac{\partial \Psi}{\partial x} dA^e. \quad (96)$$

Combining the right-hand sides of equations 93-96 gives

$$\begin{aligned} & -\int_{\Gamma^e} \left([N]^{eT} \rho_L \left(K_{xx} \frac{\partial \Psi}{\partial x} \cos \Theta_x + K_{xy} \frac{\partial \Psi}{\partial x} \cos \Theta_x + K_{yy} \frac{\partial \Psi}{\partial y} \cos \Theta_y + K_{yx} \frac{\partial \Psi}{\partial y} \cos \Theta_y \right) d\Gamma^e \right. \\ & \left. + \int_{A^e} \rho_L \left(K_{xx} \frac{\partial [N]^{eT}}{\partial x} \frac{\partial \Psi}{\partial x} + K_{yy} \frac{\partial [N]^{eT}}{\partial y} \frac{\partial \Psi}{\partial y} + K_{xy} \frac{\partial [N]^{eT}}{\partial x} \frac{\partial \Psi}{\partial y} + K_{yx} \frac{\partial [N]^{eT}}{\partial y} \frac{\partial \Psi}{\partial x} \right) dA^e \right) \end{aligned} \quad (97)$$

By substituting an approximation for the pressure head, $\Psi(x,y,t) = [N]\{\psi\}$, equation 97 can be put into final form as

$$\begin{aligned} & -\int_{\Gamma^e} \left([N]^{eT} \rho_L \left(K_{xx} \frac{\partial \Psi}{\partial x} \cos \Theta_x + K_{xy} \frac{\partial \Psi}{\partial x} \cos \Theta_x + K_{yy} \frac{\partial \Psi}{\partial y} \cos \Theta_y + K_{yx} \frac{\partial \Psi}{\partial y} \cos \Theta_y \right) d\Gamma^e \right. \\ & \left. + \int_{A^e} \rho_L \left(K_{xx} \frac{\partial [N]^{eT}}{\partial x} \frac{\partial [N]^e}{\partial x} + K_{yy} \frac{\partial [N]^{eT}}{\partial y} \frac{\partial [N]^e}{\partial y} + K_{xy} \frac{\partial [N]^{eT}}{\partial x} \frac{\partial [N]^e}{\partial y} + K_{yx} \frac{\partial [N]^{eT}}{\partial y} \frac{\partial [N]^e}{\partial x} \right) dA^e \right) \{\psi\}^e \end{aligned} \quad (98)$$

where

$\{\psi\}^e = \{\psi_i, \psi_j, \psi_k\}$ is a vector of pressure head values in the element; and
 i, j, k are the local element nodes.

Note that the variable Ψ is not replaced in the first integral term because this variable forms part of the liquid water derivative boundary condition. The second intergral term represents that portion associated with material properties, and this integral, therefore, incorporates cross terms associated with directional dependence (vectors). When properties are not directional (tensoral), however, the cross terms (xy, yx) do not appear in this equation. The remaining second-order derivatives in each of the governing equations are evaluated in a similar manner.

The second part of the derivative boundary condition for liquid water flux is obtained by evaluating integral terms associated with gravity. For example,

$$-\int_{A^e} [N]^{eT} \frac{\partial (\rho_L K_{yy})}{\partial y} dA^e. \quad (99)$$

This integral evaluation is conducted using integration-by-parts: $\int u dv = uv - \int v du$. For example, if $v = K_{yy}$, $dv = \partial K_{yy} / \partial y$, $u = [N]^T$, $du = \partial [N]^T / \partial y$, the integral can be rewritten as

$$\int_{A^e} \rho_L K_{yy} \frac{\partial [N]^{eT}}{\partial y} dA^e - [N]^{eT} \rho_L K_{yy} \cos \theta_y \Big|_{\Gamma^e}, \quad (100)$$

or

$$\int_{A^e} \rho_L K_{yy} \frac{\partial [N]^{eT}}{\partial y} dA^e - \int_{\Gamma^e} [N]^{eT} \rho_L K_{yy} \cos \theta_y d\Gamma^e. \quad (101)$$

The first and second terms in equation 101 are a force function and another part of the derivative boundary condition for liquid water flux. Similarly, evaluation of the other gravitational component results in

$$\int_{A^e} \rho_L K_{xy} \frac{\partial [N]^{eT}}{\partial x} dA^e - \int_{\Gamma^e} [N]^{eT} \rho_L K_{xy} \cos \theta_x d\Gamma^e. \quad (102)$$

By combining the first term of equation 98 with results from equations 101-102, the complete integral formulation of the flux derivative boundary condition for liquid water flux is obtained as

$$-\int_{\Gamma^e} [N]^{eT} \rho_L \left[K_{xx} \frac{\partial \psi}{\partial x} \cos \theta_x + K_{xy} \frac{\partial \psi}{\partial x} \cos \theta_x + K_{xy} \cos \theta_x + K_{yx} \frac{\partial \psi}{\partial x} \cos \theta_y + K_{yy} \frac{\partial \psi}{\partial y} \cos \theta_y + K_{yy} \cos \theta_y \right] d\Gamma^e. \quad (103)$$

This term (also known as the inter-element contribution) cancels across interior boundaries because of equal and opposite signs associated with fluxes from adjoining elements (Segerlind, 1984). Because this term does not cancel along a domain boundary, the term provides a natural way to incorporate the liquid water flux boundary condition into the model. A similar approach is used to develop boundary conditions for the heat and solute equations.

The third and fourth integral formulation types pertain to the respective point and distributed source/sink terms written as

$$-\int_{A^e} Q_{Lp} [N]^{eT} dA^e \quad \text{and} \quad (104)$$

$$-\int_{A^e} Q_{Ld} [N]^{eT} dA^e, \quad (105)$$

where

the p and d are subscripts that indicate respective point and distributed sources associated with the water equation.

The final integral formulation type involves a time derivative term given by

$$\int_{A^e} [N]^{eT} \frac{\partial \theta_L}{\partial t} dA^e. \quad (106)$$

Using the integral formulations discussed above, a general form of the residual equation for isothermal, isohaline, and liquid water flux can be written on an elemental basis as

$$\{R_{\psi\psi}\}^e = [k_{\psi L}]^e \{\psi\}^e + \{f_{\psi K}\}^e + \{f_{\psi b}\}^e - \{f_{\psi d}\}^e - \{f_{\psi p}\}^e + \Lambda [A_{\psi L}]^e \left\{ \frac{\partial \theta_L}{\partial t} \right\}^e, \quad (107)$$

where

$$[k_{\Psi L}]^e = \int_{A^e} \rho_L \left(K_{xx} \frac{\partial [N]^{eT}}{\partial x} \frac{\partial [N]^e}{\partial x} + K_{xy} \frac{\partial [N]^{eT}}{\partial x} \frac{\partial [N]^e}{\partial y} + K_{yx} \frac{\partial [N]^{eT}}{\partial y} \frac{\partial [N]^e}{\partial x} + K_{yy} \frac{\partial [N]^{eT}}{\partial y} \frac{\partial [N]^e}{\partial y} \right) dA^e, \quad (108)$$

$$\{f_{\Psi K}\}^e = \int_{A^e} \rho_L \left(K_{xy} \frac{\partial [N]^{eT}}{\partial x} + K_{yy} \frac{\partial [N]^{eT}}{\partial y} \right) dA^e, \quad (109)$$

$$\{f_{\Psi b}\}^e = \int_{\Gamma^e} [N]^{eT} \rho_L \left[K_{xx} \frac{\partial \Psi}{\partial x} \cos \theta_x + K_{xy} \frac{\partial \Psi}{\partial x} \cos \theta_x + K_{xy} \cos \theta_x + K_{yx} \frac{\partial \Psi}{\partial x} \cos \theta_y + K_{yy} \frac{\partial \Psi}{\partial y} \cos \theta_y + K_{yy} \cos \theta_y \right] d\Gamma^e = q_{Ln}, \quad (110)$$

$$\{f_{\Psi p}\}^e = \int_{A^e} \rho_L Q_{Lp} [N]^{eT} dA^e, \quad (111)$$

$$\{f_{\Psi d}\}^e = \int_{A^e} \rho_L Q_{Ld} N^{eT} dA^e, \text{ and} \quad (112)$$

$$[A_{\Psi L}]^e \left\{ \frac{d\theta_L}{dt} \right\}^e = \int_{A^e} [N]^{eT} \rho_L \Lambda \frac{\partial \theta_L}{\partial t} dA^e. \quad (113)$$

Individual Element Matrices and Vectors

The objective of this section is to derive the individual element matrix-vector coefficients for a two-dimensional model using triangular (simplex) elements. The approach involves performing integration of residual equations formulated in the previous section along with similar equations that arise from evaluation of like terms in the governing transport equations. In general, integration of these equations can be performed using the respective analytic formulas (Segerlind, 1984) given by

$$\int_{A^e} N_i^a N_j^b N_k^c dA^e = 2A^e \frac{a!b!c!}{(a+b+c+2)!}, \quad (114)$$

for area integrals, and

$$\int_{\Gamma^e} N_i^a N_j^b d\Gamma^e = 2L_{ij} \frac{a!b!}{(a+b+1)!}, \quad (115)$$

where L_{ij} is the length of an element side for boundary integrals.

In performing the first integration, the element matrix $[k_{\psi L}]^e$ is rewritten in a more compact matrix-vector form as

$$[k_{\psi L}]^e = \int_{A^e} [G]^{eT} [K]^e [G]^e dA^e = A^e [G]^{eT} [K]^e [G]^e, \quad (116)$$

where

$[G]^e$ and $[G]^{eT}$ is the respective element gradient vector and its transpose, and $[K]^e$ is the element conductivity matrix.

These matrices are given by

$$[G]^e = \begin{bmatrix} \frac{\partial [N]^e}{\partial x} \\ \frac{\partial [N]^e}{\partial y} \end{bmatrix} = \begin{bmatrix} \frac{\partial N_i}{\partial x} & \frac{\partial N_j}{\partial x} & \frac{\partial N_k}{\partial x} \\ \frac{\partial N_i}{\partial y} & \frac{\partial N_j}{\partial y} & \frac{\partial N_k}{\partial y} \end{bmatrix} = \frac{1}{2A} \begin{bmatrix} b_i & b_j & b_k \\ c_i & c_j & c_k \end{bmatrix}, \quad (117)$$

$$[G]^{eT} = \begin{bmatrix} \frac{\partial [N]^e}{\partial x} & \frac{\partial [N]^e}{\partial y} \end{bmatrix}^{eT} = \begin{bmatrix} \frac{\partial N_i}{\partial x} & \frac{\partial N_i}{\partial y} \\ \frac{\partial N_j}{\partial x} & \frac{\partial N_j}{\partial y} \\ \frac{\partial N_k}{\partial x} & \frac{\partial N_k}{\partial y} \end{bmatrix} = \frac{1}{2A} \begin{bmatrix} b_i & c_i \\ b_j & c_j \\ b_k & c_k \end{bmatrix}, \text{ and} \quad (118)$$

$$[K]^e = \rho_L \begin{bmatrix} K_{xx} & K_{xy} \\ K_{yx} & K_{yy} \end{bmatrix}. \quad (119)$$

Evaluating the integral and expanding the matrix product results in the so-called element conductance matrix given by

$$[k_{\psi L}]^e = \frac{\rho_L K_{xx}}{4A} \begin{bmatrix} b_i^2 & b_i b_j & b_i b_k \\ b_j b_i & b_j^2 & b_j b_k \\ b_k b_i & b_k b_j & b_k^2 \end{bmatrix} + \frac{\rho_L K_{yy}}{4A} \begin{bmatrix} c_i^2 & c_i c_j & c_i c_k \\ c_j c_i & c_j^2 & c_j c_k \\ c_k c_i & c_k c_j & c_k^2 \end{bmatrix} + \frac{\rho_L K_{xy}}{4A} \begin{bmatrix} b_i c_i & b_i c_j & b_i c_k \\ b_j c_i & b_j c_j & b_j c_k \\ b_k c_i & b_k c_j & b_k c_k \end{bmatrix} + \frac{\rho_L K_{yx}}{4A} \begin{bmatrix} c_i b_i & c_i b_j & c_i b_k \\ c_j b_i & c_j b_j & c_j b_k \\ c_k b_i & c_k b_j & c_k b_k \end{bmatrix}. \quad (120)$$

where

K_{xx} , K_{yy} , K_{xy} , and K_{yx} represent the average element conductivities for their respective tensor component, with $K_{xx} = (K_{xxi} + K_{xxj} + K_{xxk}) / 3$, $K_{yy} = (K_{yyi} + K_{yyj} + K_{yyk}) / 3$, and $K_{xy} = (K_{xyi} + K_{xyj} + K_{xyk}) / 3 = K_{yx}$, and ρ_L is the average element density; for example, $\rho_L = (\rho_{Li} + \rho_{Lj} + \rho_{Lk}) / 3$.

Evaluation of the gravitational element force vector $\{f_{\psi K}\}^e$ along the yy and xy directions is carried out term-by-term as

$$\{f_{\psi K_{yy}}\}^e = \int_{A^e} \rho_L K_{yy} \frac{\partial [N]^e}{\partial y} dA^e = \int_{A^e} [N]^e \{\rho_L K_{yy}\}^e \begin{Bmatrix} \frac{\partial N_i}{\partial y} \\ \frac{\partial N_j}{\partial y} \\ \frac{\partial N_k}{\partial y} \end{Bmatrix} dA^e = \frac{A(\rho_{Li} K_{yyi} + \rho_{Lj} K_{yyj} + \rho_{Lk} K_{yyk})}{6} \begin{Bmatrix} c_i \\ c_j \\ c_k \end{Bmatrix} \text{ and} \quad (121)$$

$$\{f_{\psi K_{xy}}\}^e = \int_{A^e} \rho_L K_{xy} \frac{\partial [N]^e}{\partial x} dA^e = \int_{A^e} [N]^e \{\rho_L K_{xy}\}^e \begin{Bmatrix} \frac{\partial N_i}{\partial x} \\ \frac{\partial N_j}{\partial x} \\ \frac{\partial N_k}{\partial x} \end{Bmatrix} dA^e = \frac{A(\rho_{Li} K_{xyi} + \rho_{Lj} K_{xyj} + \rho_{Lk} K_{xyk})}{6} \begin{Bmatrix} b_i \\ b_j \\ b_k \end{Bmatrix}, \quad (122)$$

where

$\{K_{yy}\}^e = \{K_{yyi}, K_{yyj}, K_{yyk}\}$ is a vector of nodal conductivities for the yy component, and $\{K_{xy}\}^e = \{K_{xyi}, K_{xyj}, K_{xyk}\}$ is a vector of nodal conductivities for the xy component.

Summing these contribution yields

$$\{f_{\psi K}\}^e = \{f_{\psi K_{yy}}\}^e + \{f_{\psi K_{xy}}\}^e. \quad (123)$$

Evaluation of the point source/sink force vector $\{f_{\psi p}\}^e$ is carried out as

$$\{f_{\psi p}\}^e = \int_{A^e} \rho_L Q_{Lp} [N]^T dA^e = \rho_L Q_{Lp} \begin{Bmatrix} N_i \\ N_j \\ N_k \end{Bmatrix}. \quad (124)$$

The point source/sink gives the value at that point, and this point value is distributed across the element on the basis of interpolation function values. When a point source/sink is located at a node, the interpolation function is equal to one at that node and zero at the other nodes. When this occurs, evaluation of the source/sink force vector becomes

$$\{f_{\psi p}\}^e = \int_{A^e} \rho_L Q_{Lp} [N]^T dA^e = \begin{Bmatrix} \rho_{Li} Q_{Lp_i} \\ 0 \\ 0 \end{Bmatrix}, \text{ or } \begin{Bmatrix} 0 \\ \rho_{Lj} Q_{Lp_j} \\ 0 \end{Bmatrix}, \text{ or } \begin{Bmatrix} 0 \\ 0 \\ \rho_{Lk} Q_{Lp_k} \end{Bmatrix}, \quad (125)$$

where

Q_{Lp_i} , Q_{Lp_j} , Q_{Lp_k} are the point source/sink for liquid-water at the corresponding node. Evaluation of the force vector for a distributed source/sink $\{f_{\psi d}\}^e$ follows

$$\{f_{\psi d}\}^e = \int_{A^e} \rho_L Q_{Ld} [N]^T dA^e = \int_{A^e} \rho_L Q_{Ld} \begin{pmatrix} N_i \\ N_j \\ N_k \end{pmatrix} dA^e = \frac{A(\rho_{Li} Q_{Ld_i} + \rho_{Lj} Q_{Ld_j} + \rho_{Lk} Q_{Ld_k})^e}{3} \quad (126)$$

where Q_{Ld_i} , Q_{Ld_j} , Q_{Ld_k} are the values of the distributed source/sink at nodes of the element.

Integration of the time-dependent term using the consistent formulation (equation 113) tends to be numerically unstable (Seegerlind, 1984). For this reason, a lumped formulation is used and described by

$$\int_{A^e} [N]^{eT} \frac{\partial \theta_L}{\partial t} dA^e = \frac{\partial \theta_L}{\partial t} \int_{A^e} [N]^{eT} dA^e = \frac{A^e}{3} \begin{bmatrix} 1 & 0 & 0 \\ 0 & 1 & 0 \\ 0 & 0 & 1 \end{bmatrix} \left\{ \frac{\partial \theta_L}{\partial t} \right\}^e = [A_{\psi L}]^e \left\{ \frac{\partial \theta_L}{\partial t} \right\}^e, \quad (127)$$

where the capacitance matrix $[A_{\psi L}]^e$ multiplies the time-derivative vector. A similar set of matrices and vectors are derived for the remaining terms in the governing equation for water transport and each term in the governing equations for heat and solute transport (assuming the appropriate substitution for variables and constants).

One additional formulation type to be integrated (not in the water equation) is associated with the liquid water flux-concentration gradient term appearing in the solute equation. In this case, the integral first is rewritten in a more compact form and then evaluated as

$$[q_{LC}]^e = \int_{A^e} [N]^T [q]^e [G]^e dA^e = A^e [N]^{eT} [q]^e [G]^e = \frac{q_{Lx}}{6} \begin{bmatrix} b_i & b_j & b_k \\ b_i & b_j & b_k \\ b_i & b_j & b_k \end{bmatrix} + \frac{q_{Ly}}{6} \begin{bmatrix} c_i & c_j & c_k \\ c_i & c_j & c_k \\ c_i & c_j & c_k \end{bmatrix}, \quad (128)$$

where

$$[N]^{eT} = \begin{bmatrix} N_i & N_i \\ N_j & N_j \\ N_k & N_k \end{bmatrix} \text{ and}$$

$$[q]^e = \begin{bmatrix} q_{Lx} & 0 \\ 0 & q_{Ly} \end{bmatrix}.$$

A similar approach is used for the velocity-concentration-capacity pressure head gradient terms appearing in the solute transport equation, for example, $V_{Lx} CC_{\psi} \frac{\partial \psi}{\partial x}$, and $V_{Ly} CC_{\psi} \frac{\partial \psi}{\partial y}$. A complete definition of individual element matrices and vectors is included in appendix 1.

By rearranging and combining like coefficients in matrix-vector form, the generalized set of residual equations now can be expressed as

Water

$$\{R_{\psi}\}^e = \Lambda \rho_L [A_{\psi L}] \left\{ \frac{\partial \theta_L}{\partial t} \right\} + \rho_L [A_{\psi V}] \left\{ \frac{\partial \theta_V}{\partial t} \right\} + [B_{\psi \psi}] \{\psi\} + [B_{\psi T}] \{T\} - [B_{\psi C}] \{C\} + \{f_{\psi K}\} - \{f_{\psi Q}\} \neq 0, \quad (129)$$

Heat

$$\{R_T\}^e = [A_{TL}] \left\{ \frac{\partial \theta_L}{\partial t} \right\} + [A_{TV}] \left\{ \frac{\partial \theta_V}{\partial t} \right\} + [A_{TC}] \left\{ \frac{\partial C}{\partial t} \right\} - [B_{T\psi}] \{\psi\} + [B_{TT}] \{T\} - [B_{TC}] \{C\} + \{f_{TK}\} - \{f_{TQ}\} \neq 0, \quad (130)$$

Solute

$$\{R_C\}^e = [A_{CL}] \left\{ \frac{\partial \theta_L}{\partial t} \right\} + [A_{CV}] \left\{ \frac{\partial \theta_V}{\partial t} \right\} - [B_{C\psi}] \{\psi\} + [B_{CT}] \{T\} + [B_{CC}] \{C\} - \{f_{CQ}\} \neq 0, \quad (131)$$

where

$\{R_{\psi}\}$, $\{R_T\}$, and $\{R_C\}$ are residual vectors for the water, heat, and solute transport equations
[kg d⁻¹m⁻¹], [cal d⁻¹m⁻¹], [mol kg⁻¹m²d⁻¹];

$\{\psi\}$, $\{T\}$, and $\{C\}$ are element vectors of pressure head, temperature, and solute concentration [m], [°C⁻¹], [mol kg⁻¹];

$\left\{ \frac{\partial \theta_L}{\partial t} \right\}$, $\left\{ \frac{\partial \theta_V}{\partial t} \right\}$, $\left\{ \frac{\partial T}{\partial t} \right\}$, and $\left\{ \frac{\partial C}{\partial t} \right\}$ are element rate change vectors of liquid water, water vapor, temperature, and solute concentration [d⁻¹], [d⁻¹], [°C d⁻¹], [mol kg⁻¹ d⁻¹];

Water transport:

$[A_{\psi L}]$ and $[A_{\psi V}]$ are element liquid and vapor capacitance matrices [m²], [m²];

$[B_{\psi \psi}]$, $[B_{\psi T}]$, and $[B_{\psi C}]$ are element conductance matrices for pressure, temperature, and solute
[kg m⁻² d⁻¹], [kg m⁻¹ d⁻¹ °C⁻¹], [kg² mol⁻¹ m⁻¹ d⁻¹];

$\{f_{\psi K}\}$ and $\{f_{\psi Q}\} = \{f_{Lp}\} + \{f_{Ld}\}$ are element force vectors accounting for gravitational potential and point source [m²], [m²].

Heat transport:

$[A_{TL}]$, $[A_{TV}]$, and $[A_{TC}]$ are element liquid water and vapor capacitance matrices
[cal m⁻¹], [cal m⁻¹ °C⁻¹], [cal m⁻¹ kg mol⁻¹];

$[B_{\psi\psi}]$, $[B_{\psi T}]$, and $[B_{\psi C}]$ are element conductance matrices for pressure, temperature, and solute
 $[\text{m d}^{-1}]$, $[\text{m}^2 \text{d}^{-1} \text{°C}^{-1}]$, $[\text{m}^2 \text{d}^{-1} \text{mol kg}^{-1}]$;
 $\{f_{TK}\}$ and $\{f_{TQ}\} = \{f_{Tp}\} + \{f_{Td}\}$ are force vectors accounting for gravitational potential and point source
 $[\text{cal m}^{-1} \text{d}^{-1}]$, $[\text{cal m}^{-1} \text{d}^{-1}]$.

Solute transport:

$[A_{CL}] = C [A_{\psi L}]$, $[A_{CT}]$, and $[A_{CC}] = \mathbf{R} [A_{\psi L}]$ are element liquid water, vapor capacitance matrices
 $[\text{mol kg}^{-1} \text{m}^2]$, $[\text{cal m}^{-1} \text{°C}^{-1}]$, $[\text{m}^2]$;
 $[B_{C\psi}]$, $[B_{CT}]$, and $[B_{CC}]$ are element conductance matrices for pressure, temperature,
and solute $[\text{mol kg}^{-1} \text{m d}^{-1}]$, $[\text{mol kg}^{-1} \text{m}^2 \text{d}^{-1} \text{°C}^{-1}]$, $[\text{m}^2 \text{d}^{-1}]$;
and
 $\{f_{CQ}\} = \{f_{Cp}\} + \{f_{Cd}\}$ is an element force vector accounting for point source
 $[\text{mol kg}^{-1} \text{m}^2 \text{d}^{-1}]$.

Derivative Boundary Conditions, Point Sources and Sinks

The two types of field conditions that occur are called specified (Dirichlet) and derivative (Neumann) boundary conditions. Both of these conditions are embodied in the following generalized mathematical equation

$$D_x \frac{\partial \phi}{\partial x} \cos \theta + D_y \frac{\partial \phi}{\partial y} \sin \theta = -M\phi_b + S, \quad (132)$$

where

D_x , D_y are physical property coefficients oriented along the principal x- and y-directions,

ϕ is the dependent field variable,

ϕ_b is an unknown value on boundary Γ , and

M and S are coefficients that depend on the applied boundary condition and equation being solved.

In the present formulation, several coefficient combinations are permissible to account for water transport at or near the solution domain boundary. For example, the water transport equation parameters may include $\phi = \psi$ [m], $\phi_b = \psi_b$ [m], $M = q_m$ [m d^{-1}], $S = q_m \psi_0$, where q_m , ψ_b , and ψ_0 are the respective liquid water boundary flux (evaporation, percolation, and/or drainage) [m d^{-1}], boundary pressure head [m], and ambient (background) pressure head [m]. Sometimes letting the boundary flux and pressure head fluctuate based solely on the amount of liquid water present may be advantageous. This condition, known as the unit hydraulic gradient, is implemented assuming $\frac{\partial \phi}{\partial x} = 0$ and $\frac{\partial \phi}{\partial y} = 1$, which leads to $M\phi_b = K$, if $S=0$.

Heat can be carried vertically to, or away from, the boundary surface by turbulent bulk flow. This turbulent flow is proportional to the temperature difference between two distances (or heights). In this case, the heat transport equation parameters may include: $\phi = T$ [°C], $\phi_b = T_b$ [°C], $M = C_a h_H$ [$\text{cal m}^{-1} \text{°C}^{-1} \text{d}^{-1}$], $S = C_a h_H T_0$ [$\text{cal m}^{-2} \text{d}^{-1}$], where h_H and T_0 are the respective turbulent transfer (convection) coefficient [$\text{cm}^{-2} \text{d}^{-1}$] and ambient air temperature [°C]. Similarly, the parameters for solute convection to, or from, a surface may include: $\phi = C$ [mol kg^{-1}], $\phi_b = C_b$, [mol kg^{-1}], $M = q_m$ [m d^{-1}], and $S = q_m C_0$ [$\text{m d}^{-1} \text{mol kg}^{-1}$], where q_m [m d^{-1}] and C_0 [mol kg^{-1}] are the respective moisture flux and background solute concentration. According to van Genuchten and Alves (1982), application of the convection boundary conditions correctly evaluates volume-averaged solute concentration for semi-infinite field profiles. This assertion is assumed to hold for the more general case of mass and energy profiles. Also, in the case of impermeable and/or insulated boundaries, or on axes of symmetry ($M=S=0$), the boundary equation simplifies to

$$D_x \frac{\partial \phi}{\partial x} \cos \theta + D_y \frac{\partial \phi}{\partial y} \sin \theta = 0. \quad (133)$$

At boundaries of outflow of fluid, a requirement that must be satisfied is continuity of mass and energy. In the case of solute, $C_0 = C_e$, where C_0 and C_e are the respective initial and boundary exit concentrations. The addition of an extra unknown (C_e) leads to an indeterminate system of equations; therefore, an additional equation is needed to fully describe the ground-water system where solutes are present. One such equation is based on the intuitive assumption that solute concentration is continuous across the boundary, where $C(x,y,t) = C_e(t)$. Substitution of this equation into the general boundary equation leads to the frequently used zero concentration gradient boundary condition given by

$$D_x \frac{\partial C}{\partial x} \cos \theta + D_y \frac{\partial C}{\partial y} \sin \theta = 0. \quad (134)$$

This equation is based on the assumption that the concentration is macroscopically continuous (Danckwerts, 1953). A similar sequence of reasoning is assumed for both water and heat fluxes across outlet boundaries.

The inclusion of the derivative boundary condition into the finite-element analysis of field problems follows the procedure outlined by Segerlind (1984), where the general inter-element contribution $\{I\}^e$ is defined as

$$\{I\}^e = -\int_{\Gamma} [N]^T \left(D_x \frac{\partial \phi}{\partial x} \cos \theta + D_y \frac{\partial \phi}{\partial y} \sin \theta \right) d\Gamma. \quad (135)$$

For a triangular element, this represents the sum of integrals for all three sides, with integration performed around the element in a counterclockwise direction. Here, the interelement contributions are identified as those that originate from a domain and/or interior boundary. In this case, the two components are written as

$$\{I\}^e = \{I_{bc}\}^e + \{I_i\}^e, \quad (136)$$

where

$\{I_{bc}\}^e$ and $\{I_i\}^e$ are the respective vector boundary and interior contributions with $\{I_i\}^e$ is a vector of zeros because of flux cancellations across interior boundaries (equal and opposite signs).

The boundary contribution is evaluated as

$$\{I\}_{bc}^e = -\int_{\Gamma_{bc}} [N]^T D_x \frac{\partial \phi}{\partial x} \cos \theta + D_y \frac{\partial \phi}{\partial y} \sin \theta = M\phi_b + S. \quad (137)$$

Substituting

$$\{I_{bc}\}^e = -\int_{\Gamma_{bc}} [N]^T (M\phi_b - S) d\Gamma, \quad (138)$$

into equation 137 and then substituting

$$\phi^e = [N]\{\phi\}^e \quad (139)$$

results in

$$\{I_{bc}\}^e = \left(\int_{\Gamma_{bc}} M[N]^T [N] d\Gamma \right) - \int_{\Gamma_{bc}} S[N]^T d\Gamma. \quad (140)$$

A similar operation is conducted for $\{I_i\}^e$ but after summarizing contributions across element boundaries from opposite directions, the net result is to cancel the contribution. This equation can be simplified as the following equation

$$\{I_{bc}\}^e = [k_M]\{\phi\} - \{f_S\}, \quad (141)$$

where

$$[k_M]^e = \int_{\Gamma_{bc}} M[N]^T [N] d\Gamma \quad \text{and} \quad (142)$$

$$\{f_S\}^e = \int_{\Gamma_{bc}} S[N]^T d\Gamma. \quad (143)$$

Considering a lumped mass approach, evaluation of these two integrals (eqs. 142-143) leads to

$$[k_M]^e = \frac{ML_{ij}}{2} \begin{bmatrix} 1 & 0 & 0 \\ 0 & 1 & 0 \\ 0 & 0 & 0 \end{bmatrix} + \frac{ML_{ik}}{2} \begin{bmatrix} 1 & 0 & 0 \\ 0 & 0 & 0 \\ 0 & 0 & 1 \end{bmatrix} + \frac{ML_{jk}}{2} \begin{bmatrix} 0 & 0 & 0 \\ 0 & 1 & 0 \\ 0 & 1 & 0 \end{bmatrix}, \quad (144)$$

$$f_S^e = \frac{SL_{ij}}{2} \begin{bmatrix} 1 \\ 1 \\ 0 \end{bmatrix} + \frac{SL_{ik}}{2} \begin{bmatrix} 1 \\ 0 \\ 1 \end{bmatrix} + \frac{SL_{jk}}{2} \begin{bmatrix} 0 \\ 1 \\ 1 \end{bmatrix}, \quad (145)$$

where L_{ij} , L_{ik} , and L_{jk} are lengths along sides of the element between nodes ij , ik , and jk . Because fluxes from adjoining elements cancel across interior boundaries, those terms that do not have a length along an exterior domain boundary drop out of equations 144-145.

Solution Procedure

In this section, the procedure used in VST2D to numerically solve the coupled water-heat-solute transport problem is described. In general, the numerical solution procedure requires time discretization of the previously derived matrix-vector relation, incorporation of derivative boundary and initial conditions, point sources and sinks, quasi-linearizing the system of equations by Picard iteration, consideration of Peclet and Courant numbers to avoid numerical oscillations, and matrix solution. In the following sections, each of these topics is discussed in more detail.

Time Discretization

To solve the time-dependent transport problem, an implicit (or backward) finite-difference approach is used because this approach is unconditionally stable and convergent. In this case, the formulation is developed with k and m representing time step and iteration number, respectively. Multiplying by the time derivative and collecting like terms results in residual equations for water, heat, and solute given by

Water

$$\begin{aligned} \{R_\psi\}^{e^{k+1,m+1}} &= \rho_L \Lambda [A_{\psi L}]^{k+1,m} \{\theta_L^{k+1,m+1} - \theta_L^k\} + \rho_L [A_{\psi V}]^{k+1,m} \{\theta_V^{k+1,m+1} - \theta_V^k\} \\ &+ \Delta t [B_{\psi \psi}]^{k+1,m} \{\psi\}^{k+1,m+1} + \Delta t [B_{\psi T}]^{k+1,m} \{T\}^{k+1,m+1} - \Delta t [B_{\psi C}]^{k+1,m} \{C\}^{k+1,m+1} + \Delta t \{f_{\psi K}\}^{k+1,m} \\ &- \Delta t \{f_{\psi Q}\}^{k+1,m} \neq 0, \end{aligned} \quad (146)$$

Heat

$$\begin{aligned} \{R_T\}^{e^{k+1,m+1}} &= [A_{TL}]^{k+1,m} \{\theta_L^{k+1,m+1} - \theta_L^k\} + [A_{TT}]^{k+1,m} \{T^{k+1,m+1} - T^k\} \\ &+ [A_{TC}]^{k+1,m} \{C^{k+1,m+1} - C^k\} - \Delta t [B_{T\psi}]^{k+1,m} \{\psi\}^{k+1,m+1} + \Delta t [B_{TT}]^{k+1,m} \{T\}^{k+1,m} \\ &- \Delta t [B_{TC}]^{k+1,m} \{C\}^{k+1,m+1} + \Delta t \{f_{TK}\}^{k+1,m} - \Delta t \{f_{TQ}\}^{k+1,m} \neq 0, \text{ and} \end{aligned} \quad (147)$$

Solute

$$\begin{aligned} \{R_C\}^{e^{k+1,m+1}} &= [A_{CL}]^{k+1,m} \{\theta_L^{k+1,m+1} - \theta_L^k\} + [A_{CC}]^{k+1,m} \{C^{k+1,m+1} - C^k\} \\ &- \Delta t [B_{C\psi}]^{k+1,m} \{\psi\}^{k+1,m+1} + \Delta t [B_{CT}]^{k+1,m} \{T\}^{k+1,m+1} + \Delta t [B_{CC}]^{k+1,m} \{C\}^{k+1,m+1} \\ &- \Delta t \{f_{CQ}\}^{k+1,m} \neq 0. \end{aligned} \quad (148)$$

Due to the nonlinear relation between coefficients dependent and variables, a Taylor series expansion is applied to the corresponding rate change of dependent variables in the governing transport equations. In turn, their corresponding matrix-vector formulation is incorporated into the numerical model to achieve satisfactory mass and energy balance. For example, consider the liquid-water derivative $\partial\theta_L$ (appearing in each of the governing equations) defined as

$$\partial\theta_L = (\theta_L^{k+1,m+1} - \theta_L^k). \quad (149)$$

Expanding $\theta^{k+1,m+1}$ by Taylor series and neglecting higher order terms gives

$$\begin{aligned} \theta_L^{k+1,m+1} &\cong \theta_L^{k+1,m} + \frac{\partial\theta_L}{\partial\psi} \Big|^{k+1,m} (\psi^{k+1,m+1} - \psi^{k+1,m}) \\ &+ \frac{\partial\theta_L}{\partial T} \Big|^{k+1,m} (T^{k+1,m+1} - T^{k+1,m}) + \frac{\partial\theta_L}{\partial C} \Big|^{k+1,m} (C^{k+1,m+1} - C^{k+1,m}). \end{aligned} \quad (150)$$

After a change in variables ($C_\psi = \partial\theta_L/\partial\psi$), substituting this result back into equation 149 gives

$$\begin{aligned} \partial\theta_L \cong & (\theta_L^{k+1,m+1} - \theta_L^{k+1,m}) + C_\psi \psi^{k+1,m+1} - C_\psi \psi^{k+1,m} + \frac{\partial\theta_L^{k+1,m}}{\partial T} T^{k+1,m+1} \\ & - \frac{\partial\theta_L^{k+1,m}}{\partial T} T^{k+1,m} + \frac{\partial\theta_L^{k+1,m}}{\partial C} C^{k+1,m+1} - \frac{\partial\theta_L}{\partial C} C^{k+1,m}. \end{aligned} \quad (151)$$

Application of this expansion to the liquid derivative term in equation 146 results in an equivalent matrix-vector formulation expressed as

$$\begin{aligned} \rho_L \Lambda [A_{\psi L}]^{k+1,m} \{ \theta_L^{k+1,m+1} - \theta_L^k \} &= \rho_L \Lambda [A_{\psi L}]^{k+1,m} \{ \Delta\theta_L \}^{k+1,m} + \rho_L \Lambda C_\psi [A_{\psi L}]^{k+1,m} \{ \psi \}^{k+1,m+1} \\ &- \rho_L \Lambda C_\psi [A_{\psi L}]^{k+1,m} \{ \psi \}^{k+1,m} + \rho_L \Lambda \frac{\partial\theta_L}{\partial T} [A_{\psi L}]^{k+1,m} \{ T \}^{k+1,m+1} - \rho_L \Lambda \frac{\partial\theta_L}{\partial T} [A_{\psi L}]^{k+1,m} \{ T \}^{k+1,m} \\ &+ \rho_L \Lambda \frac{\partial\theta_L}{\partial C} [A_{\psi L}]^{k+1,m} \{ C \}^{k+1,m+1} - \rho_L \Lambda \frac{\partial\theta_L}{\partial C} [A_{\psi L}]^{k+1,m} \{ C \}^{k+1,m}. \end{aligned} \quad (152)$$

Simplifying this expression gives

$$\begin{aligned} \rho_L \Lambda [A_{\psi L}]^{k+1,m} \{ \theta_L^{k+1,m+1} - \theta_L^k \} &= \{ f_{\psi L} \}^{k+1,m} + [A_{\psi\psi}]^{k+1,m} \{ \psi \}^{k+1,m+1} \\ &- \{ f_{\psi\psi} \}^{k+1,m} + [A_{\psi TL}] \{ T \}^{k+1,m+1} - \{ f_{\psi TL} \}^{k+1,m} + [A_{\psi CL}]^{k+1,m} \{ C \}^{k+1,m+1} - \{ f_{\psi CL} \}^{k+1,m}, \end{aligned} \quad (153)$$

where

$$\begin{aligned} [A_{\psi\psi}]^{k+1,m} &= \rho_L \Lambda C_\psi [A_{\psi L}]^{k+1,m} \text{ is an element capacitance matrix resulting from expansion of the change in liquid-water about pressure head [kg m}^{-2}\text{];} \\ \{ f_{\psi L} \}^{k+1,m} &= \rho_L \Lambda [A_{\psi L}]^{k+1,m} \{ \Delta\theta_L \}^{k+1,m} \text{ and} \\ \{ f_{\psi\psi} \}^{k+1,m} &= [A_{\psi\psi}]^{k+1,m} \{ \psi \}^{k+1,m} \text{ are force vectors resulting from the expansion of change in liquid water about pressure head [kg m}^{-1}\text{];} \\ \{ \Delta\theta_L \}^{k+1,m} &= \{ \theta_L^{k+1,m} - \theta_L^k \} [A_{\psi TL}]^{k+1,m} = \rho_L \Lambda \frac{\partial\theta_L}{\partial T} [A_{\psi L}]^{k+1,m} \text{ is an element capacitance matrix resulting from expansion of the change in liquid-water about temperature [kg m}^{-1} \text{ }^\circ\text{C}^{-1}\text{];} \\ [f_{\psi TL}]^{k+1,m} &= [A_{\psi TL}]^{k+1,m} \{ T \}^{k+1,m} \text{ is a force vector resulting from the expansion of change in liquid water about temperature [kg m}^{-1}\text{];} \\ [A_{\psi CL}]^{k+1,m} &= \rho_L \Lambda \frac{\partial\theta_L}{\partial C} [A_{\psi L}]^{k+1,m} \text{ is an element capacitance matrix resulting from expansion of the change in liquid-water about concentration [kg}^2 \text{ m}^{-1} \text{ mol}^{-1}\text{]; and} \\ [f_{\psi CL}]^{k+1,m} &= [A_{\psi CL}]^{k+1,m} \{ C \}^{k+1,m} \text{ is a force vector resulting from the expansion of change in liquid-water about concentration [kg m}^{-1}\text{].} \end{aligned}$$

Similar expressions are obtained for Taylor series expansion of the liquid derivatives appearing in the heat and solute equations; the only difference is these terms are scaled by heat and solute related coefficients instead of storativity. For example, $\{ f_{T\psi} \}^{k+1,m} = [A_{T\psi}]^{k+1,m} \{ \psi \}^{k+1,m}$ [cal m⁻¹] and $\{ f_{TL} \}^{k+1,m} = [A_{TL}]^{k+1,m} \{ \Delta\theta_L \}^{k+1,m}$ [cal m⁻¹] are force vectors for heat transport equations, where $[A_{T\psi}]^{k+1,m} = f_2 [A_{\psi\psi}]^{k+1,m}$ and $[A_{TL}]^{k+1,m} = f_2 [A_{\psi L}]^{k+1,m}$, $\{ f_{CC} \}^{k+1,m} = [A_{CC}]^{k+1,m} \{ C \}^{k+1,m}$ [m²], $\{ f_{C\psi} \}^{k+1,m} = [A_{C\psi}]^{k+1,m} \{ \psi \}^{k+1,m}$ [mol kg⁻¹ m], and $\{ f_{CL} \}^{k+1,m} = [A_{CL}]^{k+1,m} \{ \Delta\theta_L \}^{k+1,m}$ [mol kg⁻¹ m²] are force vectors for solute transport equations, where $[A_{C\psi}]^{k+1,m} = C [A_{\psi\psi}]^{k+1,m}$.

Next, the water vapor derivative associated with rate change in the water transport equation is expanded using a Taylor series given by

$$\begin{aligned} \theta_V^{k+1, m+1} &\equiv \theta_V^{k+1, m} + \left. \frac{\partial \theta_V}{\partial \psi} \right|^{k+1, m} (\psi^{k+1, m+1} - \psi^{k+1, m}) + \left. \frac{\partial \theta_V}{\partial T} \right|^{k+1, m} (T^{k+1, m+1} - T^{k+1, m}) \\ &+ \left. \frac{\partial \theta_V}{\partial C} \right|^{k+1, m} (C^{k+1, m+1} - C^{k+1, m}), \end{aligned} \quad (154)$$

$$\begin{aligned} \partial \theta_V &\equiv (\theta_V^{k+1, m} - \theta_V^k) + \frac{\partial \theta_V^{k+1, m}}{\partial \psi} \psi^{k+1, m+1} - \frac{\partial \theta_V^{k+1, m}}{\partial \psi} \psi^{k+1, m} + \frac{\partial \theta_V^{k+1, m}}{\partial T} T^{k+1, m+1} \\ &- \frac{\partial \theta_V^{k+1, m}}{\partial T} T^{k+1, m} + \frac{\partial \theta_V^{k+1, m}}{\partial C} C^{k+1, m+1} - \frac{\partial \theta_V^{k+1, m}}{\partial C} C^{k+1, m}. \end{aligned} \quad (155)$$

The corresponding matrix-vector formulations for the water vapor derivative in equation 146 can now be written as

$$\begin{aligned} \rho_L [A_{\psi V}]^{k+1, m} \{ \theta_V^{k+1, m+1} - \theta_V^k \} &= \{ f_{\psi V} \}^{k+1, m} + [A_{\psi V}]^{k+1, m} \{ \psi \}^{k+1, m+1} \\ &- \{ f_{\psi V \psi} \}^{k+1, m} + [A_{\psi TV}]^{k+1, m} \{ T \}^{k+1, m+1} \\ &- \{ f_{\psi TV} \}^{k+1, m} + [A_{\psi LV}]^{k+1, m} \{ C \}^{k+1, m+1} - \{ f_{\psi CV} \}^{k+1, m} \end{aligned} \quad (156)$$

where

$[A_{\psi V}]^{k+1, m} = \rho_L \frac{\partial \theta_V}{\partial \psi} [A_{\psi L}]^{k+1, m}$ is an element capacitance matrix resulting from expansion of the change in water vapor about pressure head [kg m⁻²],

$\frac{\partial V}{\partial \psi} \equiv \rho_s \rho_L^{-1} C_\psi (S^{-1} - 1)$ is a vapor capacitance term [m⁻¹],

$\{ f_{\psi V} \}^{k+1, m} = \rho_L [A_{\psi L}]^{k+1, m} \{ \Delta \theta_V \}^{k+1, m}$ and

$\{ f_{\psi V \psi} \}^{k+1, m} = \rho_L [A_{\psi V}]^{k+1, m} \{ \psi \}^{k+1, m}$ are force vectors resulting from the expansion of a change in water vapor about pressure head [kg m⁻¹],

$\{ \Delta \theta_V \}^{k+1, m} = \{ \theta_V^{k+1, m} - \theta_V^k \} [A_{\psi TV}]^{k+1, m} = \rho_L \frac{\partial \theta_V}{\partial T} [A_{\psi L}]$ is an element capacitance matrix resulting from expansion of the change in water vapor about temperature [kg m⁻¹ °C⁻¹],

$\{ f_{\psi TV} \}^{k+1, m} = [A_{\psi TV}]^{k+1, m} \{ T \}^{k+1, m}$ is a force vector resulting from the expansion of change in water vapor about temperature [kg m⁻¹],

$[A_{\psi CV}]^{k+1, m} = \rho_L \frac{\partial \theta_V}{\partial C} [A_{\psi L}]$ is an element capacitance matrix resulting from expansion of the change in water vapor about concentration [kg² m⁻¹ mol⁻¹], and

$\{ f_{\psi CV} \}^{k+1, m} = [A_{\psi CV}]^{k+1, m} \{ C \}^{k+1, m}$ is a force vector resulting from the expansion of change in water vapor about concentration [kg m⁻¹].

The remaining rate change derivatives occurring in the heat equation ($f_1\partial T, f_3\partial C$) are determined by applying a Taylor series expansion of heat content about temperature and concentration

$$H^{k+1, m+1} \cong H^{k+1, m} + \left. \frac{\partial H}{\partial T} \right|^{k+1, m} (T^{k+1, m+1} - T^{k+1, m}) + \left. \frac{\partial H}{\partial C} \right|^{k+1, m} (C^{k+1, m+1} - C^{k+1, m}), \quad (157)$$

$$\partial H \cong (H^{k+1, m} - H^k) + \frac{\partial H^{k+1, m}}{\partial T} T^{k+1, m+1} - \frac{\partial H^{k+1, m}}{\partial T} T^{k+1, m} + \frac{\partial H^{k+1, m}}{\partial C} C^{k+1, m+1} - \frac{\partial H^{k+1, m}}{\partial C} C^{k+1, m}, \quad (158)$$

The corresponding matrix-vector formulations for the heat content derivatives are then written as

$$[A_{\Psi L}]^{k+1, m} \{H^{k+1, m+1} - H^k\} = \{f_{TH}\}^{k+1, m} + [A_{TT}]^{k+1, m} \{T\}^{k+1, m+1} - \{f_{TT}\}^{k+1, m}, \quad (159)$$

$$[A_{\Psi L}]^{k+1, m} \{C^{k+1, m+1} - C^k\} = \{f_{TC}\}^{k+1, m} + [A_{TC}]^{k+1, m} \{T\}^{k+1, m+1} - \{f_{TCH}\}^{k+1, m}, \quad (160)$$

where

$[A_{TT}]^{k+1, m} = dH/dT [A_{\Psi L}]^{k+1, m}$ is an element capacitance matrix resulting from an expansion of the change in heat content with temperature [cal m⁻¹ °C⁻¹],

$dH/dT \cong f_1$ is the global heat capacity (assumes that small changes in heat content are approximately linear with temperature) [cal m⁻³ °C⁻¹],

$\{f_{TH}\}^{k+1, m} = [A_{\Psi L}]^{k+1, m} \{\Delta H\}^{k+1, m}$ [cal m⁻¹] and $\{f_{TT}\}^{k+1, m} = [A_{TT}]^{k+1, m} \{T\}^{k+1, m}$ [cal m⁻¹] are force vectors resulting from the expansion of a change in heat content with temperature for application to the heat transport equation,

$[A_{TC}]^{k+1, m} = dH/dC [A_{\Psi L}]^{k+1, m}$ is an element capacitance matrix resulting from expansion of the change in heat content with concentration [cal m⁻¹ kg mol⁻¹],

$dH/dC \cong f_3$ is a global latent heat term (assumes that small changes in heat content are approximately linear with concentration) [cal m⁻³ kg mol⁻¹],

$\{f_{TC}\}^{k+1, m} = [A_{\Psi L}]^{k+1, m} \{\Delta H\}^{k+1, m}$ [cal m⁻¹] and $\{f_{TCH}\}^{k+1, m} = [A_{TC}]^{k+1, m} \{C\}^{k+1, m}$ [cal m⁻¹] are force vectors resulting from an expansion of the change in heat content with concentration for application to the heat transport equation.

Lastly, the rate change derivative for concentration in the solute equation ($R\partial C$) is determined by applying a Taylor series expansion about the total solute mass (dissolved and sorbed) as

$$M_C^{k+1, m+1} \cong M_C^{k+1, m} + \left. \frac{\partial M_C}{\partial C} \right|^{k+1, m} (C^{k+1, m+1} - C^{k+1, m}), \quad (161)$$

$$\partial M_C = (M_C^{k+1, m} - M_C^k) + \frac{\partial M_C^{k+1, m}}{\partial C} C^{k+1, m+1} - \frac{\partial M_C^{k+1, m}}{\partial C} C^{k+1, m}. \quad (162)$$

The equivalent matrix-vector formulation then becomes

$$[A_{\Psi L}]^{k+1,m} \{M_C^{k+1,m+1} - M_C^k\} = \{f_{CM}\}^{k+1,m} + [A_{CC}]^{k+1,m} \{C\}^{k+1,m+1} - \{f_{CMC}\}^{k+1,m}, \quad (163)$$

where

M_C is the total solute mass [mol kg⁻¹],
 $[A_{CC}] = dM_C/dC [A_{\Psi L}]$ is a capacitance matrix resulting from an expansion of the change in mass with concentration [m²],
 $dM_C/dC \cong \mathbf{R}$, is a retardation factor (assumes that small changes in total solute content is approximately linear with concentration) [dimensionless],
 $\{f_{CM}\}^{k+1,m} = [A_{\Psi L}]^{k+1,m} \{\Delta M_C\}^{k+1,m}$ [m² mol kg⁻¹] and
 $\{f_{CMC}\}^{k+1,m} = [A_{CC}]^{k+1,m} \{C\}^{k+1,m}$ [m² mol kg⁻¹] are force vectors resulting from the expansion of a change in total solute mass with concentration for application to the water transport equation.

These matrix-vector expansions are included and the overall expression is rearranged with new and old time steps grouped on the left- and right-hand-sides, respectively. The final residual equations are written for water, heat, and solute transport as

Water

$$\begin{aligned} & ([A_{\Psi\Psi}]^{k+1,m} + [A_{\Psi V}]^{k+1,m} + \Delta t [B_{\Psi\Psi}]^{k+1,m}) \{\Psi\}^{k+1,m+1} \\ & + \Delta t B_{\Psi T}^{k+1,m} \{T\}^{k+1,m+1} - \Delta t [B_{\Psi C}]^{k+1,m} \{C\}^{k+1,m+1} = \{f_{\Psi V}\}^{k+1,m} + \{f_{\Psi\Psi}\}^{k+1,m} - \{f_{\Psi L}\}^{k+1,m} \\ & + \{f_{\Psi V\Psi}\}^{k+1,m} - \{f_{\Psi V}\}^{k+1,m} - \Delta t \{f_{\Psi K}\}^{k+1,m} + \Delta t \{f_{\Psi Q}\}^{k+1,m}, \end{aligned} \quad (164)$$

Heat

$$\begin{aligned} & ([A_{T\Psi}]^{k+1,m} - \Delta t [B_{T\Psi}]^{k+1,m}) \{\Psi\}^{k+1,m+1} + ([A_{TT}]^{k+1,m} + \Delta t [B_{TT}]^{k+1,m}) \{T\}^{k+1,m+1} \\ & + ([A_{TC}]^{k+1,m} - \Delta t [B_{TC}]^{k+1,m}) \{C\}^{k+1,m+1} = \{f_{TT}\}^{k+1,m} + \{f_{TC}\}^{k+1,m} + \{f_{T\Psi}\}^{k+1,m} - \{f_{TH}\}^{k+1,m} \\ & - \{f_{TCH}\}^{k+1,m} - \{f_{TL}\}^{k+1,m} - \Delta t \{f_{TK}\}^{k+1,m} + \Delta t \{f_{TQ}\}^{k+1,m}, \end{aligned} \quad (165)$$

Solute

$$\begin{aligned} & ([A_{C\Psi}]^{k+1,m} - \Delta t [B_{C\Psi}]^{k+1,m}) \{\Psi\}^{k+1,m+1} + \Delta t [B_{CT}]^{k+1,m+1} \{T\}^{k+1,m+1} \\ & + ([A_{CC}]^{k+1,m} + \Delta t [B_{CC}]^{k+1,m}) \{C\}^{k+1,m+1} \\ & = \{f_{CC}\}^{k+1,m} + [f_{\Psi V}]^{k+1,m} + \{f_{C\Psi}\}^{k+1,m} - \{f_{CM}\}^{k+1,m} - \{f_{CL}\}^{k+1,m} + \Delta t \{f_{CQ}\}^{k+1,m}. \end{aligned} \quad (166)$$

Combined Element Matrices and Vectors

On an elemental basis, the residual equations 166-168 now assume the familiar matrix-vector form $[M]^e \{x\}^e = \{b\}^e$, where

$$\begin{aligned}
 [M]^e = & \Delta t \begin{bmatrix} B_{\Psi\Psi_{ii}} & B_{\Psi T_{ii}} & -B_{\Psi C_{ii}} & B_{\Psi\Psi_{ij}} & B_{\Psi T_{ij}} & -B_{\Psi C_{ij}} & B_{\Psi\Psi_{ik}} & B_{\Psi T_{ik}} & -B_{\Psi C_{ik}} \\ -B_{T\Psi_{ii}} & B_{TT_{ii}} & -B_{TC_{ii}} & -B_{T\Psi_{ij}} & B_{TT_{ij}} & -B_{TC_{ij}} & -B_{T\Psi_{ik}} & B_{TT_{ik}} & -B_{TC_{ik}} \\ -B_{C\Psi_{ii}} & B_{CT_{ii}} & B_{CC_{ii}} & -B_{C\Psi_{ij}} & B_{CT_{ij}} & B_{CC_{ij}} & -B_{C\Psi_{ik}} & B_{CT_{ik}} & B_{CC_{ik}} \\ B_{\Psi\Psi_{ji}} & B_{\Psi T_{ji}} & -B_{\Psi C_{ji}} & B_{\Psi\Psi_{jj}} & B_{\Psi T_{jj}} & -B_{\Psi C_{jj}} & B_{\Psi\Psi_{jk}} & B_{\Psi T_{jk}} & -B_{\Psi C_{jk}} \\ -B_{T\Psi_{ji}} & B_{TT_{ji}} & -B_{TC_{ji}} & -B_{T\Psi_{jj}} & B_{TT_{jj}} & -B_{TC_{jj}} & -B_{T\Psi_{jk}} & B_{TT_{jk}} & -B_{TC_{jk}} \\ -B_{C\Psi_{ji}} & B_{CT_{ji}} & B_{CC_{ji}} & -B_{C\Psi_{jj}} & B_{CT_{jj}} & B_{CC_{jj}} & -B_{C\Psi_{jk}} & B_{CT_{jk}} & B_{CC_{jk}} \\ B_{\Psi\Psi_{ki}} & B_{\Psi T_{ki}} & -B_{\Psi C_{ki}} & B_{\Psi\Psi_{kj}} & B_{\Psi T_{kj}} & -B_{\Psi C_{kj}} & B_{\Psi\Psi_{kk}} & B_{\Psi T_{kk}} & -B_{\Psi C_{kk}} \\ -B_{T\Psi_{ki}} & B_{TT_{ki}} & -B_{TC_{ki}} & -B_{T\Psi_{kj}} & B_{TT_{kj}} & -B_{TC_{kj}} & -B_{T\Psi_{kk}} & B_{TT_{kk}} & -B_{TC_{kk}} \\ -B_{C\Psi_{ki}} & B_{CT_{ki}} & B_{CC_{ki}} & -B_{C\Psi_{kj}} & B_{CT_{kj}} & B_{CC_{kj}} & -B_{C\Psi_{kk}} & B_{CT_{kk}} & B_{CC_{kk}} \end{bmatrix} \\
 + & \begin{bmatrix} A_{\Psi\Psi_{ii}} + A_{\Psi V_{ii}} & 0 & 0 & 0 & 0 & 0 & 0 & 0 & 0 \\ A_{T\Psi_{ii}} & A_{TT_{ii}} & A_{TC_{ii}} & 0 & 0 & 0 & 0 & 0 & 0 \\ A_{C\Psi_{ii}} & 0 & A_{CC_{ii}} & 0 & 0 & 0 & 0 & 0 & 0 \\ 0 & 0 & 0 & A_{\Psi\Psi_{jj}} + A_{\Psi V_{jj}} & 0 & 0 & 0 & 0 & 0 \\ 0 & 0 & 0 & A_{T\Psi_{jj}} & A_{TT_{jj}} & A_{TC_{jj}} & 0 & 0 & 0 \\ 0 & 0 & 0 & A_{C\Psi_{jj}} & 0 & A_{CC_{jj}} & 0 & 0 & 0 \\ 0 & 0 & 0 & 0 & 0 & 0 & A_{\Psi\Psi_{kk}} + A_{\Psi V_{kk}} & 0 & 0 \\ 0 & 0 & 0 & 0 & 0 & 0 & A_{T\Psi_{kk}} & A_{TT_{kk}} & A_{TC_{kk}} \\ 0 & 0 & 0 & 0 & 0 & 0 & A_{C\Psi_{kk}} & 0 & A_{CC_{kk}} \end{bmatrix} \\
 \{x\}^e = & \begin{bmatrix} \Psi_i \\ T_i \\ C_i \\ \Psi_j \\ T_j \\ C_j \\ \Psi_k \\ T_k \\ C_k \end{bmatrix} \quad \{b\}^e = \begin{bmatrix} F_{\Psi_i} = f_{\Psi\Psi_i} - f_{\Psi L_i} + f_{\Psi V_i} - f_{\Psi V\Psi_i} - \Delta t(f_{\Psi K_i} - f_{\Psi Q_i}) \\ F_{T_i} = f_{TT_i} + f_{TC_i} - f_{T\Psi_i} - f_{TH_i} - f_{TCH_i} - f_{TL_i} - \Delta t(f_{TK_i} - f_{TQ_i}) \\ F_{C_i} = f_{CC_i} + f_{C\Psi_i} - f_{CL_i} - f_{CM_i} + \Delta t f_{CQ_i} \\ F_{\Psi_j} = f_{\Psi\Psi_j} - f_{\Psi L_j} + f_{\Psi V_j} - f_{\Psi V\Psi_j} - \Delta t(f_{\Psi K_j} - f_{\Psi Q_j}) \\ F_{T_j} = f_{TT_j} + f_{TC_j} + f_{T\Psi_j} - f_{TH_j} - f_{TCH_j} - f_{TL_j} - \Delta t(f_{TK_j} - f_{TQ_j}) \\ F_{C_j} = f_{CC_j} + f_{C\Psi_j} - f_{CL_j} - f_{CM_j} + \Delta t f_{CQ_j} \\ F_{\Psi_k} = f_{\Psi\Psi_k} - f_{\Psi L_k} + f_{\Psi V_k} - f_{\Psi V\Psi_k} - \Delta t(f_{\Psi K_k} - f_{\Psi Q_k}) \\ F_{T_k} = f_{TT_k} + f_{TC_k} + f_{T\Psi_k} - f_{TH_k} - f_{TCH_k} - f_{TL_k} - \Delta t(f_{TK_k} - f_{TQ_k}) \\ F_{C_k} = f_{CC_k} + f_{\Psi V_k} + f_{C\Psi_k} - f_{CL_k} - f_{CM_k} + \Delta t f_{CQ_k} \end{bmatrix}. \quad (167)
 \end{aligned}$$

The final form of the global matrix becomes

$$\begin{bmatrix}
 M_{\psi\psi_{11}} & M_{\psi T_{11}} & M_{\psi C_{11}} & M_{\psi\psi_{12}} & M_{\psi T_{12}} & M_{\psi C_{12}} & M_{\psi\psi_{13}} & M_{\psi T_{13}} & M_{\psi C_{13}} & \cdots & M_{\psi C_{1N}} \\
 M_{T\psi_{11}} & M_{TT_{11}} & M_{TC_{11}} & M_{T\psi_{12}} & M_{TT_{12}} & M_{TC_{12}} & M_{T\psi_{13}} & M_{TT_{13}} & M_{TC_{13}} & \cdots & M_{TC_{1N}} \\
 M_{C\psi_{11}} & M_{CT_{11}} & M_{CC_{11}} & M_{C\psi_{12}} & M_{CT_{12}} & M_{CC_{12}} & M_{C\psi_{13}} & M_{CT_{13}} & M_{CC_{13}} & \cdots & M_{CC_{1N}} \\
 M_{\psi\psi_{21}} & M_{\psi T_{21}} & M_{\psi C_{21}} & M_{\psi\psi_{22}} & M_{\psi T_{22}} & M_{\psi C_{22}} & M_{\psi\psi_{23}} & M_{\psi T_{23}} & M_{\psi C_{23}} & \cdots & M_{\psi C_{2N}} \\
 M_{T\psi_{21}} & M_{TT_{21}} & M_{TC_{21}} & M_{T\psi_{22}} & M_{TT_{22}} & M_{TC_{22}} & M_{T\psi_{23}} & M_{TT_{23}} & M_{TC_{23}} & \cdots & M_{TC_{2N}} \\
 M_{C\psi_{21}} & M_{CT_{21}} & M_{CC_{21}} & M_{C\psi_{22}} & M_{CT_{22}} & M_{CC_{22}} & M_{C\psi_{23}} & M_{CT_{23}} & M_{CC_{23}} & \cdots & M_{CC_{2N}} \\
 M_{\psi\psi_{31}} & M_{\psi T_{31}} & M_{\psi C_{31}} & M_{\psi\psi_{32}} & M_{\psi T_{32}} & M_{\psi C_{32}} & M_{\psi\psi_{33}} & M_{\psi T_{33}} & M_{\psi C_{33}} & \cdots & M_{\psi C_{3N}} \\
 M_{T\psi_{31}} & M_{TT_{31}} & M_{TC_{31}} & M_{T\psi_{32}} & M_{TT_{32}} & M_{TC_{32}} & M_{T\psi_{33}} & M_{TT_{33}} & M_{TC_{33}} & \cdots & M_{TC_{3N}} \\
 M_{C\psi_{31}} & M_{CT_{31}} & M_{CC_{31}} & M_{C\psi_{32}} & M_{CT_{32}} & M_{CC_{32}} & M_{C\psi_{33}} & M_{CT_{33}} & M_{CC_{33}} & \cdots & M_{CC_{3N}} \\
 \vdots & \vdots & \vdots & \vdots & \vdots & \vdots & \vdots & \vdots & \vdots & \cdots & \vdots \\
 \vdots & \vdots & \vdots & \vdots & \vdots & \vdots & \vdots & \vdots & \vdots & \cdots & \vdots \\
 \vdots & \vdots & \vdots & \vdots & \vdots & \vdots & \vdots & \vdots & \vdots & \cdots & \vdots \\
 M_{C\psi_{N1}} & M_{CT_{N1}} & M_{CC_{N1}} & M_{C\psi_{N2}} & M_{CT_{N2}} & M_{CC_{N2}} & M_{C\psi_{N3}} & M_{CT_{N3}} & M_{CC_{N3}} & \cdots & M_{C\psi_{NN}}
 \end{bmatrix}
 \begin{Bmatrix}
 \psi_1 \\
 T_1 \\
 C_1 \\
 \psi_2 \\
 T_2 \\
 C_2 \\
 \psi_3 \\
 T_3 \\
 C_3 \\
 \vdots \\
 \psi_N \\
 T_N \\
 C_N
 \end{Bmatrix}
 =
 \begin{Bmatrix}
 b_{\psi_1} \\
 b_{T_1} \\
 b_{C_1} \\
 b_{\psi_2} \\
 b_{T_2} \\
 b_{C_2} \\
 b_{\psi_3} \\
 b_{T_3} \\
 b_{C_3} \\
 \vdots \\
 b_{\psi_N} \\
 b_{T_N} \\
 b_{C_N}
 \end{Bmatrix}, \quad (169)$$

where

M 's are the global three-node element conductance-type coefficients: $M_{\psi\psi}$ [kg m^{-2}],
 $M_{\psi T}$ [$\text{kg m}^{-1} \text{ }^\circ\text{C}^{-1}$], $M_{\psi C}$ [mol m^{-1}], $M_{T\psi}$ [cal m^{-2}], M_{TT} [$\text{cal m}^{-1} \text{ }^\circ\text{C}^{-1}$],
 M_{TC} [$\text{cal kg m}^{-1} \text{ mol}^{-1}$], $M_{C\psi}$ [m mol kg^{-1}], M_{CT} [$\text{m}^2 \text{ mol kg}^{-1} \text{ }^\circ\text{C}^{-1}$],
 M_{CC} [m^2];
 b 's are the global three-node forcing coefficients: b_ψ [kg m^{-1}], b_T [cal m^{-1}],
 b_C [$\text{m}^2 \text{ mol kg}^{-1}$]; and

subscripts ψ , T , C ; and i, j, k indicate the equation type and global node numbers, respectively.

Equation 171 is nonlinear because entries in the global matrix $[M]$ and right-hand-side vector $\{b\}$ depend on unknown property values of water, heat, and solute diffusivities. Because these properties are functions of pressure head, temperature, and/or concentration, the M_{ij} values in the global matrix $[M]$ are not actually known prior to solving the equations. To solve this set of nonlinear equations, the system of equations is made quasi-linear by evaluating matrices using an iterative Picard procedure (Istok, 1989).

Dirichlet Conditions

In most field problems, the value of one or more dependent variables (pressure head, temperature, and/or solute concentration) is specified at one or more nodes, sometimes called Dirichlet nodes. These values constitute Dirichlet boundary conditions when specified along domain surfaces and are needed to solve the governing partial differential equations presented earlier. When Dirichlet conditions are specified, the system of equations must be modified before a solution can be obtained. This modification reduces the degrees of freedom (DOF) and, therefore, global system of equations. For example, if N and D are the respective number of total and Dirichlet nodes, then $DOF = N - D$ and the global dimensions are DOF by DOF .

In general, the position number of a specified field variable in vector $\{x\}$ corresponds to the row (equation number) and column that must be removed from the global matrix $[M]$. For example, if pressure head, temperature, and solute concentration were specified at node 2 (ψ_2, T_2, C_2), the global modification would result in

$$\begin{bmatrix}
 M_{\psi\psi_{11}} & M_{\psi T_{11}} & M_{\psi C_{11}} & M_{\psi\psi_{13}} & M_{\psi T_{13}} & M_{\psi C_{13}} & \cdots & M_{\psi C_{1N}} \\
 M_{T\psi_{11}} & M_{TT_{11}} & M_{TC_{11}} & M_{T\psi_{13}} & M_{TT_{13}} & M_{TC_{13}} & \cdots & M_{TC_{1N}} \\
 M_{C\psi_{11}} & M_{CT_{11}} & M_{CC_{11}} & M_{C\psi_{13}} & M_{CT_{13}} & M_{CC_{13}} & \cdots & M_{CC_{1N}} \\
 M_{\psi\psi_{31}} & M_{\psi T_{31}} & M_{\psi C_{31}} & M_{\psi\psi_{33}} & M_{\psi T_{33}} & M_{\psi C_{33}} & \cdots & M_{\psi C_{3N}} \\
 M_{T\psi_{31}} & M_{TT_{31}} & M_{TC_{31}} & M_{T\psi_{33}} & M_{TT_{33}} & M_{TC_{33}} & \cdots & M_{TC_{3N}} \\
 M_{C\psi_{31}} & M_{CT_{31}} & M_{CC_{31}} & M_{C\psi_{33}} & M_{CT_{33}} & M_{CC_{33}} & \cdots & M_{CC_{3N}} \\
 \cdot & \cdot & \cdot & \cdot & \cdot & \cdot & \cdots & \cdot \\
 \cdot & \cdot & \cdot & \cdot & \cdot & \cdot & \cdots & \cdot \\
 \cdot & \cdot & \cdot & \cdot & \cdot & \cdot & \cdots & \cdot \\
 M_{C\psi_{N1}} & M_{CT_{N1}} & M_{CC_{N1}} & M_{C\psi_{N3}} & M_{CT_{N3}} & M_{CC_{N3}} & \cdots & M_{CC_{NN}}
 \end{bmatrix}
 \begin{bmatrix}
 \psi_1 \\
 T_1 \\
 C_1 \\
 \psi_3 \\
 T_3 \\
 C_3 \\
 \cdot \\
 \cdot \\
 \cdot \\
 \psi_N \\
 T_N \\
 C_N
 \end{bmatrix}
 =
 \begin{bmatrix}
 b_{\psi_1} - b_{\psi_1}^1 \\
 b_{T_1} - b_{T_1}^1 \\
 b_{C_1} - b_{C_1}^1 \\
 b_{\psi_3} - b_{\psi_3}^3 \\
 b_{T_3} - b_{T_3}^3 \\
 b_{C_3} - b_{C_3}^3 \\
 \cdot \\
 \cdot \\
 \cdot \\
 b_{\psi_N} - b_{\psi_N}^N \\
 b_{T_N} - b_{T_N}^N \\
 b_{C_N} - b_{C_N}^N
 \end{bmatrix}, \quad (170)$$

where

$$b_{\psi_1}^1 = M_{\psi\psi_{12}} \psi_2 + M_{\psi T_{12}} T_2 + M_{\psi C_{12}} C_2, \quad (171)$$

$$b_{T_1}^1 = M_{T\psi_{12}} \psi_2 + M_{TT_{12}} T_2 + M_{TC_{12}} C_2, \quad (172)$$

$$b_{C_1}^1 = M_{C\psi_{12}} \psi_2 + M_{CT_{12}} T_2 + M_{CC_{12}} C_2 \quad (173)$$

$$b_{\psi_3}^3 = M_{\psi\psi_{32}} \psi_2 + M_{\psi T_{32}} T_2 + M_{\psi C_{32}} C_2, \quad (174)$$

$$b_{T_3}^3 = M_{T\psi_{32}} \psi_2 + M_{TT_{32}} T_2 + M_{TC_{32}} C_2, \quad (175)$$

$$b_{C_3}^3 = M_{C\psi_{32}} \psi_2 + M_{CT_{32}} T_2 + M_{CC_{32}} C_2 \quad (176)$$

$$\dots \text{ equations for nodes 4 through N-1} \quad (177)$$

$$b^N_{\psi_1} = M_{\psi\psi_{N2}}\Psi_2 + M_{\psi T_{N2}}T_2 + M_{\psi C_{12}}C_2, \quad (178)$$

$$b^N_{T_N} = M_{T\psi_{N2}}\Psi_2 + M_{TT_{N2}}T_2 + M_{TC_{N2}}C_2. \quad (179)$$

$$b^N_{C_N} = M_{C\psi_{N2}}\Psi_2 + M_{CT_{N2}}T_2 + M_{CC_{N2}}C_2 \quad (180)$$

In addition, if concentration at node 3 and pressure head at node 4 (C_3 and ψ_4) also were specified, row and column numbers 6 and 7 in the original matrix also would be deleted and additional terms would be added to the force vector components above (except equation 167 that would be used). For example, the force vector components would now become

$$b^1_{\psi_1} = M_{\psi\psi_{12}}\Psi_2 + M_{\psi T_{12}}T_2 + M_{\psi C_{12}}C_2 + M_{\psi C_{13}}C_3 + M_{\psi\psi_{14}}\Psi_4 \quad (181)$$

$$b^1_{T_1} = M_{T\psi_{12}}\Psi_2 + M_{TT_{12}}T_2 + M_{TC_{12}}C_2 + M_{TC_{13}}C_3 + M_{T\psi_{14}}\Psi_4 \quad (182)$$

$$b^1_{C_1} = M_{C\psi_{12}}\Psi_2 + M_{CT_{12}}T_2 + M_{CC_{12}}C_2 + M_{CC_{13}}C_3 + M_{C\psi_{14}}\Psi_4 \quad (183)$$

$$b^3_{\psi_3} = M_{\psi\psi_{32}}\Psi_2 + M_{\psi T_{32}}T_2 + M_{\psi C_{32}}C_2 + M_{\psi C_{33}}C_3 + M_{\psi\psi_{34}}\Psi_4 \quad (184)$$

$$b^3_{T_3} = M_{T\psi_{32}}\Psi_2 + M_{TT_{32}}T_2 + M_{TC_{32}}C_2 + M_{TC_{33}}C_3 + M_{T\psi_{34}}\Psi_4 \quad (185)$$

... equations for nodes 3 through N-1 (186)

$$b^N_{\psi_1} = M_{\psi\psi_{N2}}\Psi_2 + M_{\psi T_{N2}}T_2 + M_{\psi C_{N2}}C_2 + M_{\psi C_{N3}}C_3 + M_{\psi C_{N4}}\Psi_4 \quad (187)$$

$$b^N_{T_N} = M_{T\psi_{N2}}\Psi_2 + M_{TT_{N2}}T_2 + M_{TC_{N2}}C_2 + M_{TC_{N3}}C_3 + M_{TC_{N4}}\Psi_4 \quad (188)$$

$$b^N_{C_N} = M_{C\psi_{N2}}\Psi_2 + M_{CT_{N2}}T_2 + M_{CC_{N2}}C_2 + M_{CC_{N3}}C_3 + M_{CC_{N4}}\Psi_4 \quad (189)$$

As indicated here, not all field variables at a given node need to be specified at one time. Values can be specified at interior nodes as well as boundary nodes. When values are specified at interior nodes, these nodes become in effect a source/sink for the associated specified variable (pressure, temperature, concentration). Permissible combinations may include pressure head, pressure head-temperature, pressure head-temperature-concentration, temperature-concentration, temperature, and/or concentration. The only time concentration would be specified is in a purely diffusive problem. This situation may arise in thick unsaturated settings subject to long term semi-arid-climatic conditions.

As previously indicated, Dirichlet conditions can be specified in various combinations of dependent variables and at all nodes, boundary nodes, or a combination of interior and boundary nodes. By specifying two dependent variables at all nodes results in effectively decoupling the corresponding governing equations. If these conditions are chosen to maintain a constant-domain value (iso), the numerical solution trivializes to the classical solutions of water transport (isothermal, isohaline), heat transport (isobaric, isohaline), or solute transport (isobaric, isothermal).

Neumann Conditions

Rates of ground-water flow, heat, and/or solute (fluxes) can be specified at one or more nodes, sometimes called Neumann nodes. These values specified along domain boundaries constitute Neumann boundary conditions and can be used to represent specified flux rates of ground water, heat, and/or solute concentration into or out of the domain. When Neumann boundary conditions are specified, some entries in the global matrix $[M]$ are nonzero. The equation for computing the element contribution to the global $\{F\}$ matrix at node i was presented in the previous section titled Dirichlet Conditions.

Initial Conditions

In addition to boundary conditions, initial conditions also must be specified to solve a transient ground-water transport problem. Examples of initial conditions include moisture content or pressure head for the water equation, temperature for the heat equation, and chemical concentration for the solute equation. In the VST2D model, three initial values are required for each node point. If volumetric moisture content is specified, the program back calculates values of pressure head on the basis of the van Genuchten power function described in the “Properties and Parametric Relations” section. In general, the initial conditions usually represent some known or assumed steady state or equilibrium period. In VST2D, boundary conditions are read after the initial conditions are established so they will override initial conditions for the same boundary nodes.

Picard Iteration

A Picard iteration with an incremental solution procedure, sometimes called the modified Newton-Raphson method (Istok, 1989), is used in this model because of the sensitivity of global matrix coefficients to small changes in dependent variables. This Picard procedure requires specifying initial values of temperature, pressure head, and solute concentration. These values are used to compute a set of initial property values, for example, hydraulic conductivity, saturation, capacitance, heat capacity, latent heat of vaporization and others, which then are used to build elemental matrices. The elemental matrices then are combined to construct a global coefficient matrix $[M]$ and vector $\{b\}$ as previously described, where $[M]\{x\} = \{b\}$. Next, boundary conditions are accounted for in the system of equations and a residual vector is computed by

$$\{R\}^{m-1} = \{b\}^{m-1} - [M]^{m-1}\{x\}^{m-1}. \quad (190)$$

The system, $[M]^{m-1}\{dx\}^m = \{R\}^{m-1}$, then is solved for changes in the solution vector $\{dx\}^m$ using a flexible direct quasi-generalized minimum residual method (FDQ-GMRES; Saad, 1996). An iterative solver of this type is required for two reasons. First, the FDQ-GMRES method allows for varied step-by-step preconditioning thereby avoiding accumulated roundoff error that may otherwise occur because matrix coefficients vary over many orders-of-magnitude. Second, the FDQ-GMRES method can handle the nonsymmetric matrix that arises because of the solute transport equation. Convergence is checked by comparing the relative change between new and old values of pressure head, temperature and concentration; for example, $(\text{new} - \text{old}) / \text{new}$, with a prescribed tolerance value,

such as 0.01 percent. If all three dependent variables did not converge, the next trial solution is computed for a subsequent iteration and the procedure repeated using

$$\{x\}^m = \{x\}^{m-1} + \omega\{dx\}^m, \quad (191)$$

where ω is a weight usually set to 0.5.

Upon satisfying all three convergence criteria, the time step is advanced with current dependent variables used to formulate initial parameters, matrices, and vectors.

Peclet and Courant Numbers

The advective-dispersion transport equation can be difficult to solve numerically, particularly when advection dominates over dispersion. In this situation, the Galerkin finite-element solution can result in numerical oscillations near the concentration front. These numerical oscillations tend to be more severe as the concentration front becomes sharper, that is, when advection becomes more dominant. According to Huyakorn and Pinder (1983), if dispersion is greater than zero, numerical oscillations can be avoided when using a Galerkin finite-element approach and linear interpolation functions provided the element size is selected so the Peclet (P_e) number does not exceed 2. The dimensionless Peclet number relates the effectiveness of mass transport by advection to dispersion. The Peclet number is typically defined as $P_e = V L_{ij}/D_{ij}$, where V is the minimum domain pore velocity [m d^{-1}], L_{ij} is the maximum domain element length [m], and D_{ij} is the maximum dispersion coefficient [$\text{m}^2 \text{d}^{-1}$]. In cases of nonuniform flow, Huyakorn also noted that only minor oscillations will result even when the Peclet number is as high as 10. Moreover, Pinder and Gray (1977) have shown that a Galerkin finite-element solution can be free of oscillations with a Peclet number as high as about 5. For this reason, VST2D computes and writes to the screen and output files the maximum acceptable element length at each iteration and time step on the basis of a corresponding Peclet number of 5. The determination to stop the simulation, however, is left to the model user.

Another important criteria in solving the advection-dominated problem is associated with the time step. As a general rule-of-thumb, Huyakorn and Pinder (1983) suggest the Courant number (C_r) be less than or equal to 1. The dimensionless Courant number is defined as $C_r = V_{ij} dt/L_{ij}$, where V_{ij} [m d^{-1}] is the pore velocity, L_{ij} is the element length [m], and dt the time step [d]. By setting the Courant number equal to 1 and using the minimum domain pore velocity, the maximum time step allowed to avoid numerical dispersion of the solute front is calculated. In VST2D, the maximum allowable time step is calculated at each iteration. If the current time step exceeds the maximum allowable Courant-based time step, the time step then is set equal to the limiting value and the solution recalculated.

Mass and Energy Balance

Continuity calculations are performed as a means to check the relative accuracy of the numerical solution. If the model is performing properly, the change in amount of stored water, solute, and heat should equal the net flux (inflow minus the outflow) with time of water, solute, and heat along permeable boundaries and internally at source/sinks. Examples of sources/sinks might include water, chemical waste, or heat injection or withdrawal from wells; contaminant spills; and/or chemical or biological reactions.

In practice the difference between the amount of calculated change in stored water, solute, and heat does not balance exactly with the associated net fluxes with time. The difference between these two quantities, called residual error, is written as

$$R_{\theta} = \Delta S_{\theta} - \frac{\Delta Q_{\theta}}{\Delta t}, \quad (192)$$

$$R_C = \Delta S_C - \frac{\Delta Q_C}{\Delta t}, \quad (193)$$

$$R_H = \Delta S_H - \frac{\Delta Q_H}{\Delta t}, \quad (194)$$

where

R_{θ} , R_C , and R_H are the respective solution domain residual errors for water [m^3], solute [$\text{m}^3 \text{ mol kg}^{-1}$], and heat [cal];

ΔS_{θ} , ΔS_C , and ΔS_H are the respective changes in solution domain storage for water [m^3], solute [$\text{m}^3 \text{ mol kg}^{-1}$], and heat [cal];

ΔQ_{θ} , ΔQ_C , and ΔQ_H are the respective solution domain net fluxes along the permeable boundaries and at internal source/sinks.

Whereas a small residual error (typically less than or equal to 0.1 percent) in the water, solute, or heat calculation does not guarantee a correct solution, a large residual error (typically greater than 0.1 percent) may indicate some problem in the model mesh size.

For a steady-state or closed system problem, the change in storage will be zero. For a transient simulation, however, the change in storage may occur and can be computed for each element using the change in accumulated volume of water, solute, or heat given. Discrete volumes at a given time step are calculated using

$$V_{\theta}^e = \frac{A}{3}(\theta_{S_i} S_i + \theta_{S_j} S_j + \theta_{S_k} S_k), \quad (195)$$

$$V_C^e = \frac{A}{3}(\theta_{S_i} S_i C_i + \theta_{S_j} S_j C_j + \theta_{S_k} S_k C_k), \quad (196)$$

$$V_H^e = \frac{A}{3}(f_{1_i} T_i + f_{1_j} T_j + f_{1_k} T_k). \quad (197)$$

Total volumes for water, solute, and heat are then calculated by summing element contributions as

$$V_{\theta} = \sum_e V_{\theta}^e, \quad (198)$$

$$V_C = \sum_e V_C^e, \quad (199)$$

$$V_H = \sum_e V_H^e. \quad (200)$$

The change in storage then is calculated between time steps by

$$\Delta S_\theta^{k+1,m} = V_\theta^{k+1,m} - V_\theta^k \quad (201)$$

$$\Delta S_C^{k+1,m} = V_C^{k+1,m} - V_C^k \quad (202)$$

$$\Delta S_H^{k+1,m} = V_H^{k+1,m} - V_H^k \quad (203)$$

To compute solution domain net fluxes, inflow and outflow of water, solute, and heat along permeable boundaries and at internal source/sink nodes must be summed. Summation of fluxes includes those associated with Neumann and Dirichlet nodes. Whereas values at Neumann nodes are known, those values at Dirichlet nodes are unknown and, therefore, must be back calculated. In VST2D, the equations associated with Dirichlet conditions are written to a separate matrix for computing these flux values. In keeping with the previous example, if pressure head, temperature, and concentration are specified only at node 2 (ψ_2 , T_2 , C_2), the associated flux values are calculated according to the quasi-linear system presented below.

$$\begin{Bmatrix} Q_{\psi 2} \\ Q_{T 2} \\ Q_{C 2} \end{Bmatrix}^{k+1,m+1} = \begin{bmatrix} M_{\psi\psi_{21}} & M_{\psi T_{21}} & M_{\psi C_{21}} & M_{\psi\psi_{22}} & M_{\psi T_{22}} & M_{\psi C_{22}} & M_{\psi\psi_{23}} & M_{\psi T_{23}} & M_{\psi C_{23}} & \dots & M_{\psi\psi_{2N}} \\ M_{T\psi_{21}} & M_{TT_{21}} & M_{TC_{21}} & M_{T\psi_{22}} & M_{TT_{22}} & M_{TC_{22}} & M_{T\psi_{23}} & M_{TT_{23}} & M_{TC_{23}} & \dots & M_{TC_{2N}} \\ M_{C\psi_{21}} & M_{CT_{21}} & M_{TT_{21}} & M_{C\psi_{22}} & M_{CT_{22}} & M_{TT_{22}} & M_{C\psi_{23}} & M_{CT_{23}} & M_{TT_{23}} & \dots & M_{TT_{2N}} \end{bmatrix} \begin{Bmatrix} \psi_1 \\ T_1 \\ C_1 \\ \psi_2 \\ T_2 \\ C_2 \\ \psi_3 \\ T_3 \\ C_3 \\ \cdot \\ \cdot \\ \cdot \\ \psi_N \\ T_N \\ C_N \end{Bmatrix} + \begin{Bmatrix} b_{\psi_2} \\ -b_{T_2} \\ b_{C_2} \end{Bmatrix} / \Delta t. \quad (204)$$

where the total liquid water, heat, and solute fluxes are Q_ψ [kg d^{-1}], Q_T [cal d^{-1}], and Q_C [$\text{mol kg}^{-1} \text{m}^3 \text{d}^{-1}$] after multiplying by a unit thickness.

The actual flux values at a given time step will lag behind the updated field variables by a single iteration because the diffusivities are initially unknown. The flux of water, solute, or heat is identified as leaving or entering the domain by noting the sign; for example, negative and positive values equate to leaving and entering of flux, respectively.

The total solution domain net flux values calculated by summing element contributions given by

$$\Delta Q_{\theta} = \sum_e \Delta Q_{\theta}^e, \quad (205)$$

$$\Delta Q_C = \sum_e \Delta Q_C^e, \quad (206)$$

$$\Delta Q_H = \sum_e \Delta Q_H^e, \quad (207)$$

where ΔQ_{θ}^e , ΔQ_C^e , and ΔQ_H^e are the respective element water, solute, and heat fluxes given by

$$\Delta Q_{\theta}^e = \Delta Q_{\theta}^{k+1,m} - \Delta Q_{\theta}^k, \quad (208)$$

$$\Delta Q_C^e = \Delta Q_C^{k+1,m} - \Delta Q_C^k, \quad (209)$$

$$\Delta Q_H^e = \Delta Q_H^{k+1,m} - \Delta Q_H^k, \quad (210)$$

Assumptions

The following list gives a summary of key assumptions invoked during the formulation of this numerical model. The order does not indicate relative importance in model development and/or application.

- Dependent variables (pressure head, temperature, and concentration) vary linearly within elements.
- Global coordinates are oriented along a Cartesian system: x (horizontal) and y (vertical).
- Physical properties are consistent with notion of representative elementary volume.
- The finite-element domain is two-dimensional: horizontal or vertical plane.

MODEL DOCUMENTATION

A flow chart depicting the (a) operational and (b) matrix sequencing for VST2D and some of the supporting subroutines is given in figure 7. A general description of the program structure and organization of subroutines is provided below.

General Program Structure

The computer program VST2D is designed for simulating transient, coupled water-heat-solute transport in heterogeneous, anisotropic, two-dimensional, ground-water systems. All data input to the main program are read from four data storage files (with the extension .IN), namely, ELEMENT, PROPERTY, BOUNDARY, and INITIAL. The ELEMENT file contains element data, including coordinates; PROPERTY contains material properties (physical, thermal and chemical); BOUNDARY file contains input boundary conditions; and INITIAL contains solution criteria and initial conditions.

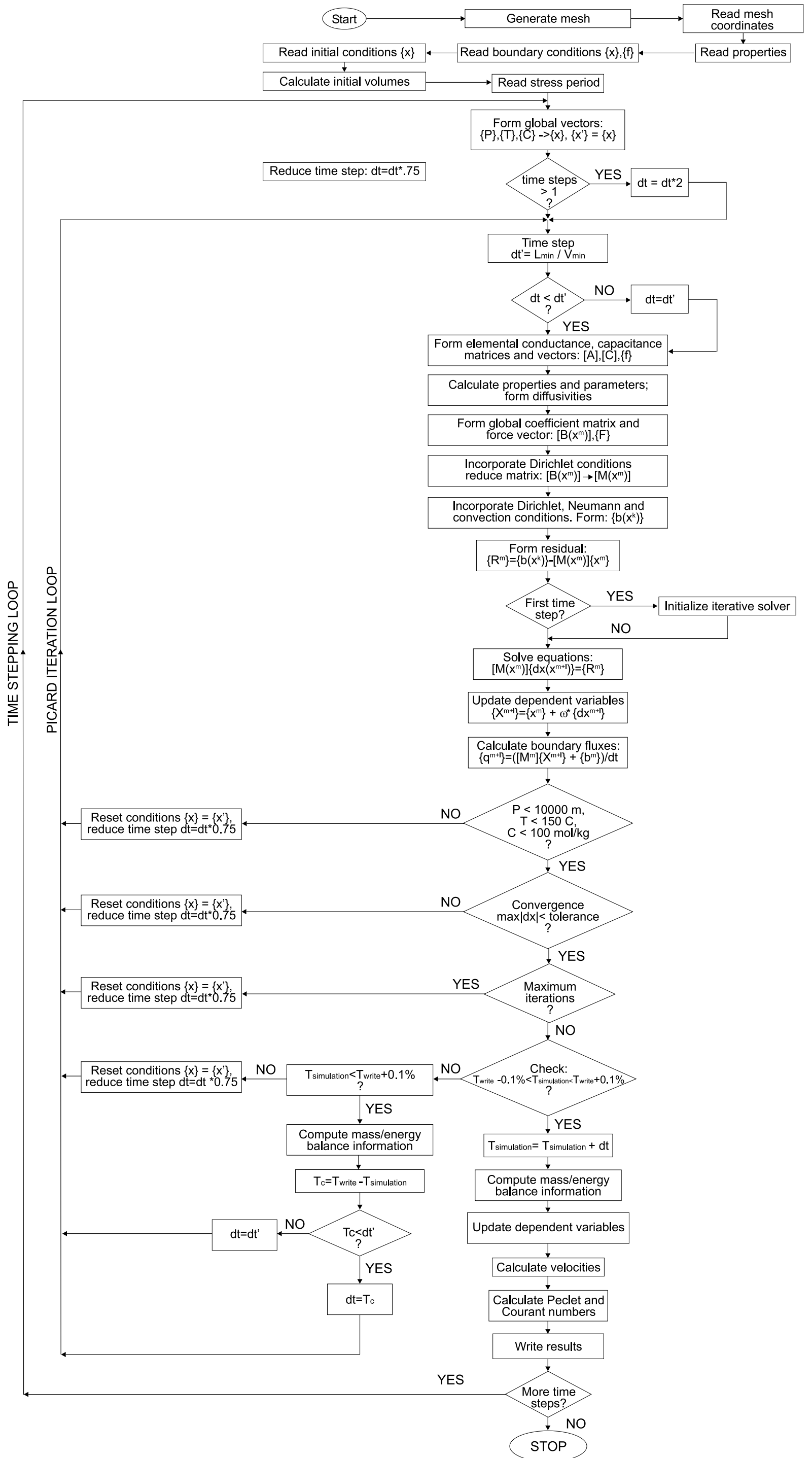


Figure 7. Flowchart depicting (a) operational and (b) matrix sequencing for the VST2D model.

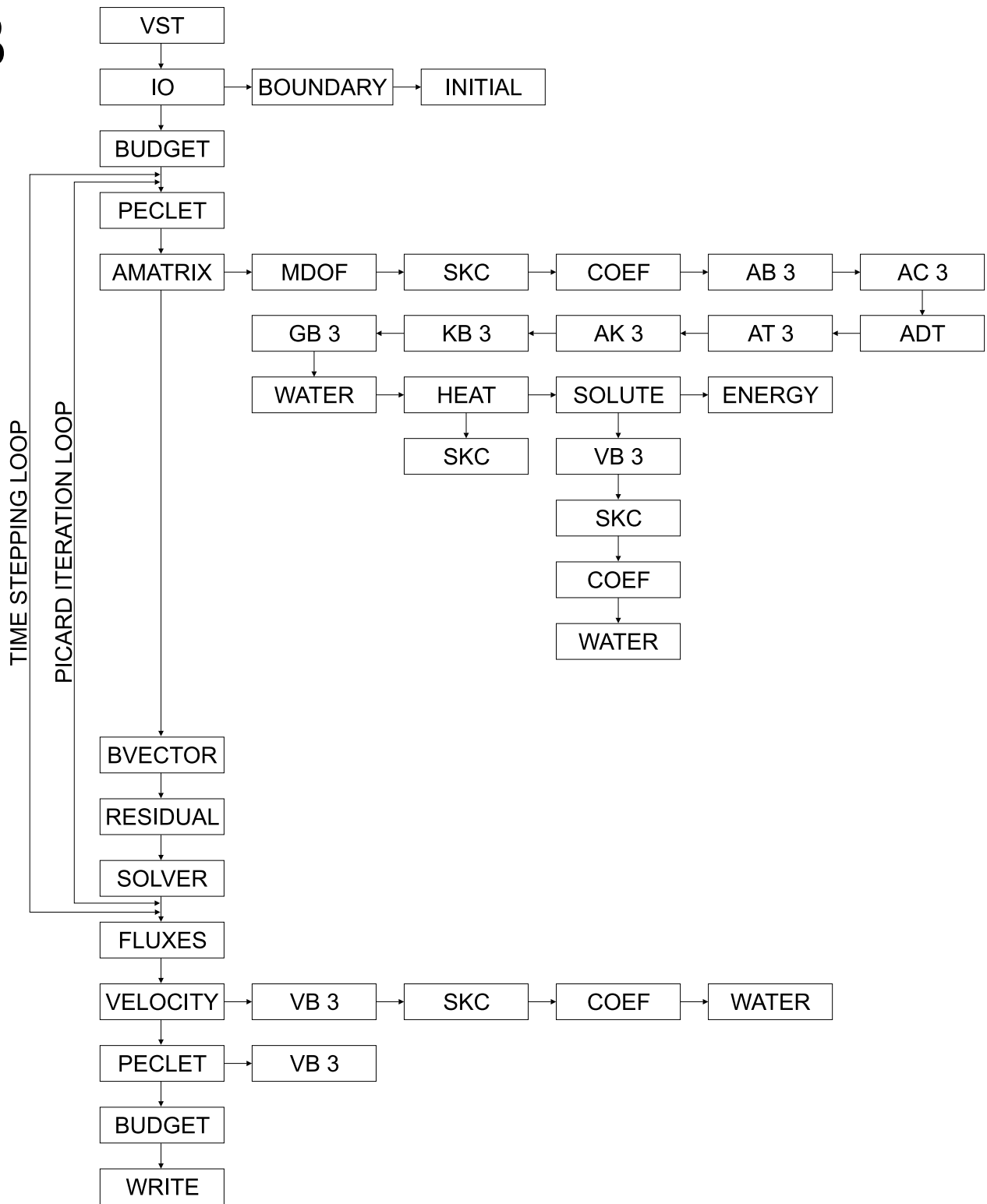
B

Figure 7. Continued.

One preprocessor that can be used with the VST2D program is a finite-element grid generator called GRID. Upon reading an input file (with the extension .IN) called GRID, the preprocessor generates a mesh of linear triangular (simplex) elements. The GRID file is created using a text editor and includes information about the problem, such as title, number of regions in the solution domain, x, y coordinates of the boundary nodes for a region, regional connectivity data, material properties, and other information about grid generation (appendix 2). An illustrated example can be found in the VARSAT2D documentation by Nieber, Friedel, and Munir (1994). The output from this grid generator is written to a file called ELEMENT.IN for use with VST2D (see “Data Input Files”).

Main Program and Related Subroutines

The main program, VST2D, is supported by 24 subroutines (with the extension .FOR). All data transfer between the main program and subroutines is performed using common blocks. The tasks performed by the main routine and each of the subroutines are given below.

- AB3: Computes element contribution associated with time derivative which is used in computing capacitance terms.
- AC3: Computes element contribution because of a convective solute boundary condition.
- AMATRIX: Computes and adds elemental and capacitance to form global matrix $[M]$. Computes transient changes in vapor, and liquid contents, incorporates Dirichlet conditions, and modifies global matrix accordingly. Delegates tasks to subroutines MDOF, COEF, SKC, AB3, AC3, KB3, GB3, CB3, WATER, HEAT, and SOLUTE.
- BOUNDARY: Assigns specified moisture/pressure head, temperature, solute concentration (Dirichlet conditions) and point source/sink or distributed fluxes (Neumann conditions) to appropriate nodes. Fills control arrays to track Dirichlet conditions.
- BUDGET: Computes water, heat, and solute budgets.
- BVECTOR: Assembles global right-hand-side vector $\{b\}$ for system of equations where $[A]\{x\} = \{b\}$. Includes summation of contributions from the application of Dirichlet conditions and functions related to the water $[\text{kg m}^{-1}]$, heat $[\text{cal m}^{-1}]$, and solute $[\text{mol kg}^{-1} \text{m}^3]$ equations. Specific contributions to the water equation arise because of Dirichlet and flux boundary conditions, Taylor series expansion of capacitance, time discretization of liquid and vapor, and gravitational potential. Specific contributions to the heat equation arise because of Dirichlet and flux-boundary conditions, Taylor series expansion of moisture capacitance, time discretization of liquid water, and time discretization of solute concentration. Individual contributions to the solute equation arise because of Dirichlet, flux and convective boundary conditions, and time discretization of solute concentration.
- COEF: Computes a , b , and c , coefficients used in interpolation (basis) functions; for example, $N_i = 1/2A (a_i + b_i x + c_i y)$, and derivatives of interpolation functions.
- DNPCR: Converts a densely stored matrix into a row oriented compactly sparse matrix (Saad, 1996).
- FLUXES: Computes liquid fluxes at permeable boundary nodes for use in mass-balance calculations.
 - GB3: Computes elemental contribution because of gravitational potential associated with the water equation.
 - GB3T: Computes elemental contribution because of gravitational potential associated with the heat equation.
- HEAT: Computes nodal and elemental thermal contributions (B_{Tc} $[\text{cal kg mol}^{-1} \text{m}^{-1} \text{d}^{-1}]$, B_{Tv} $[\text{cal m}^{-2} \text{d}^{-1}]$, B_{TT} $[\text{cal m}^{-1} \text{°C}^{-1} \text{d}^{-1}]$). Specific properties calculated include latent heat of vaporization $[\text{cal g}^{-1}]$, specific heat of liquid water and water vapor $[\text{cal g}^{-1} \text{°C}^{-1}]$, volumetric heat capacity $[\text{cal cm}^{-3} \text{°C}^{-1}]$, thermal conductivities $[\text{mcal cm}^{-1} \text{°C}^{-1} \text{sec}^{-1}]$, global heat capacity $[\text{cal m}^{-3} \text{°C}^{-1}]$, global heat of vaporization $[\text{cal m}^{-3}]$. Individual diffusivities calculated include the molecular diffusivity of water in air $[\text{m}^2 \text{s}^{-1}]$, liquid water diffusivity $[\text{m}^2 \text{d}^{-1}]$, thermal liquid

diffusivity [$\text{m}^2 \text{d}^{-1} \text{ }^\circ\text{C}^{-1}$], thermal vapor diffusivity [$\text{m}^2 \text{d}^{-1} \text{ }^\circ\text{C}^{-1}$], and average elemental thermal diffusivity in x and y directions.

- IO: Reads element numbers, nodal coordinates, and hydraulic, thermal, and chemical properties. This information then is written to VST.OUT for the user's review.
- ILUT: Preconditions global matrix $[M]$ prior to solution by the iterative solver RUNRC (Saad, 1996).
- INITIAL: Reads time information (number and maximum time steps, time function, maximum time increment, and output times) and initial values (moisture or pressure head, temperature, and solute concentration). Computes initial pressure head if moisture, saturation, and conductivity are specified. Delegates tasks to COEF and writes initial dependent field variables to INPUT.DAT and OUTPUT.DAT.
- KB3: Computes element contribution because of conductivity in water equation which is added to conductance matrix associated with liquid water flow.
- MDOF: Computes degrees of freedom.
- PECLET: Computes Peclet and Courant numbers. Values are written to PECLET.DAT. Delegates tasks to VB3.
- RESIDUAL: Computes the vector of residual error: $\{R\} = \{b\} - [M]\{x\}$.
- RUNRC: Solves system of equations using flexible direct version of quasi-general minimum residual method. Delegates tasks to BISINIT, MGSRO, GIVENS, LUSOL, LUTSOL, DQGMR, AMUX, and ATMUX (Saad, 1996).
- SKC: Computes nodal and elemental saturation, conductivity, and capacitance.
- SOLUTE: Computes nodal and elemental solute contributions to global capacitance (B_{CC} because of osmotic gradient [$\text{m}^2 \text{d}^{-1}$], $B_{C\psi}$ is specific moisture gradient [$\text{m mol kg}^{-1} \text{d}^{-1}$], and B_{CT} because of temperature gradient [$\text{m}^2 \text{mol kg}^{-1} \text{ }^\circ\text{C}^{-1} \text{d}^{-1}$]). Specific properties calculated include the salt-sieving coefficient [dimensionless], solute dispersion coefficient in water [$\text{m}^2 \text{d}^{-1}$], solute dispersion coefficient in soil [$\text{m}^2 \text{d}^{-1}$], hydrodynamic dispersion coefficient [$\text{m}^2 \text{s}^{-1}$], dispersion-diffusion coefficient [$\text{m}^2 \text{s}^{-1}$], dispersion coefficient of solute because of salt sieving [$\text{m}^2 \text{mol kg}^{-1} \text{s}^{-1}$], dispersion coefficient of solute because of salt sieving, [mol kg^{-1}], diffusion coefficient in soil solution because of temperature gradients [$\text{m}^2 \text{mol kg}^{-1} \text{K}^{-1} \text{s}^{-1}$], diffusion coefficient of solute because of temperature gradients [$\text{m}^2 \text{mol kg}^{-1} \text{K}^{-1} \text{d}^{-1}$], dispersion coefficients [$\text{m}^2 \text{d}^{-1}$], diffusion-dispersion coefficient [$\text{m}^2 \text{d}^{-1}$], bulk density of soil [Mg m^{-3}], density of liquid phase [kg m^{-3}], radius of pore assuming capillary bundle theory; tortuosity [dimensionless] and wetted thickness [angstroms]. This subroutine also delegates the calculation of pore water velocity [m d^{-1}] and specific discharge (apparent velocity) [m d^{-1}] to VB3.
- VB3: Computes specific discharge and pore water velocity components along principal directions. Computes derivatives of interpolation functions and individual liquid flux contributions because of isothermal, thermal, and osmotic gradients. Delegates computational tasks to SKC, COEF, WATER.
- VELOCITY: Computes apparent ground-water discharge, velocity, and angle. Delegates tasks to VB3 for calculating specific discharge and pore water velocity components in principal directions.
- VOLUME: Computes initial moisture volume initial solute mass initial heat storage through this subroutine.
- VST: This is the main program. Tasks are delegated to the subroutines (BOUNDARY, INITIAL, AMATRIX, BVECTOR, RESIDUAL, DNSCRS, ILUT, RUNRC, FLUXES, VOLUME, VELOCITY, PECLET), whereas simulation time, output time, and time step is advanced. This program subroutine also checks for convergence and mass balance error. The screen output for specified time originates from this subroutine.
- WATER: Computes nodal and elemental contributions to the conductance matrix ($B_{w\psi}$ [$\text{kg m}^{-2} \text{d}^{-1}$], $B_{\psi T}$ [$\text{kg m}^{-1} \text{d}^{-1} \text{ }^\circ\text{C}^{-1}$] and $B_{\psi C}$ [$\text{kg}^2 \text{mol}^{-1} \text{m}^{-1} \text{d}^{-1}$]). Specific properties calculated include a gain factor used to compensate for underestimation of temperature-induced changes when only surface tension is considered (function of water and clay content; exceeds 1), interfacial tension

of water on air [mN m^{-1}], relative humidity as a function of osmotic potential [percent], relative humidity as a function of matric potential [percent], total relative humidity [percent], saturated density [kg m^{-3}], dp_s/dT [$\text{kg m}^{-3} \text{ }^\circ\text{C}^{-1}$], pore radius assuming capillary bundle theory [m], hydrated radius of solute and water [nm], bulk density of soil [Mg m^{-3}], saturated water vapor density [kg m^{-3}], and liquid density [kg m^{-3}]. Specific diffusivities include the thermal diffusivity matrix [$\text{m}^2 \text{ d}^{-1} \text{ }^\circ\text{C}^{-1}$], pressure diffusivity matrix [m d^{-1}], molecular diffusivity of water vapor in air [$\text{m}^2 \text{ s}^{-1}$], liquid water diffusivity because of solute concentration [$\text{m}^2 \text{ kg mol}^{-1} \text{ s}^{-1}$], moisture vapor diffusivity (D_{mv}) [$\text{m}^2 \text{ d}^{-1}$], isothermal vapor diffusivity [$\text{m}^2 \text{ d}^{-1}$], thermal liquid diffusivity [$\text{m}^2 \text{ d}^{-1} \text{ }^\circ\text{C}^{-1}$], thermal vapor diffusivity [$\text{m}^2 \text{ d}^{-1} \text{ }^\circ\text{C}^{-1}$], and thermal diffusivity [$\text{m}^2 \text{ d}^{-1} \text{ }^\circ\text{C}^{-1}$].

WRITE: Writes generalized results to 10 scratch files (with the extension .OUT): BUDGET, DIFFC, DIFFPT, DISP, LFLUX, PECLT, NODES, NODES1D, NODES2D, VST, VELOCITY. A complete description of the information written to each of these files can be found in the section Data Output Files.

Data Input Files

The data needed to execute VST2D are read in “free” format from four files (each has the extension *.IN): ELEMENT, PROPERTY, BOUNDARY, INITIAL; therefore, all input can be separated by a comma, space, or blank line. Whereas using the accompanying finite-element grid generator called GRID.EXE to create the ELEMENT and PROPERTY files (see appendix 2), the BOUNDARY and INITIAL files should be created using a text editor. An example of typical input for each of these files is given below.

ELEMENT:

Parameter	Definition
1. TITLE	Problem title (up to 80 alphanumeric characters).
2. IVERT	Section type flag: 0 = horizontal, 1 = vertical.
3. NUMELM	Number of elements.
4. NUMNOD	Number of nodes.
5. NODNUM(I,J)	Node numbers (read as triplet for each element).
6. X(I),Y(I)	Cartesian coordinates (read in X,Y pairs) [m].
7. E, PROP(I,J)	Element number, Material properties (19 properties are read for each element from PROPERTY.IN).

PROPERTY: One set of 20 properties is read in for each element.

Parameter	Definition
1. KXS	Saturated conductivity x-direction [m d^{-1}].
2. KYS	Saturated conductivity y- (or z-) direction [m d^{-1}].
3. CA	van Genuchten alpha parameter [m^{-1}].
4. CN	van Genuchten N parameter [dimensionless].
5. TR	Residual moisture content [dimensionless].
6. TS	Saturated moisture content [dimensionless].
7. CPS	Volumetric heat capacity of solid [$\text{cal cm}^{-3} \text{ }^\circ\text{C}^{-1}$].
8. DELT	Angle between local element principal directions and global cartesian coordinates (degrees).
9. LAMBDAs	Thermal conductivity of silt [$\text{mcal cm}^{-1} \text{ }^\circ\text{C}^{-1} \text{ s}^{-1}$].
10. XO	Fractional organic carbon content [dimensionless].
11. SSA	Specific surface area [$\text{m}^2 \text{ kg}^{-1}$].
12. RHOB	Bulk density [Mg m^{-3}].

13. AL	Longitudinal dispersivity [m].
14. AT	Transverse dispersivity [m].
15. KD	Distribution coefficient [$\text{m}^3 \text{kg}^{-1}$].
16. DECAY	Decay constant [d^{-1}].
17. Xsnd	Fractional sand [dimensionless].
18. Xslt	Fractional silt [dimensionless].
19. Xcly	Fractional clay [dimensionless].
20. PMC	Porous medium compressibility [$\text{m}^2 \text{N}^{-1}$].

BOUNDARY:

Parameter	Definition
1. NSPN	Number of specified pressure head (or moisture content) nodes.
2. J,XPSI(J)	Node number, Specified pressure [m] (or moisture content).
3. NLFN	Number of specified moisture flux nodes; for example.
4. J,FLUXPM(J)	Node number, Specified moisture flux [$\text{m}^3 \text{d}^{-1}$](point source/sink).
5. NSTN	Number of specified temperature nodes.
6. J,TEMPC(J)	Node number, Specified temperature [$^{\circ}\text{C}$].
7. NHFN	Number of specified heat flux nodes.
8. J,FLUXPT(J)	Node number, Specified heat flux [cal m^{-3}](point source/sink).
9. NSCN	Number of specified solute concentration nodes.
10. J,CS(J)	Node number, Specified solute concentration [mol kg^{-1}].
11. ISFLAG	Flux (ISFLAG=0), Convective boundary condition (ISFLAG=1).
12. NSFN	Number of specified solute flux nodes.
13. J,FLUXPC(J)	Node number, Specified solute point source/sink [1], Or
14. J,CIN(J)	Node number, Specified background solute concentration [mol kg^{-1}].
15. IFLOW(I),NS(I,1),NS(I,2)	Permeable boundary node, Boundary node end points.
16. NSMF	Number of distributed moisture flux nodes; for example NSMF = 0.
17. J,FLUXDM(J)	Node number, Distributed moisture flux [$\text{m}^3 \text{d}^{-1}$]. Note: if a -99 is entered, then the unit hydraulic boundary condition is activated.
18. NSHF	Number of distributed heat flux nodes.
19. J,FLUXDT(J)	Node number, Distributed heat flux [cal m^{-3}].
20. NSCF	Number of distributed solute flux nodes.
21. J,FLUXDC(J)	Node number, distributed concentration flux [mol kg^{-1}].

INITIAL:

Parameter	Definition
1. MAXTS	Maximum number of time steps.
2. MAXIT	Maximum number of Picard iterations.
3. TOL1	Tolerance criteria for pressure head [m].
4. TOL2	Tolerance criteria for temperature [$^{\circ}\text{C}$].
5. TOL3	Tolerance criteria for concentration [mol kg^{-1}].
6. REFT	Temperature used to calculate reference values of density, surface tension, viscosity, and latent heat of vaporization [$^{\circ}\text{C}$].
7. FLAGDV	Flag indicating type of fluid density, surface tension, and viscosity calculations: 1 = constant, 2= temperature dependent, and 3= temperature and concentration dependent.
8. RS	Hydrated radius of solute molecule [nm].

9. GF	Gain factor used to multiply temperature coefficient in D_{TL} . Compensates for underestimation of temperature-induced changes in matric potential ($1 < GF < 5$).
10. TF	Tortuosity factor (scales tortuosity).
11. FDTL2	Factor multiplying change in osmotic potential with respect to temperature in D_{TL} for example, FDTL2 = 1 for new theory (Nassar, 1992) or FDTL2 = 0 to remove liquid water flux because of a concentration gradient (de Vries, 1958).
12. FDCL2	Factor multiplying change in osmotic potential with respect to concentration in D_{CL} ; for example, FDCL2 = 1 if new theory (Nassar, 1992), FDCL2 = 0 to remove liquid water flux due to concentration gradient (De Vries, 1958).
13. SCALE	Scales time step used in alternate Picard iteration set. For example, if convergence is not achieved, time step is decreased by SCALE and Picard procedure restarted [d].
14. OMEGA	Relaxation factor ($0 < OMEGA < 1$). Determined by trial-and-error.
15. OMEGADT	Time increment multiplier [d].
16. NUMSTEP(ICOUNT)	Number of time steps.
17. DT(ICOUNT)	Time-step increment [d].
18. -1	End-flag for number of time steps.
19. -1	End-flag for time step increment.
20. TIME(ICOUNT),	Beginning time [d].
21. TFUNC(ICOUNT)	Beginning time function [dimensionless].
22. TIME(ICOUNT),	Ending time [d].
23. TFUNC(ICOUNT)	Ending time function (linear interpolation) [dimensionless].
24. -1	End-flag for ending time.
25. -1	End-flag for ending time function.
26. DTMAXX	Maximum allowable time increment [d].
27. NTHOUT	Write results every N th time step; If NTHOUT = 0 then results are written at user specified times.
28. IFLAG	Indicates initial uniform pressure field (IFLAG = 0) , or uniform moisture content field (IFLAG = 1), or read nodal pressure pairs (IFLAG = 2), or read nodal moisture pairs (IFLAG = 3).
29. XINIT	Uniform moisture value [$\text{cm}^3 \text{cm}^{-3}$]; or uniform pressure value [m]; or node #, pressure head [m] pairs; or node #, moisture [$\text{cm}^3 \text{cm}^{-3}$] pairs. Total pairs = NUMNOD.
30. IFLAGT	Indicates initial uniform temperature field (IFLAGT = 0) or read nodal temperature pairs (IFLAGT = 1).
31. DEGREESC	Uniform temperature value [$^{\circ}\text{C}$]; or node #, temperature [$^{\circ}\text{C}$] pairs. Total pairs = NUMNOD.
32. IFLAGC	Indicates initial uniform concentration field (IFLAGC = 0) , or read nodal concentration pairs (IFLAGC = 1).
33. SOLC	Uniform concentration value [mol kg^{-1}]; or node #, concentration [mol kg^{-1}] pairs. Total pairs = NUMNOD.
34. ICOUNT	Number time steps for which data will be written.
35. TIM (ICOUNT)	Output time(s) [d] at which data will be written.
36. ICOUNT	Number of nodes for which data will be written.
37. NODEOUT(I) = NOD	Node number(s) for which results are written.

Data Output Files

Output from the main program is stored in 11 scratch files (with the extension .OUT): BUDGET, DIFFC, DIFFPT, DISP, LFLUX, PECLT, NODES, NODES1D, NODES2D, VST, VELOCITY. Because all data are written to files in column fashion, the files can be used with many commercial graphing and/or contour packages. The various parameters and dependent variables associated with each scratch file are described below. The actual argument or parameter used in the VST2D model is presented in upper case and between parentheses.

- BUDGET:** This file contains incremental and cumulative water, solute, and heat balance information. Specific incremental information is written out for each time increment (DT) and includes the volume ($VOLM, VOLH, VOLC$), total flux in ($QMIN, QHIN, QCIN$), total flux out ($QMOUT, QHOUT, QCOUT$), net flux change (dQm, dQh, dQc), storage change (dSm, dSh, dSc), and residual error ($VOLERRm, VOLERRh, VOLERRc$). Cumulative information is written out for total time (T) and includes the volume ($cVOLM, cVOLH, cVOLM$), total flux in ($cQMIN, cQHIN, cQCIN$), total flux out ($cQMOUT, cQHOUT, cQCOUT$), cumulative net flux change ($cdQm, cdQh, cdQc$), cumulative storage change ($cdSm, cdSh, cdSc$), absolute change ($cVOLERRm, cVOLERRh, cVOLERRc$), and cumulative residual error ($rVOLERRm, rVOLERRh, rVOLERRc$).
- DIFFC:** This file contains the node number ($NODE$), Cartesian coordinate (X, Y), molecular diffusivity of water vapor in air (D), isothermal moisture diffusivity (Dm), diffusion coefficient of solute because of temperature gradients (D_{TS}), diffusion coefficient of solute because of salt sieving multiplied by moisture capacity in x- and y-directions ($D_{xsiev} C, D_{ysiev} C$), and moisture capacity (C).
- DIFFPT:** This file contains the node ($NODE$), Cartesian coordinates (X, Y), isothermal liquid diffusivity in the x-direction (D_{ml-x}), isothermal liquid diffusivity in the y-direction (D_{ml-y}), isothermal vapor diffusivity (D_{mv}), thermal liquid diffusivity in the x- and y-directions (D_{tl-x}, D_{tl-y}), thermal vapor diffusivity (D_{TV}), liquid water diffusivity because of solute concentration in x-direction (D_{cl-x}), liquid water diffusivity because of solute concentration in the y-direction (D_{cl-y}), vapor diffusivity because of solute concentration (D_{CV}), moisture capacity (C), and osmotic coefficient (OEC).
- DISP:** This file contains the time step (TS), iteration (IT), element (E), and mechanical dispersion coefficients in the xx, yy, and xy directions ($D_{hxx}, D_{hyy}, D_{hxy}$).
- LFLUX:** This file contains the element number ($ELEM$), liquid flux because of thermal gradient in the x- and y-directions ($QTLXE, QTLYE$), liquid isothermal flux in x- and y-directions ($QMLXE, QMLYE$), and liquid flux because of solute gradient in the x- and y-directions ($QCLXE, QCLYE$).
- PECLT:** This file contains the time step (TS), iteration (IT), element (E), Peclet number in the x- and y-directions ($Pe-x, Pe-y$), maximum Courant number in the x- and y-directions ($Cr-x, Cr-y$), dispersion coefficient in the x-direction (D_{xx}), dispersion coefficient in the y-direction (D_{yy}), average element velocity in the x-direction (VXE), and average element velocity in y-direction (VYE).
- NODES:** This file contains the global control array that tracks Dirichlet conditions ($ISFV2$), global control array that tracks modified Dirichlet conditions ($ISFV3$), and local control arrays that indicate specified pressure head (ISP), temperature (IST), and concentration (ISC).
- NODES1D:** This file contains two blocks of data written for selected nodes along a one-dimensional profile. The first block includes node number ($NODE$), pressure head ($PRES$), temperature ($TEMP$), solute concentration ($CONC$), moisture ($MOIST$), liquid saturation ($SAT-liquid$), vapor saturation ($SAT-vapor$), and hydraulic conductivity in x-direction (K_x), and hydraulic conductivity in the y-direction (K_y). The second block includes node number ($NODE$), Cartesian coordinate in x-direction (X), Cartesian coordinate in the y-direction (Y), isothermal liquid diffusivity in the x- and y-directions (D_{ml-x}, D_{ml-y}), isothermal vapor diffusivity (D_{mv}), thermal liquid diffusivity in the x- and y-directions (D_{tl-x}, D_{tl-y}), thermal vapor diffusivity (D_{TV}), liquid water diffusivity

because of solute concentration in the x - and y -directions (D_{cl-x} , D_{cl-y}), vapor diffusivity because of solute concentration (D_{CV}), moisture capacity (C), and osmotic coefficient (OE).

NODES2D: This file contains a block of data for all nodes (2-dimensions) at a given time step. For example, number ($NODE$), pressure head ($PRES$), temperature ($TEMP$), solute concentration ($CONC$), moisture ($MOIST$), and saturation (SAT).

VST: This file contains echoed input from **ELEMENT**, **BOUNDARY**, **INITIAL**, and **PROPERTY**. The file also includes output time, iteration number when the solution converged, and associated mass and energy budgets.

VELOCITY: This file contains element number ($ELEM$), pore water velocity in the x -direction (V_x), pore water velocity in the y -direction (V_y), specific discharge in the x -direction (Q_x), specific discharge in the y -direction (Q_y), apparent velocity (V), and angle ($ANGLE$).

MODEL VERIFICATION

To ensure that the governing equations and finite-element model formulations are derived and implemented correctly, the accuracy of VST2D calculations are verified in two parts. First, the transient response of individual dependent variables (pressure head, temperature or concentration) are compared to numerical solutions by decoupling the governing equations through application of appropriate boundary conditions. In this report, VST2D is checked against numerical solutions for water (Nieber and others, 1994), heat (Blomberg and Claessen, 1998), and solute (van Genuchten and Alves, 1982) transport under simplified, unsaturated, conditions. Second, the simultaneous, one-dimensional, steady-state, interaction of water-heat-solute is verified against laboratory observations of a closed-system as described by Nassar and Horton (1989). A comparison in this way is appropriate because of the unavailability of recently developed steady-state models involving water-heat-solute transport (Nassar and Horton, 1992; Noborio and others, 1996).

The following sections describe numerical experiments involving the simulation of water or solute, and water-heat-solute transport through homogeneous Ida silt loam (Nassar and Horton, 1989), and heat transport through heterogeneous crystalline rock. Important model properties include bulk density, dispersivities (longitudinal and transverse), fractional soil constituents (sand, silt, clay, and organic carbon), moisture retention, saturated hydraulic conductivity, and specific surface area. A summary of properties for the soil and rock are provided in tables 2 and 3, respectively. Many of these properties were determined previously using laboratory methods, however, those properties with an asterisk indicate assumed literature or fitted values. For example, the three parameters (α , n , and $m = 1/1-n$) used to describe a moisture retention function were determined by fitting a curve to the observed moisture-pressure head measurements for Ida silt loam (Nassar and Horton, 1989) using the RETC computer program (van Genuchten, 1980). These observations and fitted curve are presented in figure 3.

The numerical calculations using VST2D are for a two-dimensional domain, however, the applied boundary conditions result in one-dimensional transport. As such, the results are written to files for nodes specified along the center-axis of each finite-element mesh. In this way, transport profiles simulated using VST2D can be compared with the other one-dimensional numerical and analytic solutions.

Case 1: Water Transport Under Nonisobaric, Isothermal, Isohaline Conditions

In this first case, the accumulation of water is simulated as it migrates into a vertical and closed column (sides and bottom) of moist, homogeneous and isotropic Ida silt loam. The conditions involve continuous surface ponding with constant 20 °C temperature (isothermal) and 0.00 mol kg⁻¹ solute concentration (isohaline) throughout the soil. A summary of the input properties and conditions are provided in tables 2 and 4, respectively. The finite-element mesh used during this simulation is shown in figure 8, and the input data files is provided in appendix 3. Surface boundaries are numbered from 1 to 4 beginning at x equal to zero (far left) and moving counterclockwise.

Table 2. Summary of properties used in the VST2D model validation process involving Ida silt loam

[Mg m⁻³, million grams per cubic meter; m, meter; mg kg, milligram per kilogram; cm³/cm³, cubic centimeter per cubic centimeter; m d⁻¹, meter per day; m² kg⁻¹, meter squared per kilogram; cal cm⁻³, calorie per cubic centimeter; °C, degrees Celsius; * estimated or assumed value]

Physical Property	Magnitude
1. Angle between local principal directions and global Cartesian coordinates, δ	0.0 degrees
2. Bulk density, ρ_b	1.09 Mg m ⁻³
3. Decay constant, λ^*	0.0 d ⁻¹
4. Dispersivity-longitudinal, α_L^*	0.007 m
5. Dispersivity-transverse, α_T^*	0.001 m
6. Distribution coefficient, K_d^*	0.0 L kg ⁻¹
7. Fractional organic carbon, X_o^*	0.0002 cm ³ /cm ³
8. Fractional sand, X_{snd}^*	0.1 cm ³ /cm ³
9. Fractional silt, X_{slt}^*	0.686 cm ³ /cm ³
10. Fractional clay, X_{cly}^*	0.214 cm ³ /cm ³
11. Moisture retention property, α^*	0.5857 m ⁻¹
12. Moisture retention property, n^*	1.546
13. Moisture content-saturated (porosity), θ_s	0.67 cm ³ /cm ³
14. Moisture content-residual, θ_r^*	0.05 cm ³ /cm ³
15. Porous media compressibility, ω	1.01 × 10 ⁻⁸ m ² N ⁻¹
16. Saturated hydraulic conductivity, x-direction, K_x	0.229 m d ⁻¹
17. Saturated hydraulic conductivity, y-direction, K_y	0.229 m d ⁻¹
18. Specific surface area, S_a	1.01 × 10 ⁻⁵ m ² kg ⁻¹
19. Thermal conductivity of silt, λ_s	10 mcal cm ⁻¹ °C ⁻¹ s ⁻¹
20. Volumetric heat capacity of solids, C_{ps}	0.48 cal cm ⁻³ °C ⁻¹

Table 3. Summary of properties used in the VST2D model validation process involving crystalline rock

[Mg m⁻³, million grams per cubic meter; m, meter; mg kg, milligram per kilogram; cm³/cm³, cubic centimeter per cubic centimeter; m d⁻¹, meter per day; m² kg⁻¹, meter squared per kilogram; cal cm⁻³, calorie per cubic centimeter; °C, degrees Celsius; * estimated or assumed value]

Physical Property	Magnitude
1. Angle between local principal directions and global Cartesian coordinates, δ	0.0 degrees
2. Bulk density, ρ_b	1.07 Mg m ⁻³
3. Decay constant, λ^*	0.0 d ⁻¹
4. Dispersivity-longitudinal, α_L^*	0.0 m
5. Dispersivity-transverse, α_T^*	0.0 m
6. Distribution coefficient, K_d^*	0.0 L kg ⁻¹
7. Fractional organic carbon, X_o^*	0.0 cm ³ /cm ³
8a. Fractional sand (unit 1), X_{snd}^*	0.995 cm ³ /cm ³
9a. Fractional silt (unit 1), X_{slt}^*	0.005 cm ³ /cm ³
10a. Fractional clay (unit 1), X_{cly}^*	0.0 cm ³ /cm ³
8b. Fractional sand (unit 2), X_{snd}^*	0.005 cm ³ /cm ³
9b. Fractional silt (unit 2), X_{slt}^*	0.095 cm ³ /cm ³
10b. Fractional clay (unit 2), X_{cly}^*	0.0 cm ³ /cm ³
11. Moisture retention property, α^*	0.5857 m ⁻¹
12. Moisture retention property, n^*	1.546
13. Moisture content-saturated (porosity), θ_s	0.095 cm ³ /cm ³
14. Moisture content-residual, θ_r^*	0.09 cm ³ /cm ³
15. Porous media compressibility, ω	1.01 × 10 ⁻⁸ m ² N ⁻¹
16. Saturated hydraulic conductivity, x-direction, K_x	0.229 m d ⁻¹
17. Saturated hydraulic conductivity, y-direction, K_y	0.229 m d ⁻¹
18. Specific surface area, S_a	1.01 × 10 ⁻⁵ m ² kg ⁻¹
19. Thermal conductivity of silt, λ_s	10 mcal cm ⁻¹ °C ⁻¹ s ⁻¹
20. Volumetric heat capacity of soil solids, C_{ps}^*	0.48 cal cm ⁻³ °C ⁻¹

Table 4. Summary of conditions used in the VST2D validation process for water transport [cm³/cm³, cubic centimeter per cubic centimeter; m d⁻¹, meter per day; °C, degrees Celsius; mol kg⁻¹, mole per kilogram; Γ , surface boundary]

Initial conditions: $\theta(x,y,0)$, initial moisture content at all nodes; $T(x,y,0)$, initial temperature at all nodes; $C(x,y,0)$, initial concentration at all nodes

Dirichlet conditions: $\theta(x,1.40,t)$, moisture content on Γ_4 ; $T(x,y,t)$, temperature at all nodes; $C(x,y,t)$, concentration at all nodes

Neumann conditions: $q_\theta(0.00,y,t)$, liquid flux on Γ_1 ; $q_\theta(0.08,y,t)$, liquid flux on Γ_3 ; $q_\theta(x,0.00,t)$, liquid flux on Γ_2 .

Initial conditions	Dirichlet conditions	Neumann conditions
$\theta(x,y,0) = 0.15 \text{ cm}^3/\text{cm}^3$	$\theta(x,1.4,t) = 0.67$	$q_\theta(0.00,y,t) = 0.0 \text{ m d}^{-1}$
$T(x,y,0) = 20.0 \text{ }^\circ\text{C}$	$T(x,y,t) = 20.0 \text{ }^\circ\text{C}$	$q_\theta(0.08,y,t) = 0.0 \text{ m d}^{-1}$
$C(x,y,0) = 0.00 \text{ mol kg}^{-1}$	$C(x,y,t) = 0.00 \text{ mol kg}^{-1}$	$q_\theta(x,0.00,t) = 0.0 \text{ m d}^{-1}$

The results of this simulation are verified to a numerical solution obtained with the computer program VARSAT2D (Nieber and others, 1994). For this case, the simulated pressure head profiles for vertical flow range from 0.1 to 2.0 days (fig. 9). Excellent visual agreement is indicated between both numerical models. Differences between both methods were less than 0.1 percent with maximum VST2D mass-balance errors for time step and total time on the order of 10^{-8} and 10^{-7} , respectively.

The corresponding VST2D moisture and saturation profiles are shown in figures 10a-10b. As expected, the profiles in these figures indicate water percolates into the soil column in response to the pressure and gravitational potentials. Upon reaching the column bottom, the moisture front saturates the soil and begins accumulating in time.

Case 2: Heat Transport Under Isobaric, Nonisothermal, Isohaline Conditions

In the second case, time dependent heat transport is simulated as it migrates into a heterogeneous, isotropic, crystalline rock block. With moisture content set to residual and no applied water pressure, latent heat by vapor or sensible heat by moving vapor and liquid is not transferred. Under these conditions, the VST2D simulated transfer of heat, which is by molecular conduction, can be compared to the results from the program HEAT2 (Blomberg and Claessen, 1998). The input properties and applied conditions describing this case are given in tables 3 and 5, respectively. The finite-element mesh used is shown in figure 11 and the input data files are provided in appendix 4.

The simulated time-dependent temperature profiles derived using VST2D (isobaric, isohaline) and HEAT2 models are shown in figure 12. These numerical models appear in agreement (after 1.44 minutes and 144 minutes) with a characteristic break in temperature slope at the point where thermal properties change. The VST2D mass relative balance error was on the order of 10^{-3} but not available for the HEAT2 model.

Case 3: Solute Transport Under Isobaric, Isothermal, Nonisohaline Conditions

In this third case, the accumulation of solute is simulated as it is transported into a vertical column of homogeneous and isotropic Ida silt loam. By applying a constant pressure head and temperature at both ends of the soil column, the moisture content (and therefore velocity, 0.019 m d^{-1}) and hydrodynamic dispersion ($0.00919 \text{ m}^2 \text{ d}^{-1}$) are constant throughout the domain. Also, the constant-moisture profile with no sorption or decay (distribution coefficient and decay constant equal to zero) results in a conventional retardation factor equal to one. Assuming that a uniform and external solute source is present, transport into the column occurs across the upper boundary due solely to the gravitational potential gradient. At the outlet end, the transient build-up of solute is governed by the permissible solute flux across that boundary. The implementation of these conditions together with convective solute boundary conditions in VST2D permits verification with a one-dimensional, steady-state analytical solution using ALVE2 (van Genuchten and Alves, 1982). A summary of the input properties and conditions is provided in

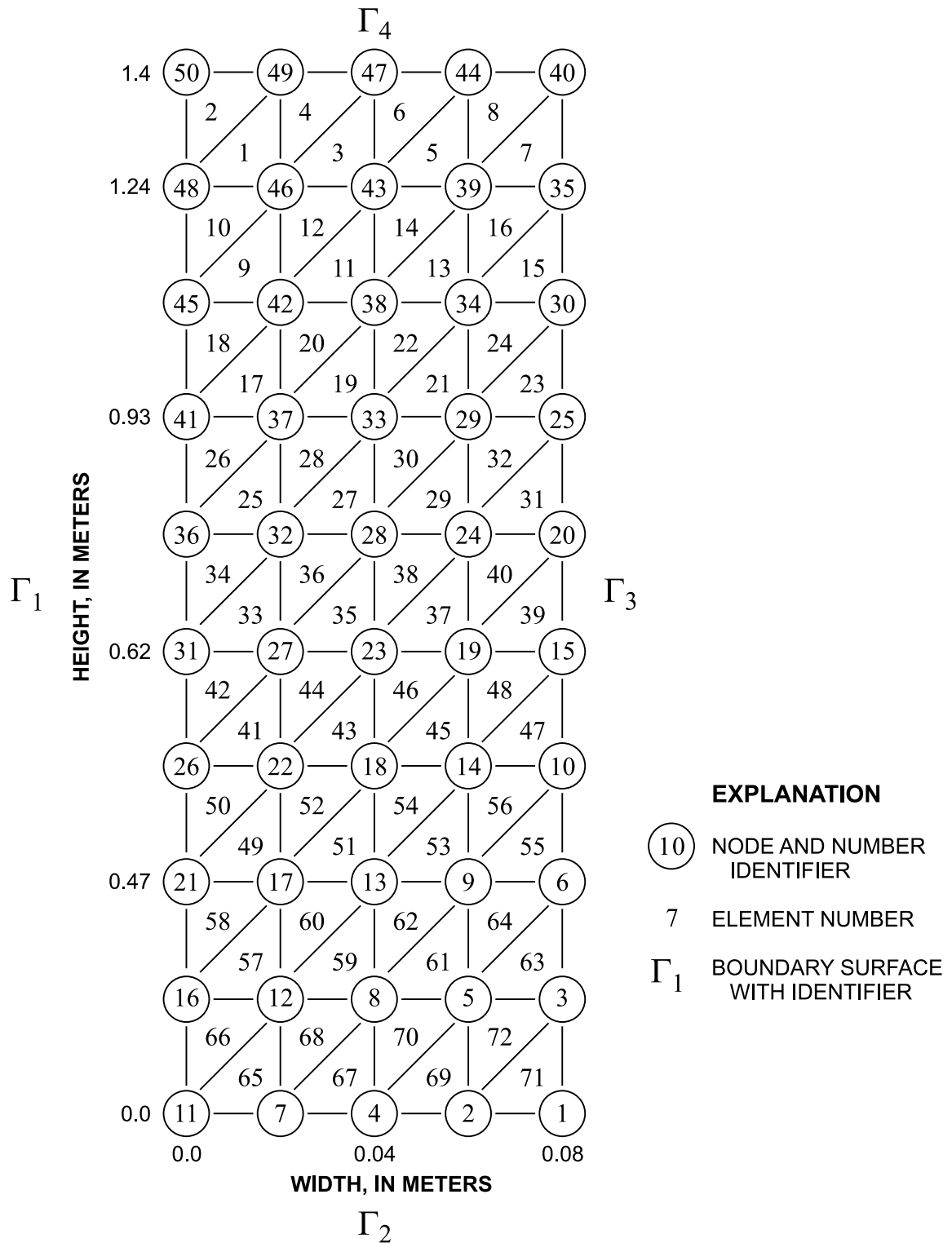


Figure 8. Finite-element mesh used in the verification of water transport under isothermal and isohaline conditions.

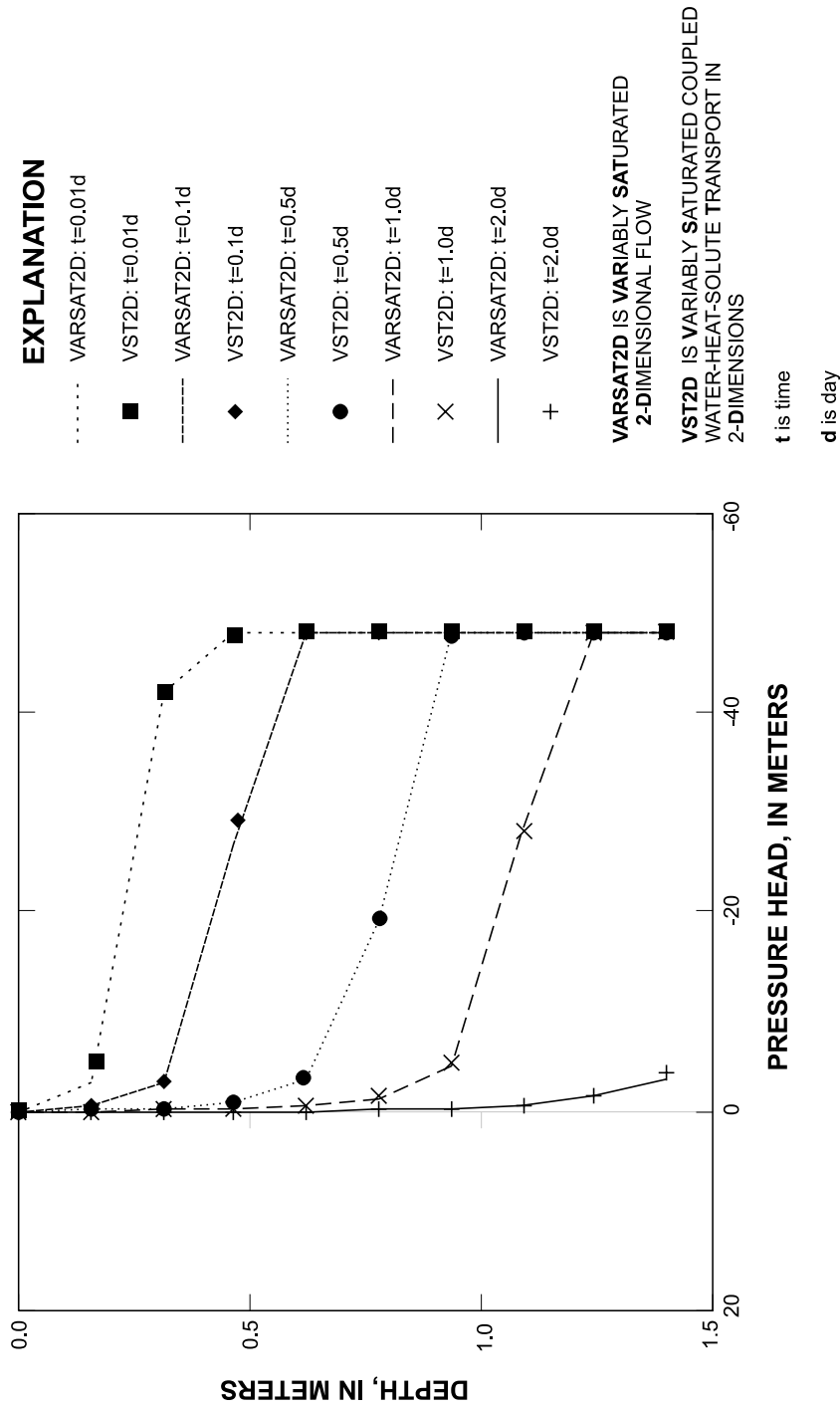


Figure 9. Comparison of transient pressure head profiles for vertical water transport simulated under isothermal and isohaline conditions using the VST2D and VARSAT2D models.

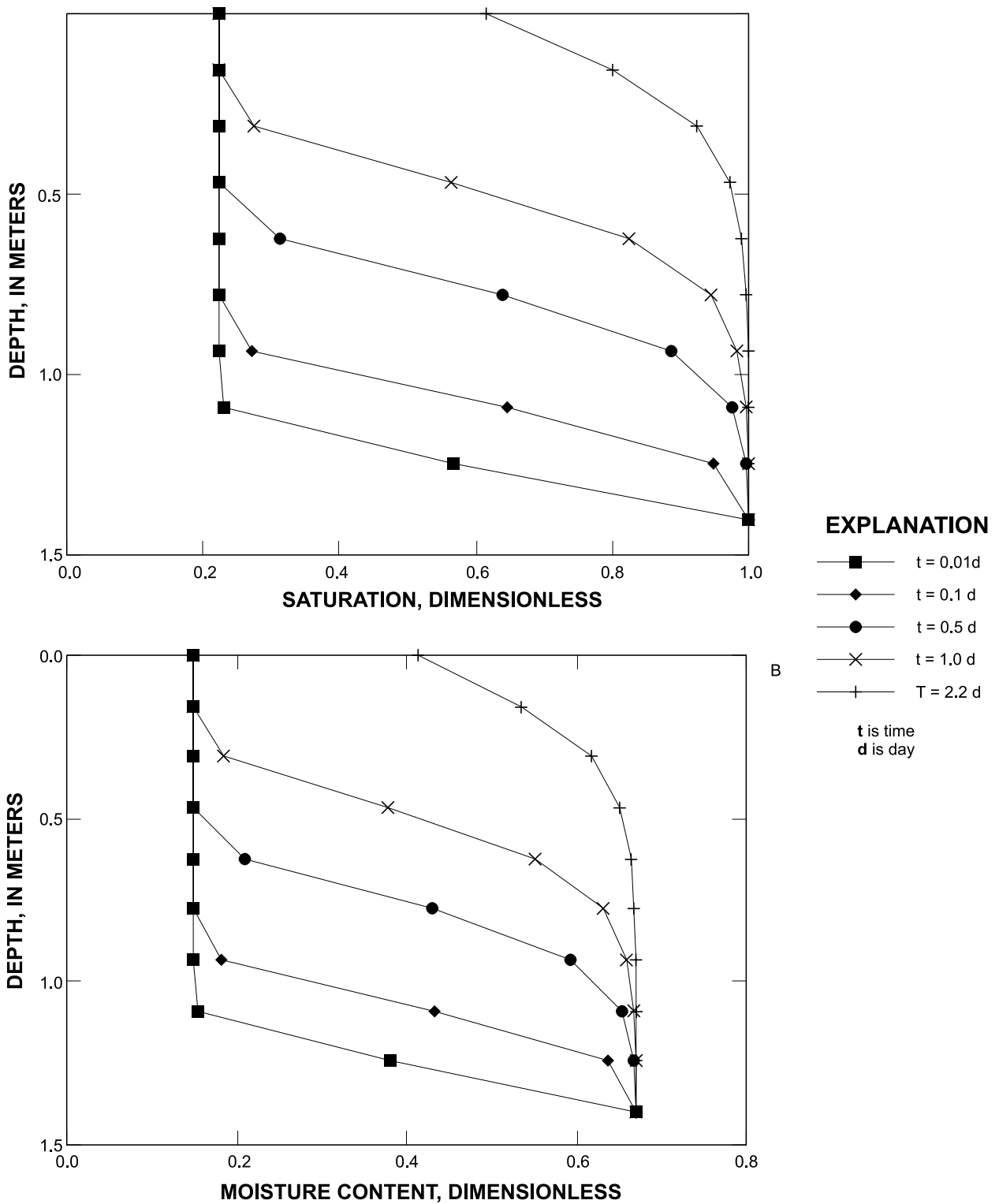


Figure 10. Comparison of transient (A) moisture and (B) saturation profiles for vertical water transport simulated under isothermal and isohaline conditions using the VST2D model.

Table 5. Summary of conditions used in the VST2D validation process for heat transport [cm³/cm³, cubic centimeter per cubic centimeter; m d⁻¹, meter per day; °C, degrees Celsius; mol kg⁻¹, mole per kilogram; Γ , surface boundary]

Initial conditions: $\psi(x,y,0)$, initial moisture content at all nodes; $T(x,y,0)$, initial temperature at all nodes; $C(x,y,0)$, initial concentration at all nodes

Dirichlet conditions: $\psi(x,y,t)$, pressure head at all nodes; $T(0.00,y,t)$, temperature on Γ_1 ; $T(0.08,y,t)$, temperature on Γ_3 ; $C(x,y,t)$, concentration at all nodes

Neumann conditions: $q_T(x,0.00,t)$, heat flux on Γ_1 ; $q_T(x,0.08,t)$, heat flux on Γ_3

Initial conditions	Dirichlet conditions	Neumann conditions
$\psi(x,y,0) = -10.0$ m	$\psi(x,y,t) = -10.0$ m	$q_T(x,0.00,t) = 0.0$ cal d ⁻¹
$T(x,y,0) = 10.0$ °C	$T(0.00,y,t) = 1.0$ °C	$q_T(x,0.08,t) = 0.0$ cal d ⁻¹
$C(x,y,0) = 0.00$ mol kg ⁻¹	$T(0.08,y,t) = 20.0$ °C	
	$C(x,y,t) = 0.00$ mol kg ⁻¹	

tables 2 and 6, respectively. The finite-element mesh used in this simulation is shown in figure 14. The input data files are provided in appendix 5.

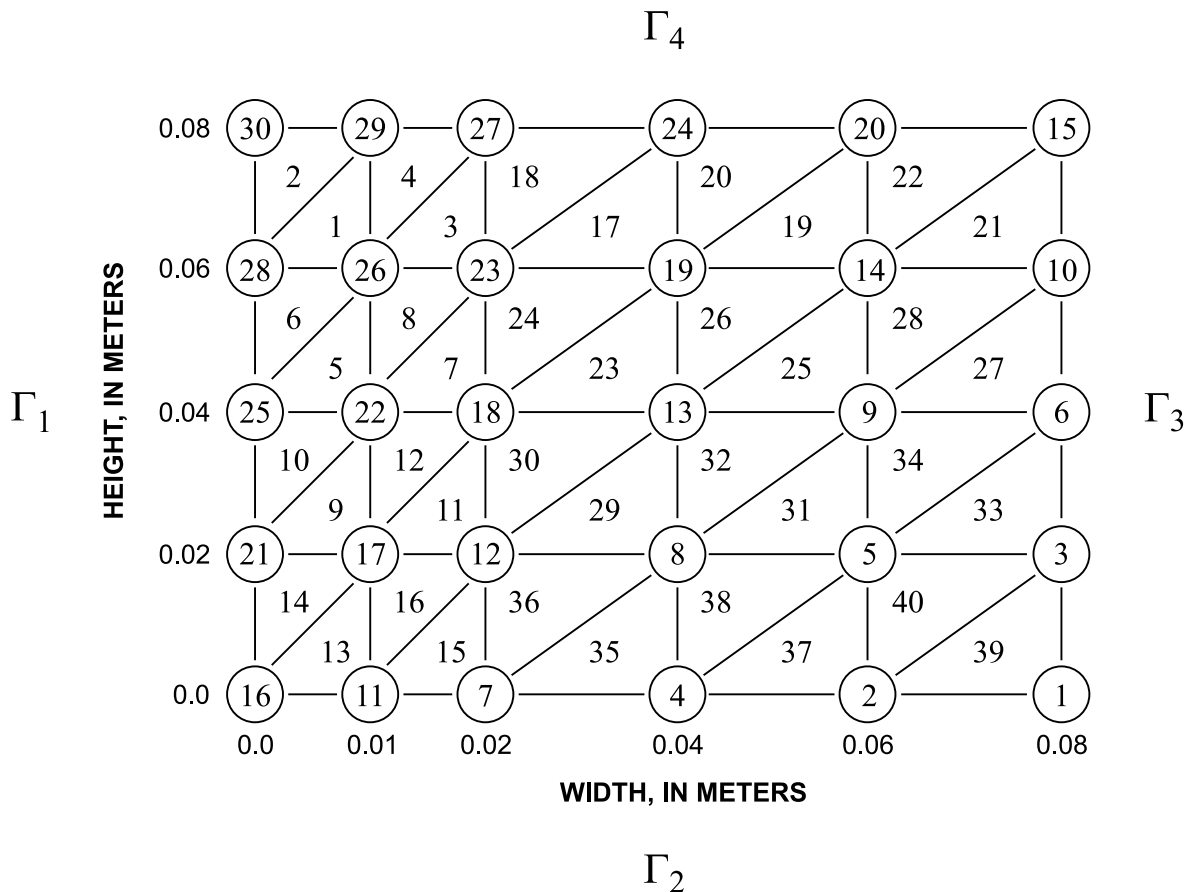
In performing these simulations, the Peclet and Courant numbers of 1.57 and 0.0046 calculated in VST2D gave a maximum allowable element size and time step of 0.3 m and 0.218 day, respectively. The resulting time-dependent solute concentration profiles for 1, 5, 10, 15, and 25 days are shown in figure 13. The solute is determined to move into the domain along a relatively sharp concentration front and in time saturates the column (fig. 13). Despite the relatively good mass balance error of 10^{-5} and 10^{-3} for water and solute, respectively, the VST2D curve tends to under and over simulate the analytical solution at the leading and trailing edges of the respective concentration front.

Case 4: Coupled Water-Heat-Solute Transport Under Nonisobaric, Nonisothermal, Nonisohaline Conditions

In the final verification case, experimental observations of interactive heat and mass transport are used to test and verify the capability of VST2D to simulate a coupled ground-water system. The laboratory observations used here were recorded during an experiment performed with temperature applied to a horizontal column under closed-system conditions (Nassar and Horton, 1989). Soil moisture, temperature and solute concentration profiles simulated for this closed horizontal column are computed and compared with profiles observed after attaining steady-state (31-day period). The respective finite-element mesh and boundary conditions used are presented in figure 15 and table 7. The input data files are provided in appendix 6.

In simulating coupled energy and mass transport in a horizontal closed-column subject to heat at each end, a simple trial-and-error calibration was conducted to fit the longitudinal dispersivity (α_L) and thermal diffusivity gain factor ($G_{\psi T}$). Assuming an initial longitudinal dispersivity equal to 10 percent of the total domain length (0.014 m), the gain factor was increased from zero until the calculated average moisture and solute concentrations matched the steady state conditions (the net mass flux equal to zero). Next, the longitudinal dispersivity was decreased until the solute profile matched the observed results.

General agreement is apparent between the dependent variables (moisture, temperature, and concentration) measured in the laboratory and those variables calculated simultaneously using VST2D (figs. 16a-c). The best correspondence is between the simulated and observed solute profiles. The mismatch between the modeled linear and observed nonlinear temperature profiles suggests the likely increased effect of sensible heat transfer by liquid movement in the laboratory. Other possible reasons for discrepancies between the modeled and laboratory results may be due to the use of numerous estimated and assumed values as input to the model (see table 2). Also shown are calculated results based on the Philip and de Vries (1957) theory, which neglects water fluxes due to solute gradients. These results underscore the importance of accounting for effects of solute on water movement in moist, salinized soil.



EXPLANATION

- $\textcircled{10}$ NODE AND NUMBER IDENTIFIER
- 7 ELEMENT NUMBER
- Γ_1 BOUNDARY SURFACE WITH IDENTIFIER

Figure 11. Finite-element mesh used in the verification of heat transport under isobaric and isohaline conditions.

SUMMARY

The occurrence of temperature, pressure head, and chemical concentration gradients in geologic materials can cause the simultaneous transport of heat, water, and solute. The computer model called VST2D was designed to simulate coupled water-heat-solute transport in heterogeneous, anisotropic, two-dimensional, ground-water systems with variable fluid density. This report documents the theoretical development of governing equations, parametric relations, finite-element formulation, solution procedure, initial and boundary conditions, and mass/energy balance considerations incorporated into VST2D, and it provides a user's document for implementation of the model. The advantages and limitations of model implementation also are discussed together with the model's validation.

The coupling of governing equations for water, heat, and solute transport, allows the VST2D model to solve simultaneously for one or more dependent variables (pressure, temperature, and concentration) at nodes in a horizontal or vertical mesh using a quasi-linearized general minimum residual method. Heterogeneous

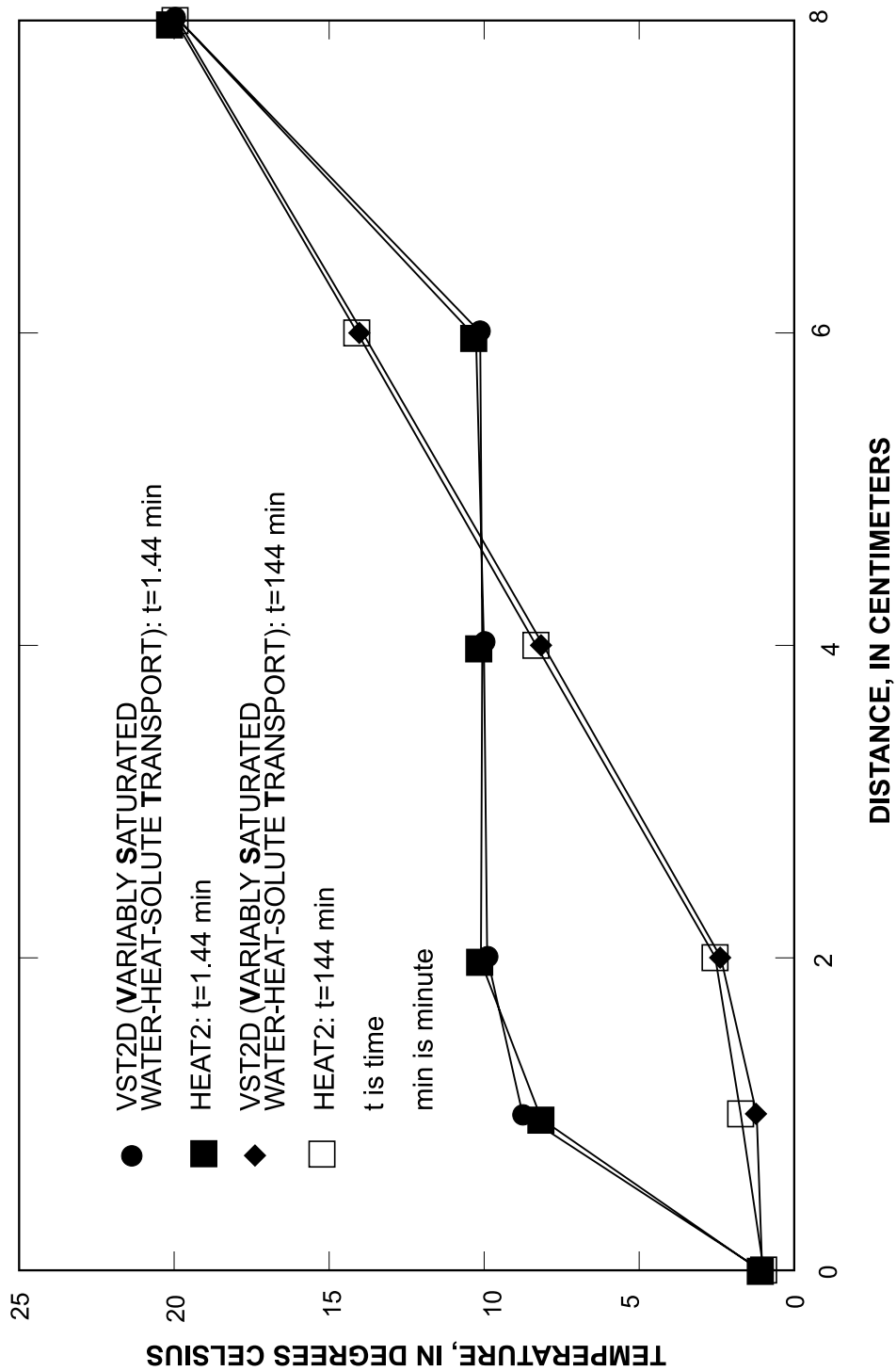


Figure 12. Comparison of transient temperature profiles simulated under isobaric and isohaline conditions using VST2D and HEAT2.

Table 6. Summary of conditions used in the VST2D model validation process for solute transport

[m, meter; m d⁻¹, meter per day; °C, Celsius; cal d⁻¹, calorie per day; mol kg⁻¹, mole per kilogram; mol kg⁻¹ d⁻¹, mole per kilogram day; Γ , surface boundary]

Initial conditions: $\psi(x,y,0)$, initial pressure head at all nodes; $T(x,y,0)$, initial temperature at all nodes; $C(x,y,0)$, initial concentration at all nodes

Dirichlet conditions: $\psi(x,0.00,t)$, pressure head on Γ_1 ; $\psi(x,1.40,t)$, pressure head on Γ_2 ;
 $T(x,0.00,t)$, temperature on Γ_1 ; $T(x,1.40,t)$, temperature on Γ_2 ;
 $C(-\infty,0.00,t)$, ambient concentration outside domain but along Γ_1 ;
 $C(x,1.40,t)$, concentration on Γ_2

Neumann conditions: $q_\theta(0.00,y,t)$, liquid flux on Γ_1 ; $q_\theta(0.08,y,t)$, liquid flux on Γ_3 ;
 $q_T(0.00,y,t)$, heat flux on Γ_1 ; $q_T(0.08,y,t)$, heat flux on Γ_3 ;
 $q_C(0.00,y,t)$, solute flux on Γ_2 ; $q_C(0.08,y,t)$, solute flux on Γ_3 ;
 $q_C(x,0.00,t)$, solute flux on Γ_4

Initial conditions	Dirichlet conditions	Neumann conditions
$\psi(x,y,0) = -0.5$ m	$\psi(x,0.00,t) = -0.5$ m	$q_\theta(0.00,y,t) = 0.0$ m d ⁻¹
$\psi(x,y,0) = -0.5$ m	$\psi(x,1.40,t) = -0.5$ m	$q_\theta(0.08,y,t) = 0.0$ m d ⁻¹
$T(x,y,0) = 20.0$ °C	$T(x,0.00,t) = 20.0$ °C	$q_T(0.00,y,t) = 0.0$ cal d ⁻¹
$C(x,y,0) = 0.00$ mol kg ⁻¹	$T(x,1.40,t) = 20.0$ °C	$q_T(0.08,y,t) = 0.0$ cal d ⁻¹
	$C(\infty,0.00,t) = 1.00$ mol kg ⁻¹	$q_C(0.00,y,t) = 0.0$ mol kg ⁻¹ d ⁻¹
	$C(x,1.40,t) = 0.00$ mol kg ⁻¹	$q_C(0.08,y,t) = 0.0$ mol kg ⁻¹ d ⁻¹
		$q_C(x,0.00,t) = 0.0$ mol kg ⁻¹ d ⁻¹

and anisotropic conditions are implemented locally using individual element property descriptions. Boundary conditions can include time-varying pressure head (or moisture content), heat, and/or concentration; fluxes distributed along domain boundaries and/or at internal node points; and/or convective moisture, heat, and solute fluxes along the domain boundaries; and/or unit hydraulic gradient along domain boundaries. Other model features include temperature and concentration dependent density (liquid and vapor) and viscosity, sorption and/or decay of a solute, and capability to determine moisture content beyond residual to zero.

The VST2D model was validated against analytic and numerical solutions for problems of water transport under isohaline and isothermal conditions, heat transport under isobaric and isohaline conditions, and solute transport under isobaric and isothermal conditions. The coupled water-heat-solute transport problem was compared to measured laboratory results for which no known analytic solutions or numerical models are available. The test results indicate the model is accurate and applicable for a wide range of conditions, including when water (liquid and vapor), heat (sensible and latent), and solute are coupled in ground-water systems. The cumulative residual errors for the coupled problem tested was less than 10⁻⁸ cubic centimeter per cubic centimeter, 10⁻⁵ moles per kilogram, and 102 calories per cubic meter for liquid water content, solute concentration and heat content, respectively. This model should be useful to hydrologists, engineers, and researchers interested in studying coupled processes associated with variably saturated transport in ground-water systems.

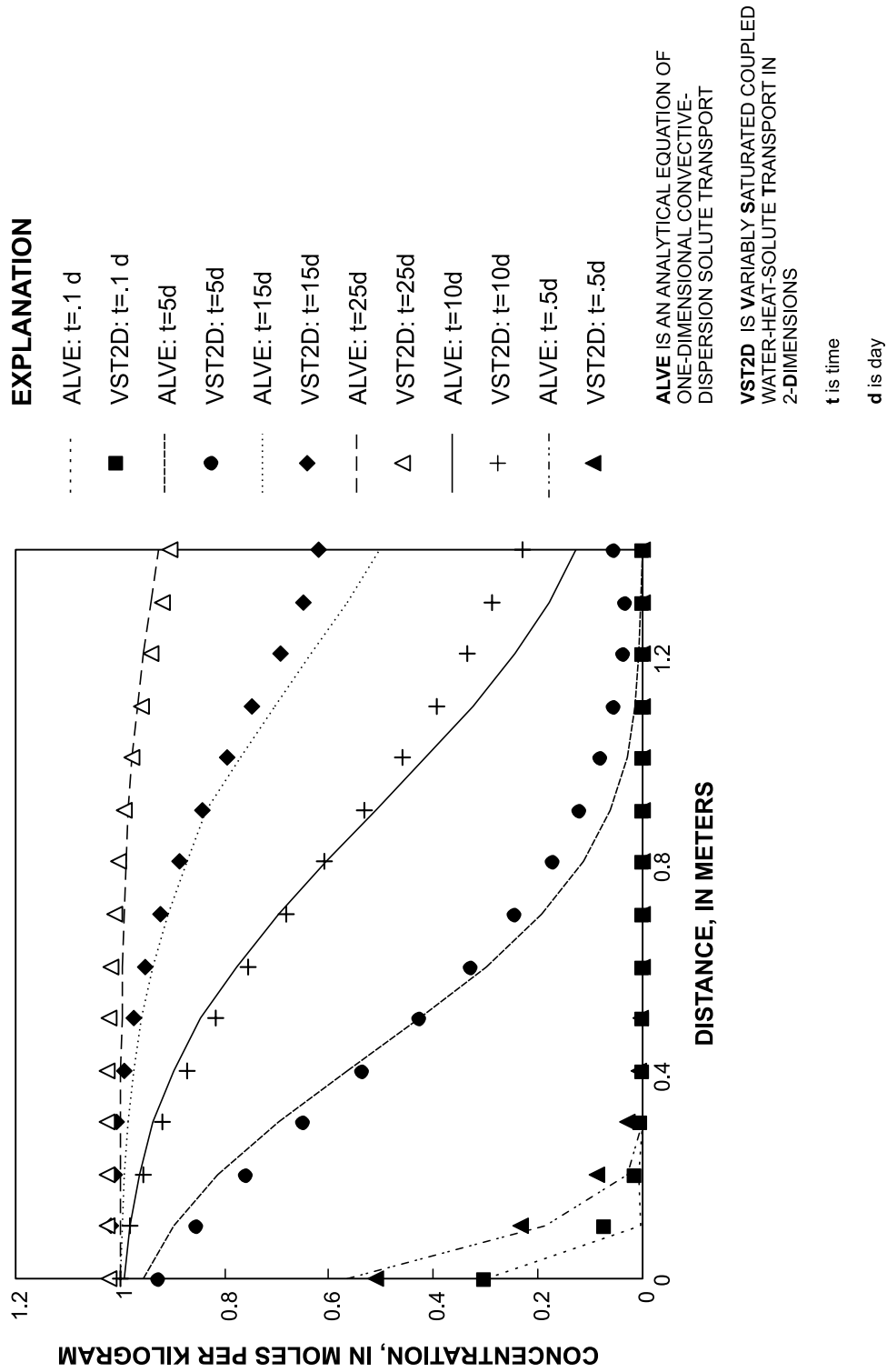


Figure 13. Comparison of transient solute profiles simulated under isobaric and isothermal conditions using VST2D and ALVE2.

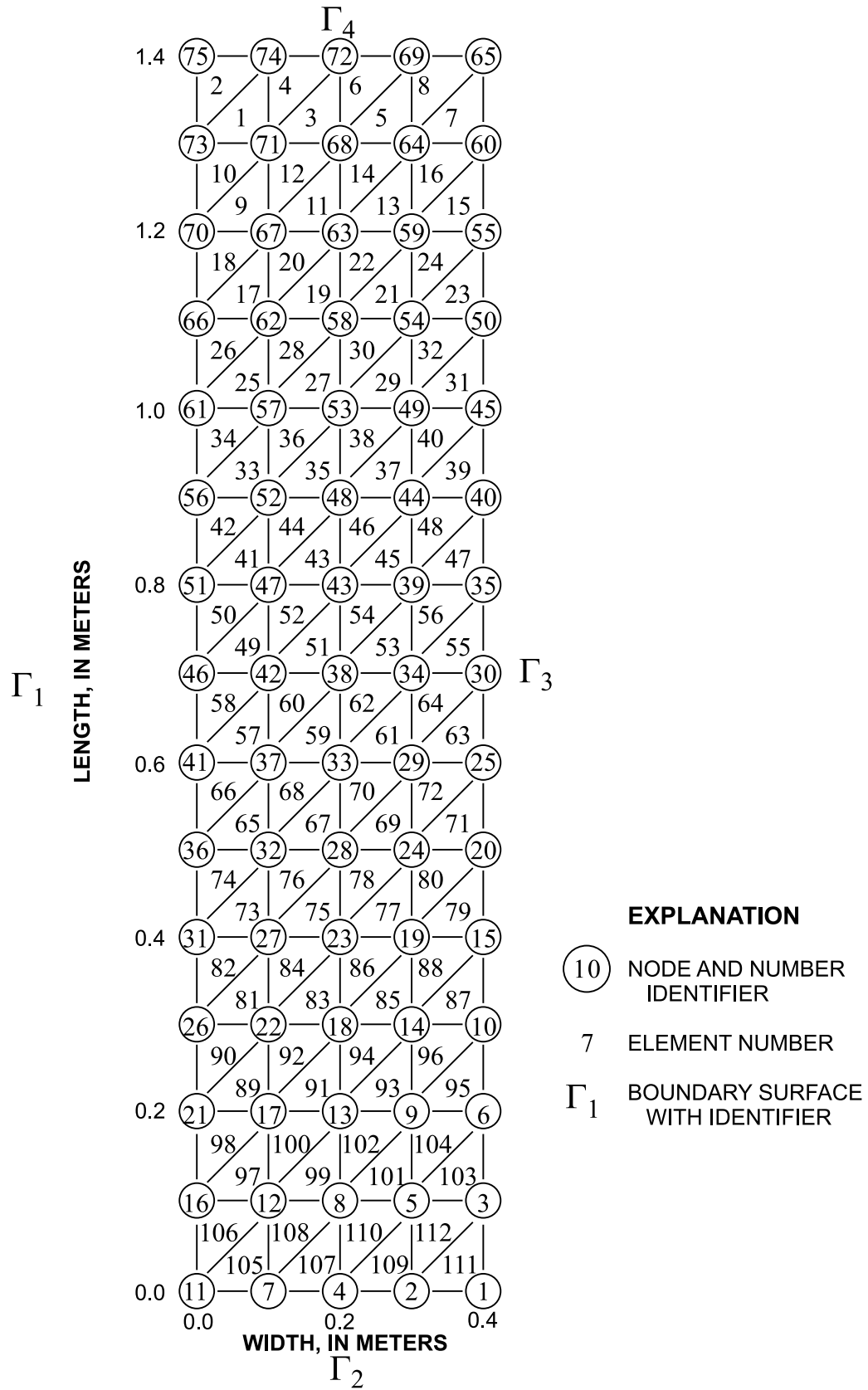


Figure 14. Finite-element mesh used in verification of solute transport simulated under isobaric and isothermal conditions.

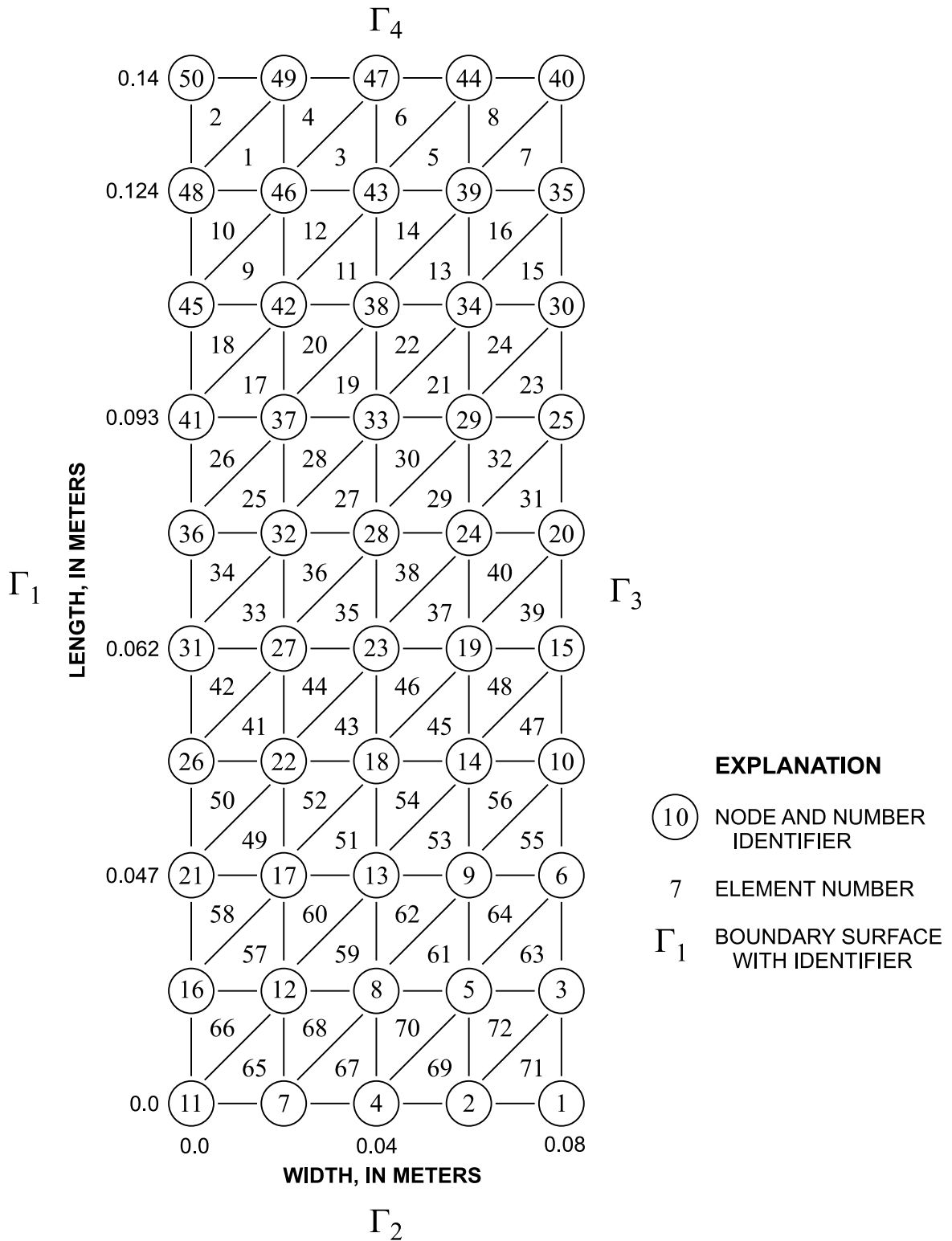


Figure 15. Finite-element mesh used in the verification of steady-state water-heat-solute transport conditions.

Table 7. Summary of conditions used in the VST2D validation process for coupled water-heat-solute transport

[cm³/cm³, cubic centimeter per cubic centimeter; °C, Celsius; m d⁻¹, meter per day; mol kg⁻¹, mol per kilogram; cal d⁻¹, calorie per day; mol kg⁻¹ d⁻¹, mole per kilogram day; Γ , surface boundary]

Initial conditions: $\theta(x,y,0)$, initial moisture content at all nodes; $T(x,y,0)$, initial temperature at all nodes; $C(x,y,0)$, initial concentration at all nodes

Dirichlet conditions: $T(x,0.00,t)$, temperature on Γ_2 ; $T(x,0.14,t)$, temperature on Γ_4 .

Neumann conditions: $q_\theta(0.00,y,t)$, liquid flux on Γ_1 ; $q_\theta(x,0.00,t)$, liquid flux on Γ_2 ;
 $q_\theta(0.008,y,t)$, liquid flux on Γ_3 ; $q_\theta(x,0.14,t)$, liquid flux on Γ_4 ;
 $q_T(0.00,y,t)$, heat flux on Γ_1 ; $q_T(x,0.00,t)$, heat flux on Γ_2 ;
 $q_T(0.008,y,t)$, heat flux on Γ_3 ; $q_T(x,0.14,y,t)$, heat flux on Γ_4 ;
 $q_C(0.00,y,t)$, solute flux on Γ_1 ; $q_C(x,0.00,t)$, solute flux on Γ_2 ;
 $q_C(0.0080,y,t)$, solute flux on Γ_3 ; $q_C(x,0.14,t)$, solute flux on Γ_4

Initial conditions	Dirichlet conditions	Neumann conditions
$\theta(x,y,0) = 0.144 \text{ cm}^3/\text{cm}^3$	$T(x,0.00,t) = 19.2 \text{ }^\circ\text{C}$	$q_\theta(0.00,y,t) = 0.0 \text{ m d}^{-1}$
$T(x,y,0) = 14.0 \text{ }^\circ\text{C}$	$T(x,0.14,t) = 8.93 \text{ }^\circ\text{C}$	$q_\theta(0.008,y,t) = 0.0 \text{ m d}^{-1}$
$C(x,y,0) = 0.794 \text{ mol kg}^{-1}$		$q_\theta(x,0.00,t) = 0.0 \text{ m d}^{-1}$
		$q_\theta(x,0.14,t) = 0.0 \text{ m d}^{-1}$
		$q_T(0.00,y,t) = 0.0 \text{ cal d}^{-1}$
		$q_T(0.008,y,t) = 0.0 \text{ cal d}^{-1}$
		$q_T(x,0.00,t) = 0.0 \text{ cal d}^{-1}$
		$q_T(x,0.14,y,t) = 0.0 \text{ cal d}^{-1}$
		$q_C(0.00,y,t) = 0.0 \text{ mol kg}^{-1} \text{ d}^{-1}$
		$q_C(0.008,y,t) = 0.0 \text{ mol kg}^{-1} \text{ d}^{-1}$
		$q_C(x,0.00,t) = 0.0 \text{ mol kg}^{-1} \text{ d}^{-1}$
		$q_C(x,0.14,t) = 0.0 \text{ mol kg}^{-1} \text{ d}^{-1}$

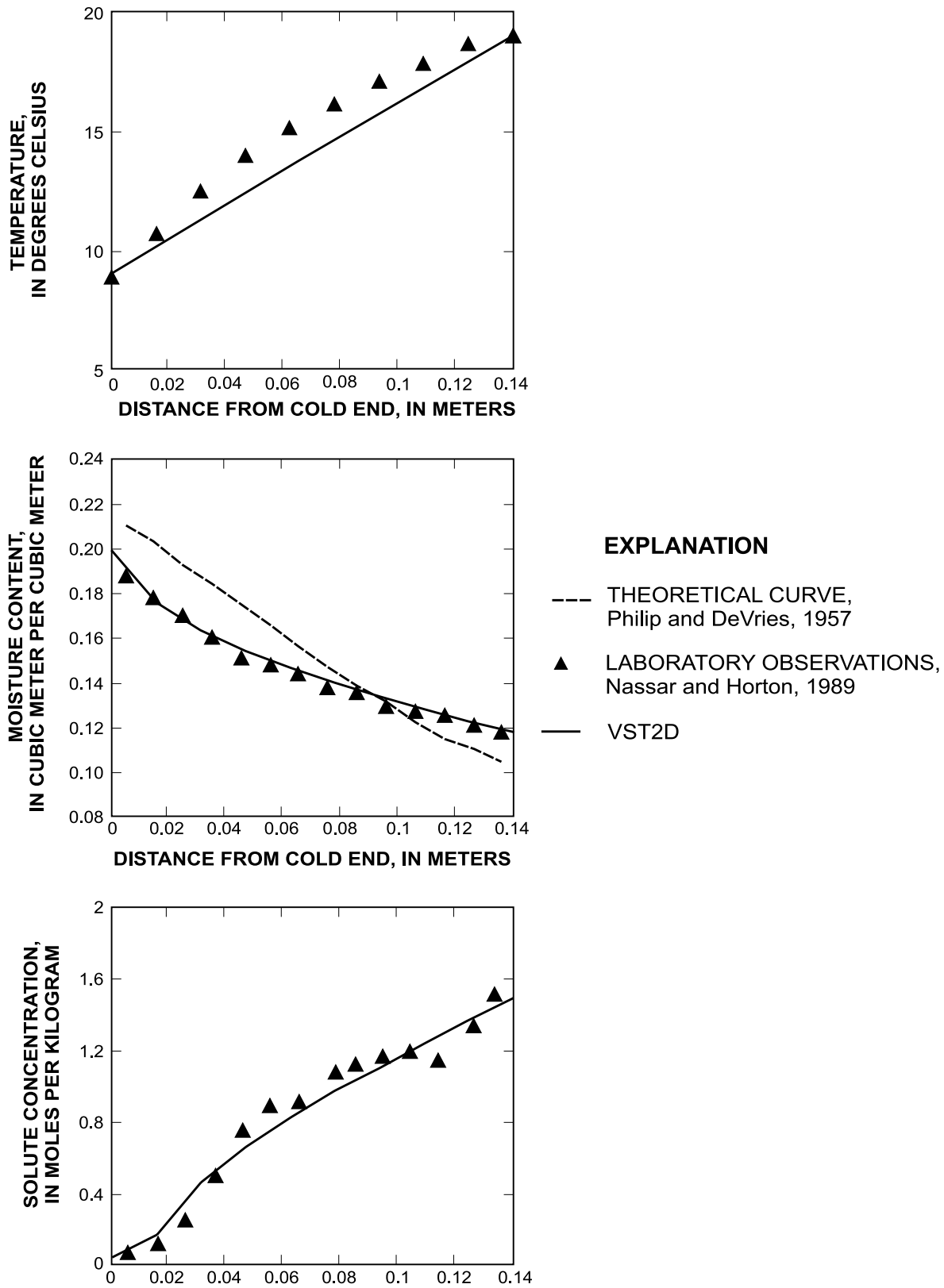
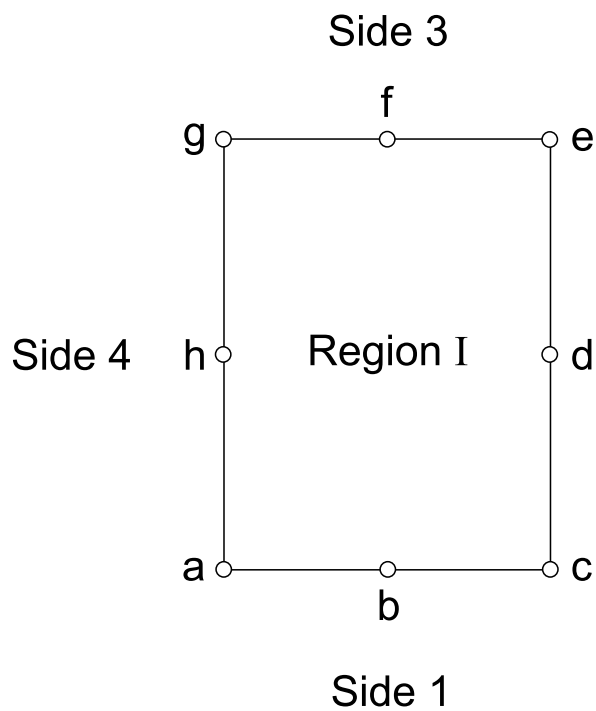
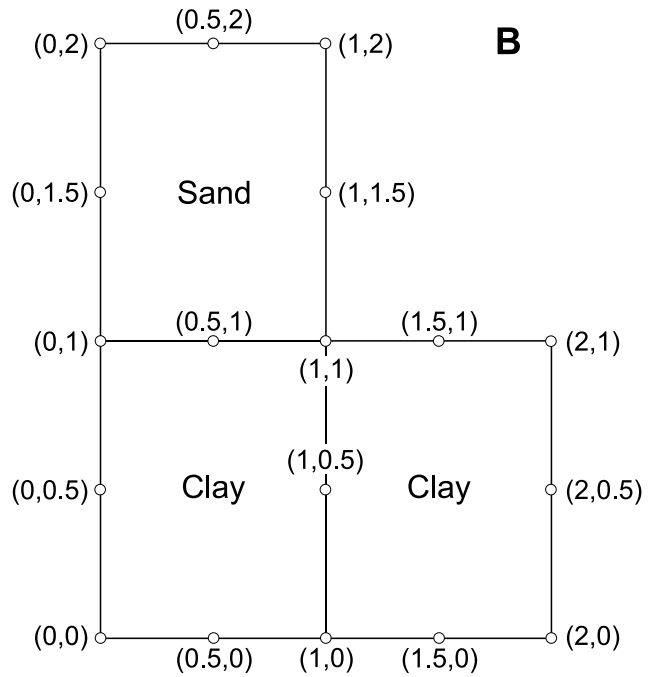
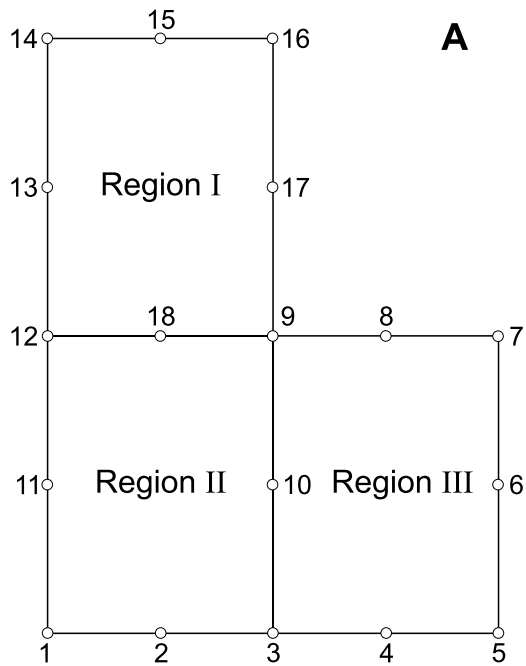


Figure 16. Comparison of measured and simulated steady-state profiles within a moist, salinized, horizontal column subject to differential heat: (A) temperature, (B) moisture content, (C) solute concentration.



C

EXPLANATION

- 7 REGIONAL NODE AND NUMBER IDENTIFIER
- e REGIONAL NODE AND CONNECTIVITY IDENTIFIER
- (2,1) NODE COORDINATES, IN METERS
- Clay ELEMENT MATERIAL TYPE
- Region I REGION NUMBER ONE
- Side 3 SIDE THREE OF REGION ONE

Figure 17. Concepts for finite element mesh generation using GRID. Regions and node numbers (A) unit types, (B) coordinate distances, and (C) regional connectivity conditions.

REFERENCES

- Beke, G.J., and Palmer, C.J., 1989, Subsurface occurrences of mabilite in a mollisol of southern Alberta, Canada: A case study: Soil Science Society of America Journal.
- Blomberg, T., and Claesson, J., 1998, HEAT2: A PC program for heat transfer in two-dimensions: Blocon USA. 37 p.
- Braud, I., Dantas-Antonio, A.C., Vauclin, M., Thony, J.L., and Ruelle, P., 1995, A simple soil-plant-atmosphere transfer model (SiSPAT) development and field verification: Elsevier, v. 166, p. 213-250.
- Cass, A., Campbell, G.S., and Jones, T.L., 1984, Enhancement of thermal water vapor diffusion in soil: Soil Science Society of America Journal, v. 48, p. 25-32.
- Chemical Society of Japan (eds.), 1975, Kagaku binran, Kisohen (Basic chemical tables), 2nd ed. (In Japanese): Tokyo, Maruzen Publishers, 453 p.
- Danckwerts, P.V., 1953, Continuous flow systems: Chemical Engineering Science, v. 2, p. 1-13.
- de Vries., D.A., 1958, Simultaneous transfer of heat and moisture in porous media: Transactions: American Geophysical Union, v. 39, no. 5, p. 909-915.
- 1963, Thermal properties of soils *in* Van Wijk, W.R., ed., Physics of plant environment: Amsterdam, North-Holland Publishing Company, p. 210-235.
- Friedel, M., and Nieber, J., 1995, SWHT: Simultaneous Water and Heat Transfer: Bureau of Mines, Open-File Report 85-95, 28 p.
- Harned, H.S., and Owen, B.B., 1958, The physical chemistry of electrolytic solutions, 3rd ed.: New York, Reinhold Publishing Corporation, 458 p.
- Healy, R.W., 1990, Simulation of solute transport in variably saturated porous media with supplemental information on modifications to the U.S. Geological Survey's computer program VS2D: U.S. Geological Survey Water-Resources Investigations Report 90-4025, 125 p.
- Healy, R.W., and Ronan, A.D., 1996, Documentation of computer program VS2DH for simulation of energy transport in variably saturated porous media—Modification of the U.S. Geological Survey's computer program VS2DT: U.S. Geological Survey Water-Resources Investigations Report 96-4230, 36 p.
- Huyakorn, P.S., and Pinder, G.F., 1983, Computational methods in subsurface flow: New York, Academic Press, 473 p.
- Istok, J., 1989, Groundwater modeling by the finite-element method: Water Resources Monograph, American Geophysical Union, 495 p.
- Jamieson, D.T., Irving, J.B., and Tudhope, J.S., 1975, Liquid thermal conductivity, A data survey to 1973: Edinburgh, Scotland, National Engineering Laboratory, Her Majesty's Stationary Office, 334 p.
- Jessup, R.S., 1927, Refrigerating brines, *in* Washburn, E.W., ed., International critical tables of numerical data, physics, chemistry and technology: New York, v. 2, McGraw-Hill, p. 327-328.
- Karickhoff, S.W., Brown, D.S., and Scott, T.A., 1979, Sorption of hydrophobic pollutants on natural sediments: Water Research, v. 13, p. 241-248.
- Karickhoff, S.W., 1984, Organic pollutant sorption in aquatic systems: Journal of Hydraulic Engineering, v. 110, no. 6, p. 707-735.
- Kimball, B.A., Jackson, R.D., Reginato, R.J., Nakayama, F.S., and Idso, S.B., 1976, Comparison of field-measured and calculated soil-heat fluxes: Soil Science Society of America Journal, v. 40, p.18-25.
- Milly, P.C.D., 1982, Moisture and heat transport in hysteretic, in homogeneous porous media: A matric head-based formulation and a numerical model: Water Resources Research, v. 20, p. 489-498.
- 1984, A simulation analysis of thermal effects on evaporation from soil: Water Resources Research, p. 1087-1098.
- Letej, J., and Kemper, W.D., 1969, Movement of water and salt through clay-water system: Experimental verification of Onsager reciprocal relation: Soil Science Society of America Journal, v. 33, p. 25-29.
- Lobo, V.M.M., and Quaresma, J.L., 1989, Handbook of electrolyte solutions, Part B: Elsevier, New York, Physical Sciences Data, 234 p.
- Nassar, I.N., and Horton, R., 1989a, Water transfer in unsaturated, nonisothermal, salty soil: I. Experimental results: Soil Science Society of America Journal, v. 53, no. 5, p. 1323-1329.
- 1989b, Water transport in unsaturated nonisothermal salty soil: II. Theoretical developments: Soil Science Society of America Journal, v. 53, no. 5, p. 1330-1337.
- 1992, Simultaneous transfer of heat, water, and solute in porous media: theoretical development: Soil Science Society of America Journal, v. 56, no. 5, p. 1350-1356.
- Nassar, I.N., Horton, R., and Globus, A.M., 1992, Simultaneous transfer of heat, water, and solute in porous media: II Experiment and analysis: Soil Science Society of America Journal, v. 56, p. 1357-1365.

- National Research Council, 1990, Ground Water Models, Scientific and regulatory applications: Washington, D.C., Commission on Groundwater Model Assessment, Water Science and Technology Board, Natural Resource Council, National Academy Press, 303 p.
- Nieber, J.L., Friedel, M.J., and Munir, H.M., 1994, VARSAT2D: Finite-element analysis of variably saturated two-dimensional flow: Bureau of Mines, Information Circular 9373, 30 p.
- Nimmo, J.R., and Miller, E.E., 1986, The temperature dependence of isothermal moisture vs. potential characteristics of soils: Soil Science Society of America Journal, v. 50, p. 1105-1113.
- Noborio, K., McInnes, K.J., and Heilman, J.L., 1996, Two-dimensional model for water, heat, and solute transport in furrow-irrigated soil: II Field evaluation: Soil Science Society American Journal, v. 60, p. 1016-1021.
- Olmstead, J.M.J., 1961, Advanced calculus: Englewood Cliffs, N.J., Prentice-Hall, 348 p.
- Passerat de Silans, A., Bruckler, L., Thony, J.S., and Vauclin, M., 1989, Numerical modeling of coupled heat and water flows during drying in a stratified bare soil-comparison with field observations: Journal of Hydrology, v. 105, p. 109-138.
- Philip, J.R., and DeVries, D.A., 1957, Moisture movement in porous materials under temperature gradients: Transactions of American Geophysical Union, v. 38, p. 222-232.
- Pinder, G.F., and Gray, W.G., 1977, Finite element simulation in surface and subsurface hydrology: New York, Academic Press, 373 p.
- Robinson, R.A., and Stokes, R.H., 1965, Electrolyte solutions, 2nd ed.: London, Butterworths.
- Saad, Y., 1996, Iterative methods for sparse linear systems: Boston, Massachusetts, PWS Publishers, 447 p.
- Scanlon, B.R., and Milly, P.C.D., 1994, Water and heat fluxes in desert soils, 2, Numerical simulations: Water Resources Research, v. 20, p. 721-733.
- Segerlind, L.J., 1984, Applied finite-element analysis, 2nd ed.: New York, John Wiley & Sons, 385 p.
- Segol, G., 1994, Classic groundwater simulations, Proving and improving numerical models: Englewood Cliffs, N.J., Prentice-Hall, 531 p.
- Simunke, J., Vogel, T., and van Genuchten, M.T., 1994, The SWMS-2D code for simulating water flow and solute transport in two-dimensional variably saturated media, version 1.21: Riverside, California, U.S. Salinity Laboratory, Agricultural Research Service, U.S. Department of Agriculture, 197 p.
- Strack, O.D.L., 1989, Groundwater Mechanics: Newark, New Jersey, Prentice-Hall, 732 p.
- van Genuchten, T., 1980, A closed form equation for predicting the hydraulic conductivity of unsaturated soils: Soil Science Society of America Journal, v. 44, p. 892-898.
- van Genuchten, M. Th., and Alves, W.J., 1982, Analytical equations of the one-dimensional convective-dispersion solute transport equation: U.S. Department of Agricultural Technical Bulletin, v. 166, 149 p.
- van Genuchten, M. Th., and Parker, J.C., 1984, Boundary conditions for displacement experiments through short soil columns: Soil Science Society of America Journal, v. 48, p. 703-708.
- Voss, C., 1984, SUTRA: Saturated-unsaturated transport: U.S. Geological Survey Water-Resources Investigations Report 84-4369, 409 p.
- Yeh, T-C, J., Srivastava, R., Guzman, A., and Harter, T., 1993, A numerical model for water flow and chemical transport in variably saturated porous media: Groundwater, v. 31, no. 4, p. 634-639.
- Young, T.F., and Harkins, W.D., 1928, Surface-tension data for pure liquids between 0 and 360 °C and for all types of solutions at all temperatures, in Washburn, E.W., ed., International critical tables of numerical data, physics, chemistry, and technology: New York, McGraw-Hill, v. 6, p. 446-475.

APPENDIXES

APPENDIX 1. ELEMENTAL MATRIX-VECTOR REPRESENTATION FOR WATER, HEAT, AND SOLUTE EQUATIONS

Water:

$$[B_{\psi\psi}]^e = [K_{\psi L}]^e + [D_{\psi V}]^e + [K_{\psi q}]^e \quad (211)$$

$$[K_{\psi L}]^e = \frac{\rho_L K_{xx}}{4A} \begin{bmatrix} b_i^2 & b_i b_j & b_i b_k \\ b_j b_i & b_j^2 & b_j b_k \\ b_k b_i & b_k b_j & b_k^2 \end{bmatrix} + \frac{\rho_L K_{yy}}{4A} \begin{bmatrix} c_i^2 & c_i c_j & c_i c_k \\ c_j c_i & c_j^2 & c_j c_k \\ c_k c_i & c_k c_j & c_k^2 \end{bmatrix} + \frac{\rho_L K_{xy}}{4A} \begin{bmatrix} b_i c_i & b_i c_j & b_i c_k \\ b_j c_i & b_j c_j & b_j c_k \\ b_k c_i & b_k c_j & b_k c_k \end{bmatrix} + \frac{\rho_L K_{yx}}{4A} \begin{bmatrix} c_i b_i & c_i b_j & c_i b_k \\ c_j b_i & c_j b_j & c_j b_k \\ c_k b_i & c_k b_j & c_k b_k \end{bmatrix} \quad (212)$$

$$[D_{\psi V}]^e = \frac{D_{\theta V} \rho_L C_{\psi}}{4A} \begin{bmatrix} b_i^2 & b_i b_j & b_i b_k \\ b_j b_i & b_j^2 & b_j b_k \\ b_k b_i & b_k b_j & b_k^2 \end{bmatrix} + \frac{D_{\theta V} \rho_L C_{\psi}}{4A} \begin{bmatrix} c_i^2 & c_i c_j & c_i c_k \\ c_j c_i & c_j^2 & c_j c_k \\ c_k c_i & c_k c_j & c_k^2 \end{bmatrix} \quad (213)$$

$$[K_{\psi q}]^e = \frac{\rho_L q_{ij}}{2} \begin{bmatrix} 1 & 0 & 0 \\ 0 & 1 & 0 \\ 0 & 0 & 0 \end{bmatrix} + \frac{\rho_L q_{ik}}{2} \begin{bmatrix} 1 & 0 & 0 \\ 0 & 0 & 0 \\ 0 & 0 & 1 \end{bmatrix} + \frac{\rho_L q_{jk}}{2} \begin{bmatrix} 0 & 0 & 0 \\ 0 & 1 & 0 \\ 0 & 0 & 1 \end{bmatrix} \quad (214)$$

$$[B_{\psi T}]^e = [B_{TL}]^e + [B_{TV}]^e \quad (215)$$

$$[B_{TL}]^e = \rho_L \left(\psi G_{\psi T} \gamma_{T'} - \sigma_0 \frac{\partial O}{\partial T} \right) [K_{\psi L}]^e \quad (216)$$

$$[B_{TV}]^e = \frac{\rho_L D_{TV}}{4A} \begin{bmatrix} b_i^2 & b_i b_j & b_i b_k \\ b_j b_i & b_j^2 & b_j b_k \\ b_k b_i & b_k b_j & b_k^2 \end{bmatrix} + \frac{\rho_L D_{TV}}{4A} \begin{bmatrix} c_i^2 & c_i c_j & c_i c_k \\ c_j c_i & c_j^2 & c_j c_k \\ c_k c_i & c_k c_j & c_k^2 \end{bmatrix} \quad (217)$$

$$[B_{\psi C}]^e = [B_{CL}]^e + [B_{CV}]^e \quad (218)$$

$$[B_{CL}]^e = \rho_L \left(\psi \gamma_C' - \sigma_0 \frac{\partial O}{\partial C} \right) [K_{\psi L}]^e \quad (219)$$

$$[B_{CV}]^e = \frac{\rho_L D_{CV}}{4A} \begin{bmatrix} b_i^2 & b_i b_j & b_i b_k \\ b_i b_j & b_j^2 & b_j b_k \\ b_i b_k & b_j b_k & b_k^2 \end{bmatrix} + \frac{\rho_L D_{CV}}{4A} \begin{bmatrix} c_i^2 & c_i c_j & c_i c_k \\ c_i c_j & c_j^2 & c_j c_k \\ c_i c_k & c_j c_k & c_k^2 \end{bmatrix} \quad (220)$$

$$[A_{\Psi L}]^e = \frac{A}{3} \begin{bmatrix} 1 & 0 & 0 \\ 0 & 1 & 0 \\ 0 & 0 & 1 \end{bmatrix} = [A_{\Psi V}]^e \quad [A_{\Psi \Psi}]^e = \rho_L \Lambda C_{\Psi} [A_{\Psi L}]^e \quad (221)$$

$$\{f_{\Psi Q}\}^e = \rho_L Q_{\Psi} \begin{pmatrix} N_i \\ N_j \\ N_k \end{pmatrix} \quad \{f_{\Psi k}\}^e = \frac{\rho_L (K_{yyi} + K_{yyj} + K_{yyk})}{6} \begin{Bmatrix} c_i \\ c_j \\ c_k \end{Bmatrix} + \frac{\rho_L (K_{xyi} + K_{xyj} + K_{xyk})}{6} \begin{Bmatrix} b_i \\ b_j \\ b_k \end{Bmatrix} \quad (222)$$

$$\{f_{\Psi V}\}^e = [A_{\Psi V}] \{\Delta \theta_V\} \quad \{f_{\Psi \Psi}\}^e = \rho_L \Lambda [A_{\Psi \Psi}] \{\Psi\} \quad \{f_{\Psi L}\}^e = \rho_L \Lambda [A_{\Psi L}] \{\Delta \theta_L\} \quad (223)$$

Heat:

$$[B_{TT}]^e = \frac{\sigma}{4A} \begin{bmatrix} b_i^2 & b_i b_j & b_i b_k \\ b_i b_j & b_j^2 & b_j b_k \\ b_i b_k & b_j b_k & b_k^2 \end{bmatrix} + \frac{\sigma}{4A} \begin{bmatrix} c_i^2 & c_i c_j & c_i c_k \\ c_i c_j & c_j^2 & c_j c_k \\ c_i c_k & c_j c_k & c_k^2 \end{bmatrix} + C_L T [B_{TL}]^e \quad (224)$$

$$[B_{T\Psi}]^e = \frac{\sigma'}{4A} \begin{bmatrix} b_i^2 & b_i b_j & b_i b_k \\ b_i b_j & b_j^2 & b_j b_k \\ b_i b_k & b_j b_k & b_k^2 \end{bmatrix} + \frac{\sigma'}{4A} \begin{bmatrix} c_i^2 & c_i c_j & c_i c_k \\ c_i c_j & c_j^2 & c_j c_k \\ c_i c_k & c_j c_k & c_k^2 \end{bmatrix} + C_L T [K_{\Psi L}]^e. \quad (225)$$

$$[B_{TC}]^e = \frac{\sigma''}{4A} \begin{bmatrix} b_i^2 & b_i b_j & b_i b_k \\ b_i b_j & b_j^2 & b_j b_k \\ b_i b_k & b_j b_k & b_k^2 \end{bmatrix} + \frac{\sigma''}{4A} \begin{bmatrix} c_i^2 & c_i c_j & c_i c_k \\ c_i c_j & c_j^2 & c_j c_k \\ c_i c_k & c_j c_k & c_k^2 \end{bmatrix} + C_L T [B_{CL}]^e \quad (226)$$

$$[A_{TT}]^e = f_1 [A_{\Psi L}] \quad [A_{T\Psi}]^e = f_2 [A_{\Psi \Psi}] \quad (227)$$

$$[A_{TC}]^e = f_3[A_{\Psi L}] \quad [A_{TL}]^e = f_2[A_{\Psi L}] \quad (228)$$

$$\{f_{Tk}\}^e = \frac{C_L T(K_{xy_i} + K_{xy_j} + K_{xy_k})}{2} \begin{pmatrix} b_i \\ b_j \\ b_k \end{pmatrix} + \frac{C_L T(K_{yy_i} + K_{yy_j} + K_{yy_k})}{2} \begin{pmatrix} c_i \\ c_j \\ c_k \end{pmatrix} \quad \{f_{TQ}\} = Q_T \begin{pmatrix} N_i \\ N_j \\ N_k \end{pmatrix} \quad (229)$$

$$\{f_{TT}\}^e = [A_{TT}]\{T\} \quad \{f_{TC}\}^e = [A_{\Psi L}]\{C\} \quad \{f_{T\psi}\}^e = [A_{T\psi}]\{\psi\} \quad \{f_{TL}\}^e = [A_{TL}]\{d\theta_L\} \quad (230)$$

$$\{f_{TH}\}^e = [A_{\Psi L}]\{\Delta H\} \quad \{f_{CTC}\}^e = [A_{TC}]\{C\} \quad \{f_{CH}\}^e = [A_{\Psi L}]\{\Delta H\} \quad (231)$$

Solute:

$$[B_{CC}]^e = [D_{hC}]^e + [q_{LC}]^e + [\lambda_{LC}]^e \quad (232)$$

$$[D_{hC}]^e = \frac{D_{hxx}}{4A} \begin{bmatrix} b_i^2 & b_i b_j & b_i b_k \\ b_j b_i & b_j^2 & b_j b_k \\ b_k b_i & b_k b_j & b_k^2 \end{bmatrix} + \frac{D_{hyy}}{4A} \begin{bmatrix} c_i^2 & c_i c_j & c_i c_k \\ c_j c_i & c_j^2 & c_j c_k \\ c_k c_i & c_k c_j & c_k^2 \end{bmatrix} + \frac{D_{hxy}}{4A} \begin{bmatrix} b_i c_i & b_i c_j & b_i c_k \\ b_j c_i & b_j c_j & b_j c_k \\ b_k c_i & b_k c_j & b_k c_k \end{bmatrix} + \frac{D_{hyx}}{4A} \begin{bmatrix} c_i b_i & c_i b_j & c_i b_k \\ c_j b_i & c_j b_j & c_j b_k \\ c_k b_i & c_k b_j & c_k b_k \end{bmatrix} \quad (233)$$

$$[q_{LC}]^e = \frac{q_{Lx}}{6} \begin{bmatrix} b_i & b_j & b_k \\ b_i & b_j & b_k \\ b_i & b_j & b_k \end{bmatrix} + \frac{q_{Ly}}{6} \begin{bmatrix} c_i & c_j & c_k \\ c_i & c_j & c_k \\ c_i & c_j & c_k \end{bmatrix} \quad (234)$$

$$[\lambda_{LC}]^e = \frac{A\lambda C(\theta_L + \rho_d K_d)}{3} \begin{bmatrix} 1 & 0 & 0 \\ 0 & 1 & 0 \\ 0 & 0 & 1 \end{bmatrix} \quad (235)$$

$$[B_{C\psi}]^e = [D_{C\psi}] + [V_{LC}] \quad (236)$$

$$[D_{C\psi}]^e = \beta' C [K_{\Psi L}]^e \quad (237)$$

$$[V_{LC}]^e = \frac{V_{Lx} C C_{\Psi}}{6} \begin{bmatrix} b_i & b_j & b_k \\ b_i & b_j & b_k \\ b_i & b_j & b_k \end{bmatrix} + \frac{V_{Ly} C C_{\Psi}}{6} \begin{bmatrix} c_i & c_j & c_k \\ c_i & c_j & c_k \\ c_i & c_j & c_k \end{bmatrix} \quad (238)$$

$$[B_{CT}]^e = \frac{D_{CT}}{4A} \begin{bmatrix} b_i^2 & b_i b_j & b_i b_k \\ b_i b_j & b_j^2 & b_j b_k \\ b_i b_k & b_j b_k & b_k^2 \end{bmatrix} + \frac{D_{CT}}{4A} \begin{bmatrix} c_i^2 & c_i c_j & c_i c_k \\ c_i c_j & c_j^2 & c_j c_k \\ c_i c_k & c_j c_k & c_k^2 \end{bmatrix} \quad (239)$$

$$\{f_{CV}\}^e = \frac{(\theta_{Li} V_{Lxi} + \theta_{Lj} V_{Lxj} + \theta_{Lk} V_{Lxk})}{6} \begin{Bmatrix} b_i \\ b_j \\ b_k \end{Bmatrix} + \frac{(\theta_{Li} V_{Lyi} + \theta_{Lj} V_{Lyj} + \theta_{Lk} V_{Lyk})}{6} \begin{Bmatrix} c_i \\ c_j \\ c_k \end{Bmatrix} \quad \{f_{TQ}\}^e = Q_T \begin{pmatrix} N_i \\ N_j \\ N_k \end{pmatrix} \quad (240)$$

$$[A_{C\psi}]^e = CC_\psi [A_{\psi L}] \quad [A_{CL}]^e = C [A_{\psi L}] \quad [A_{CC}]^e = (\theta_L + \rho_d K_d) [A_{\psi L}] \quad (241)$$

$$\{f_{CC}\}^e = [A_{CC}] \{T\} \quad \{f_{C\psi}\}^e = [A_{CL}] \{\psi\} \quad \{f_{CL}\}^e = [A_{CL}] \{d\theta_L\} \quad (f_{CM})^e = [A_{\psi L}] \{dM_C\} \quad (242)$$

APPENDIX 2. INPUT/OUTPUT FOR FINITE-ELEMENT GRID GENERATOR (GRID).

The GRID.IN data file described below is used as input to GRID.EXE for generating a grid of linear triangular elements with element and node numbers. Information from GRID.EXE is written to three files: ELEMENT.IN, PROPERTY.IN, and GRID.PLT. The first two files are used as input to VST.EXE, whereas the latter can be used in conjunction with a graphics package (for example, VIEW.EXE of the SURFER package) to view the finite-element grid, coordinate geometry, and node numbers.

GRID.IN

The information comprising this file is shown below with input in bold and computer code parameters in parentheses. An explanation of additional information for each input item or group of items is provided in regular type, and an example is shown in italic type. For this hypothetical example, a schematic depicting regions, node numbers, unit types (sand and clay), and coordinate distances is provided in figure 16.

1. **Title (TITLE):** alpha-numeric string of up to 40 characters.

Sample grid with three subregions and two material property sets.

2. **Number of regions, number of boundary node points (NP), number of material property sets (NMPSET).**
3,18,2

3. **X-coordinates for each boundary node (X); enter NP values of X.**

0.,.5,1.,1.5,2.,2.,2.,1.5,1.,1.,0.,0.,0.,0.,.5,1.,1.,.5

4. **Y-coordinates for each boundary node (Y); enter NP values of Y.**

0.,0.,0.,0.,0.,.5,1.,1.,1.,.5,1.,1.5,2.,2.,2.,1.5,1.

5. **Region number, regions of connectivity.** Enter zeros for sides not connected to any region.

1,2,0,0,0

2,0,3,1,0

3,0,0,0,2

6. **Read (NMPSET) set of 19 material properties (KXS,KYS,CA, CN, TR, TS, CPS, DELT, LAMBDA, X0, SSA, RHOB, AL, AT, KD, DECAY, Xsnd, Xslt, Xcly - see Data Input section)**

0.255 0.255 0.5111 1.322 0.05 0.67 0.480 0.0000 0. 0.0002 1.01 1.04 0.0070 0.0010 000.00 0 0.1 0.686 0.214

0.229 0.229 0.5857 1.546 0.05 0.67 0.480 0.0000 0. 0.0002 1.01 1.04 0.0070 0.0010 000.00 0 0.1 0.686 0.214

7. **Region number, material property number for that region, number of rows needed for that region, number of columns needed for that region, eight boundary nodes for that region.** Enter boundary nodes in a counterclockwise order.

1,1,10,10,12,18,9,17,16,15,14,13

2,2,10,10,1,2,3,10,9,18,12,11

3,2,10,10,3,4,5,6,7,8,9,10

ELEMENT.IN

In the sample file provided below, four sets of information are written. First is the problem title. Second is a flag indicating default vertical section (0), number of elements (486), and number of nodes (280). Third, a set of three nodes are written (i, j, k) for each element beginning with element 1 and ending with 486. Fourth, the Cartesian coordinates for each node are given beginning with 1 and ending with 280. Because of the large number of element and nodal sets, only the first and last three lines are provided for the readers convenience.

Sample grid with 3 subregions and 2 sets of properties

```
0      486      280
278 276 279 278 279 280 276 273 277 276 277 279 273 269 274      ((NOD(I,J),J=1,3),I=1,NELEM)
273 274 277 269 264 270 269 270 274 264 258 265 264 265 270
258 251 259 258 259 265 251 243 252 251 252 259 243 234 244
...
22 23 30 16 11 17 16 17 23 11 7 12 11 12 17
7 4 8 7 8 12 4 2 5 4 5 8 2 1 3
2 3 5
2.000 0.000 1.889 0.000 2.000 0.111 1.778 0.000      (X(I),Y(I),I=1,NNP)
1.889 0.111 2.000 0.222 1.667 0.000 1.778 0.111
1.889 0.222 2.000 0.333 1.556 0.000 1.667 0.111
...
0.333 1.889 0.444 2.000 0.000 1.667 0.111 1.778
0.222 1.889 0.333 2.000 0.000 1.778 0.111 1.889
0.222 2.000 0.000 1.889 0.111 2.000 0.000 2.000
```

PROPERTY.IN

In the file below, the property information for each element is written beginning with element 1 and ending with 486. Again, only a nominal amount of information is provided for comparison.

```
1 0.2550 0.2550 0.5111 1.3220 0.0500 0.6700 0.4800 0.0000 0.0000 0.0002 1.0100 1.0400 0.0070
0.0010 0.0000 0.0000 0.1000 0.6860 0.2140 0.1e-7
... repeat elements 2 to 162
162 0.2550 0.2550 0.5111 1.3220 0.0500 0.6700 0.4800 0.0000 0.0000 0.0002 1.0100 1.0400
0.0070 0.0010 0.0000 0.0000 0.1000 0.6860 0.2140 0.1e-7
163 0.2290 0.2290 0.5857 1.5460 0.0500 0.6700 0.4800 0.0000 0.0000 0.0002 1.0100 1.0400
0.0070 0.0010 0.0000 0.0000 0.1000 0.6860 0.2140 0.1e-7
... repeat elements 164 to 485
486 0.2290 0.2290 0.5857 1.5460 0.0500 0.6700 0.4800 0.0000 0.0000 0.0002 1.0100 1.0400
0.0070 0.0010 0.0000 0.0000 0.1000 0.6860 0.2140 0.1e-7
```

APPENDIX 3. MODEL INPUT FILES IN CASE 1 VALIDATION (WATER TRANSPORT)

ELEMENT.IN

Water transport through Ida Silt Loam in 1.4 m vertical column

```

1      72      50
48 46 49 48 49 50 46 43 47 46 47 49 43 39 44
43 44 47 39 35 40 39 40 44 45 42 46 45 46 48
42 38 43 42 43 46 38 34 39 38 39 43 34 30 35
34 35 39 41 37 42 41 42 45 37 33 38 37 38 42
33 29 34 33 34 38 29 25 30 29 30 34 36 32 37
36 37 41 32 28 33 32 33 37 28 24 29 28 29 33
24 20 25 24 25 29 31 27 32 31 32 36 27 23 28
27 28 32 23 19 24 23 24 28 19 15 20 19 20 24
26 22 27 26 27 31 22 18 23 22 23 27 18 14 19
18 19 23 14 10 15 14 15 19 21 17 22 21 22 26
17 13 18 17 18 22 13 9 14 13 14 18 9 6 10
9 10 14 16 12 17 16 17 21 12 8 13 12 13 17
8 5 9 8 9 13 5 3 6 5 6 9 11 7 12
11 12 16 7 4 8 7 8 12 4 2 5 4 5 8
2 1 3 2 3 5
0.080 0.000 0.060 0.000 0.080 0.156 0.040 0.000
0.060 0.156 0.080 0.311 0.020 0.000 0.040 0.156
0.060 0.311 0.080 0.467 0.000 0.000 0.020 0.156
0.040 0.311 0.060 0.467 0.080 0.622 0.000 0.156
0.020 0.311 0.040 0.467 0.060 0.622 0.080 0.778
0.000 0.311 0.020 0.467 0.040 0.622 0.060 0.778
0.080 0.933 0.000 0.467 0.020 0.622 0.040 0.778
0.060 0.933 0.080 1.089 0.000 0.622 0.020 0.778
0.040 0.933 0.060 1.089 0.080 1.244 0.000 0.778
0.020 0.933 0.040 1.089 0.060 1.244 0.080 1.400
0.000 0.933 0.020 1.089 0.040 1.244 0.060 1.400
0.000 1.089 0.020 1.244 0.040 1.400 0.000 1.244
0.020 1.400 0.000 1.400

```

PROPERTY.IN

```

1 0.229 0.229 0.5857 1.546 0.05 0.67 0.480 0.0000 10 0.0002 1.01 1.07 0.1000 0.0100 0.0 0 0.1 0.686 0.214 0.1e-7
2 0.229 0.229 0.5857 1.546 0.05 0.67 0.480 0.0000 10 0.0002 1.01 1.07 0.1000 0.0100 0.0 0 0.1 0.686 0.214 0.1e-7
3 0.229 0.229 0.5857 1.546 0.05 0.67 0.480 0.0000 10 0.0002 1.01 1.07 0.1000 0.0100 0.0 0 0.1 0.686 0.214 0.1e-7
4 0.229 0.229 0.5857 1.546 0.05 0.67 0.480 0.0000 10 0.0002 1.01 1.07 0.1000 0.0100 0.0 0 0.1 0.686 0.214 0.1e-7
5 0.229 0.229 0.5857 1.546 0.05 0.67 0.480 0.0000 10 0.0002 1.01 1.07 0.1000 0.0100 0.0 0 0.1 0.686 0.214 0.1e-7
6 0.229 0.229 0.5857 1.546 0.05 0.67 0.480 0.0000 10 0.0002 1.01 1.07 0.1000 0.0100 0.0 0 0.1 0.686 0.214 0.1e-7
7 0.229 0.229 0.5857 1.546 0.05 0.67 0.480 0.0000 10 0.0002 1.01 1.07 0.1000 0.0100 0.0 0 0.1 0.686 0.214 0.1e-7
8 0.229 0.229 0.5857 1.546 0.05 0.67 0.480 0.0000 10 0.0002 1.01 1.07 0.1000 0.0100 0.0 0 0.1 0.686 0.214 0.1e-7
9 0.229 0.229 0.5857 1.546 0.05 0.67 0.480 0.0000 10 0.0002 1.01 1.07 0.1000 0.0100 0.0 0 0.1 0.686 0.214 0.1e-7
10 0.229 0.229 0.5857 1.546 0.05 0.67 0.480 0.0000 10 0.0002 1.01 1.07 0.1000 0.0100 0.0 0 0.1 0.686 0.214 0.1e-7
11 0.229 0.229 0.5857 1.546 0.05 0.67 0.480 0.0000 10 0.0002 1.01 1.07 0.1000 0.0100 0.0 0 0.1 0.686 0.214 0.1e-7
12 0.229 0.229 0.5857 1.546 0.05 0.67 0.480 0.0000 10 0.0002 1.01 1.07 0.1000 0.0100 0.0 0 0.1 0.686 0.214 0.1e-7
13 0.229 0.229 0.5857 1.546 0.05 0.67 0.480 0.0000 10 0.0002 1.01 1.07 0.1000 0.0100 0.0 0 0.1 0.686 0.214 0.1e-7
14 0.229 0.229 0.5857 1.546 0.05 0.67 0.480 0.0000 10 0.0002 1.01 1.07 0.1000 0.0100 0.0 0 0.1 0.686 0.214 0.1e-7
15 0.229 0.229 0.5857 1.546 0.05 0.67 0.480 0.0000 10 0.0002 1.01 1.07 0.1000 0.0100 0.0 0 0.1 0.686 0.214 0.1e-7
16 0.229 0.229 0.5857 1.546 0.05 0.67 0.480 0.0000 10 0.0002 1.01 1.07 0.1000 0.0100 0.0 0 0.1 0.686 0.214 0.1e-7
17 0.229 0.229 0.5857 1.546 0.05 0.67 0.480 0.0000 10 0.0002 1.01 1.07 0.1000 0.0100 0.0 0 0.1 0.686 0.214 0.1e-7
18 0.229 0.229 0.5857 1.546 0.05 0.67 0.480 0.0000 10 0.0002 1.01 1.07 0.1000 0.0100 0.0 0 0.1 0.686 0.214 0.1e-7
19 0.229 0.229 0.5857 1.546 0.05 0.67 0.480 0.0000 10 0.0002 1.01 1.07 0.1000 0.0100 0.0 0 0.1 0.686 0.214 0.1e-7
20 0.229 0.229 0.5857 1.546 0.05 0.67 0.480 0.0000 10 0.0002 1.01 1.07 0.1000 0.0100 0.0 0 0.1 0.686 0.214 0.1e-7
21 0.229 0.229 0.5857 1.546 0.05 0.67 0.480 0.0000 10 0.0002 1.01 1.07 0.1000 0.0100 0.0 0 0.1 0.686 0.214 0.1e-7
22 0.229 0.229 0.5857 1.546 0.05 0.67 0.480 0.0000 10 0.0002 1.01 1.07 0.1000 0.0100 0.0 0 0.1 0.686 0.214 0.1e-7

```


21	
1	0.0
2	0.0
4	0.0
7	0.0
11	0.0
16	0
21	0
26	0
31	0
36	0
41	0
45	0
48	0
3	0
6	0
10	0
15	0
20	0
25	0
30	0
35	0
50	
40	20.00
44	20.00
47	20.00
49	20.00
50	20.00
1	20.00
2	20.00
4	20.00
7	20.00
11	20.00
16	20
21	20
26	20
31	20
36	20
41	20
45	20
48	20
3	20
6	20
10	20
15	20
20	20
25	20
30	20
35	20
12	20
8	20
5	20

17	20
13	20
9	20
22	20
18	20
14	20
27	20
23	20
19	20
32	20
28	20
24	20
37	20
33	20
29	20
42	20
38	20
34	20
46	20
43	20
39	20
0	
0	
50	
40	0.00
44	0.00
47	0.00
49	0.00
50	0.00
1	0.00
2	0.00
4	0.00
7	0.00
11	0.00
16	0
21	0
26	0
31	0
36	0
41	0
45	0
48	0
3	0
6	0
10	0
15	0
20	0
25	0
30	0
35	0
12	0
8	0

5 0
17 0
13 0
9 0
22 0
18 0
14 0
27 0
23 0
19 0
32 0
28 0
24 0
37 0
33 0
29 0
42 0
38 0
34 0
46 0
43 0
39 0
0
0
26
50,49,49
49,50,47
47,49,44
44,47,40
40,44,44
1,2,2
2,4,1
4,7,2
7,11,4
11,7,7
16,21,11
21,26,16
26,31,21
31,36,26
36,41,31
41,45,36
45,48,41
48,50,45
35,30,45
30,25,35
25,20,30
20,15,25
15,10,20
10,6,15
6,3,10
3,1,6
2,50,49

4,49,47
6,47,44
8,44,40
7,40,35
15,35,30
23,30,25
31,25,20
39,20,15
47,15,10
5,10,6
63,6,3
71,3,1
71,1,2
69,4,2
6,7,4
65,11,7
66,16,11
58,21,16
50,26,21
42,31,26
34,36,31
26,41,36
18,45,41
10,48,45
2,50,48
0
0
0
0

INITIAL.IN

1.
10000000 .01
-1 -1
0.0 1.0
10000000 1.0
-1 -1
5
1
1
1 0.15
50 0.15
-1 -1
1 20.00
50 20.00
-1 -1
1 0.00000
50 0.00000
-1 -1
14
0.01

0.1
0.3
0.5
0.7
0.9
1.0
1.1
1.3
1.5
2.5
5.0
10.0
50.0
10
4
8
13
18
23
28
33
38
43
47

APPENDIX 4. MODEL INPUT FILE IN CASE 2 VALIDATION (HEAT TRANSPORT)

ELEMENT.IN

Heat conduction throughout heterogeneous rock block

```

0  40  30
28 26 29 28 29 30 26 23 27 26 27 29 25 22 26
25 26 28 22 18 23 22 23 26 21 17 22 21 22 25
17 12 18 17 18 22 16 11 17 16 17 21 11 7 12
11 12 17 23 19 24 23 24 27 19 14 20 19 20 24
14 10 15 14 15 20 18 13 19 18 19 23 13 9 14
13 14 19 9 6 10 9 10 14 12 8 13 12 13 18
8 5 9 8 9 13 5 3 6 5 6 9 7 4 8
7 8 12 4 2 5 4 5 8 2 1 3 2 3 5
0.080 0.000 0.060 0.000 0.080 0.020 0.040 0.000
0.060 0.020 0.080 0.040 0.020 0.000 0.040 0.020
0.060 0.040 0.080 0.060 0.010 0.000 0.020 0.020
0.040 0.040 0.060 0.060 0.080 0.080 0.000 0.000
0.010 0.020 0.020 0.040 0.040 0.060 0.060 0.080
0.000 0.020 0.010 0.040 0.020 0.060 0.040 0.080
0.000 0.040 0.010 0.060 0.020 0.080 0.000 0.060
0.010 0.080 0.000 0.080

```

PROPERTY.IN

```

1  0.229 0.229 0.5857 1.546 0.09 0.095 0.480 0.0000 10 0.00000 1.01 1.07 0.0000 0.0100 000.00 0.0 0.995 0.005 0.000 0.1e-7
2  0.229 0.229 0.5857 1.546 0.09 0.095 0.480 23.8830 10 0.00000 1.01 1.07 0.0000 0.0100 000.00 0.0 0.995 0.005 0.000 0.1e-7
3  0.229 0.229 0.5857 1.546 0.09 0.095 0.480 0.0000 10 0.00000 1.01 1.07 0.0000 0.0100 000.00 0.0 0.995 0.005 0.000 0.1e-7
4  0.229 0.229 0.5857 1.546 0.09 0.095 0.480 0.0000 10 0.00000 1.01 1.07 0.0000 0.0100 000.00 0.0 0.995 0.005 0.000 0.1e-7
5  0.229 0.229 0.5857 1.546 0.09 0.095 0.480 0.0000 10 0.00000 1.01 1.07 0.0000 0.0100 000.00 0.0 0.995 0.005 0.000 0.1e-7
6  0.229 0.229 0.5857 1.546 0.09 0.095 0.480 23.8830 10 0.00000 1.01 1.07 0.0000 0.0100 000.00 0.0 0.995 0.005 0.000 0.1e-7
7  0.229 0.229 0.5857 1.546 0.09 0.095 0.480 0.0000 10 0.00000 1.01 1.07 0.0000 0.0100 000.00 0.0 0.995 0.005 0.000 0.1e-7
8  0.229 0.229 0.5857 1.546 0.09 0.095 0.480 0.0000 10 0.00000 1.01 1.07 0.0000 0.0100 000.00 0.0 0.995 0.005 0.000 0.1e-7
9  0.229 0.229 0.5857 1.546 0.09 0.095 0.480 0.0000 10 0.00000 1.01 1.07 0.0000 0.0100 000.00 0.0 0.995 0.005 0.000 0.1e-7
10 0.229 0.229 0.5857 1.546 0.09 0.095 0.480 23.8830 10 0.00000 1.01 1.07 0.0000 0.0100 000.00 0.0 0.995 0.005 0.000 0.1e-7
11 0.229 0.229 0.5857 1.546 0.09 0.095 0.480 0.0000 10 0.00000 1.01 1.07 0.0000 0.0100 000.00 0.0 0.995 0.005 0.000 0.1e-7
12 0.229 0.229 0.5857 1.546 0.09 0.095 0.480 0.0000 10 0.00000 1.01 1.07 0.0000 0.0100 000.00 0.0 0.995 0.005 0.000 0.1e-7
13 0.229 0.229 0.5857 1.546 0.09 0.095 0.480 0.0000 10 0.00000 1.01 1.07 0.0000 0.0100 000.00 0.0 0.995 0.005 0.000 0.1e-7
14 0.229 0.229 0.5857 1.546 0.09 0.095 0.480 23.8830 10 0.00000 1.01 1.07 0.0000 0.0100 000.00 0.0 0.995 0.005 0.000 0.1e-7
15 0.229 0.229 0.5857 1.546 0.09 0.095 0.480 0.0000 10 0.00000 1.01 1.07 0.0000 0.0100 000.00 0.0 0.995 0.005 0.000 0.1e-7
16 0.229 0.229 0.5857 1.546 0.09 0.095 0.480 0.0000 10 0.00000 1.01 1.07 0.0000 0.0100 000.00 0.0 0.995 0.005 0.000 0.1e-7
17 0.229 0.229 0.5857 1.546 0.09 0.095 0.480 0.0000 10 0.00000 1.01 1.07 0.0000 0.0100 000.00 0.0 0.005 0.995 0.000 0.1e-7
18 0.229 0.229 0.5857 1.546 0.09 0.095 0.480 0.0000 10 0.00000 1.01 1.07 0.0000 0.0100 000.00 0.0 0.005 0.995 0.000 0.1e-7
19 0.229 0.229 0.5857 1.546 0.09 0.095 0.480 0.0000 10 0.00000 1.01 1.07 0.0000 0.0100 000.00 0.0 0.005 0.995 0.000 0.1e-7
20 0.229 0.229 0.5857 1.546 0.09 0.095 0.480 0.0000 10 0.00000 1.01 1.07 0.0000 0.0100 000.00 0.0 0.005 0.995 0.000 0.1e-7
21 0.229 0.229 0.5857 1.546 0.09 0.095 0.480 0.0000 10 0.00000 1.01 1.07 0.0000 0.0100 000.00 0.0 0.005 0.995 0.000 0.1e-7
22 0.229 0.229 0.5857 1.546 0.09 0.095 0.480 0.0000 10 0.00000 1.01 1.07 0.0000 0.0100 000.00 0.0 0.005 0.995 0.000 0.1e-7
23 0.229 0.229 0.5857 1.546 0.09 0.095 0.480 0.0000 10 0.00000 1.01 1.07 0.0000 0.0100 000.00 0.0 0.005 0.995 0.000 0.1e-7
24 0.229 0.229 0.5857 1.546 0.09 0.095 0.480 0.0000 10 0.00000 1.01 1.07 0.0000 0.0100 000.00 0.0 0.005 0.995 0.000 0.1e-7
25 0.229 0.229 0.5857 1.546 0.09 0.095 0.480 0.0000 10 0.00000 1.01 1.07 0.0000 0.0100 000.00 0.0 0.005 0.995 0.000 0.1e-7
26 0.229 0.229 0.5857 1.546 0.09 0.095 0.480 0.0000 10 0.00000 1.01 1.07 0.0000 0.0100 000.00 0.0 0.005 0.995 0.000 0.1e-7
27 0.229 0.229 0.5857 1.546 0.09 0.095 0.480 0.0000 10 0.00000 1.01 1.07 0.0000 0.0100 000.00 0.0 0.005 0.995 0.000 0.1e-7
28 0.229 0.229 0.5857 1.546 0.09 0.095 0.480 0.0000 10 0.00000 1.01 1.07 0.0000 0.0100 000.00 0.0 0.005 0.995 0.000 0.1e-7
29 0.229 0.229 0.5857 1.546 0.09 0.095 0.480 0.0000 10 0.00000 1.01 1.07 0.0000 0.0100 000.00 0.0 0.005 0.995 0.000 0.1e-7
30 0.229 0.229 0.5857 1.546 0.09 0.095 0.480 0.0000 10 0.00000 1.01 1.07 0.0000 0.0100 000.00 0.0 0.005 0.995 0.000 0.1e-7
31 0.229 0.229 0.5857 1.546 0.09 0.095 0.480 0.0000 10 0.00000 1.01 1.07 0.0000 0.0100 000.00 0.0 0.005 0.995 0.000 0.1e-7

```


1	-10
2	-10
4	-10
7	-10
11	-10
17	-10
12	-10
8	-10
5	-10
22	-10
18	-10
13	-10
9	-10
26	-10
23	-10
19	-10
14	-10
0	
10	
15	20.0
10	20.0
6	20.0
3	20.0
1	20.0
16	1.00
21	1.00
25	1.00
28	1.00
30	1.00
8	
29	0.00
27	0.00
24	0.00
20	0.00
2	0.0
4	0.0
7	0.0
11	0.0
0	
30	
16	0.00
21	0.00
25	0.00
28	0.00
30	0.00
29	0.00
27	0.00
24	0.00
20	0.00
15	0.00
10	0
6	0

3 0
1 0
2 0
4 0
7 0
11 0
17 0
12 0
8 0
5 0
22 0
18 0
13 0
9 0
26 0
23 0
19 0
14 0
0
0
18
6,21,21
21,16,25
25,21,28
28,25,30
30,28,28
29,30,27
27,29,24
24,27,20
20,24,15
15,20,20
10,15,6
6,10,3
3,6,1
1,3,3
2,1,4
4,7,2
7,11,4
11,16,7
14,16,21
10,21,25
6,25,28
2,28,30
2,30,29
4,29,27
18,27,24
20,24,20
22,20,15
21,15,10
27,10,6
33,6,3
39,3,1

39,1,2
37,4,2
35,7,4
15,11,7
13,11,16
0
0
0
0

INITIAL.IN

0.25
1.0
1.0
1.0
0.1
0.5
1.
10000000 .0001
-1 -1
0.0 1.0
10000000 1.0
-1 -1
5
0
0
1 0.0
50 0.0
-1 -1
1 10.00
50 10.00
-1 -1
1 0.00000
50 0.00000
-1 -1
18
0.0007
0.0024
0.0028
0.0056
0.0069
.1
.5
1.
2
3
4
5.
7
8
9

10.
25
50
6
6
9
13
18
22
25

APPENDIX 5. MODEL INPUT FILE IN CASE 3 VALIDATION (SOLUTE TRANSPORT)

ELEMENT.IN

NASSAR Model-convective solute boundary condition

```

1      72      50
48 46 49 48 49 50 46 43 47 46 47 49 43 39 44
43 44 47 39 35 40 39 40 44 45 42 46 45 46 48
42 38 43 42 43 46 38 34 39 38 39 43 34 30 35
34 35 39 41 37 42 41 42 45 37 33 38 37 38 42
33 29 34 33 34 38 29 25 30 29 30 34 36 32 37
36 37 41 32 28 33 32 33 37 28 24 29 28 29 33
24 20 25 24 25 29 31 27 32 31 32 36 27 23 28
27 28 32 23 19 24 23 24 28 19 15 20 19 20 24
26 22 27 26 27 31 22 18 23 22 23 27 18 14 19
18 19 23 14 10 15 14 15 19 21 17 22 21 22 26
17 13 18 17 18 22 13 9 14 13 14 18 9 6 10
9 10 14 16 12 17 16 17 21 12 8 13 12 13 17
8 5 9 8 9 13 5 3 6 5 6 9 11 7 12
11 12 16 7 4 8 7 8 12 4 2 5 4 5 8
2 1 3 2 3 5
0.080 0.000 0.060 0.000 0.080 0.156 0.040 0.000
0.060 0.156 0.080 0.311 0.020 0.000 0.040 0.156
0.060 0.311 0.080 0.467 0.000 0.000 0.020 0.156
0.040 0.311 0.060 0.467 0.080 0.622 0.000 0.156
0.020 0.311 0.040 0.467 0.060 0.622 0.080 0.778
0.000 0.311 0.020 0.467 0.040 0.622 0.060 0.778
0.080 0.933 0.000 0.467 0.020 0.622 0.040 0.778
0.060 0.933 0.080 1.089 0.000 0.622 0.020 0.778
0.040 0.933 0.060 1.089 0.080 1.244 0.000 0.778
0.020 0.933 0.040 1.089 0.060 1.244 0.080 1.400
0.000 0.933 0.020 1.089 0.040 1.244 0.060 1.400
0.000 1.089 0.020 1.244 0.040 1.400 0.000 1.244
0.020 1.400 0.000 1.400

```

PROPERTY.IN

```

1 0.229 0.229 0.5857 1.546 0.05 0.67 0.480 0.0 10 0.00 1.01 1.07 0.1000 0.00000 000.00 0 0.1 0.686 0.214 0.1e-7
2 0.229 0.229 0.5857 1.546 0.05 0.67 0.480 0.0 10 0.00 1.01 1.07 0.1000 0.00000 000.00 0 0.1 0.686 0.214 0.1e-7
3 0.229 0.229 0.5857 1.546 0.05 0.67 0.480 0.0 10 0.00 1.01 1.07 0.1000 0.00000 000.00 0 0.1 0.686 0.214 0.1e-7
4 0.229 0.229 0.5857 1.546 0.05 0.67 0.480 0.0 10 0.00 1.01 1.07 0.1000 0.00000 000.00 0 0.1 0.686 0.214 0.1e-7
5 0.229 0.229 0.5857 1.546 0.05 0.67 0.480 0.0 10 0.00 1.01 1.07 0.1000 0.00000 000.00 0 0.1 0.686 0.214 0.1e-7
6 0.229 0.229 0.5857 1.546 0.05 0.67 0.480 0.0 10 0.00 1.01 1.07 0.1000 0.00000 000.00 0 0.1 0.686 0.214 0.1e-7
7 0.229 0.229 0.5857 1.546 0.05 0.67 0.480 0.0 10 0.00 1.01 1.07 0.1000 0.00000 000.00 0 0.1 0.686 0.214 0.1e-7
8 0.229 0.229 0.5857 1.546 0.05 0.67 0.480 0.0 10 0.00 1.01 1.07 0.1000 0.00000 000.00 0 0.1 0.686 0.214 0.1e-7
9 0.229 0.229 0.5857 1.546 0.05 0.67 0.480 0.0 10 0.00 1.01 1.07 0.1000 0.00000 000.00 0 0.1 0.686 0.214 0.1e-7
10 0.229 0.229 0.5857 1.546 0.05 0.67 0.480 0.0 10 0.00 1.01 1.07 0.1000 0.00000 000.00 0 0.1 0.686 0.214 0.1e-7
11 0.229 0.229 0.5857 1.546 0.05 0.67 0.480 0.0 10 0.00 1.01 1.07 0.1000 0.00000 000.00 0 0.1 0.686 0.214 0.1e-7
12 0.229 0.229 0.5857 1.546 0.05 0.67 0.480 0.0 10 0.00 1.01 1.07 0.1000 0.00000 000.00 0 0.1 0.686 0.214 0.1e-7
13 0.229 0.229 0.5857 1.546 0.05 0.67 0.480 0.0 10 0.00 1.01 1.07 0.1000 0.00000 000.00 0 0.1 0.686 0.214 0.1e-7
14 0.229 0.229 0.5857 1.546 0.05 0.67 0.480 0.0 10 0.00 1.01 1.07 0.1000 0.00000 000.00 0 0.1 0.686 0.214 0.1e-7
15 0.229 0.229 0.5857 1.546 0.05 0.67 0.480 0.0 10 0.00 1.01 1.07 0.1000 0.00000 000.00 0 0.1 0.686 0.214 0.1e-7
16 0.229 0.229 0.5857 1.546 0.05 0.67 0.480 0.0 10 0.00 1.01 1.07 0.1000 0.00000 000.00 0 0.1 0.686 0.214 0.1e-7
17 0.229 0.229 0.5857 1.546 0.05 0.67 0.480 0.0 10 0.00 1.01 1.07 0.1000 0.00000 000.00 0 0.1 0.686 0.214 0.1e-7

```


44	-.500
47	-.500
49	-.500
50	-.500
1	-.500
2	-.500
4	-.500
7	-.500
11	-.500
16	
16	0
21	0
26	0
31	0
36	0
41	0
45	0
48	0
3	0
6	0
10	0
15	0
20	0
25	0
30	0
35	0
50	
40	20.00
44	20.00
47	20.00
49	20.00
50	20.00
1	20.00
2	20.00
4	20.00
7	20.00
11	20.00
16	20
21	20
26	20
31	20
36	20
41	20
45	20
48	20
3	20
6	20
10	20
15	20
20	20
25	20
30	20

35	20
12	20
8	20
5	20
17	20
13	20
9	20
22	20
18	20
14	20
27	20
23	20
19	20
32	20
28	20
24	20
37	20
33	20
29	20
42	20
38	20
34	20
46	20
43	20
39	20
0	
0	
0	
5	
40	1.00
44	1.00
47	1.00
49	1.00
50	1.00
21	
1	0.00
2	0.00
4	0.00
7	0.00
11	0.00
16	0
21	0
26	0
31	0
36	0
41	0
45	0
48	0
3	0
6	0
10	0
15	0

20 0
25 0
30 0
35 0
26
50,49,49
49,50,47
47,49,44
44,47,40
40,44,44
1,2,2
2,4,1
4,7,2
7,11,4
11,7,7
16,21,11
21,26,16
26,31,21
31,36,26
36,41,31
41,45,36
45,48,41
48,50,45
35,30,45
30,25,35
25,20,30
20,15,25
15,10,20
10,6,15
6,3,10
3,1,6
2,50,49
4,49,47
6,47,44
8,44,40
7,40,35
15,35,30
23,30,25
31,25,20
39,20,15
47,15,10
5,10,6
63,6,3
71,3,1
71,1,2
69,4,2
6,7,4
65,11,7
66,16,11
58,21,16
50,26,21
42,31,26

34,36,31
26,41,36
18,45,41
10,48,45
2,50,48
0
0
0
0

INITIAL.IN

20.0 ! TREF - Reference temperature used to calculate density, viscosity, latent heat
3.0 ! FLAGRG - Flag indicating type of density, viscosity calculations: 1 = reference value, 2 = T
dependence, 3 = T,C dependence
0.26 ! RS - Radius of solute
1.0 ! GF - Gain factor used to multiply first term in Dtl
1.0 ! TF - Factor used to multiply tortuosity
0.0 ! FDTL2 - Factor used to multiply second term in Dtl
0.1 ! FDCL2 - Factor used to multiply second term in Dcl
0.5 ! SCALE
1.0 ! OMEGA
100000. .001
-1 -1
0.0 1.0
10000000 1.0
-1 -1
5
0
0
1 -0.5
50 -0.5
-1 -1
1 20.00
50 20.00
-1 -1
1 0.00000
50 0.00000
-1 -1
13
.1
.5
1.
2
3
4
5.
7
8
9
10.
25

50
10
4
8
13
18
23
28
33
38
43
47

APPENDIX 6. MODEL INPUT FILE IN CASE 4 VALIDATION (WATER-HEAT-SOLUTE TRANSPORT)

ELEMENT.IN

NASSAR Model - water-heat-solute transport in moist,salinized horizontal column

```

0      72      50
48 46 49 48 49 50 46 43 47 46 47 49 43 39 44
43 44 47 39 35 40 39 40 44 45 42 46 45 46 48
42 38 43 42 43 46 38 34 39 38 39 43 34 30 35
34 35 39 41 37 42 41 42 45 37 33 38 37 38 42
33 29 34 33 34 38 29 25 30 29 30 34 36 32 37
36 37 41 32 28 33 32 33 37 28 24 29 28 29 33
24 20 25 24 25 29 31 27 32 31 32 36 27 23 28
27 28 32 23 19 24 23 24 28 19 15 20 19 20 24
26 22 27 26 27 31 22 18 23 22 23 27 18 14 19
18 19 23 14 10 15 14 15 19 21 17 22 21 22 26
17 13 18 17 18 22 13 9 14 13 14 18 9 6 10
9 10 14 16 12 17 16 17 21 12 8 13 12 13 17
8 5 9 8 9 13 5 3 6 5 6 9 11 7 12
11 12 16 7 4 8 7 8 12 4 2 5 4 5 8
2 1 3 2 3 5
0.0080 0.0000 0.0060 0.0000 0.0080 0.0156 0.0040 0.0000
0.0060 0.0156 0.0080 0.0311 0.0020 0.0000 0.0040 0.0156
0.0060 0.0311 0.0080 0.0467 0.0000 0.0000 0.0020 0.0156
0.0040 0.0311 0.0060 0.0467 0.0080 0.0622 0.0000 0.0156
0.0020 0.0311 0.0040 0.0467 0.0060 0.0622 0.0080 0.0778
0.0000 0.0311 0.0020 0.0467 0.0040 0.0622 0.0060 0.0778
0.0080 0.0933 0.0000 0.0467 0.0020 0.0622 0.0040 0.0778
0.0060 0.0933 0.0080 0.1089 0.0000 0.0622 0.0020 0.0778
0.0040 0.0933 0.0060 0.1089 0.0080 0.1244 0.0000 0.0778
0.0020 0.0933 0.0040 0.1089 0.0060 0.1244 0.0080 0.1400
0.0000 0.0933 0.0020 0.1089 0.0040 0.1244 0.0060 0.1400
0.0000 0.1089 0.0020 0.1244 0.0040 0.1400 0.0000 0.1244
0.0020 0.1400 0.0000 0.1400

```

PROPERTY.IN

```

1 0.229 0.229 0.5857 1.546 0.05 0.67 0.480 0.0000 0. 0.0002 1.01 1.04 0.0070 0.0010 000.00 0 0.1 0.686 0.214 0.1e-7
2 0.229 0.229 0.5857 1.546 0.05 0.67 0.480 0.0000 0. 0.0002 1.01 1.04 0.0070 0.0010 000.00 0 0.1 0.686 0.214 0.1e-7
3 0.229 0.229 0.5857 1.546 0.05 0.67 0.480 0.0000 0. 0.0002 1.01 1.04 0.0070 0.0010 000.00 0 0.1 0.686 0.214 0.1e-7
4 0.229 0.229 0.5857 1.546 0.05 0.67 0.480 0.0000 0. 0.0002 1.01 1.04 0.0070 0.0010 000.00 0 0.1 0.686 0.214 0.1e-7
5 0.229 0.229 0.5857 1.546 0.05 0.67 0.480 0.0000 0. 0.0002 1.01 1.04 0.0070 0.0010 000.00 0 0.1 0.686 0.214 0.1e-7
6 0.229 0.229 0.5857 1.546 0.05 0.67 0.480 0.0000 0. 0.0002 1.01 1.04 0.0070 0.0010 000.00 0 0.1 0.686 0.214 0.1e-7
7 0.229 0.229 0.5857 1.546 0.05 0.67 0.480 0.0000 0. 0.0002 1.01 1.04 0.0070 0.0010 000.00 0 0.1 0.686 0.214 0.1e-7
8 0.229 0.229 0.5857 1.546 0.05 0.67 0.480 0.0000 0. 0.0002 1.01 1.04 0.0070 0.0010 000.00 0 0.1 0.686 0.214 0.1e-7
9 0.229 0.229 0.5857 1.546 0.05 0.67 0.480 0.0000 0. 0.0002 1.01 1.04 0.0070 0.0010 000.00 0 0.1 0.686 0.214 0.1e-7
10 0.229 0.229 0.5857 1.546 0.05 0.67 0.480 0.0000 0. 0.0002 1.01 1.04 0.0070 0.0010 000.00 0 0.1 0.686 0.214 0.1e-7
11 0.229 0.229 0.5857 1.546 0.05 0.67 0.480 0.0000 0. 0.0002 1.01 1.04 0.0070 0.0010 000.00 0 0.1 0.686 0.214 0.1e-7
12 0.229 0.229 0.5857 1.546 0.05 0.67 0.480 0.0000 0. 0.0002 1.01 1.04 0.0070 0.0010 000.00 0 0.1 0.686 0.214 0.1e-7
13 0.229 0.229 0.5857 1.546 0.05 0.67 0.480 0.0000 0. 0.0002 1.01 1.04 0.0070 0.0010 000.00 0 0.1 0.686 0.214 0.1e-7
14 0.229 0.229 0.5857 1.546 0.05 0.67 0.480 0.0000 0. 0.0002 1.01 1.04 0.0070 0.0010 000.00 0 0.1 0.686 0.214 0.1e-7
15 0.229 0.229 0.5857 1.546 0.05 0.67 0.480 0.0000 0. 0.0002 1.01 1.04 0.0070 0.0010 000.00 0 0.1 0.686 0.214 0.1e-7
16 0.229 0.229 0.5857 1.546 0.05 0.67 0.480 0.0000 0. 0.0002 1.01 1.04 0.0070 0.0010 000.00 0 0.1 0.686 0.214 0.1e-7
17 0.229 0.229 0.5857 1.546 0.05 0.67 0.480 0.0000 0. 0.0002 1.01 1.04 0.0070 0.0010 000.00 0 0.1 0.686 0.214 0.1e-7

```


40	0.	! Node #, Moisture flux
44	0.	!
47	0.	
49	0.	
50	0.	
1	0.	
2	0.	
4	0.	
7	0.	
11	0.	
16	0	
21	0	
26	0	
31	0	
36	0	
41	0	
45	0	
48	0	
3	0	
6	0	
10	0	
15	0	
20	0	
25	0	
30	0	
35	0	
10		! Number of specified temperature values
40	19.02	! Node #, Temperature
44	19.02	
47	19.02	
49	19.02	
50	19.02	
1	8.93	
2	8.93	
4	8.93	
7	8.93	
11	8.93	
0		! Number of convective heat flux nodes
16		! Number of specified heat flux nodes
16	0	! Node #, Heat flux
21	0	
26	0	
31	0	
36	0	
41	0	
45	0	
48	0	
3	0	
6	0	
10	0	
15	0	
20	0	

25	0	
30	0	
35	0	
0		! Number of specified solute concentration nodes
0		! Number of convective solute flux nodes
26		! Number of specified solute flux nodes
40	0.00	! Node #, solute flux
44	0.00	
47	0.00	
49	0.00	
50	0.00	
1	0.00	
2	0.00	
4	0.00	
7	0.00	
11	0.00	
16	0	
21	0	
26	0	
31	0	
36	0	
41	0	
45	0	
48	0	
3	0	
6	0	
10	0	
15	0	
20	0	
25	0	
30	0	
35	0	
26		! Number of boundary nodes
50,49,49		! Boundary node #, adjacent boundary node numbers
49,50,47		
47,49,44		
44,47,40		
40,44,44		
1,2,2		
2,4,1		
4,7,2		
7,11,4		
11,7,7		
16,21,11		
21,26,16		
26,31,21		
31,36,26		
36,41,31		
41,45,36		
45,48,41		
48,50,45		
35,30,45		

30,25,35
 25,20,30
 20,15,25
 15,10,20
 10,6,15
 6,3,10
 3,1,6
 2,50,49
 4,49,47
 6,47,44
 8,44,40
 7,40,35
 15,35,30
 23,30,25
 31,25,20
 39,20,15
 47,15,10
 5,10,6
 63,6,3
 71,3,1
 71,1,2
 69,4,2
 6,7,4
 65,11,7
 66,16,11
 58,21,16
 50,26,21
 42,31,26
 34,36,31
 26,41,36
 18,45,41
 10,48,45
 2,50,48
 0 !
 0 !
 0 !
 0 !

INITIAL.IN

20.0 ! TREF - Reference temperature used to calculate density, viscosity, latent heat
 3.0 ! FLAGRG - Flag indicating type of density, viscosity calculations: 1 = reference value, 2 = T
 dependence, 3 =T,C dependence
 0.25 ! RS - Radius of solute
 4.1 ! GF - Gain factor used to multiply first term in Dtl
 1.0 ! TF - Factor used to multiply tortuosity
 1.0 ! FDTL2 - Factor used to multiply second term in Dtl
 1.0 ! FDCL2 - Factor used to multiply second term in Dcl
 0.5 ! SCALE
 1.0 ! OMEGA
 10000000 .002 ! NUMSTEP(ICOUNT),DT(IDT)
 -1 -1 ! EOF

```

0.0  1.0      ! TIME(ICOUNT),TFUNC(ICOUNT) Beginning
10000000 1.0 ! TIME(ICOUNT),TFUNC(ICOUNT) Ending
-1  -1      ! EOF
4      ! DTMAXX
0      ! NTHOUT - write results every Nth time steps
1      ! IFLAG 0 = Pressure, 1 = Moisture
1  0.144    ! First node, Initial moisture
50  0.144   ! Last node, Initial moisture
-1  -1      ! EOF
1  10.00    ! Start node, Initial temperature
50  10.00   ! End node, Initial temperature
-1  -1      ! EOF
1  0.794    ! Start node, Initial concentration
50  0.794   ! End node, Initial concentration
-1  -1      ! EOF
20     ! NTOUT - number of times to write results
0.001
0.01   ! Write time 1 (0.1 day)
0.05
0.1
0.2
0.3    ! Write time 2
0.5
0.7
0.9
1.0
1.1
1.3
1.5
2.5
5.0
10.0
15.
20.0
30.
35.0
10     ! Number of nodes to write values
4      ! Write node number 4
8
13
18
23
28
33
38
43
47

```



Friedel—DOCUMENTATION AND VERIFICATION OF VST2D: A MODEL FOR SIMULATING TRANSIENT, VARIABLY SATURATED, COUPLED WATER-HEAT-SOLUTE
TRANSPORT IN HETEROGENEOUS, ANISOTROPIC, 2-DIMENSIONAL, GROUND-WATER SYSTEMS WITH VARIABLE FLUID DENSITY—U.S. Geological Survey
Water-Resources Investigations Report 00-4105

U.S. GEOLOGICAL SURVEY
221 NORTH BROADWAY AVE.
URBANA, ILLINOIS 61801